

Some Sorption and Salt Occlusion Properties  
of Silicalite-1

By

Tracey K. Flynn

Thesis presented for the degree of

Doctor of Philosophy

University of Edinburgh

1987



**To Mum and Dad**

## ACKNOWLEDGEMENTS

This work would not have been possible without the guidance and enthusiasm of Drs. B.M. Lowe and H.F. Leach. Their supervision was much appreciated. The provision of funds by the University of Edinburgh for a four period demonstratorship and a James Watt Bursary is gratefully acknowledged. I am also indebted to the members of the zeolite group for the many useful discussions.

## DECLARATION

This thesis is of my own composition and is an accurate account of the research carried out by myself at the University of Edinburgh between October 1982 and September 1985.

## ABSTRACT

Silicalite is the all silica polymorph of the ZSM-5 series. Its surface is usually considered to be an array of Si-O-Si bonds. The central theme of this work is concerned with the internal surface of this material. The properties of the surface are very dependent on the conditions used for the synthesis and the subsequent treatment of samples. In turn, the hydrophobic and organophilic properties are governed by the presence or absence of species such as silanol groups or cations in the channels of silicalite-1.

Silicalite-1 was synthesised from a number of different reaction mixtures. The pretreatment of the resultant samples was varied - calcination temperature, washing procedures, ion-exchange and activation temperature - to give a range of pretreated samples.

The gas phase sorption of organic and polar molecules by these different samples was investigated to note the effect of varying the synthesis and pretreatment procedures. Two techniques were used in the sorption measurements. In the determination of isotherms and diffusion rates, a Cahn electrobalance was used. A technique developed during this work - the "multi-equilibration" method - was used to obtain maximum uptakes of sorbates, quickly and simply.

A range of organic and polar salts were occluded from aqueous solutions. In particular, the occlusion of three sodium alkylsulphonates was examined in detail to observe the effect of varying the length of the alkyl chain.

The occlusion of salts obviously alters the sorption properties of the molecular sieve. This was investigated further. In particular, how the sorption of molecules from the gas phase varies with the quantity of salt occluded was measured using an adapted version of the "multi-equilibration" technique.

Finally, the occlusion and subsequent decomposition of alkaline salts - acetates and carbonates - was carried out to note the effect on the structure and sorption properties of silicalite-1.

# TABLE OF CONTENTS

<b>1 GENERAL INTRODUCTION</b>	<b>1</b>
1.1 SYNTHESIS OF ZEOLITES	3
1.2 STRUCTURE	7
1.3 ION EXCHANGE	13
1.4 ZEOLITE CATALYSIS	17
1.5 THIS WORK	17
1.6 REFERENCES	20
<b>2 SYNTHESIS AND INITIAL CHARACTERISATION</b>	<b>26</b>
2.1 EXPERIMENTAL TECHNIQUES	26
2.1.1 X-ray Diffraction	26
2.1.2 Thermal Analysis	29
2.1.3 X-ray Fluorescence	33
2.1.4 Microscopy	33
2.1.5 pH Measurements	34
2.2 SYNTHESIS	34
2.2.1 Synthesis of ZSM-5	34
2.2.2 Pretreatment of ZSM-5	35
2.2.3 Synthesis of Silicalite	35
2.2.4 Pretreatment of Samples	37
2.2.5 Terminology	38
2.3 RESULTS	39
2.3.1 ZSM-5	39
2.3.2 Silicalite	41
2.4 REFERENCES	49
<b>3 SORPTION PROPERTIES OF SILICALITE</b>	<b>51</b>
3.1 INTRODUCTION	51
3.2 SORPTION ISOTHERMS	53
3.2.1 The Langmuir Isotherm	53
3.2.2 Sorption Isotherm with Sorbate-sorbate Interactions	55
3.3 ENERGETICS OF SORPTION	56
3.4 INTERACTIONS	57
3.5 DIFFUSION	59
3.6 FACTORS AFFECTING SORPTION	61
3.6.1 Effect of Cations	61
3.6.2 Si/Al Ratio	63
3.6.3 Nature Of Sorbate	63
3.6.4 Temperature	64
3.6.5 Structure	64
3.6.6 Salt Occlusion	64
3.7 ZSM-5 AND SILICALITE-1	64
3.8 HYDROXYLATION OF SILICA	67
3.9 HYDROXYLATION OF ZSM-5/SILICALITE	69
3.10 EXPERIMENTAL TECHNIQUES	71
3.10.1 Cahn R.G. Automatic Electrobalance	71
3.10.2 The Multi-equilibration Method	77
3.10.3 Comparison of techniques	85

3.11	SORPTION PROPERTIES OF ZSM-5	90
3.12	SORPTION PROPERTIES OF SILICALITE	95
3.12.1	Uptakes of n-alkanes by [TPA,PIP]-SIL	95
3.12.2	Uptake of n-heptane by silicalite	98
3.12.3	Sorption of Methanol	101
3.12.4	Uptake of Water by Silicalite	115
3.12.5	Low Pressure Hysteresis of Isotherms	122
3.12.6	Hydroxylation and Methoxylation of Silicalite	138
3.12.7	Uptake of Water by Various Forms of Silicalite	140
3.13	CONCLUSION	147
3.14	REFERENCES	149
<b>4</b>	<b>OCCLUSION OF SALTS BY SILICALITE</b>	<b>154</b>
4.1	INTRODUCTION	154
4.1.1	Aluminous Zeolites	155
4.1.2	High Silica Molecular Sieves	158
4.2	INTRODUCTION TO EXPERIMENTAL TECHNIQUES	159
4.3	EXPERIMENTAL	164
4.3.1	Apparatus	164
4.3.2	Procedure	165
4.3.3	Materials	166
4.4	ISOPIESTIC RESULTS	167
4.4.1	Hexamethonium bromide + Silicalite	167
4.4.2	CsNO <sub>3</sub> + Silicalite	169
4.4.3	Tetramethylammoniumbromide + Silicalite	170
4.4.4	Sodium benzenesulphonate + Silicalite	172
4.4.5	Occlusion of Sodium alkylsulphonates	173
4.5	SORPTION PROPERTIES OF SALT OCCLUDED SILICALITE	194
4.5.1	Sorption Properties of CsCl/Silicalite and NaCl/Silicalite	196
4.5.2	Uptake of n-heptane by Hexamethonium bromide/Silicalite and Decamethonium bromide/Silicalite	198
4.5.3	Uptake of N-heptane by Sodium benzenesulponate/Silicalite	200
4.5.4	Uptakes of sorbates by Sodium alkylsulphonates	201
4.6	CONCLUSION	207
4.7	REFERENCES	209
<b>5</b>	<b>210</b>	
5.1	ISOPIESTIC MEASUREMENTS	211
5.1.1	Experimental	211
5.1.2	Results	211
5.2	SORPTION PROPERTIES	222
5.2.1	Experimental	222
5.2.2	Results	223
5.3	FURTHER EXPERIMENTS	234
5.4	REPEATED OCCLUSION/DECOMPOSITION/ION-EXCHANGE CYCLES	256
5.5	CONCLUSION	265
5.6	REFERENCES	266
<b>6</b>	<b>CONCLUSION</b>	<b>267</b>
<b>A</b>	<b>LECTURE COURSES</b>	<b>271</b>

# CHAPTER 1

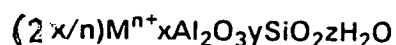
## GENERAL INTRODUCTION

Very few materials display such a diversity of structures and variety of properties as do zeolites. Consequently they have found numerous applications and provide an expanding field for scientific research.

Zeolites were first recognised as a separate mineral group in 1756 with the discovery of Stilbite[1]. Although, further zeolites were identified in nature and the first zeolite synthesis reported in 1862[2], it was not until the 1940's that zeolite science became a research area in its own right. In the 1950's, developments occurred on two fronts. Barrer and Milton with their respective co-workers, separately started research of a systematic nature on zeolites and in particular on their synthesis[3]. In the late 1950's exploration revealed the existence of some large deposits of natural zeolites[4]. Since then zeolite research has expanded in all areas of synthesis, ion exchange, sorption and catalysis.

Zeolites are arrays of  $\text{SiO}_4$  and  $\text{AlO}_4$  tetrahedra linked together through their apical oxygen atoms to form three-dimensional networks. The frameworks are not tight structures but open ones with channels and cages permeating throughout. The trivalent aluminium in the framework results in an overall negative charge which is balanced by occluded cations in the channels. Other species such as water, salts and/or organic molecules may also occupy the voids within the structure. These species may have considerable freedom of movement.

The composition of zeolites may be empirically described by the formula





As Al-O-Al linkages are not found in zeolites,  $y$  is always greater than or equal to  $2x$ . No zeolite has a unique composition. Each synthetic zeolite can only be prepared with a characteristic range of composition and in particular with a range of framework Si/Al ratios. As many properties of zeolites are related to their aluminium content, they are arbitrarily classified into three groups according to their Si/Al ratio. Some examples are shown in Table 1.1.

Over 30 natural zeolites have been identified and many more have been synthesised. For some synthetic zeolites no counterpart in nature has yet been discovered. These different zeolites exhibit a wide variety of properties. The synthesis of these materials and the properties they possess are discussed further in the following sections. Previous work on sorption and salt occlusion is discussed in more detail in chapters 3 and 4 respectively

## **1.1 Synthesis of Zeolites**

Zeolite synthesis has attracted a considerable amount of attention by researchers as shown by the many patents, papers and reviews[5,6,7,8] which have been published. This research has been concerned with three aspects:-

1. Synthesis of new and novel materials.
2. The mechanism of synthesis.
3. The parameters that affect synthesis.

It is outwith the scope of this work to give more than the briefest outline of this broad subject. Zeolites were first synthesised under conditions of high pressure and high temperature, but later, it was discovered that they may be prepared using relatively mild conditions[9]. These days, the majority of zeolites are synthesised under hydrothermal conditions with autogenous or atmospheric pressure and temperatures in the range 25-175°C. They are crystallised from aqueous alkaline aluminosilicate gels prepared from sources of alumina, silica and aqueous base. A large number of different silica and alumina materials can

Table 1.1. Classification of Zeolites with respect to Si/Al ratio.

Si/Al ratio	examples
$1 < \text{Si/Al} < 2$	zeolite A, zeolite X
$2 < \text{Si/Al} < 10$	zeolite L, Mordenite
$10 < \text{Si/Al}$	ZSM-5, ZSM-11

be used, but, the product may depend on the source and pretreatment of the reagents. When the components are mixed an amorphous aluminosilicate gel is formed. The appearance of the gel varies and is dependent on the exact nature of the starting materials. The crystallisation of zeolites takes place in three stages: pre-nucleation, nucleation and crystal growth[10]. Two different mechanisms have been proposed for the formation of zeolites from gels[11]. One considers that the zeolite crystallisation occurs by dissolution of the amorphous gel to produce aluminosilicate ions in solution. These species then grow by consumption of the gel to form nuclei and then crystals. The second mechanism considers that the nucleation and crystallisation processes occur in the solid phase and result from the partial depolymerisation of the gel by the hydroxide ions present.

When crystallisation occurs from solutions which can give rise to a number of different products (as in zeolite synthesis) the first product formed will be the least thermodynamically stable. If this is allowed to remain in contact with its mother liquor at the same reaction temperature, it will subsequently recrystallise to a more stable material. Zeolites are often thermodynamically unstable products and these must be separated from the reaction mixture before they recrystallise to denser materials. The situation is very complex as the reaction mixtures are invariably heterogeneous and the nucleation is a kinetically controlled rather than a thermodynamically controlled process. So as aforementioned, the treatment of reactants prior to crystallisation, their chemical and physical nature, the influence of other additives such as cations, organics and salts will all play a part in determining which products appear.

The  $\text{H}_2\text{O}/\text{SiO}_2$  and  $\text{HO}^-/\text{SiO}_2$  ratios have a strong influence on the species present in the reaction mixture and the rate at which they interconvert by

hydrolysis to ultimately form the zeolite product[12]. In general, the higher the pH the shorter the time taken for the product to crystallise. The role played by the cations in zeolite formation is often significant. It is noticed that the crystallisation of some zeolites is favoured by the addition of a given cation to the reaction mixture[5]. For example, a reaction mixture which contains  $K^+$  ions yields zeolite L, whereas if  $Na^+$  ions are present zeolite Y is formed instead[13]. The synthesis of a number of zeolites is facilitated if the reaction mixture contains two different cations[14]. The substitution of organic bases and cations for inorganic ones was initiated by Barrer and Denny[15], and Kerr and Kokatailo[16]. In most cases, the organic ions serve to stabilise the aluminosilicate species in solution[17]. The organic ions are occluded into the zeolite framework during the course of synthesis. Many of the organic ions incorporated are larger than the pore openings, and can only be removed from the framework by heating at a sufficiently high temperature to decompose them. Calcination usually leaves the framework intact, although, some structures are known to collapse when subjected to such treatment[13,14].

The use of organic cations in reaction mixtures produced zeolites with higher Si/Al ratios than had been previously attained. The reasons for this are no doubt complex. But one explanation put forward is in essence simple[15]. The size of the organic ion limits the number of ions that may be accommodated within the framework. This in turn restricts the anionic charge on the zeolite framework which results in higher Si/Al ratios.

Continuation of this research yielded many zeolites of a siliceous nature. Among these new zeolites were the now well known ZSM-5[18] and ZSM-11[19]. These two zeolites may be synthesised over a wide range of Si/Al ratios from Si/Al=10 to infinity. It is debatable whether such structures with

large Si/Al ratios - where the aluminium content is much less than one aluminium atom per unit cell - can truly be called zeolites. In this thesis, the term 'molecular sieve' will be used generally to refer to materials with any Si/Al ratio whereas 'zeolite' will refer only to structures with an experimentally significant amount of aluminium in their framework.

The formation of ZSM-5 is favoured by tetrapropylammonium ions( $\text{TPA}^+$ ) and these are normally a component of the reaction mixture[18,20]. However ZSM-5 has been synthesised with other "template" ions. E.g. other quaternary ammonium ions[21], amines[22], alcohols[23], alkanamines[24], carboxylic acids[25] and organic transition metal complexes[26]. ZSM-5 has also been synthesised in the absence of organic cations[27]. Analysis of the 'as-made' material has shown that four  $\text{TPA}^+$  cations are occluded per unit cell during synthesis[28]. This corresponds to one  $\text{TPA}^+$  per channel intersection: there being four intersections per unit cell. In the late 1970's both Mobil Oil Corporation and Union Carbide Company produced patents which appeared to cover the same material - that is an aluminium free ZSM-5[29,30]. This material, now usually known as Silicalite-1, was synthesised from a reaction mixture that contained reactive silica,  $\text{TPA}^+$ ,  $\text{OH}^-$ ,  $\text{Na}^+$ , and water but no aluminium species. Any traces of aluminium in the resultant framework came from impurities in the reagents and the reaction vessels. Other siliceous materials have been made, for example Silicalite-2[31] which is the end member of the ZSM-11 series.

These high silica molecular sieves have unique properties that distinguish them from the more aluminous zeolites.

## 1.2 Structure

Although zeolites have been recognised since the early 18th century, elucidation of their complex structures had to wait for the development of crystallography early this century.

The complete classification of zeolites with respect to their structures has been pioneered by Barrer[32], Breck[33] and Meier[34,35,36]. The primary building blocks of zeolites are the  $\text{SiO}_4$  and  $\text{AlO}_4$  tetrahedra. In 1967 Meier proposed seven secondary building units (SBUs) that can be used to construct all known zeolite topologies. These SBUs are shown in Figure 1.1. For clarity, the oxygen atoms have been omitted and only the T-atoms are shown in the Figure. A zeolite framework may be built up using only one type of SBU. However a number of zeolite networks may be built from different SBU. In Table 1.2 some zeolites are listed with the SBU's from which they may be built.

A number of larger cage-like polyhedral units can be defined within certain zeolite frameworks. These cage-like units are designated by greek letters- $\alpha$ ,  $\beta$ ,  $\gamma$ ,  $\delta$ ,  $\epsilon$  etc (Figure 1.2). The  $\beta$ -cage can be alternatively described in terms of 4- and 6-membered rings and is seen in the structure of zeolite A (Figure 1.3). In this zeolite the  $\beta$ -cages are linked by double four-rings to form a cubic structure. The large cavities that result from such an arrangement are termed  $\alpha$ -cages.

The dimensions and arrangement of the channel and cage network control many of the properties of a zeolite. Access of sorbate molecules to the channel system is governed by the dimensions of the pore openings. The dimensions of these pores depend on the number of Si or Al atoms (often

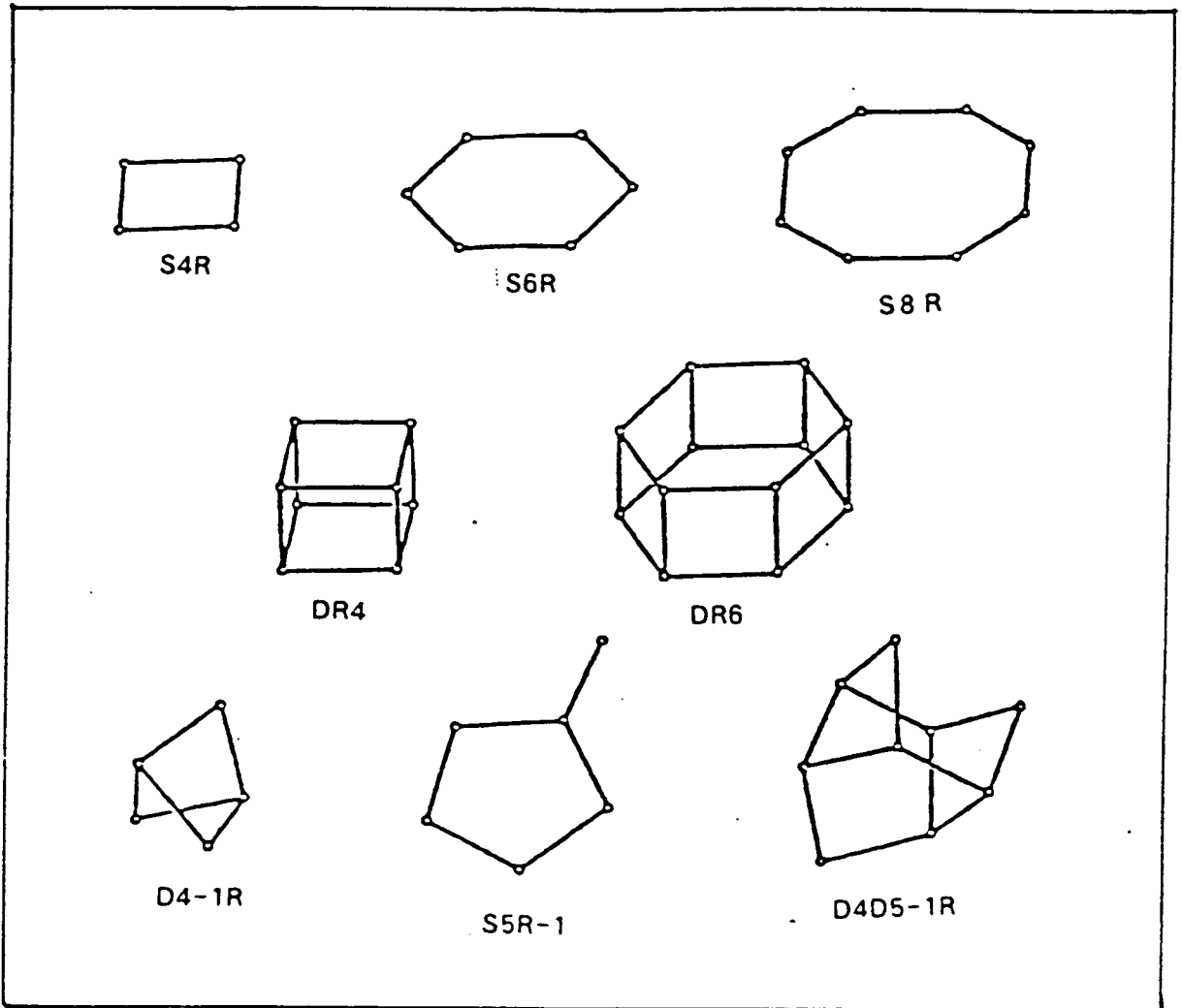


Figure 1.1. Secondary Building Units.

Group	S.B.U.	Example
1	Single 4-ring S4R	Phillipsite
2	Single 6-ring S6R	Erionite
3	Double 4-ring DR4	zeolite A
4	Double-6 ring DR6	zeolite X
5	Complex 4-1 D4-1R	Thomsonite
6	Complex 5-1 S5R-1	Mordenite
7	Complex 4-4-1 D4D5-1R	Clinoptilolite

Table 1.2 Some examples of Zeolites with respective SBU's



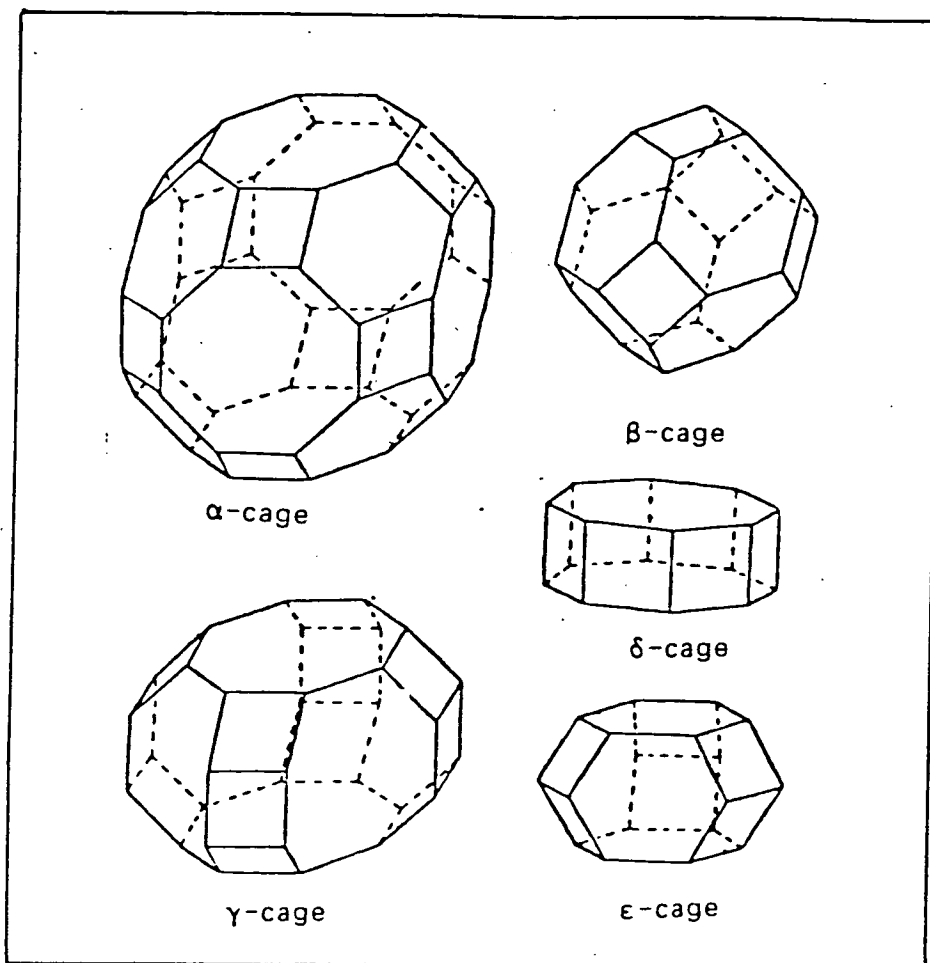


Figure 1.2. Some Polyhedral Units.

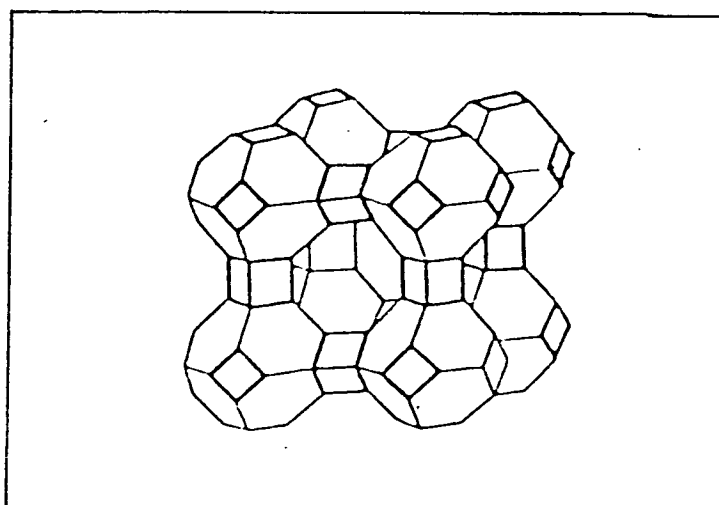


Figure 1.3 Zeolite A

referred to as T-atoms) in the ring. There may be 4,5,6,8,10 or 12 T-atoms in the ring with concomitant free dimensions as shown in Table 1.3[37]. Channels and cavities accessed only by 4 or 5 T-atoms are seldom of interest as their dimensions prohibit entry of all but the smallest molecules. The free dimensions quoted assume a planar configuration of the T-atoms. Frequently, this configuration is distorted so the dimensions are altered as in Offerite and Ferrierite[38].

The channels that permeate the structure may be parallel to one another or interconnected to yield 1-, 2-, or 3-dimensional networks[39]. Some examples are shown in Table 1.4. Whether the channels are parallel or interconnected has consequences for sorption and catalysis.

As much of the work to be discussed is based on ZSM-5 and Silicalite, it is appropriate to give details of this structure[40]. ZSM-5 and Silicalite have the same framework structure; they differ only in composition. They can be formed from a building unit[36,41] shown in Figure 1.4 which in turn may be constructed from 5-1 rings. The resultant framework is permeated by sinusoidal and straight channels as shown in Figure 1.5. The sinusoidal channels are circular with a cross-section of  $5.4\text{\AA}$  whereas the straight channels are elliptical with dimensions of  $5.2\text{\AA}$  by  $5.8\text{\AA}$ .

### 1.3 Ion Exchange

Cations are present in the channels of zeolites to balance the negative charge on the trivalent aluminium. As these cations are mobile, they may be ion exchanged with other cations from melts[42,43] or more commonly from aqueous solution[44-47]. Such exchange of ions is usually reversible. The exchange capacity of a zeolite is obviously related to its Si/Al ratio. Zeolites

T-atoms	dimensions/A
4	1.2
5	2.0
6	2.8
8	4.5
10	6.3
12	8.0

Table 1.3. Dimensions of pore openings of zeolites.

Channel Type	Example
1-D	Omega
2-D	Mordenite
3-D	zeolite A

Table 1.4. Some examples of Zeolites with different channel systems.

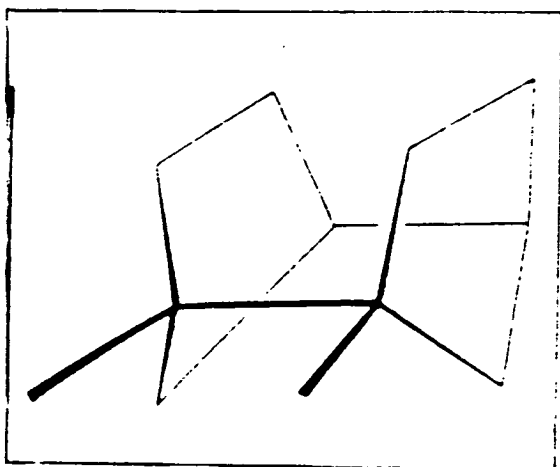


Figure 1.4. A Building Unit of ZSM-5/Silicalite.

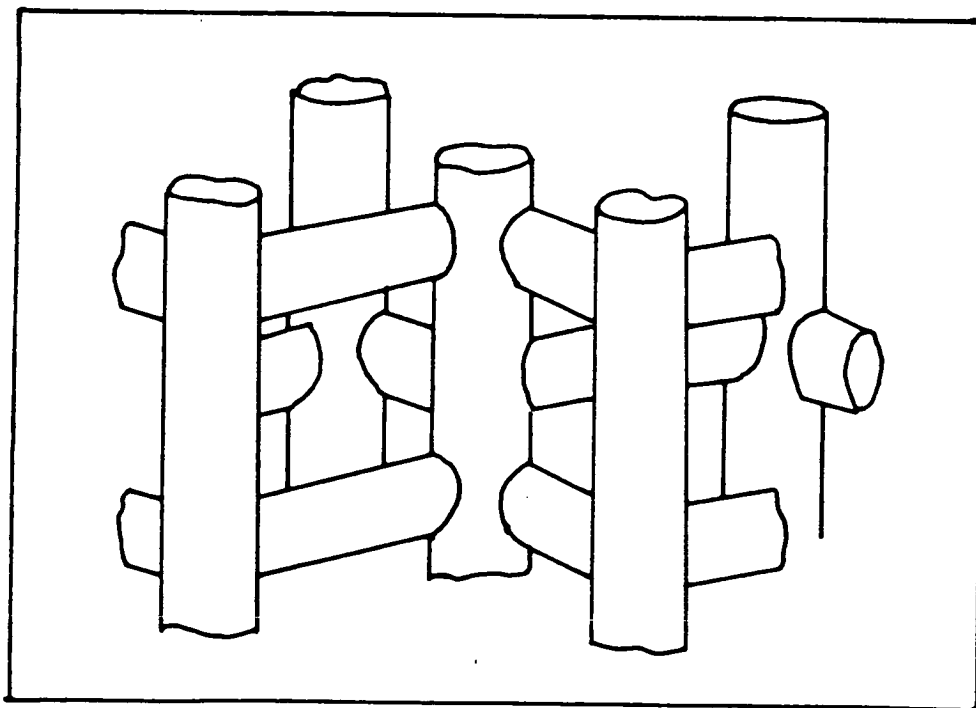


Figure 1.5. The Channel System of ZSM-5/Silicalite.

with low Si/Al ratio have the highest exchange capacities.

The use of zeolites as ion exchangers has attracted a growing interest. They have not tended to displace the established organic resins but rather have found uses in new applications where organic ion exchangers are unsuitable. Their advantages are that they undergo no appreciable changes in structure dimensions on exchange, have greater stability to temperature and ionising radiation and a higher selectivity for certain ions than do the organic resins. This has led to their use in detergents, in ammonium removal from waste water, in removal of radioisotopes from nuclear waste and in agriculture[48].

The nature of cation exchange in zeolites depends on a number of variables:-

1. The radii of the hydrated and the anhydrous cation and its charge.
2. Temperature of the system.
3. Concentration of the solution.
4. The anions associated with the cations in solution.
5. The nature of the channels and cavities of the zeolite.

Ion sieving effects are observed with small pore zeolites and with larger ions. It is observed that some cations are exchanged even though their hydrated ionic diameters exceed those of the zeolite pores[43]. In this case, an exchange of solvent molecules must also occur. If the solvation shell is bound tightly to the ion, the diffusion of the ion into the zeolite will be slow. Cations

with anhydrous diameters that exceed the pore diameters are totally excluded. The size of the cation will also govern its entry to cages within the framework. Larger ions may be excluded on steric grounds from the smaller cages. For example,  $\text{Cs}^+$  ions can replace only 68% of  $\text{Na}^+$  ions in zeolite Y because  $\text{Cs}^+$  is too large to enter the sodalite cages where 16 $\text{Na}^+$  are located. The extent of ion-exchange may also be limited because of the volume occupied by the cation. Zeolite X will sorb 33  $\text{C}(\text{CH}_3)_4$  molecules per unit cell[10]. As  $\text{N}(\text{CH}_3)_4^+$  is of a similar size it can only exchange a fraction of the 82  $\text{Na}^+$  ions in a unit cell[49].

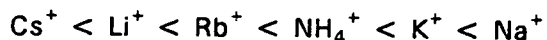
The location of cations within the framework depends on the nature of the zeolite[50]. In most zeolites the number of sites exceeds the number of cations required to balance the charge on the framework. Not all these sites will be identical. How the cations distribute themselves amongst the available sites depends on the size and charge of ions as well as the temperature and the degree of hydration of the zeolite.

In the ion-exchange of cations from aqueous solutions, the zeolite competes with the water molecules in solution for the cation. The preference of a zeolite for a given cation will depend on the Si/Al ratio and the pore volume of the zeolite and the ionic radius, charge and hydration energy of the cation. This is clearly shown if the selectivities series of two very different zeolites are examined - zeolite A and ZSM-5[47,51].

Zeolite A has a low Si/Al ratio and so the field strength of the anionic framework is very strong. "Strong field" zeolites like zeolite A show greatest preference for cations with small ionic radii and high charge even though such ions are also strongly attracted by the solution phase. As a result zeolite A

shows a greater preference for multivalent ions than univalent cations.

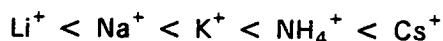
The selectivity for univalent cations is:-



It is observed that even a zeolite with a strong field like zeolite A cannot compete with the strong interaction of the lithium cations with water molecules in the solution phase.

ZSM-5 has a high Si/Al ratio and consequently it possesses a much weaker field in its channels than zeolite A. It is observed that zeolites such as this show greatest selectivity for cations with large ionic radii and small charge. So it is found that univalent cations are more preferred than multi-valent cations by zeolites like ZSM-5.

The selectivity series for ZSM-5 is:-



Zeolites may be exchanged in solutions with a pH < 7 to give hydrogen exchanged zeolites. Zeolites such as Y and A undergo structural collapse when in contact with acid solutions[13] but the hydrogen form of zeolites with higher Si/Al ratios such as ZSM-5 and mordenite may be prepared by this method[52]. Even in these high silica materials, this treatment often results in dealumination. An alternative method for the preparation of hydrogen zeolites involves exchange with ammonium ions[53], followed by calcination at a temperature > 400°C which liberates ammonia leaving protons in the channels. However, even by this method complete exchange of zeolite A and zeolite X cannot be achieved. The temperature used to calcine the ammonium exchanged molecular sieve is important as it has been shown that the catalytic activity of the zeolite is dependent on the temperature at which the ammonium ion

exchanged zeolite is calcined[54].

## **1.4 Zeolite Catalysis**

In the early 1960's researchers in the laboratories of Mobil Oil Corporation and Union Carbide Company both demonstrated intracrystalline catalytic activity of zeolites. This activity varied from zero to excellent and was dependent on the choice of zeolite, Si/Al ratio, and the nature of the cations in the channels[55]. The rare-earth and hydrogen forms of some zeolites were found to possess cracking activity several orders of magnitude greater than conventional silica-alumina catalysts. This enhanced activity may be explained in terms of a greater concentration of active sites. It may also be increased by a molecular sieve effect which permits catalytic conversion of only those molecules that can penetrate the channel system. The dimensions of the channel system also control the nature of the transition state that can be formed[56]. Zeolites have made a tremendous impact on the petroleum industry because of this enhanced catalytic activity. Catalysed reactions include isomerisation, alkylation, dealkylation, hydration of alkenes, dehydration of alcohols, aromatisation, hydrocracking and cracking[57].

## **1.5 This Work**

The properties of a molecular sieve may be altered by the occlusion of salt, even in small amounts. The primary object of this work was to systematically quantify how the sorption properties of molecular sieves are modified by the occlusion of salts. Since the ingress of both sorbate molecules and salts depends on the nature of the guest-molecular sieve interactions, such an investigation should also yield information about the internal surface of the molecular sieve. The uptake of salts by zeolites has been investigated by a number of other workers. But only one paper has dealt with the consequent



effect on sorption properties and it did so in a qualitative manner[58].

In this paper, a study was made of the effect of salt occlusion in a number of zeolites, upon the kinetics of sorption and the molecular sieving behaviour towards different sorbates. Salts were occluded in zeolite L, offerite and H-mordenite. Salts were chosen for their thermal stability, KCl, KBr,  $K_2SO_4$  and  $K_2CrO_4$ .

Barrer and workers carried out the occlusion by soaking the zeolite in the appropriate salt solution for 16h at 80°C, filtering and repeating the procedure twice. Several different concentrations of salt solutions were used. A number of samples were further treated; referred to as "washed" or "extracted". Washed samples were filtered with distilled water. Extracted samples were stirred in distilled water for 16h at 80°C. The sorption properties of these different samples was investigated. The presence of salt in the channels of the zeolite was observed to hinder the diffusion of sorbates into the molecular sieves, lower the equilibrium uptakes and in some cases alter the molecular sieving behaviour.

Samples that had either been "washed" or "extracted" generally exhibited less modification to their sorption properties. The different salts were observed to modify the uptakes of sorbates by a given zeolite to different extents.

This paper has shown that the occlusion of salts into the pores and channels of zeolites alters the sorption behaviour of a zeolite. The modification being dependent on the concentration of the salt solution, the zeolite, the salt and the washing procedure. However, the results are of a very qualitative

nature.

Corresponding information about the salt occlusion properties of high silica molecular sieves is scarce. In the light of this and the present interest in high silica molecular sieves it was felt pertinent to examine the properties of these materials. Research was concentrated on the all silica polymorph of the ZSM-5 series - Silicalite-1. In theory the treatment of Silicalite-1 should be more straightforward than that of zeolitic materials which contain aluminium in their framework and cations in their channels. In practice, complications arose that were a consequence of imperfect structures. However, these were of interest in themselves and were investigated further.

The result is an accumulation of information in four interrelated areas.

1. Synthesis and pretreatment of Silicalite-1 and preliminary characterisation.
2. Sorption of polar and non-polar molecules by samples of silicalite-1 prepared and pretreated by different procedures.
3. Occlusion of various salts into Silicalite-1 and their effect on its sorptive behaviour.
4. Occlusion and subsequent decomposition of salts in Silicalite-1 and the effect on structure and sorption properties.

## 1.6 References

1. A.F. Cronstedt, *Akad. Handl.*, Stockholm, 1756, 15, 120.
2. H. de St Claire–Deville, *Compt. Rend.* 1862, 54, 324.
3. E.M. Flanigen, "Zeolites: Science and Technology", NATO ASI Series (ed. F.R. Ribeiro, A.E. Rodrigues, L.D. Rollmann, C. Naccache), Martinus Nijkoff, The Hague, 1984, p3.
4. F.A. Mumpton, "Natural Zeolites, Occurrence, Properties, Use", (ed. L.B. Sand and F.A. Mumpton), Pergamon, London, 1978, p3.
5. R.M. Barrer, *Zeolites*, 1981, 1, 130.
6. H. Robson, *ChemTech*, 1978, 8, 176.
7. L.D. Rollmann, "Zeolites: Science and Technology", NATO ASI Series (ed. F.R. Ribeiro, A.E. Rodrigues, L.D. Rollmann, C. Naccache), Martinus Nijkoff, The Hague, 1984, p109.
8. E.M. Flanigen, *Adv. Chem. Ser.*, 1973, 121, 119.
9. D.W. Breck and R.M. Milton, *J. Amer. Chem. Soc.*, 1956, 78, 2338.
10. R.M. Barrer, "Hydrothermal Chemistry of Zeolites", Academic Press, London, 1982.

11. B.D. Nicol, G.T. Pott and K.R. Loos, *J. Phys. Chem.*, 1972, 76, 3388.
12. L.D. Rollman, *Adv. Chem. Ser.*, 1979, 173, 387.
13. D.W. Breck, "Zeolite Molecular Sieves", John Wiley and Sons, New York, 1974.
14. R. Aiello and R.M. Barrer, *J. Chem. Soc., A*, 1970, 1470.
15. R.M. Barrer and P.J. Denny, *J. Chem. Soc.* 1961,971.
16. G.T. Kerr and G. Kokotailo, *J. Amer. Chem. Soc.*, 1961, 83, 4675.
17. W. Sieber and W.M. Meier, *Helv. Chim. Acta*, 1974, 57, 1533.
18. R.J. Arguar and G.R. Landoit, U.S. Patent 3,702,866(1972)
19. P. Chu, U.S. Patent 3,709,979(1973).
20. N.Y. Chen, S.J. Lucki and W.E. Garwood, U.S. Patent 3,702,886,(1972).
21. S.B. Kulkarni, V.P. Shiralkar, A.N. Kotasthane, R.B. Borade and P. Ratnasamy, *Zeolites*, 1982, 2, 313.
22. L.D. Rollman and E.W. Valyocsik, U.S. Patent 4,139,600(1973).
23. J.L. Casci, B.M. Lowe and T.V. Whittam, European Patent Application 42,225(1981)

24. W.J. Ball, K.W. Palmer and D.G. Stewart, U.S. Patent 4,407,728(1983).
25. K.I. Iwayama, T. Kamano, K. Tada and T. Inoue, European Patent Application, 57,016(1982).
26. L.A. Rantiel and E.W. Valyocsik, U.S. Patent 4,388,285(1983).
27. B.M. Lok, T.R. Cannan and C.A. Messina, *Zeolites* 1983, 3, 252.
28. E.G. Derouane, S. Detremmerie, Z. Gabelica and N. Blom, *Appl. Catal.* 1981, 1, 201.
29. F.G. Dwyer and E.E. Jenkins, U.S. Patent 3,941,871(1976).
30. R.W. Grose and E.M. Flanigen, U.S. Patent 4,061,724(1977).
31. D.M. Bibby, N.B. Milestone and L.P. Aldridge, *Nature* 1979, 280, 664.
32. R.M. Barrer, *Adv. Chem. Ser.*, 1973, 121, 1.
33. D.W. Breck, *Adv. Chem. Ser.*, 1971, 101, 1.
34. W.M. Meier, "Molecular Sieves", Soc. Chem. Ind., London, 1968, p10.
35. W.M. Meier and D.H. Olson, *Adv. Chem. Ser.*, 1971, 101, 155.
36. R. Gramlich-Meier and W.M. Meier, *J.Solid State Chem.*, 1982, 44, 41.

37. R.M. Barrer, "Zeolites and Clay Minerals as Sorbents and Molecular Sieves", Academic Press, London, 1978.
38. R.M. Barrer and I.S. Kerr, *Trans. Farad. Soc.*, 1959, 55, 1915.
39. W.M. Meier and D.H. Olson, "Atlas of Zeolite Structure Types", published by the structure commission of the International Zeolite Association(1978).
40. G.T. Kokotailo, S.L. Lawton, D.H. Olson and W.M. Meier, *Nature* 1978, 272, 437.
41. G.Boxhoorn, O.Sudmeijer and P.H.G. van Kasteren, *J. Chem. Soc. Chem. Comm.*, 1983,1416
42. M. Liquornik and Y. Marcus, *J. Phys. Chem.*, 1968, 72, 2885.
43. M. Liquornik and Y. Marcus, *J. Phys. Chem.*, 1968, 72, 4704
44. H.S. Sherry, "Molecular Sieve Zeolites 1", (ed. E.M. Flanigen and L.B. Sand), 1971, p329.
45. R.M. Barrer, "Proc. 5th Int. Conf. on Zeolites", (ed. L.V.C. Rees), Naples, 1980, p273.
46. A. Cremers, "Molecular Sieve Zeolites 2", ACS Symposium series, 1977, 40, 179.
47. J.D. Sherman, "Zeolites: Science and Technology",NATO ASI Series (Edit.

F.R. Ribeiro, A.E. Rodrigues, L.D. Rollman, C. Naccache), Martinus Nijkoff, The Hague, 1984, p583.

48. R.P. Townsend, *Chem. Ind*, 1984,7, 246.
49. H.S. Sherry, *J. Phys. Chem*, 1966, 70, 1158.
50. W.J. Mortier, "Compilation of Extra Framework Sites in Zeolites", Butterworth Scientific Ltd., 1982.
51. P. Chu and F.G. Dwyer, "Intrazeolite Chemistry", (ed. G.D. Stucky and F.G. Dwyer), ACS Symposium Series, 218, 1983, p59.
52. R.M. Barrer and M.B. Makki, *Can. J. Chem*, 1964, 42, 1481.
53. R.M. Barrer, *Nature* 1949, 164, 112.
54. P.A. Jacobs, "Carboniogenic activity of Zeolites", Elsevier, Amsterdam, 1977.
55. F. Figueras, R. Gormez and M. Primet, *Adv. Chem. Ser*, 1973, 121, 480.
56. E.G. Derouane, "Zeolites: Science and Technology", NATO ASI Series (Ed. F.R. Ribeiro, A.E. Rodrigues, L.D. Rollman, C. Naccache), Martinus Nijkoff, The Hague, 1984, p347.
57. J.A. Rabo, R.D. Bezman and M.L. Poutsma, *Acta. Phys. Chem*, 1978, 24, 39.

58. R.M. Barrer, D.A. Harding and A. Sikand, *J. Chem. Soc., Faraday 1*, 1980, 76, 180.



## CHAPTER 2

# SYNTHESIS AND INITIAL CHARACTERISATION

In the first part of this chapter the techniques used in the initial characterisation of molecular sieves are reviewed. In the second part, details are given of the synthesis of the molecular sieves used in this work. Finally the results of synthesis and initial characterisation experiments are given and discussed.

### 2.1 Experimental Techniques

There are a large number of experimental techniques available to aid in the characterisation of a molecular sieve. As their use has been well documented elsewhere, only details of the techniques used in this work are given[1,2].

#### 2.1.1 X-ray Diffraction

X-ray powder diffraction is an universally used technique in the characterisation of molecular sieves. The strength of this technique lies in its ability to identify molecular sieves by a "finger-print" method. Each type of molecular sieve gives a different pattern, although there is some dependence on the Si/Al ratio, cation content and degree of hydration of a given sample. The diffraction pattern of a "new" sample can often be identified by comparison with diffraction patterns of known molecular sieves[3].

This technique may be used to assess the degree of crystallinity of a sample, for example, in following the crystallisation of a reaction. The reaction mixture is sampled at regular intervals. The solid is filtered from the mother liquor, dried and an XRD powder pattern obtained. As crystallisation proceeds, the % crystalline phase increases and the area of the XRD peaks increase

correspondingly.

X-ray diffraction powder patterns can provide information about the structure of the crystalline lattice of molecular sieves. There may however be some problems in the determination of the exact space group symmetry[4]. Meier developed a method to determine the appropriate model in order to obtain the space group symmetry of zeolites[5].

The space group symmetry of some molecular sieves has been reported to alter upon certain treatments such as calcination, ion-exchange, dealumination and hydration/dehydration. For example, the lattice parameters in Faujasite were found to vary with aluminium content[6] and the Chabazite framework undergoes distortion on dehydration which causes a change in the space group symmetry[7]. Particularly relevant to this work are the reported changes in the space group symmetry of ZSM-5 that occur upon calcination or ion exchange of the material[8]. The x-ray diffraction patterns of the as-made ZSM-5 are consistent with the framework having orthorhombic symmetry. A change to apparent monoclinic symmetry may be observed upon calcination and/or ion exchange.

The transformation from orthorhombic to monoclinic is recognised by several changes in the XRD patterns. There are changes in relative line intensities: the lines at  $7.9^\circ$  and  $8.9^\circ$   $2\theta$  increase in intensity whereas those at  $11.9^\circ$  and  $12.5^\circ$   $2\theta$  decrease in intensity. The doublet at  $14.7^\circ$   $2\theta$  merges to a singlet, the line at  $23.9^\circ$   $2\theta$  becomes less distinct, whereas, the doublet at  $23.2^\circ$   $2\theta$  becomes more apparent. There is also the appearance of a doublet in the line at  $24.4^\circ$   $2\theta$ .

The symmetry changes appear to be reversible and can occur at low temperatures. This suggests that they are not due to "reconstructive transformations" but that they result from changes in the chemical content of the channels and voids of the framework.

Variables such as cation content, organic species, Si/Al ratio and degree of hydration were all found to affect the change from apparent orthorhombic to monoclinic symmetry. The higher the Si/Al ratio the easier it was observed for the ZSM-5 framework to undergo the orthorhombic/monoclinic change. The x-ray diffraction pattern of a sample with a high sodium content was found to still exhibit an orthorhombic pattern after calcination. When the sodium content was lowered by ion-exchange the monoclinic pattern appeared. In other samples with lower sodium content only calcination of the samples was necessary to cause the x-ray diffraction patterns of these materials to display the monoclinic pattern. An x-ray diffraction pattern of a sample that had been recently calcined was obtained. It displayed an orthorhombic pattern. However, when an x-ray diffraction pattern of a sample that been equilibrated with atmospheric water vapour for 3 days was obtained, it was found to display a monoclinic pattern. Here, the water vapour had allowed a rearrangement of the cations in the channels of the ZSM-5 framework.

Bibby et al[9] observed that the spacing between two peaks at  $45^\circ$  and  $45.5^\circ$   $2\theta$  in XRD powder patterns varied with the aluminium content of the ZSM-5 zeolite. After calcination, they used the separation of these peaks to determine the aluminium content of their ZSM-5 samples.

Von Ballmoos and Meier[10] observed that the peaks of higher aluminium ZSM-5 samples were considerably broadened. They suggested that this was

due to the inhomogenous distribution of aluminium within the individual crystals.

In this work, XRD patterns were obtained with a Philips semi-automatic diffractometer. This consisted of a P1965/60 goniometer with a PW1730 stabilised x-ray generator which produced Cu  $K_{\alpha 12}$  radiation. The output was analysed with a PW1390 channel control unit and displayed on a PM8203 pen recorder. Samples carefully packed in diffraction slides were loaded by a PW1170 automatic sample changer. The scanning was controlled by a PW1394 motor control unit.

Before XRD patterns were obtained, samples were equilibrated with the atmospheric moisture. Approximately 1g of sample was gently ground in a mortar and pestle. This was then gently pressed into the diffraction slide with a glass microscope slide.

The conditions used for the majority of runs are shown below.

Scanspeed	$2^{\circ} \text{ min}^{-1}$
Time constant	2
Range	$1 \times 10^4$
Angles scanned	$40^{\circ}$ to $4^{\circ} 2\theta$

### 2.1.2 Thermal Analysis

In thermal analysis either the change in weight or the change in energy of the sample as a function of temperature is measured[11]. Two thermal analysis techniques were used: thermal gravimetric analysis and differential thermal analysis.

## **Thermal Gravimetric Analysis**

The technique of thermal gravimetric analysis(TGA) records the change in sample weight as a function of temperature. The sample is heated in a linear manner and its weight is recorded continuously along with its temperature. In the analysis of molecular sieves, the resultant weight-change versus temperature curve(referred to as the TG curve in this thesis) provides information on the %weight of water and/or organic along with the temperature at which desorption or decomposition occurred. It is also possible to observe dehydroxylation of samples at higher temperatures.

The shape of the TG curve is affected by a number of factors. These can be separated into two types: those that arise from variables in the thermobalance and those that result from variations in the sample used. These factors are listed below.

### **1. Instrumentation**

- Furnace
- Chart speed
- Furnace atmosphere
- Geometry of the furnace
- Sensitivity of the chart recorder
- Material of sample holder

### **2. Sample Characteristics**

- Amount of sample
- Particle size
- Heat of reaction
- Sample packing
- Nature of sample
- Thermal conductivity

Although some of the above factors are constant for any given thermobalance, care must be taken to ensure that as many of the other variables are kept as

constant as possible so that results from different runs may be meaningfully compared.

Two factors must be chosen with care: the heating rate and the chart speed. When more than one reaction is involved, the rate of heating may well determine whether or not the different reactions will be separated. In TGA a slower rate of heating is preferable although this has to be balanced against the time taken to obtain a run. This is because for any given temperature interval, the extent of decomposition is greater at a slow rate of heating than for a similar sample heated at a faster rate. A relatively slow chart speed is desirable as a fast chart speeds tend to minimize differing rates of weight-loss.

The TG analyses in this work were carried out using a Stanton Redcroft TG 770 thermal balance. Samples were equilibrated over saturated NaCl solution at 25°C ( $a_w = 0.753$ ). Between 5–10mg of sample was placed in a platinum sample holder. The apparatus was calibrated prior to each run.

The conditions used were:-

Chart speed	2mm/min
Heating rate	10°C/min
Atmosphere	air
Flow rate	4.5 ml/min
Temperature range	room temperature to 1000°C

The sample weight was recorded as a full scale deflection of 50% or 100% so that the %weight loss could be read directly from the recorder chart.

### **Differential Thermal Analysis**

In the technique of differential thermal analysis(DTA) the difference in

temperature between a substance and a reference material against either time or temperature is recorded. Changes in the sample that are not accompanied by weight losses – such as structure transitions and melting – can be observed with this technique.

The factors that effect the DTA curve are similar to those listed for the TG curve. However, variations in conditions have a more pronounced effect on the DTA curve. Again, the rate of heating must be carefully considered. In DTA, fast heating rates increase the sensitivity but unfortunately lower the resolution. A fast heating rate will cause the heat given out or taken in by the sample in a given time interval to increase because more reaction will take place in the same time interval and the displacement of the peak from the baseline will be greater.

Differential thermal analysis was carried out using a Stanton-Redcroft DTA 674. A sample weight of 50–100mg was required. The sample and reference (dry alumina,  $\text{Al}_2\text{O}_3$ ) were packed into dimpled sample holders until the dimples were just covered. To ensure samples were packed evenly each time, a machined loading die was used. Conditions used are given below.

Atmosphere	static air
Heating rate	10°C/min
Chart speed	2mm/min

Some samples, particularly salts, lose a large % of their weight. In order to avoid problems associated with this, it was necessary to mix the sample with an inert material. The inert material used was  $\text{Al}_2\text{O}_3$ . A side effect of this is to reduce the sensitivity.

### **2.1.3 X-ray Fluorescence**

The composition of the molecular sieves was determined by X-ray fluorescence analyses. Approximately 1g of calcined sample was further heated at 1100°C for 30min. 5.33 times the sample weight of lithium borate flux was added. This mixture was heated at 1100°C for 20min. Once cooled the mixture was reweighed and any weight loss made up by further addition of flux. The mixture was then heated strongly until "liquid" and poured into a graphite mould. The glass discs were cooled carefully to avoid cracking. Once cool, the discs were gently removed from the mould and labelled. The analysis of samples was carried out in the Department of Geology, University of Edinburgh. The instrument used was a Philips spectrometer(model PW1450). By this method the % weight of Na, Si, Al, K could be determined. The % weight of Li, Rb and Cs had to be inferred from the totals.

### **2.1.4 Microscopy**

Scanning electron microscopy can give information on the shape and size of the molecular sieve crystals. It may also give information about their surface. Gel material may be distinguished from crystalline particles.

The instrument used was a Cambridge Instruments type 604 stereoscan electron microscope. Samples were finely ground and spread on an aluminium peg before being coated with a thin film of gold.

An optical microscope(Vickers model M41 photoplan microscope) was also used.



## 2.1.5 pH Measurements

pH measurements were made with a Pye unicam 290 pH meter with a plastic bodied pH electrode (EIL, type 1180/200/UKP). The electrode was regularly standardised in a reference buffer solution (pH = 9.2). The pH meter was set to record measurements at 20°C.

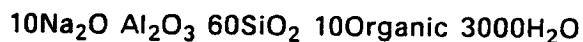
In order to measure the pH of a reaction mixture, a sample of  $\sim 8\text{cm}^3$  was taken and allowed to cool to room temperature in a stoppered glass sample bottle. Once cool the electrode was placed in the mixture. Some drift in the reading was observed initially but this stabilised relatively quickly and stable readings were obtained after 10–15 minutes. The electrode was thoroughly washed in distilled water between readings.

## 2.2 Synthesis

### 2.2.1 Synthesis of ZSM-5

As mentioned in section 1.1, ZSM-5 may be prepared using a variety of organic salt or bases. In this work, it was synthesised from reaction mixtures which contained either hexane-1,6-diol(DIOL) or piperazine(PIP)[12,13,14].

The stoichiometric ratios in molar oxides were:-



The source and purity of reagents are given below.

<u>Chemical</u>	<u>Purity</u>	<u>Source</u>
SiO <sub>2</sub> (Cab-o-sil,M5)		BDH
Al <sub>2</sub> O <sub>3</sub>	99%	BDH
Piperazine hexahydrate	98%	Aldrich
Hexane-1,6-diol	99%	Aldrich
NaOH	99%	Fisons Scientific

The same procedure was used to mix the reagents in all preparations of ZSM-5. The Cab-o-sil was thoroughly mixed with a large quantity of water in a 2 litre plastic beaker. The alumina was dissolved in hot aqueous sodium hydroxide solution. Once cool this solution was stirred into the Cab-o-sil/water mix. Finally the organic was stirred in and the rest of the water added. The total weight of reaction mixture was 750g.

The reaction mixtures were stirred at 300rpm in a 1 litre autoclave at 150°C for 42h. The resultant zeolite was filtered off from the solution and washed with a large quantity of water.

### **2.2.2 Pretreatment of ZSM-5**

In the as-synthesised form of ZSM-5 the channels are occupied by the organic molecules. In order to carry out experiments on these zeolites it is necessary to calcine them at a sufficiently high temperature to decompose the organic molecules. Preparations synthesised with hexane-1,6-diol were calcined at 450°C for 12h and then at 550°C for a further 12h. Those synthesised with piperazine were calcined at 550°C for 24h followed by 12h at 800°C.

Both zeolites were ion-exchanged with 1M NaCl solutions for 12h at 70°C. After ion-exchange the zeolites were washed until the washings were free of Cl<sup>-</sup> ions, as determined by addition of silver nitrate solution.

### **2.2.3 Synthesis of Silicalite**

Silicalite samples were synthesised from a number of different reaction mixtures. Some contained inorganic ions, other did not. The mole ratios of the reaction mixtures used are given below[15,16,17].

10PIP 2TPABr 20SiO<sub>2</sub> 1000H<sub>2</sub>O

3.5M<sub>2</sub>O 2TPABr 20SiO<sub>2</sub> 1000H<sub>2</sub>O

where M = Li, Na, K, Rb, Cs and TMA.

The source and purity of chemicals used, are listed below.

<u>Chemical</u>	<u>Purity</u>	<u>Source</u>
LiOH	99%	BDH
KOH	85%	Fisons
RbOH	98%	Fluka
CsOH.H <sub>2</sub> O	95%	Fluka
TMAOH	>98%	Fluka
TPABr	99%	Fluka

The water of hydration and/or solution was taken into account when determining the quantities of hydroxide and water required. The Cab-o-sil was mixed with a large quantity of water. The TPABr was dissolved in hot aqueous hydroxide solution or piperazine solution. The mixtures were stirred in 1 litre polypropene bottles at 150rpm at 95°C until synthesis was complete. Some evaporation of water occurred from the reaction mixture so small quantities of water were added daily to maintain the total. The mixtures could be sampled through holes cut in the tops of the bottles. Further description of the apparatus can be found in references 14 and 15. The total weight of reaction mixture used was 500g.

Completion of reaction was determined in one or more of a number of ways.

1. Sample appearance. As synthesis reaches completion, the solid separates from the solution leaving it clear.

2. XRD. Samples were separated from the mother liquor and an XRD pattern

obtained.

3. Microscopy. The sample was examined to observe whether or not any gel phase was still present.

4. pH Measurements. The pH of samples could be measured to determine whether synthesis had reached completion, as the pH of the liquor changes throughout the reaction[13,16,17].

#### **2.2.4 Pretreatment of Samples**

Samples that were synthesised from reaction mixtures that contained piperazine were generally calcined at 550°C for 18h and a further 1h at 800°C. Other samples were usually calcined at 550°C for 18h. Some samples were calcined at higher or lower temperatures than those given here. When this is the case, it is specified in the sample code (see Section 2.2.5.)

Hydrogen ion-exchange of the cation forms was carried out by stirring the molecular sieve with 0.1M HCl solution at room temperature for 18h. A number of such ion-exchanged samples were subsequently heated at elevated temperatures.

Soxhlet extraction of some calcined samples was carried out. This is method by which the samples may be continuously washed with fresh pure hot water. About 3g was placed in the thimble and continually washed with water for 3 days.

## 2.2.5 Terminology

An example of the way in which samples are named is given below.



This is a silicalite that was prepared with TPA and LiOH in the reaction mixture. These species are denoted in the name in square brackets. The parent silicalite was calcined at 400°C, as shown in the curved brackets. If the temperature used for calcination is that given in the procedure - 550°C - then this term may be omitted. The silicalite has been hydrogen ion-exchanged, the ion-exchange cation being unenclosed and prefixing the name. After ion-exchange the sample was further calcined at 800°C as given by the temperature in the curly brackets. Finally the preparation number is given as Px, where x is the preparation number, at the end of the name.

A list of all preparations of silicalite is given below.

<u>Preparation Number</u>	<u>Reaction Mixture</u>
1	3.5TMAOH 2TPABr 20SiO <sub>2</sub> 1000H <sub>2</sub> O
2-15	10PIP 2TPABr 20SiO <sub>2</sub> 1000H <sub>2</sub> O
16-17	3.5Na <sub>2</sub> O 2TPABr 20SiO <sub>2</sub> 1000H <sub>2</sub> O
18	3.5K <sub>2</sub> O 2TPABr 20SiO <sub>2</sub> 1000H <sub>2</sub> O
19	3.5Li <sub>2</sub> O 2TPABr 20SiO <sub>2</sub> 1000H <sub>2</sub> O
20	3.5Rb <sub>2</sub> O 2TPABr 20SiO <sub>2</sub> 1000H <sub>2</sub> O
21	3.5CsO <sub>2</sub> 2TPABr 20SiO <sub>2</sub> 1000H <sub>2</sub> O

## 2.3 Results

In this section the results from the synthesis and initial characterisation of samples are given and discussed.

### 2.3.1 ZSM-5

The XRF results are given below as moles of oxides.

	Na <sub>2</sub> O	Al <sub>2</sub> O <sub>3</sub>	SiO <sub>2</sub>
(H,Na)-[Na,PIP]-ZSM-5	0.12	1.00	31.5
Na-[Na,DIOL]-ZSM-5	0.95	1.00	35.8

The results for Na-[Na,DIOL]-ZSM-5 show that there is close to 1 Na<sup>+</sup> ion for every Al. The small deficiency of Na<sup>+</sup> ions needed to balance the charge on Al in the framework, must be compensated for by a small number of hydroxyl groups present - either on the surface or in the channels.

However in (H,Na)-[Na,PIP]-ZSM-5 there is a very low Na content. There is only one Na<sup>+</sup> ion present for 10 Al atoms. The zeolite is predominantly in the hydrogen form. It is interesting to note that this must also be true of the calcined material before sodium ion-exchange, and it is clear the hydrogens in this material are not readily ion-exchanged. They are presumably present as acid sites of the form



The reason for the difference between the two zeolites lies with the different organics used to synthesis the materials. Piperazine can carry a positive charge and so as the 'template' itself can balance the trivalent aluminium in the framework, the presence of Na<sup>+</sup> ions is not required. (It is well known that the use of amines in the synthesis of ZSM-5 reduces the alkali metal content of the as-synthesised material). Hexane-1,6-diol however cannot carry a positive charge and so cannot itself balance the charge on the trivalent atoms in the

framework and therefore in this case, Na<sup>+</sup> ions are required to ensure electrical-neutrality.

It is observed that the Si/Al ratio of both the samples is considerably higher than that of the reaction mixture.

The XRD patterns of [DIOL,Na]-ZSM-5 and [PIP,Na]-ZSM-5 and the corresponding ion-exchanged calcined forms are shown in Figure 2.1. The XRD patterns of the two zeolites are similar. Calcination results in an increase in intensity of the lines at lower angles. This has been recognised and reported by other workers[9]. It is due to the presence of organic material in the as-made samples which lowers the intensities of XRD lines at lower angles. It was observed that the changes in the intensities of the lines at 7.9° and 8.9° 2θ was more marked for [Na,PIP]-ZSM-5 than for [Na,DIOL]-ZSM-5. Araya and Lowe[18] noted this observation and commented that the peak intensities of the as-made materials were expected to differ because of different intracrystalline content but that it was surprising that those of the calcined materials showed such marked differences. All the XRD patterns shown in this figure exhibit predominantly orthorhombic patterns. No change to a monoclinic pattern was observed. As aforementioned, the XRD patterns of ZSM-5 samples with lower Si/Al ratios are not so prone to transformation to 'monoclinic' patterns on calcination as those with higher Si/Al ratios.

### **2.3.2 Silicalite**

#### **Reaction Times**

The times taken by the different mixtures to crystallise are given in Table 2.1 along with approximate crystal size. The presence of inorganic cations in

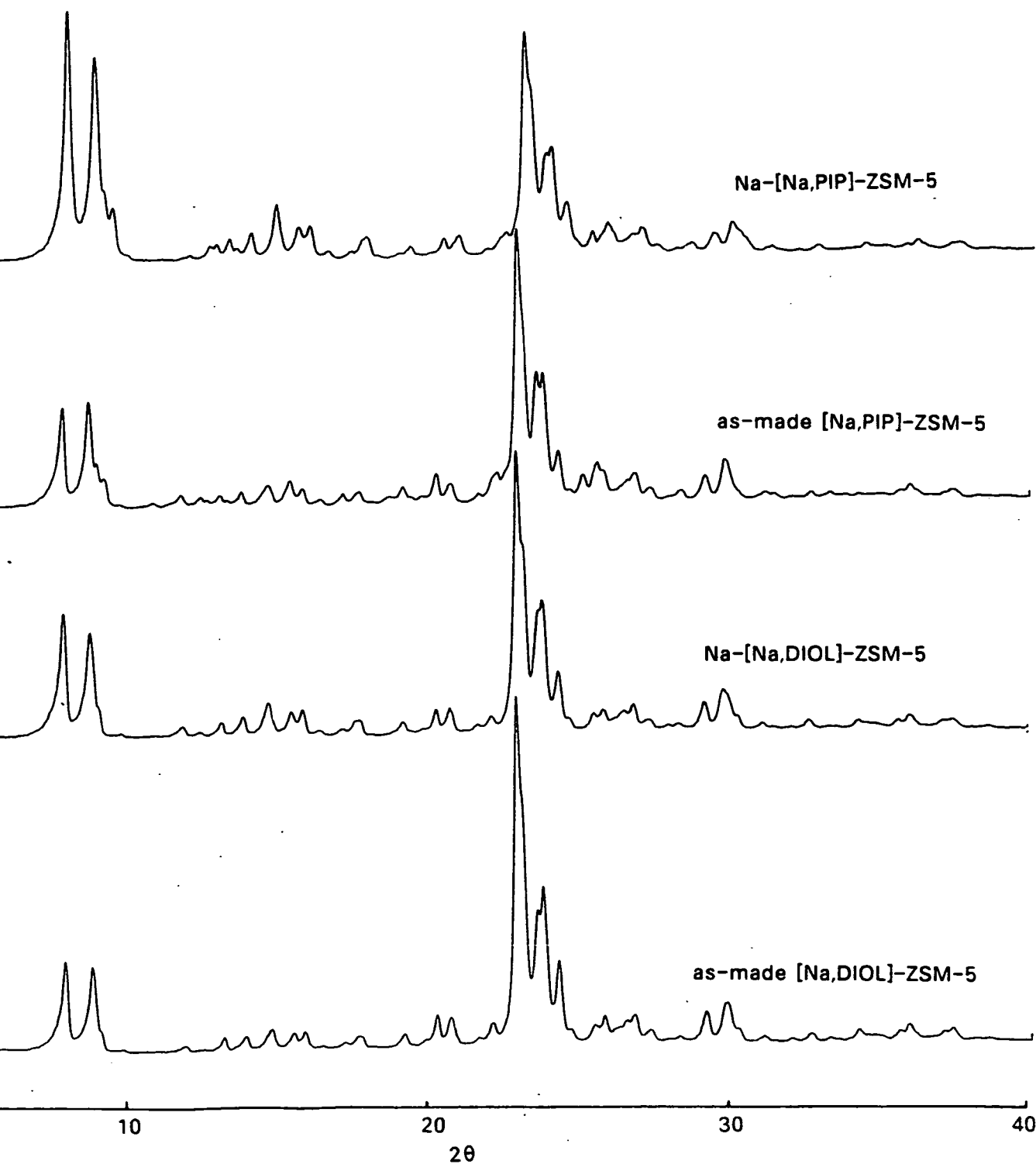


Figure 2.1 XRD patterns of ZSM-5.



Silicalite	reaction time	crystal size
Li- [Li, TPA] -SIL	14d	<1u
Na- [Na, TPA] -SIL	10d	1-2u
K- [K, TPA] -SIL	16d	1-2u
Rb- [Rb, TPA] -SIL	5 weeks	<1u
Cs- [Cs, TPA] -SIL	8 weeks	<1u
[TPA, PIP] -SIL	8 weeks	5-10u

Table 2.1                      Reaction times and crystal sizes of synthesis mixtures given in section 2.2.3.

the reaction mixture effects the crystallisation of the silicalite. The effect on reaction time in the cation reaction system, TPA<sup>+</sup>, M<sup>+</sup> is Na<sup>+</sup> > K<sup>+</sup> > Li<sup>+</sup> > Cs<sup>+</sup>. The presence of Cs<sup>+</sup> ions leaves the reaction time unaffected compared to the [TPA ,PIP] mix. The reaction mixture that contained TMAOH produced a very small yield, < 0.2g.

### **XRF results**

The results obtained from XRF for the various forms of pretreated silicalites are shown in Table 2.2. The Si/Al ratio is about 1000/1 for all the samples except Cs-[Cs,TPA]-SIL where it is 400/1. This is possibly due to impurities in the CsOH used.

It is noted that no Cs<sup>+</sup> ions are occluded in the framework during synthesis. Nastro et al.[19] investigated the synthesis of ZSM-5 from a mixture that contained Li<sup>+</sup>, Na<sup>+</sup>, K<sup>+</sup>, Rb<sup>+</sup> or Cs<sup>+</sup> ions. They postulated that neither Rb<sup>+</sup> or Cs<sup>+</sup> ions are present in the channels but rather are found only on the surface of the crystals. When Na<sup>+</sup> and K<sup>+</sup> ions were present in the reaction mixture, approximately four cations were incorporated per unit cell. In the Li<sup>+</sup> form there appears to be a greater number of cations present.

The results for the hydrogen ion-exchange forms of sodium and potassium show that the ion-exchange procedure does indeed remove all the cations from the framework. It is observed that soxhlet extraction removes a fraction but not all of the cations in the framework.

### **XRD patterns**

The XRD patterns of the calcined forms and pretreated forms of silicalite are shown in Figure 2.2. With one exception, the samples are crystalline and

	$SiO_2$	$Al_2O_3$	$Na_2O$	$K_2O$	$Li_2O$	$Rb_2O$	$Cs_2O$
Li- (Li, TPA) -SIL	88	0.05	0.10	-	11.8	-	-
max Li- (Li, TPA) -SIL	88	0.05	-	-	8.7	-	-
Na- (Na, TPA) -SIL	88	0.05	2.0	-	-	-	-
H- (Na, TPA) -SIL	88	0.08	-	-	-	-	-
K- (K, TPA) -SIL	88	0.04	-	2.1	-	-	-
H- (K, TPA) -SIL	88	0.04	-	-	-	-	-
Rb- (Rb, TPA) -SIL	88	0.58	-	-	-	5.8	-
Cs- (Cs, TPA) -SIL	88	0.12	1.78	-	-	-	-

Table 2.2

XRF results for a number of different silicalites.

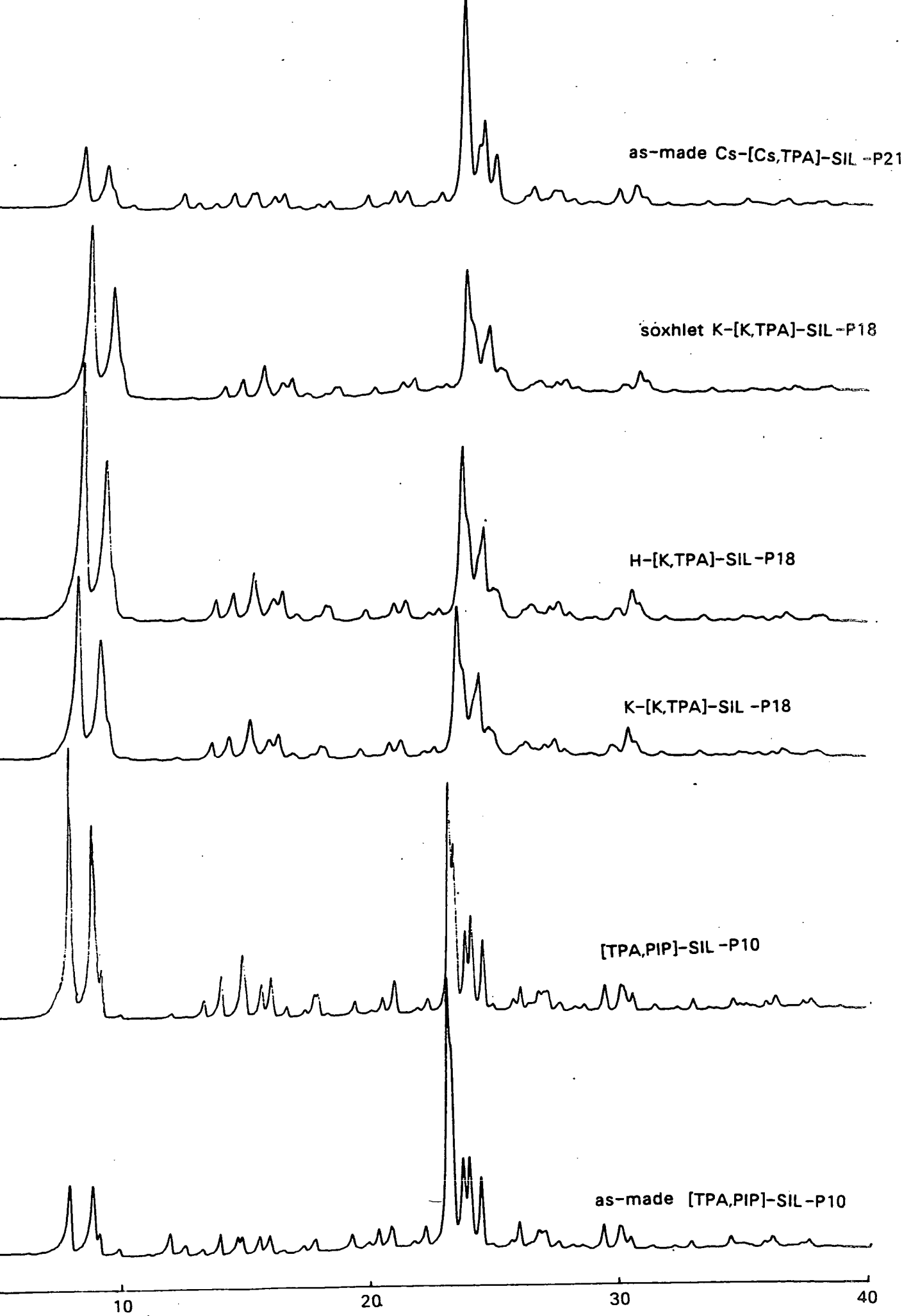
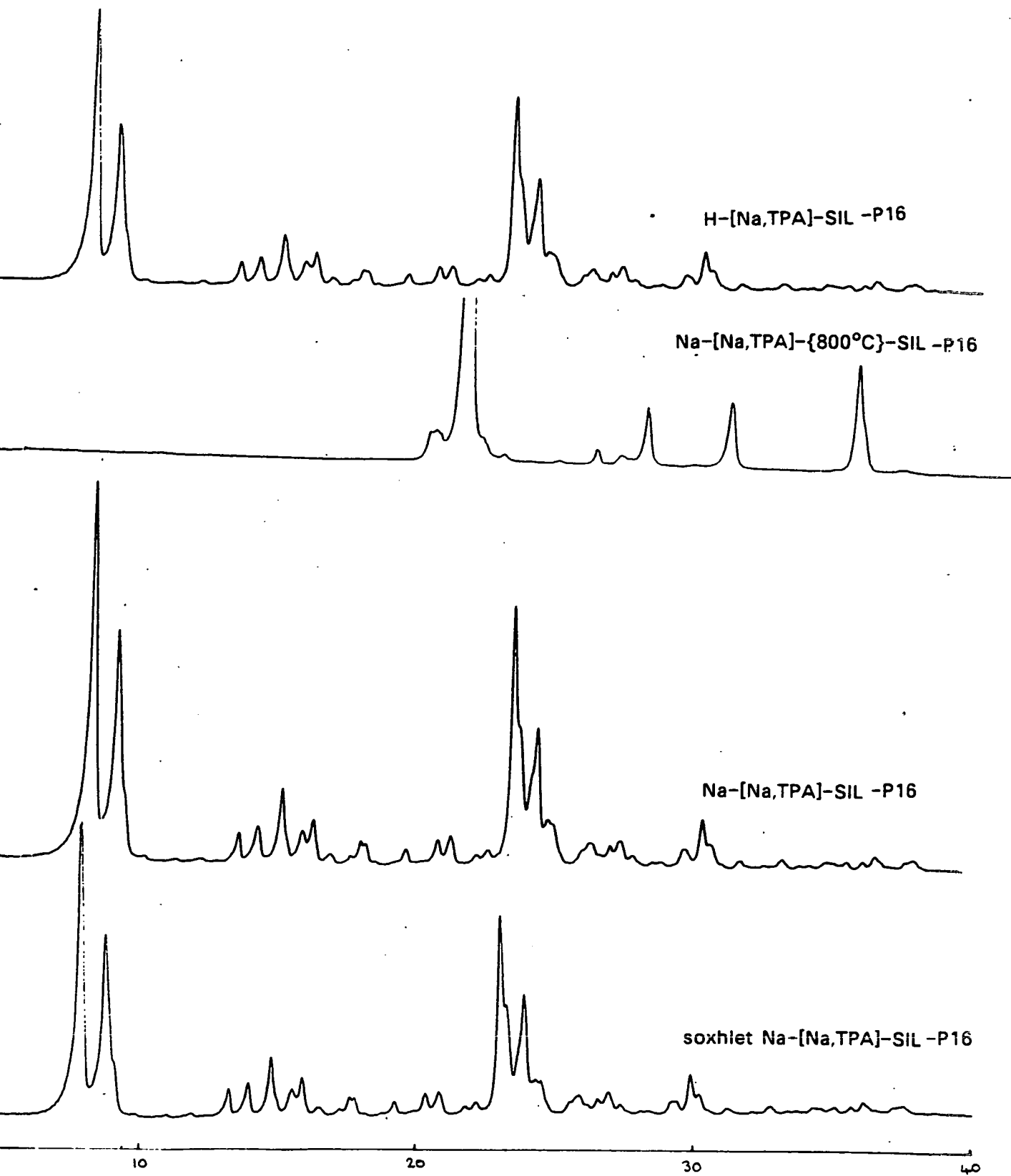


Figure 2.2 XRD patterns of silicalite-1.



20

Figure 2.2 Continued

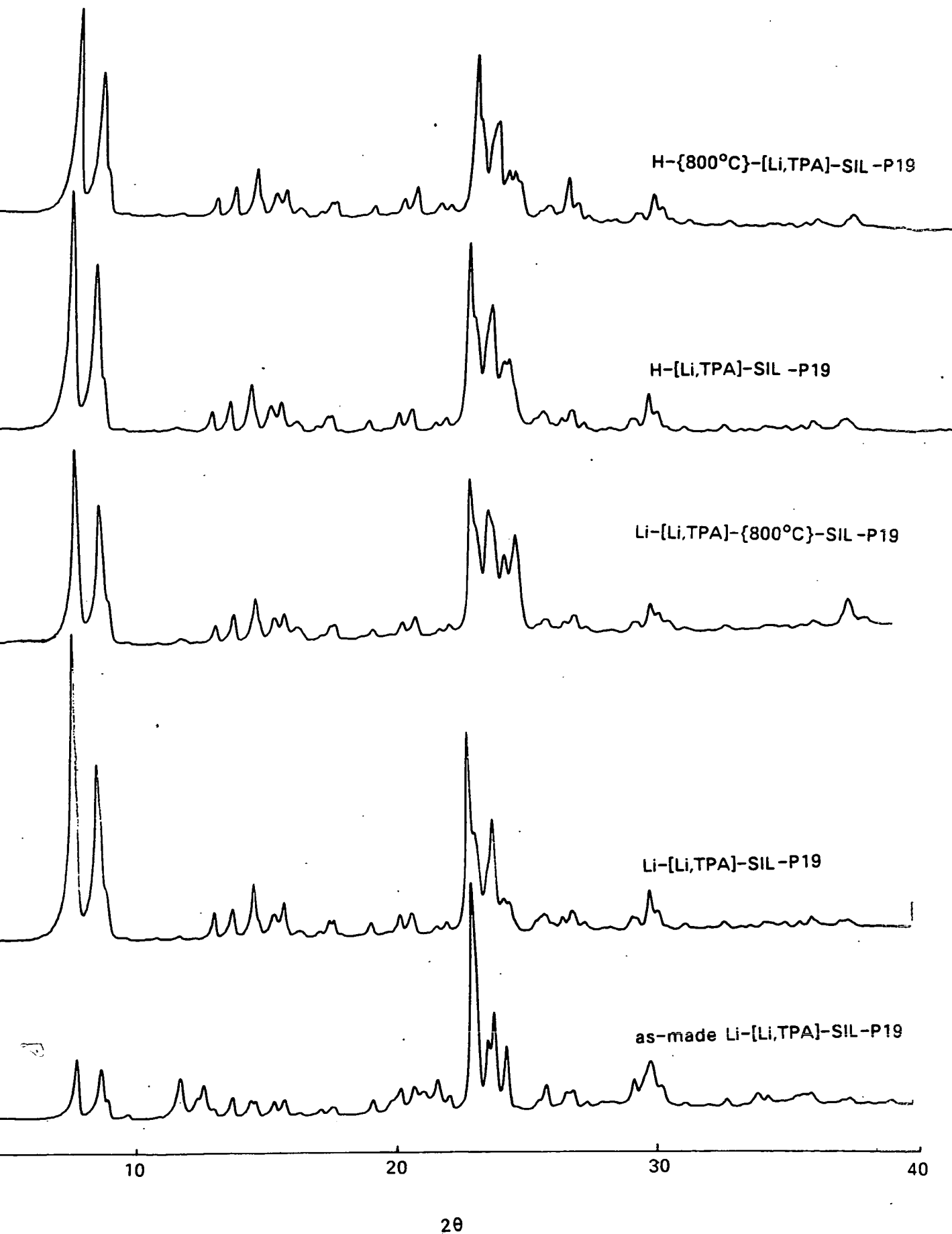


Figure 2.2 Continued

the only phase that is present is silicalite-1. The only exception is the Na-[Na,TPA]-SIL sample that was calcined at 800°C. This sample has undergone a solid phase transformation from silicalite to  $\alpha$ -cristobalite. Some of the XRD patterns are indicative of 'orthorhombic' symmetry, others of 'monoclinic' symmetry. The XRD pattern of the as-made Li-[Li,TPA]-SIL is orthorhombic but all the further treated forms of this silicalite display monoclinic XRD patterns. The most extreme case being that of the Li-[Li,TPA]-SIL sample calcined at 800°C. Treatment of the sodium and potassium silicalites change the XRD patterns from that of orthorhombic to a more monoclinic form. The transition though is not extreme as observed in the case of the lithium silicalite. This may be a result of there being a greater number of lithium cations present than there are sodium or potassium ions. This is also supported by the fact that the [TPA,PIP]-SIL displays a predominantly orthorhombic pattern even after calcination at 800°C.

In the next chapters the properties of these samples of ZSM-5 and silicalite are examined in some detail.

## 2.4 References

1. H. Lechert, "Zeolites: Science and Technology", NATO ASI series, (ed. F.R. Ribeiro, A.E. Rodrigues, L.D. Rollman, C. Naccache) Martinus Nijkoff, The Hague, 1984, p151.
2. D.W. Breck, "Zeolite Molecular Sieves", Wiley-Interscience, 1974.
3. R. von Ballmoos, "Collection of Simulated XRD powder patterns for zeolites", Butterworth and Co. Ltd, 1984.
4. K.F. Fischer, "Molecular Sieves", ACS 121 (ed. W.M. Meier and J.B. Uytterhoeven), Washington DC, 1973, p31.
5. W.M. Meier, "Molecular Sieves", ACS 121 (ed. W.M. Meier and J.B. Uytterhoeven), Washington DC, 1973, p39.
6. E. Dempsey, G.H. Kuehl and D.H. Olson, *J. Phys. Chem.*, 1969, 73, 387.
7. J.V. Smith, *Acta Crystallogr.*, 1962, 15, 835.
8. E.L. Wu, S.L. Lawton, D.H. Olson, A.C. Rohrman, Jr. and G.T. Kokotailo, *J. Phys. Chem.*, 1979, 83, 2777.
9. D.M. Bibby, L.P. Aldridge and N.B. Milestone, *J. Catal.*, 1981, 72, 373.
10. R. von Ballmoos and W.M. Meier, *Nature*, 1981, 289, 782.
11. W. W. Wendland, "Thermal Methods of Analysis", John Wiley and Sons,



New York, 1974.

12. J.L. Casci, B.M. Lowe and T.V. Whittam, European Patent Application 42, 225(1981).
13. J.L. Casci and B.M. Lowe, *Zeolites*, 1986, 6, 111.
14. J.L. Casci, Ph.D Thesis, Edinburgh, 1981.
15. S.G. Fegan, Ph.D Thesis, Edinburgh, 1985.
16. S.G. Fegan and B.M. Lowe, *J. Chem. Soc., Faraday Trans.1*, 1986, 82, 801.
17. S.G. Fegan and B.M. Lowe, *J. Chem. Soc., Faraday Trans.1*, 1986, 82, 785.
18. A. Araya and B.M. Lowe, *Zeolites*, 1986, 6, 111.
19. A. Nastro, Z. Gablica, P. Bodart and J.B. Nagy, "Catalysis on the Energy Scene", (ed. S. Kaliaguine and A. May), Elsevier Science Publications, Amsterdam, 1984, p131.

# CHAPTER 3

## SORPTION PROPERTIES OF SILICALITE

### 3.1 Introduction

The ability of molecular sieves to sorb molecules has been recognised for many years. For sorption to occur the molecular sieves must be activated by heating preferably in vacuo and the sorbate molecules must be of the correct size and shape to pass through the windows into the channel system beyond. The dimensions of the windows and channels are comparable to those of small molecules, consequently whether they are sorbed or excluded from the channel system is very sensitive to their dimensions and shape[1]. Because the channels are small the electric fields produced at the channel walls often overlap. The electric field experienced by a molecule in the channels of a molecular sieve will vary from one type of molecular sieve to another and from sorbate to sorbate. So unlike carbon molecular sieves, zeolite molecular sieves may preferentially sorb or exclude a molecule on account of its electronic nature. The regularity of the molecular sieve pore system simplifies the vapour phase sorption behaviour, which in consequence is not as complicated as that of more irregular amorphous solids[2].

In molecular sieves the specific surface area is of little physical importance. In general, any attempts to compare the "monolayer equivalent" with the experimental sorption capacity of molecular sieves have been unconvincing[3]. What is of concern is the pore volume available to sorbate molecules. It is found in many instances that molecular sieves obey the Gurvitsch Rule[4]. This rule embodies the principle that the maximum amounts of different sorbates taken up by a given molecular sieve will concur if the uptake is expressed as a volume of liquid. There are a number of exceptions to this rule. However,



these deviations usually occur with larger molecules that give lower volumes and so may well be a consequence of difficulties in packing of the molecules in the channels.

The exclusion of some molecules from the channels of a molecular sieve may be caused by size and or shape differences between the pore diameter of the molecular sieve and those of the sorbate molecule. Several attempts have been made to correlate the crystallographic pore dimensions with those of the sorbate molecules. The use of the equilibrium diameter of a sorbate molecule based on the Van der Waals radii is in many cases unsatisfactory since it is observed that some molecules that are easily sorbed have an equilibrium diameter larger than the pore diameter of the molecular sieve. This is a consequence of the change in dimensions which occurs as the atoms in the framework and the sorbate vibrate. As a result it is usually the kinetic diameter of a molecule that is of interest rather than the equilibrium diameter[5]. The kinetic diameter of a molecule can be found from the Lennard-Jones potential[6]; this potential is described by equation 3.1.

$$\phi(r) = 4\epsilon[(\sigma/r)^{12} - (\sigma/r)^6] \quad (3.1)$$

where the parameters  $\sigma$  and  $\epsilon$  are constants which are characteristic of a given molecule. At large separations the attractive component  $(\sigma/r)^6$  is the dominant term. As the separations of the two molecules decreases the repulsive component  $(\sigma/r)^{12}$  becomes dominant. When the potential  $\phi(r)$  equals zero, the diameter  $r$  is equal to  $\sigma$ , where  $\sigma$  is known as the kinetic diameter. The kinetic diameter is the intermolecular distance of closest approach for two molecules colliding with zero kinetic energy. The maximum energy of attraction occurs at  $r_{\min}$  where  $r_{\min} = 2^{1/6}\sigma$  and is known as the equilibrium diameter of the molecule.

Sorption of molecules of known dimensions provides a simple and routine method for the characterisation of the pore diameters of molecular sieves. The effective pore diameter of a molecular sieve can be estimated from the largest molecule that can be sorbed under a given set of conditions.

### 3.2 Sorption Isotherms

The uptake  $U$  of a sorbate by a molecular sieve is dependent on the pressure of the sorbate,  $p$ , the temperature  $T$ , and the nature of the sorbate and molecular sieve.

$$U = f(p, T, \text{sorbate}, \text{molecular sieve}) \quad (3.2)$$

For a given molecular sieve and sorbate the uptake of sorbate depends only on the pressure and temperature. Hence at constant temperature,

$$U = f(p)_T \quad (3.3)$$

It follows from this that the isotherm of a given sorbate and sieve may be obtained experimentally by measurement of the uptake of a sorbate at different pressures. The experimental isotherms are difficult to predict from a theoretical model. Many attempts have been made but they have only had limited success. The equation that has perhaps the widest application is that of the Langmuir Isotherm[7].

#### 3.2.1 The Langmuir Isotherm

The Langmuir isotherm equation was originally applied to the physical sorption of molecules in a monolayer on a surface. This gave rise to a rectangular shaped isotherm known as the type I isotherm[8]. The Langmuir equation may be written as

$$\theta = U/U_{\max} = Kp/(1+Kp) \quad (3.4)$$

where  $K$  is in effect the equilibrium constant for the sorption process. A large  $K$  is indicative of strong sorption.  $U$  is the uptake of sorbate at a given

pressure  $p$ , and  $U_{\max}$  is the maximum uptake at equilibrium. Equation (3.4) may be rewritten as in equation 3.5.

$$p/U = 1/U_{\max}K + p/U_{\max} \quad (3.5)$$

If an isotherm follows the Langmuir equation a plot of  $p/U$  against  $p$  should yield a straight line of slope  $1/U_{\max}$  and an intercept of  $1/KU_{\max}$ . At very low pressures  $Kp$  is very small compared to unity and so at low pressures equation (3.5) simplifies to

$$U = U_{\max}Kp \quad (3.6)$$

This implies that the uptake is proportional to pressure and consequently at low pressures the isotherm is a straight line passing through the origin, and Henry's Law is obeyed. At high pressures the value of  $Kp$  is much greater than unity and the equation reduces to

$$U = U_{\max} \quad (3.7)$$

The isotherm rises steeply at low pressures and at high pressures becomes horizontal. The model on which the Langmuir equation is based involves a number of assumptions.

1. There are a number of fixed sorption sites with sorption of one molecule per site. In a molecular sieve the number of sites that may be occupied depends on the size of the sorbate molecule. So this assumption of one molecule/sorption site cannot be applied to molecular sieves.

2. The surface is energetically homogeneous. This is blatantly untrue for many molecular sieves, particularly more aluminous zeolites.

3. The sorbate molecules do not interact with each other. There is considerable evidence that many sorbates in the channels of a molecular sieve interact quite strongly with each other[9].

Why then do molecular sieve isotherms often agree with the Langmuir

equation? In many cases this is a result of compensation between the heat of sorption and the entropy of sorption. As the heat of sorption increases due to favourable sorbate-sorbate interactions the entropy may decrease due to increased packing of the sorbate molecules in the channels. This may result in compensation between the heat of sorption and the thermal entropy of sorption. Consequently many molecular sieves obey the Langmuir isotherm in an empirical fashion rather than by strict agreement with the Langmuir model.

Deviation from the Langmuir isotherm may itself be a source of information[10]. The slope  $dp/dU$  close to the origin reflects the strength of sorbate-molecular sieve interactions. If the molecular sieve is energetically heterogeneous then the sorbate uptake at low pressures will be higher than predicted from the Langmuir isotherm equation. As a result  $p/U$  will be smaller and deviations at low pressures will be observed on the Langmuir plot. The existence of sorbate-sorbate interactions will lead to deviations from the Langmuir plot at higher pressures.

### 3.2.2 Sorption Isotherm with Sorbate-sorbate Interactions

If the sorbate molecules are considered to be sorbed on specific sites and sorbate-sorbate interactions to occur only between nearest neighbours then the potential energy of the sorbate will be increased by an amount  $w$  for every pair of nearest neighbours[11]. This quantity  $w$  may be positive(repulsive) or negative(attractive). The isotherm is described by equation 3.8.

$$p = k[\theta/1-\theta]\exp[(2w/kT)/\theta] \quad (3.8)$$

If this isotherm is followed, a plot of  $\log p$  against  $\log(\theta/1-\theta)$  should yield a straight line if  $w = 0$ . If  $w$  is negative, that is the sorbate-sorbate interactions are attractive and the isotherm is s-shaped.

This isotherm like the Langmuir isotherm is only an approximation since it assumes that the sorption is localised. It does however show that strong sorbate-sorbate interactions can result in s-shape isotherms.

### 3.3 Energetics of Sorption

From the thermodynamic equation

$$\Delta G = \Delta H - T\Delta S \quad (3.9)$$

it is clear that if sorption is to occur then  $(\Delta H - T\Delta S) < 0$  and  $\Delta H < T\Delta S$ .  $\Delta S$  is always negative as sorption results in greater order, so  $\Delta H$  must also be negative.

There are three terms that are used to describe to the heat of sorption[12].

1. The isothermal integral heat of sorption. This is used to refer to the total heat involved in the sorption process from zero uptake of sorbate to some final uptake.
2. The differential heat of sorption  $\Delta H^s$ . This is the change in integral heat of sorption with a change in sorbate uptake. It may be defined as

$$\Delta H^s = (H^s - H^g) \quad (3.10)$$

where  $H^g$  is the molar enthalpy of the sorbate in the gas phase and  $H^s$  is the partial molar enthalpy of the sorbate. The differential heat of sorption is found to be dependent on pressure, temperature and uptake.

3. The isosteric heat of sorption  $q_{st}$ . This is related to the differential heat of sorption as shown in equation 3.11.

$$-q_{st} = \Delta H^s \quad (3.11)$$

The isosteric heat of sorption can be found experimentally from a set of isotherms at different temperatures with use of the Clausius-Clapeyron

equation.

The Clapeyron equation is

$$dp/dT = q_{st}/T\Delta V \quad (3.12)$$

where  $\Delta V$  is the difference between the volume of one mole gas and one mole sorbate. If it is assumed that the gas behaves in an ideal manner, the volume of the gas may be replaced by  $RT/p$ . Now, since the volume of gas is very much greater than the volume of the sorbed species,  $\Delta V$  may be replaced by  $RT/p$ . These approximations lead to the Clausius-Clapeyron equation

$$d\ln p/dT = -q_{st}/RT^2 \quad (3.13)$$

If it is also assumed that  $\Delta H$  does not vary with temperature then the isosteric heat of sorption may be determined from a plot of  $\log p$  against  $1/T$  for a given uptake of sorbate. Experimentally the pressure required to give a certain uptake is measured at different temperatures. This is repeated at a variety of uptakes so that the variation of  $q_{st}$  with  $U$  is obtained.

The differential entropy of sorption may also be obtained from these plots of  $\log p$  against  $1/T$ . The differential molar entropy  $S_a$  of sorption is given by

$$S_a = S_g + RT\ln(p^0/p) + \Delta H^s/T \quad (3.14)$$

where  $S_g$  is the molar entropy of the gas at standard pressure,  $p^0$ , and temperature,  $T$ . Since  $S_g$  is known and  $\Delta H^s$  can be measured,  $S_a$  can be determined for various uptakes, and a plot of  $S_a$  against  $U$  can be obtained.

### 3.4 Interactions

The sorption of a gas by a molecular sieve occurs as a consequence of net attraction between the molecules of the gas and the atoms or ions of the molecular sieve framework. The forces of interaction which result in sorption always involve dispersion forces, which are attractive in nature, and short range



repulsive forces[13]. If the molecular sieve and/or the sorbate is polar, electrostatic forces will also be involved. The London dispersion forces are a result of rapid fluctuations in electron density within each atom. A fluctuation in one atom induces an electrical moment in a near neighbour and so attraction occurs between the two atoms. The interaction  $\phi_D$  between two atoms separated by a distance,  $r$ , that results from this force can be defined as

$$\phi_D = -C_1 r^{-6} \quad (3.15)$$

where  $C_1$  is the dispersion coefficient associated with the induced dipole-induced dipole interactions.

The short-range repulsive forces lead to an interaction  $\phi_R$  that can be expressed as

$$\phi_R = B r^{-12} \quad (3.16)$$

If the molecular sieve is polar an electric field of strength  $F$  results, which induces a dipole in the sorbate molecule. This dipole depends on the polarisability,  $\alpha$  of the sorbate molecule. The interaction  $\phi_p$  that results from this is:-

$$\phi_p = -0.5\alpha^2 F \quad (3.17)$$

Now if the sorbate molecule possesses a permanent dipole moment  $\mu$  it will interact with the field produced by the molecular sieve. This interaction is:-

$$\phi_{F\mu} = -F\mu \cos \tau \quad (3.18)$$

where  $\tau$  is the angle between the field and the axis of the dipole.

If the sorbate has a quadrupole moment this will also interact with the field gradient  $F$  of the electric field to produce a further contribution  $\phi_{FQ}$  to the total interaction energy.

A sorbate molecule may interact with another sorbate molecule. This

interaction will contribute to the total interaction energy. The sorbate-sorbate interaction is denoted  $\phi_{SP}$ . This term tends to zero at low uptakes and includes dispersion, and close-range repulsion energies as well as dipole-dipole and dipole-induced dipole energies for polar molecules.

The total interaction energy  $\phi$  can be expressed as

$$\phi = \phi_D + \phi_R + \phi_P + \phi_{F\mu} + \phi_{FQ} + \phi_{SP} \quad (3.19)$$

The dispersion and close-range repulsive interactions are present in every case. The magnitude of the dispersion interactions may vary considerably as they depend on the nature of the sorbate. The dispersion energy of interaction may be of considerable importance when the dipole and quadrupole interactions are not involved. This energy of interaction increases with an increase in the number of atoms in a sorbate molecule[14]. It also increases the more tightly packed the sorbate molecules are in the channels of the molecular sieve. The polarization energy term will only be present if the molecular sieve is heteropolar. This arises with aluminous zeolites since their structure contains negative aluminium ions and positive cations. This term will be of negligible importance in the case of silicalite where the framework consists of near homopolar  $\text{SiO}_2$  groups. As a result of the very small electric field in the silicalite channels the terms resulting from dipole and quadrupole moments will also be negligible.

### 3.5 Diffusion

The diffusion of sorbate molecules into molecular sieves can be very complex. In small crystals there are several possible rate-controlling steps[10]

1. Intracrystalline diffusion

2. Intercrystalline diffusion and flow

### 3. Transmission through surface skins

4. Evolution of heat on sorption and cooling on desorption which results in time-dependent drifts in sorption equilibria.

5. A combination of any of the above.

If intracrystalline diffusion is the rate-controlling step then the sorption rate curves may be used to obtain the differential intrinsic diffusivities  $D$ [15]. If the particles are approximately spherical of radius  $r_0$  the diffusion equation at constant pressure is

$$U_t/U_{\max} = 6/r_0(Dt/\pi)^{1/2} \quad (3.20)$$

where  $U_t$  is the amount sorbed after time  $t$ ,  $U_{\max}$  is the amount sorbed at equilibrium, and  $D$  is the diffusion coefficient. This equation only applies for small amounts of sorption, in the region of which the sorption isotherm follows Henry's Law. Thus a plot of  $U_t/U_{\max}$  against  $t^{1/2}$  is linear and has a slope of  $6/r_0(D/\pi)$ . At larger times,  $t$ , the equation takes the form:

$$U_t/U_{\max} = 1 - 6/\pi^2 \exp(-D\pi^2 t/r_0^2) \quad (3.21)$$

so a plot of  $\ln(1-U_t/U_{\max})$  against  $t$  approaches a straight line of slope  $-D\pi^2/r_0^2$ .

The diameter of the sorbate is an important parameter that governs diffusion into a molecular sieve. But other features of the sorbate must also be considered. For example, in the diffusion of  $n$ -alkanes into zeolite 5A: diffusion decreases and its activation energy increase as the carbon number of the alkane increases[16]. However diffusion of  $n$ -alkanes into zeolite T, though still dependent on chain length, is more complex[17]. A phenomenon termed the "window effect" was observed.  $N$ -dodecane was measured to diffuse several orders of magnitude faster than  $n$ -octane. The length of the  $n$ -dodecane

molecule is such that both ends of the molecule just extend through the 8-membered rings that enclose the cavities. Such a configuration aids the diffusion of this molecule through the internal network of cages. N-octane on the other hand is just too long to fit entirely into the erionite cage but too small to extend both ends through the ring openings. So it must assume a configuration with one end of the molecule extending through the 8-membered ring. This configuration hinders the diffusion of n-octane compared to the diffusion of n-dodecane.

### **3.6 Factors affecting Sorption**

The sorption properties of a molecular sieve will depend on a number of factors some of which have already been mentioned. In this section the influence of these factors on the sorption behaviour of molecular sieves is examined in more detail.

#### **3.6.1 Effect of Cations**

The nature of cations in the molecular sieve channels may have a pronounced effect on its sorption behaviour. Both the position and the size of the cation are important, and both may cause considerable hindrance to the movement of the sorbate molecules. Cations affect the sorption behaviour in several ways:

1. They restrict the diffusion of molecules in the channels.
2. They reduce the space in the channels that is available to sorbate molecules. This effect is more pronounced in less open structures.
3. If the cations are located near the pore openings they may restrict entry to the channels. As a result molecules that are sorbed in the absence of

cations may be excluded from the framework if sufficiently large cations are present[18].

Experimentally it has been observed that the isosteric heat of sorption for a given sorbate varies with the type of cation present. This effect is highlighted by the sorption of  $N_2$  at 178K by zeolite X containing different alkali cations[19]. It is found that the highest initial heat of sorption is given by zeolite Li-X followed by Na-X with the lowest value being given by K-X. This shows that Li-X has the highest affinity for  $N_2$  at low uptakes. However K-X shows very little change in the heat of sorption with uptake indicating the surface is fairly homogeneous whereas Li-X shows a considerable reduction in  $q_{st}$  with uptake. Another example is the sorption of Ar,  $O_2$ ,  $N_2$ , NO, and CO by Li, Na, K and Cs mordenites[20]. The value of  $q_{st}$  was found to increase in the order Cs-mordenite < K-mordenite < Na-mordenite < Li-mordenite irrespective of the sorbate gas. The heat of sorption of CO by H-mordenites was measured and  $q_{st}$  found to fall between those for Na-mordenite and K-mordenite. The hydrogen atom is bonded to just one oxygen atom to produce an acidic silanol group which has a strong covalent character in H-mordenite. A low electric field results even though the cation is very small[21].

If the sorbate is polar very strong interactions between the cation and the sorbate may arise. This may lead to sorption that is more chemical than physical in nature. An example of this is the sorption of water in some zeolites. Ideally, the water exists in the zeolite as discrete molecules and may be easily removed by heating. In practice the water molecules form hydration complexes with the cations and interact electrostatically with the framework oxygens. In addition the cation may polarize the water molecule sufficiently that it splits into an hydroxyl group which bonds to the cation and a proton

which attaches itself to a framework oxygen[22].

### 3.6.2 Si/Al Ratio

An increase in the Si/Al ratio of the framework has two effects,

1. The amount of framework aluminium present is reduced; the surface becomes less heterogeneous, and the electric field strength is lowered.
2. The number of cations needed to balance the charge on the framework aluminium is reduced and so the number of cations present is reduced.

Chen has shown for a series of dealuminized H-mordenites that the water sorbed decreases linearly with decreasing aluminium content[23]. This was attributed to the increase in the number of nearly homopolar -Si-O-Si- bonds and a corresponding decrease in the number of hydrophilic aluminium tetrahedra and associated cation centres. Nakamoto and Takahashi also showed that the uptake of methanol by H-ZSM-5 varies with Si/Al ratio[24]. These workers also measured the uptake of hydrocarbons by samples of H-ZSM-5 with different Si/Al ratios. They found that there was little variation except that at the highest aluminium content the uptake of hydrocarbon actually increased. They suggest that this arose from the polarisation of the hydrocarbon molecules by the electrostatic field of the proton.

### 3.6.3 Nature Of Sorbate

The most important features of the sorbate are its size and shape relative to those of the molecular sieve channels. Another important factor is the presence or absence of a dipole moment, as already explained, this can affect the strength of its interaction with both the cation and lattice. The ability of the molecule to flex and assume the most favourable configuration to pass through the pores and pack into the channel system also has a significant effect. A

molecule that is very rigid and inflexible may be excluded from the channel system whereas a molecule of similar size but with a greater flexibility may be sorbed.

#### **3.6.4 Temperature**

The higher the temperature the lower the uptake of sorbate at a given pressure and the less rectangular the sorption isotherms. The higher the temperature the faster the diffusion of molecules into the molecular sieve provided the diffusion is intracrystalline controlled. However, in many cases the maximum sorption capacity expressed as a volume/weight basis decreases as the temperature increases. This is probably a consequence of the decrease in density of the sorbate with increasing temperature.

#### **3.6.5 Structure**

The channel network may be 1-D, 2-D or 3-D, and this affects the sorption behaviour of a molecular sieve. The presence of large cages in the framework such as in zeolite X will lead to liquid bead-like clusters of sorbate. The presence of stacking faults in the framework may reduce the sorption capacity and the diffusion rate of the sorbates[10].

#### **3.6.6 Salt Occlusion**

The occlusion of salt molecules in the channel system can considerably alter the sorption properties of a molecular sieve[25]. This will be discussed in some detail in chapter 4.

### **3.7 ZSM-5 and Silicalite-1**

Although the sorption behaviour of ZSM-5 and silicalite has been the subject of several studies there still remains much to be done. In particular, there are discrepancies between the the results obtained for sorption of

unsaturated hydrocarbons and more polar molecules. The sorption of these molecules appears to be very sensitive to the exact nature of the internal surface. The discrepancies are probably due to differences in synthesis conditions, pretreatment, and the actual technique and conditions used to observe the sorption properties.

Several workers have shown that the uptake of water by a series of ZSM-5 zeolites which contain different amounts of aluminium, varies linearly with the aluminium content extrapolating back to  $\sim 0$  for the end member, silicalite[23,24,26]. The very small uptake of water at zero aluminium content reported by references [26] and [24] is postulated to be due to sorption on the surface hydroxyl groups. Chen found that the slopes of the plots of uptake against  $\text{wt}\% \text{Al}_2\text{O}_3$  corresponds to the sorption of  $4\text{H}_2\text{O}$  to each aluminium in the framework[23]. At  $p/p_0=0.05$ , Chen found that a ZSM-5 zeolite with 2% alumina did not sorb water. However Olson et al[26] measured the uptake of water with  $p/p_0=0.006$  and  $T = 0^\circ\text{C}$  and found that there was still a small uptake at zero alumina content. At 2% alumina the uptake of water was measured to be  $0.0010\text{gg}^{-1}$ . No mention is made of how long the samples were equilibrated nor were desorption curves reported. Nakamoto and Takahashi also showed that the uptake of methanol varied linearly with  $\text{wt}\% \text{alumina}$ . The uptake extrapolated to  $0.0045\text{gg}^{-1}$  at zero alumina again with  $P/P_0 = 0.006$  and  $T = 100^\circ\text{C}$ . The uptakes of benzene and n-heptane remained constant with Si/Al ratio. Other workers report that at higher  $p/p_0$  and at ambient temperatures that the uptakes of water and methanol are no longer insignificant[27,28,29]. Flanigen and workers report that the uptake of water by silicalite is  $0.047\text{gg}^{-1}$  at room temperature, and an uptake of  $0.153\text{gg}^{-1}$  for methanol is quoted[27]. Qin-Hua Xu and workers reported that the uptake of water by a H-ZSM-5 series was  $>0.10\text{gg}^{-1}$  at  $p/p_0 = 0.6$ [28]. These results



show that silicalite and ZSM-5 may in fact sorb methanol to an extent which completely fills the pores and that a substantial uptake of water by silicalite can take place (~25% of the pore volume). Hill and Seddon[29] measured the sorption isotherms of water on H-ZSM-5 using two different procedures. In the first, the sample was allowed to equilibrate with a given pressure of water vapour, and once a steady reading was obtained the uptake of sorbate at that pressure was noted. The sample was then evacuated and heated to remove all the sorbed water before determining the next point on the sorption isotherm. In the second method the sample was contacted with increasing pressures of water vapour and the uptakes at each pressure were noted. The first method produced sorption isotherms that were lower than those obtained by the second method. Also hysteresis was noted in the isotherms of water obtained by the second method. No explanations for the hysteresis were provided.

Though silicalite and ZSM-5 with little aluminium in the framework may be considered hydrophobic with respect to more aluminous zeolites, they still sorb polar molecules to a significant extent and so it may be more correct to call them organophilic rather than hydrophobic.

Doelle et al reported the sorption of methanol, dimethyl ether, and benzene was reversible on three different ZSM-5 zeolites[30]. However they found that the sorption of ethene, propene and cyclohexane to be irreversible. They also found rather pronounced differences in sorption behaviour between the three different zeolites. These had been synthesised and pretreated in different ways, and the results emphasise the importance of procedures used to prepare the zeolite.

The variation of heat of sorption with sorbate uptake has been measured

for a number of different sorbates[33,35,31,32,28]. Lechert found the isosteric heat of sorption, particularly for the sorption of polar molecules on ZSM-5 showed an initial decrease with uptake of sorbate. It was found that the heat of sorption is highest for alkanes, least for water and intermediate for sorbates such as aromatics.

The variation of heat of sorption,  $q_{st}$ , for n-hexane, toluene and benzene has been investigated by Stach and workers[27]. The sorption of n-hexane shows an increase in  $q_{st}$  with uptake of sorbate. The  $q_{st}$  of toluene and benzene remains constant for low uptakes except at very low uptakes where a sharp decrease in  $q_{st}$  was observed. This suggests that there were a few hydrophilic sites in the channels.

Olson and workers observed hysteresis at intermediate pressures in the isotherm of p-xylene on ZSM-5 at 70°C[34]. This, they postulated, was due to the packing of the p-xylene molecules in the channel system. However, when Pope studied the sorption properties of p-xylene in ZSM-5 he found that hysteresis only occurred in samples of ZSM-5 with low Si/Al ratios.[33].

### **3.8 Hydroxylation of Silica**

Silicalite is a silica polymorph and its internal surface is essentially an array of Si-O-Si linkages. Consequently, the sorption behaviour of silicalite might be expected to show some similarities to that of other silica materials. One of the notable characteristics of silica surfaces is that their water sorption behaviour is very sensitive to the pretreatment of the sample[36]. This sensitivity to pretreatment procedures is due to varying degrees of hydroxylation of the surface. The degree of hydroxylation may range from 0 to 100%. Dehydroxylation of the surface occurs when the sample is heated at

temperatures above 350°C. At a temperature of 1100°C the surface is almost completely dehydroxylated. At intermediate temperatures partial dehydroxylation of the surface results. However, on contact with water vapour rehydroxylation of the surface occurs.

Sorption of water on a completely hydroxylated surface involves hydrogen bonding which is essentially physical in nature. The isotherm is found to be reversible in the low pressure range. However, this is not so with the sorption of water on a partially dehydroxylated silica surface. When such a sample is contacted with water vapour, the water molecules are initially physically sorbed via hydrogen bonds to the remaining hydroxyl groups. The water molecules may then chemically interact with the surface with the formation of further silanol groups. As hydroxylation involves a rearrangement of atoms, and the formation of new chemical bonds it is an activated process and so its rate is slow. Because of the limited rate of this process it will occur slowly during the determination of the isotherm and hence low pressure hysteresis results. It is observed that this low pressure hysteresis does not occur unless the desorption run commences from some  $p/p^{\circ}$  value which is above a threshold value required to initiate hydroxylation. The sorption/desorption isotherm of water on a silica that has been heated at 1000°C shows hysteresis over an extensive pressure range[37].

Sorption of methanol on such surfaces may also result in low pressure hysteresis as the methanol can chemically interact with a siloxane bond to form a methoxyl group and a hydroxyl group. As methanol is a less polar molecule than water the rate of methoxylation will be slower and possibly less extensive than that of hydroxylation.

### 3.9 Hydroxylation of ZSM-5/Silicalite

There are two aspects concerning hydroxyl groups that will affect subsequent use of samples.

1. The presence of internal hydroxyl groups remaining after calcination and pretreatment processes.
2. The formation of hydroxyl or methoxyl groups as a result of exposure to water or methanol.

A number of different workers have reported evidence that supports the presence of internal hydroxyl groups[38,39,40,41,42]. Boxhoorn et al using an application of high resolution  $^{29}\text{Si}$  solid-state n.m.r. showed that around 18% of silicon atoms were hydroxylated in their as-made material[38]. However, after calcination the majority of these groups had been eliminated. They postulate that the highly strained 4-membered rings are not fully closed in the as-made material. Complete closure of these rings only occurs after heating at elevated temperatures.

On the contrary, Wooley et al still observed hydroxyl groups even after removal of the organic template and cations[39]. These conflicting results may be due to differences in preparation and pretreatment of the materials. Scholle and workers examined the sorption of water by H-ZSM-5 using magic angle spinning proton n.m.r.[40]. They observed two different sorption sites in H-ZSM-5 which they assigned to the interaction of water with Si-O-Al sites and SiOH sites. They also observed that the spectra obtained for water/silicalite were more complicated than those for water/H-ZSM-5. No attempt to account for this was made. Von Ballmoos and Meier investigated the  $^{18}\text{O}$ -exchange kinetics between ZSM-5 and water[43]. The conclusions they

reached were that not only Si-O-Al but also Si-O-Si bridges were cleaved under relatively mild conditions in the presence of water. They commented, *"This throws new light on the reactivity of Si-O-Si bridging oxygens which (at least in zeolite chemistry) have all too frequently been assumed to be inert"*. It was suggested that defects in the framework may be of consequence in determining the mobility of framework atoms. Ison and Gorte examined the sorption of water and methanol on H-ZSM-5 by use of several techniques: TPD, TGA, and transmission I.R.[44]. They discovered that the sorbed water could not be completely desorbed even by evacuation at room temperature. Under these conditions they observed strong interaction between the water molecules and the cations. The water could only be completely desorbed by raising the temperature to 373K under vacuum. The methanol molecules were found to interact with the hydrogen cation but not with the silanol groups. The results showed that methanol was sorbed in two different environments. A strongly bound state that corresponded to one methanol sorbed per cation and a more loosely sorbed methanol. As with sorption of water these workers found that the sorption of methanol at room temperature was not completely reversible. They expressed surprise at the irreversible nature of both methanol and water sorption in light of the low heats of sorption found for both sorbates. They suggested that the irreversible nature of these sorbates may be due to the coupling of desorption and diffusion processes.

Although Ison and Gorte did not observe interaction of methanol with silanol groups, Barrer presented evidence for the chemisorption of methanol by zeolite-X, using I.R absorption spectroscopy[22]. A strongly bonded form of methanol was detected. Barrer suggested that the methanol had reacted with silanol groups present, to give a  $-\text{Si}-\text{O}-\text{CH}_3$  group.

### **3.10 EXPERIMENTAL TECHNIQUES**

Many techniques have been developed over the years to characterise the sorption properties of sorbents. These techniques have been the subject of a number of reviews and so only the techniques used in this work are discussed here[45]. These techniques are the Cahn Electrobalance and the "multi-equilibration" technique. The latter was developed particularly for this work. The techniques differ considerably in their methods of operation and they possess different advantages and disadvantages.

#### **3.10.1 Cahn R.G. Automatic Electrobalance**

A microbalance such as the Cahn R.G. Automatic Electrobalance can measure very small changes in sample weight. As a result with auxiliary apparatus to control sample temperature and sorbate pressure it is possible to measure the uptake of sorbate with time at a given temperature and pressure or the uptake of sorbate at different pressures or temperatures. From such measurements diffusion data, isotherms and heats of sorption can be obtained.

The Cahn Electrobalance employs the null-balance principle which allows it to measure rapid changes in sample weight very quickly and accurately. The electrobalance and its components are shown schematically in Figure 3.1. A change in sample weight deflects the beam. This moves the attached flag which alters the amount of light that reaches the phototube and so the phototube current is altered. This is amplified in a two-stage servo amplifier and applied to the coil attached to the beam. The coil is in a magnetic field. The current in the coil acts like a d.c. motor and exerts a force on the beam that restores it to its original position. This process occurs so quickly that the beam appears to be stationary. In fact it is in dynamic equilibrium. The force that restores the beam to its original position is proportional to the current in

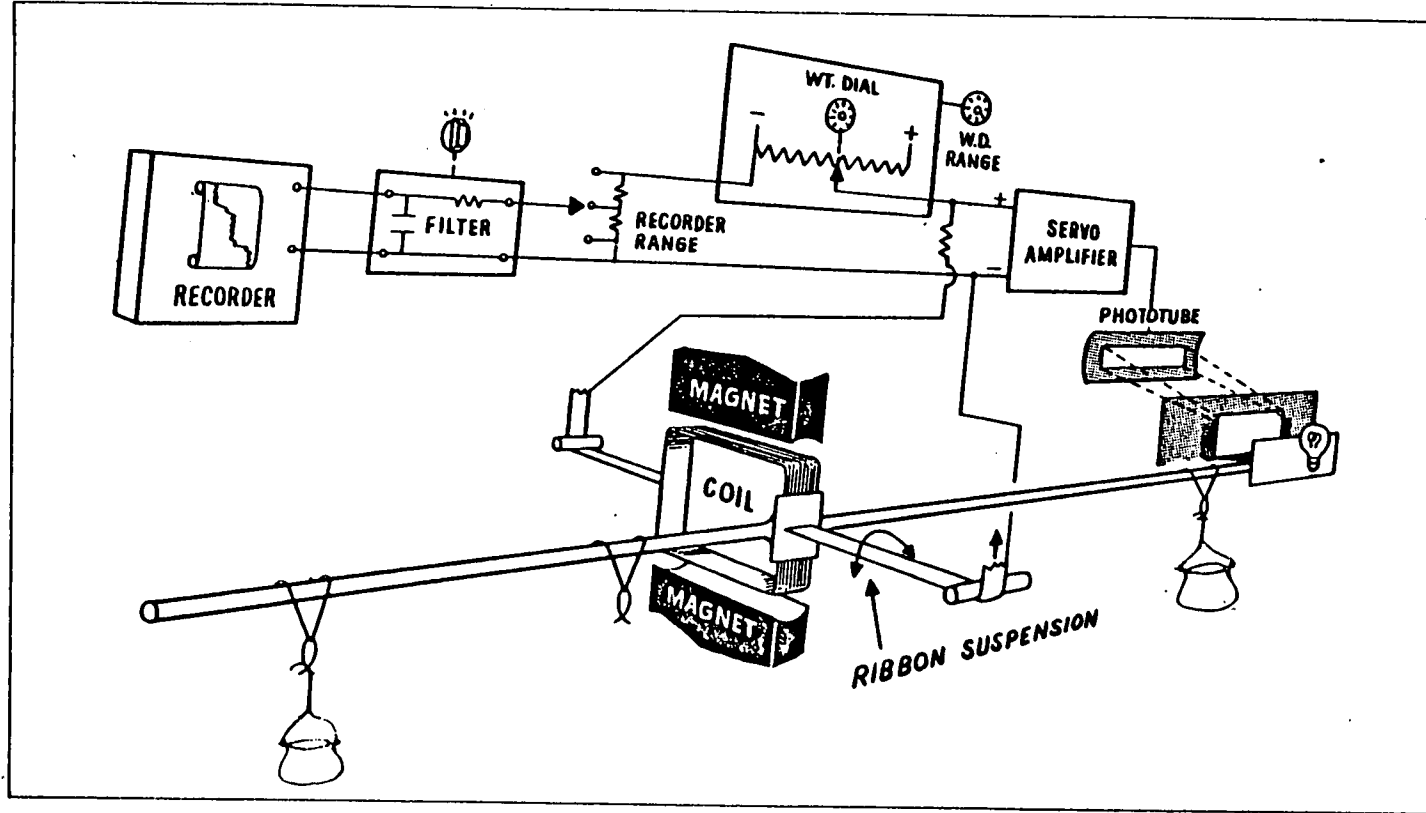


Figure 3.1

Schematic diagram of the Cahn electrobalance.

the coil which in turn is proportional to the change in sample weight.

To display this on a recorder it is necessary to subtract a known proportion of the weight voltage and apply only the excess to the recorder. The mass dial on the potentiometer shows in milligrams the amount of voltage that has been subtracted.

The sorbate handling section of the apparatus was constructed of Pyrex glassware. The taps used were Springham greaseless taps. The use of grease was avoided where possible as it might interact with the sorbates. Where needed, either silicon or Apiezon "T" grease was used. To ensure the sorbates were pure they were frozen-pumped-thawed several times prior to use. A McLeod gauge was used to detect small pressures and vacuum tests were carried out prior to sorption runs.

The system was evacuated using two mercury diffusion pumps backed with two oil rotary pumps. The vacuum achieved was in the region of  $10^{-5}$  Torr. The hangdown tube that contained the sample was outgassed using a close fitting non-inductively wound furnace. The temperature was controlled by a thermocouple linked to a Stanton Redcroft linear temperature programmer which incorporated a Eurotherm control unit. The sample temperature was measured using another thermocouple placed down a silica pocket in the hangdown tube in a position level with the sample bucket. This thermocouple was connected to a digital voltmeter.

Sample temperatures above 30°C were controlled with the furnace. Lower sample temperature were controlled using water or slush baths of the appropriate temperature.



## Procedure

The balance was calibrated according to the manufacturers instructions using standardised calibration weights. The sample weights were 50mg or less with substitution weights of 20mg or 30mg. The weight of the sample was determined by summation of the mass dial value, the recorder reading and the substitution weight.

An approximate weight of sample was added and the system outgassed at 550°C for 18h. After this time, the sample was cooled. In the case of ZSM-5 some increase in sample weight was noted as the sample cooled. This weight gain was not wholly reproducible between runs. However, with silicalite samples, only small weight gains were observed and these were reproducible between runs. It was noted that even the cooling of a glass sample from 550°C to room temperature showed a small increase in sample weight. The small reproducible weight gains were thought to be the result of temperature gradients in the hangdown sample tube at elevated temperatures.

To obtain sorption isotherms a small amount of sorbate was allowed into the sorption chamber and after equilibration had been reached, the pressure was noted from the mercury manometer and a further amount of sorbate was admitted into the sorption chamber. Desorption was measured in a similar way except sorbate was removed from the sorption chamber.

Kinetic measurements could be obtained as the weight is continuously recorded. However it was difficult to obtain kinetic measurements within the first sixty seconds as the sorbate entering the chamber caused large fluctuations in the recorder measurements.

After each run the sample was regenerated by initial evacuation at 550°C and then contacted with 400 Torr of oxygen before evacuation again at 550°C for 18h.

The reproducibility of this apparatus was found by repeated runs. The uptake of n-heptane and of methanol by silicalite samples are shown in figures 3.2 and 3.3. The reproducibility was excellent when the sorbate was n-heptane, the error being less than  $0.003\text{gg}^{-1}$ . The sorption of methanol was less reproducible than n-heptane, this is because methanol is more sensitive to the previous history of the sample. The greatest error in the methanol isotherms is in the low pressure region, but at higher pressures the error is much lower approaching that found for the sorption of n-heptane.

### **3.10.2 The Multi-equilibration Method**

For much of the work in this project, it was necessary to have a technique that could measure the uptakes of different sorbates by many samples at one time quickly, simply and in a reproducible manner. There are few such techniques described in the literature[46,47]. One technique is described by Landolt in a paper entitled "Method for rapid determination of sorption properties of zeolites". In this technique the molecular sieve is activated externally from the sorption system and then transferred rapidly to the sorption chamber. The sorption chamber is connected by a common manifold and solenoid valve to a gas line which contains the sorbates. The sorbate pressure is controlled by means of a mercury manostat which operates the solenoid valve via a relay. The whole system is evacuated by a rotary vacuum oil pump. The sorbate uptakes of eleven samples can be determined at one time.

For the present work Landolt's method was further simplified by elimination

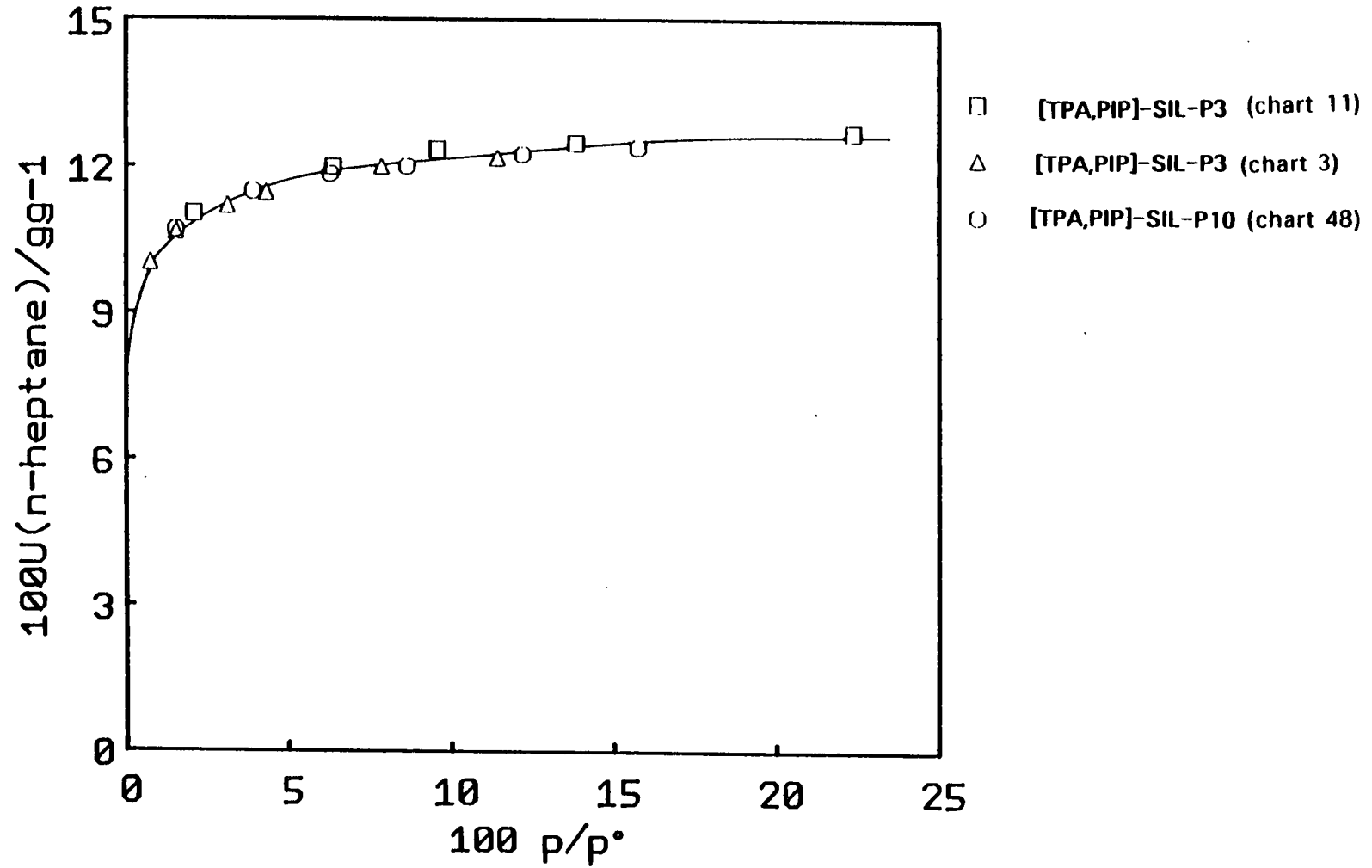


Figure 3.2

The reproducibility of sorption results  
obtained with the Cahn electrobalance.

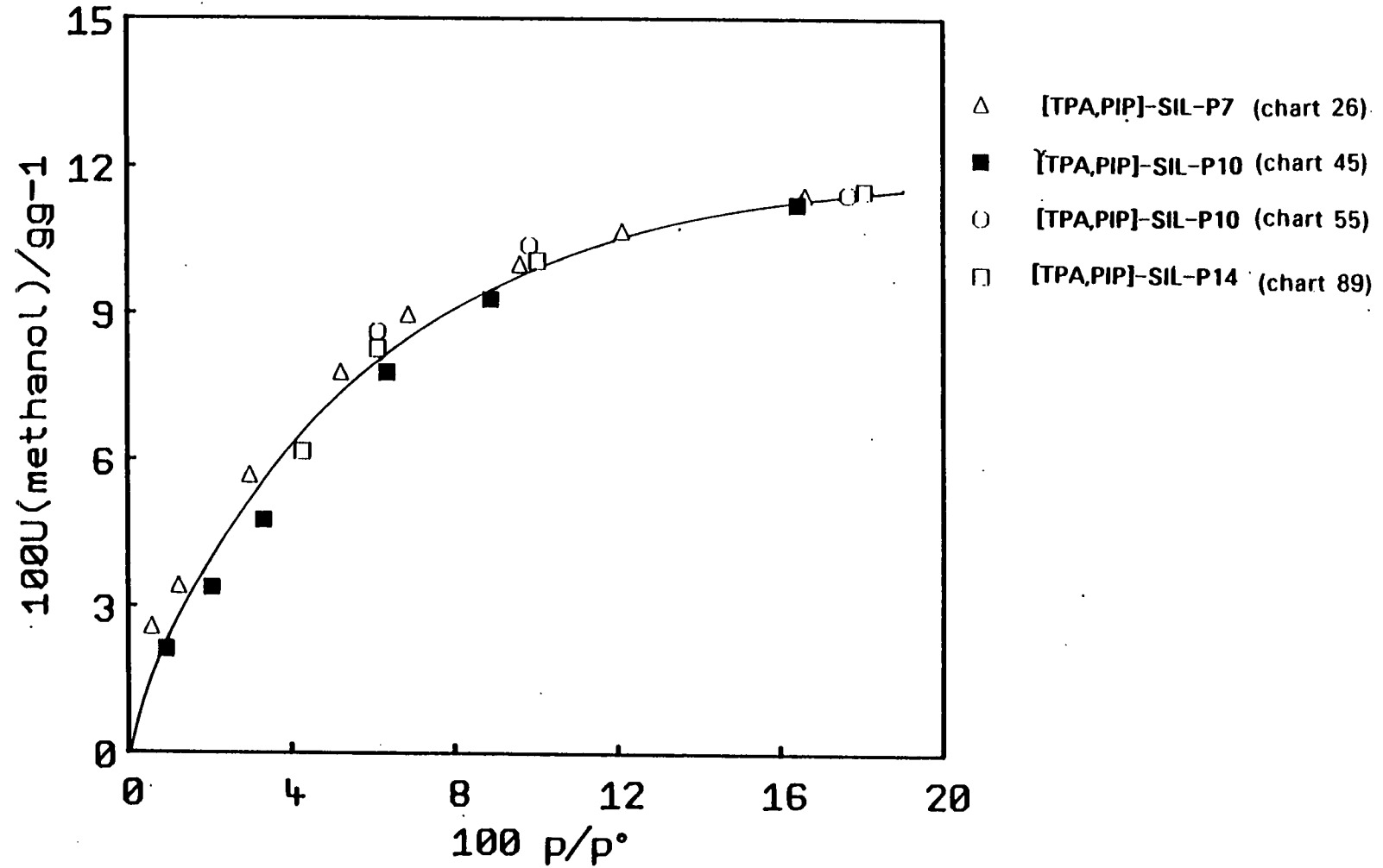


Figure 3.3

The reproducibility of the Cahn electrobalance.  
 The uptakes of methanol by [TPA,PIP]-SIL with sorbate  
 pressure in four separate runs.

of the circuit that controls the sorbate pressure and gas line. A dry-seal 6" Jencon desiccator was used as the sorption chamber. Small glass sample tubes with plastic caps contained the molecular sieve. The sample tubes were placed in a metal block as shown in Figure 3.4. The block was designed to enable the upper part to be replaced while the samples were still in the furnace. This is to help to prevent the samples from "picking up" water from the atmosphere. This method is referred to as the "multi-equilibration" technique.

The sorbate is added to the system as liquid in a glass dish. The desiccator is evacuated by a rotary oil pump. Sorption occurs from the gas phase provided the sorbate has a high enough vapour pressure and sufficient time is allowed for equilibration.

In order to prevent capillary condensation which occurs when  $p/p^0$  of the sample approaches unity, another liquid with a kinetic diameter greater than the pores of the molecular sieve and with a low vapour pressure is added to the sorbate to lower the pressure. The liquid used was dibutylphthalate(DBP).

Generally, capacity sorption is reached in molecular sieves at low values of  $p/p_0$  so the sorbate uptake measured by this technique is the maximum uptake at that temperature. The procedure followed was:

1. The sample tubes and tops were weighed.
2. 0.2g-0.5g of molecular sieve was added to each sample tube.
3. The sample tubes were placed in the bottom half of a metal block and heated to remove any water or gases sorbed from the atmosphere.

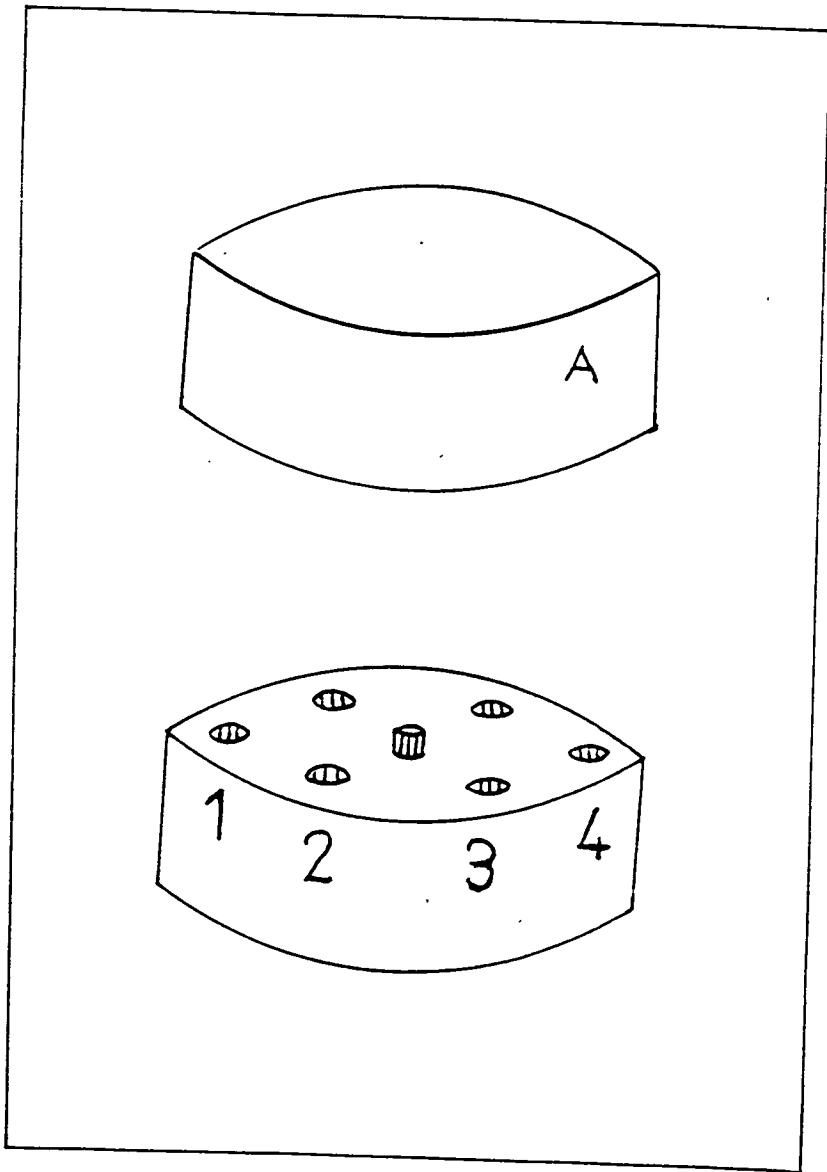


Figure 3.4 Stainless steel blocks used in the "multi-equilibration" technique.

4. The top of the block was replaced and the block allowed to cool in vacuo over  $P_2O_5$ .
5. Once cool the tops of the sample tubes were quickly replaced and immediately reweighed to find the weight of dry molecular sieve in each tube.
6. The sorption mixture of  $2\text{cm}^3$  sorbate and  $2\text{cm}^3$  DBP in a glass dish was placed in the desiccator with the sample tubes and evacuated. The desiccator was then placed in a water bath at  $25^\circ\text{C}$  and left to equilibrate. The time taken to reach equilibrium varied from 16h to 3d, depending on the vapour pressure of the sorbate under investigation.
7. After equilibration the tops of the sample tubes were replaced. The sample tubes were then reweighed to obtain the weight of sorbate taken up.

The uptake of sorbate,  $U$ , is expressed in grams sorbed per gram of dry molecular sieve.

If water is used as the sorbate, the procedure is a little different. The water is added as a saturated salt solution in contact with excess solid salt. In this case the pressure of the sorbate is known and so if desired a complete isotherm could be obtained.

In order to ascertain the accuracy and the reproducibility of the "multi-equilibration" technique several preliminary experiments were carried out. In these experiments zeolite 5A was used because it was available commercially in a large batch and its sorption properties have been widely

reported in the literature[48,49,50,51].

Five samples of zeolite A were dried and the weight of anhydrous zeolite was found as described in the procedure. The weights of these five samples were then monitored over a period of time. During this time, the tops of two samples were left on, the tops of two others were removed and in one case the top was removed and replaced prior to weighing.

The tubes were weighed after 3, 5, 15 and 70 minutes and finally after 20h. The results are shown in Table 3.1. The weight gained by zeolite 5A in the sample tubes with the tops on is very small. This is so even when the top was removed for a short time prior to weighing. However, substantial weight gain was observed when the tops were removed. This is the result of sorption of gases and water vapour from the atmosphere.

In another experiment the weight of anhydrous zeolite 5A was found as before. The samples were placed in two desiccators (one with  $P_2O_5$ , one without) and left for 18h before they were weighed again. The results are shown in Tables 3.2 and 3.3 and demonstrated that the presence of  $P_2O_5$  in the desiccator helps to prevent the sorption of water by the zeolite. It is observed that the more zeolite there is in a sample tube, the lower the weight gain per gram of anhydrous zeolite.

In another experiment, samples of anhydrous zeolite 5A were equilibrated over  $2\text{cm}^3$  DBP. The weight gained by the zeolite sample in g and  $\text{gg}^{-1}$  are shown in Table 3.4. There is little more weight gained than when the samples were equilibrated over  $P_2O_5$ . Probably hydrophobic molecular sieves such as ZSM-5 and silicalite would gain even less weight.



time	weight gain/g				
	TOPS ON		TOPS REMOVED		TOP REMOVED/REPLACED
wt. zeolite	0.2727	0.3418	0.3538	0.2387	0.3012
3min	0.0002	0.0001	0.0005	0.0004	0.0001
5min	0.0002	0.0003	0.0007	0.0005	0.0001
15min	0.0004	0.0005	0.0013	0.0009	0.0003
70min	0.0009	0.0010	0.0038	0.0031	0.0008
20h	0.0015	0.0018	0.0344	0.0304	0.0012

Table 3.1 Weight gains by samples of zeolite 5A in sample tubes.

wt. zeolite/g	wt. gain/g	wt. gain/gg-1
0.1803	0.0010	0.0053
0.2213	0.0008	0.0038
0.2435	0.0011	0.0045
0.2853	0.0008	0.0034
0.2735	0.0012	0.0044

Table 3.2

Weight gains by samples of zeolite 5A in desiccator with  $P_2O_5$ .

wt. zeolite/g	wt. gain/g	wt. gain/gg-1
0.1828	0.0020	0.0104
0.2389	0.0021	0.0088
0.2452	0.0028	0.0108
0.2838	0.0021	0.0080
0.2807	0.0024	0.0083
0.2872	0.0019	0.0085

Table 3.3

Weight gains by samples of zeolite 5A in a desiccator without  $P_2O_5$  present.

wt. zeolite/g	wt. gain/g	wt. gain/gg-1
0.0812	0.0008	0.0111
0.1828	0.0011	0.0060
0.2158	0.0013	0.0060
0.2688	0.0018	0.0062
0.3312	0.0018	0.0048

Table 3.4 Weight gains by samples of zeolite after equilibration over DBP.

	uptake of n-heptane/gg-1					average	standard deviation
run 1	0.1475	0.1488	0.1470	0.1489		0.1471	0.0003
run 2	0.1488	0.1478	0.1488	0.1488	0.1489	0.1488	0.0004
run 3	0.1477	0.1473	0.1485	0.1489	0.1483	0.1470	0.0005
run 4	0.1478	0.1470	0.1478	0.1488		0.1472	0.0005

Table 3.5 The uptake of n-heptane by samples of zeolite 5A measured in four separate runs.

The uptake of n-heptane by zeolite 5A was measured in four individual runs. Four or five samples of zeolite were activated and the uptake of n-heptane measured. This was repeated three times using different samples each time. The results are shown in Table 3.5. The average uptake and standard deviation for each run is shown also in the table.

The results from the preliminary experiments suggest that the "multi-equilibration" method is an ideal technique to obtain uptakes of sorbates by many samples at one time, quickly, simply and in a reproducible manner.

### 3.10.3 Comparison of techniques

The Cahn electrobalance provides a much more sophisticated method for the determination of sorption properties than does the "multi-equilibration" technique and as a result it has the potential to provide a great deal more information. Its main disadvantage however, is that only one sample may be examined at one time. In order to compare the uptakes of say 18 samples, it would take three weeks if the Cahn Balance was used, whereas with the "multi-equilibration" method results could be obtained within 24h. The Cahn balance requires constant supervision but the "multi-equilibration" method requires none. If the sorbate vapour pressure is low and the equilibration time is long, it may not be possible to use the Cahn balance. In the case of the "multi-equilibration" method samples can be left to equilibrate for weeks if necessary. Problems were found with the "multi-equilibration" method when samples with high vapour pressure such as methanol were used. Evacuation of the desiccator resulted in most of the sorbate being removed from the system and non-reproducible data then resulted.

How do the results from these two techniques compare? The isotherm of

the uptake of n-heptane by [TPA,PIP]-SIL-P10 is shown in Figure 3.5. The Langmuir plot of this isotherm is shown in Figure 3.6. The maximum uptake,  $U_m$ , calculated from this plot is  $0.133 \pm 0.004 \text{gg}^{-1}$ . This compares well with the value of  $0.134 \pm 0.001 \text{gg}^{-1}$  obtained with the "multi-equilibration" method. The value of the equilibrium constant calculated from the Langmuir plot of this isotherm was  $2.7 \pm 0.6 \text{mmHg}^{-1}$ .

Also compared are the corresponding values for the sorption of p-xylene. The sorption isotherm for the uptake of p-xylene by [TPA,PIP]-SIL is shown in Figure 3.7. The Langmuir plot is shown in Figure 3.8. The maximum uptake of sorbate,  $U_{\text{max}}$  calculated from the Langmuir plot was  $0.151 \text{gg}^{-1} \pm 0.003$ . The uptake of p-xylene found with use of the "multi-equilibration" method was  $0.154 \pm 0.001 \text{gg}^{-1}$ . The equilibrium constant for the sorption of p-xylene was found to be  $5.0 \pm 0.9 \text{mmHg}^{-1}$ .

These uptake values show that results obtained from the equilibration method and the Cahn balance agree within experimental error.

### 3.11 Sorption Properties of ZSM-5

The sorption behaviour of two samples of ZSM-5 prepared by different routes, i.e. (Na,H)-[Na,PIP]-ZSM-5 and Na-[Na,DIOL]-ZSM-5, was investigated. The preparation of both these zeolites was described in chapter two. These two zeolites have substantially different  $\text{Na}^+$  content as a consequence of different methods of preparation. In Figure 3.9 the uptakes of n-heptane, p-xylene and cyclohexane with time at  $23^\circ\text{C}$  are shown for both zeolites. The pressure of the sorbate was controlled using a p-xylene slush bath. The uptake of n-heptane by both zeolites is rapid but the equilibrium uptake is higher for (Na,H)-[Na,PIP]-ZSM-5 than Na-[Na,DIOL]-ZSM-5. The diffusion of

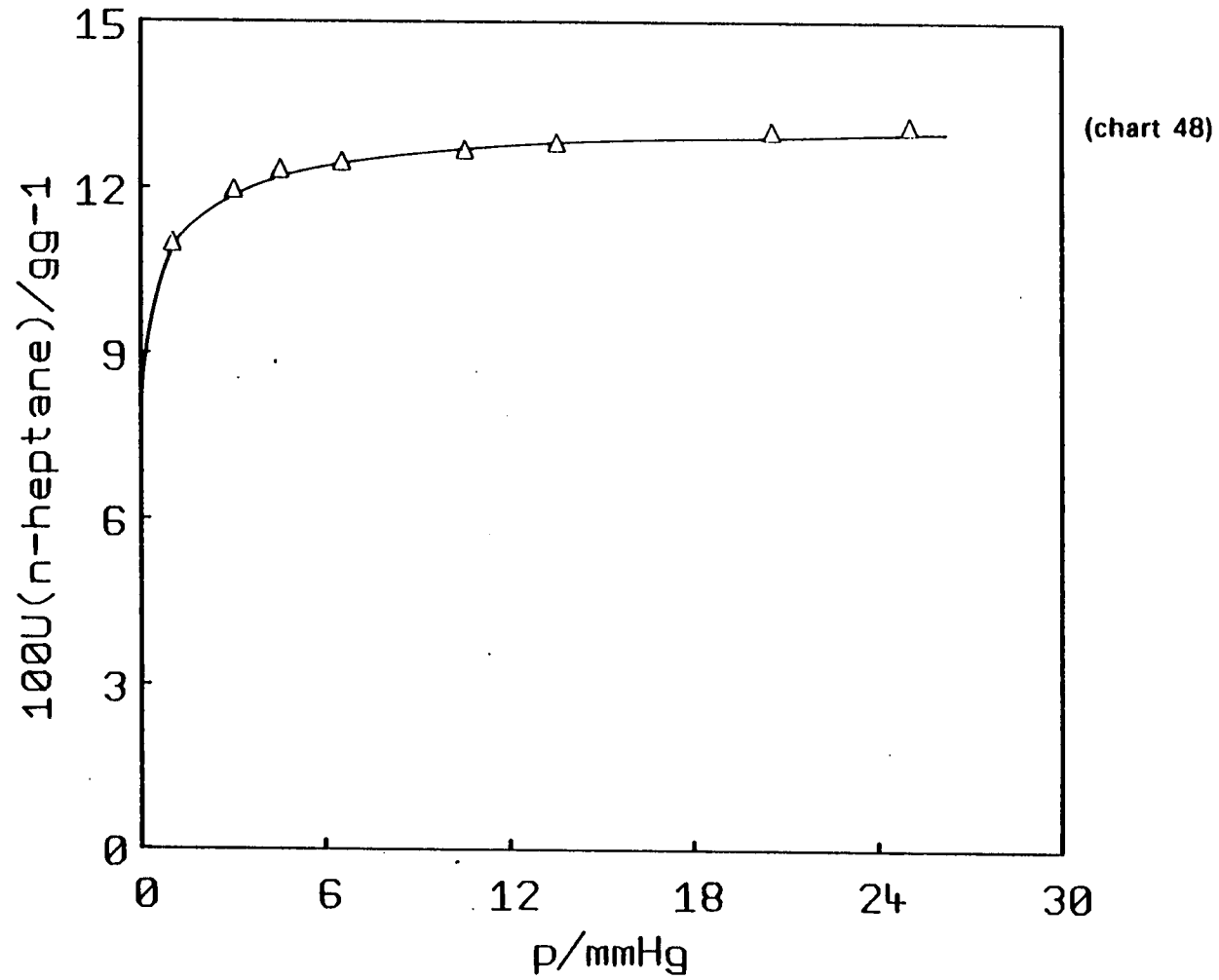


Figure 3.5

The uptakes of n-heptane by [PTA,PIP]-SIL-P10 plotted against sorbate pressure,  $p$ , at 24°C.

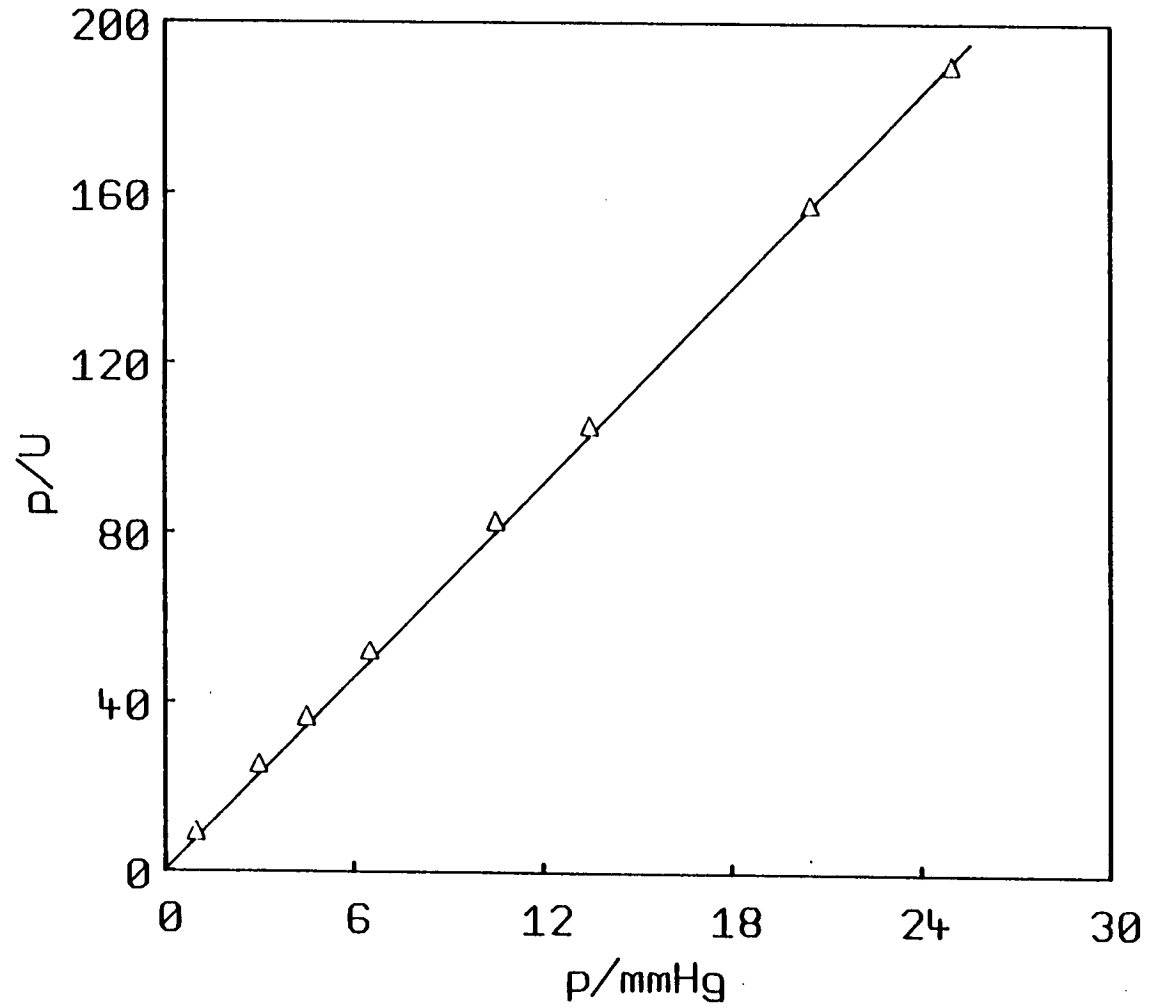


Figure 3.6

The langmuir plot of the n-heptane isotherm plotted in Figure 3.5.

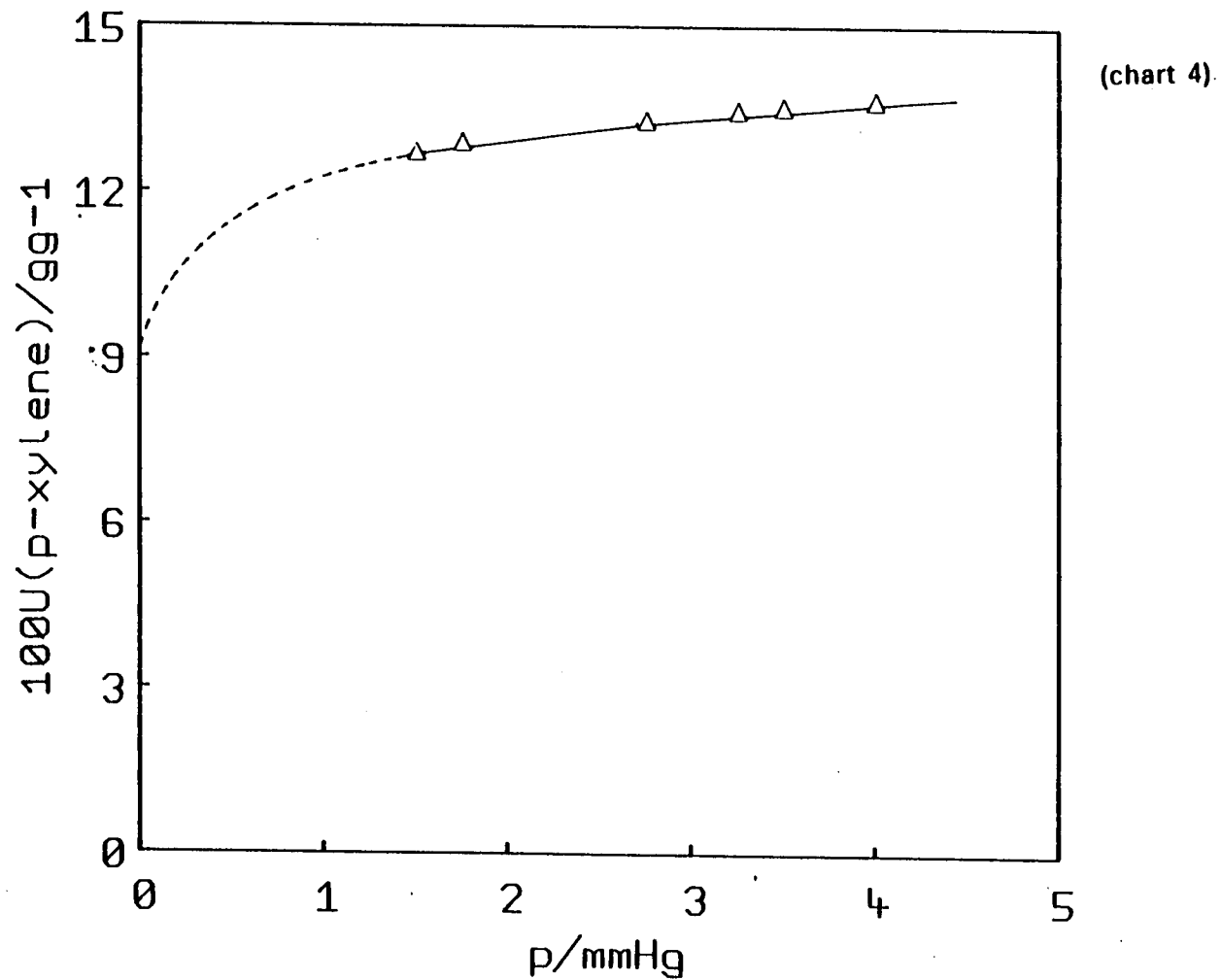


Figure 3.7

The uptake of p-xylene, U, by [TPA,PIP]-SIL-P10 plotted against sorbate pressure, p, at 24°C.



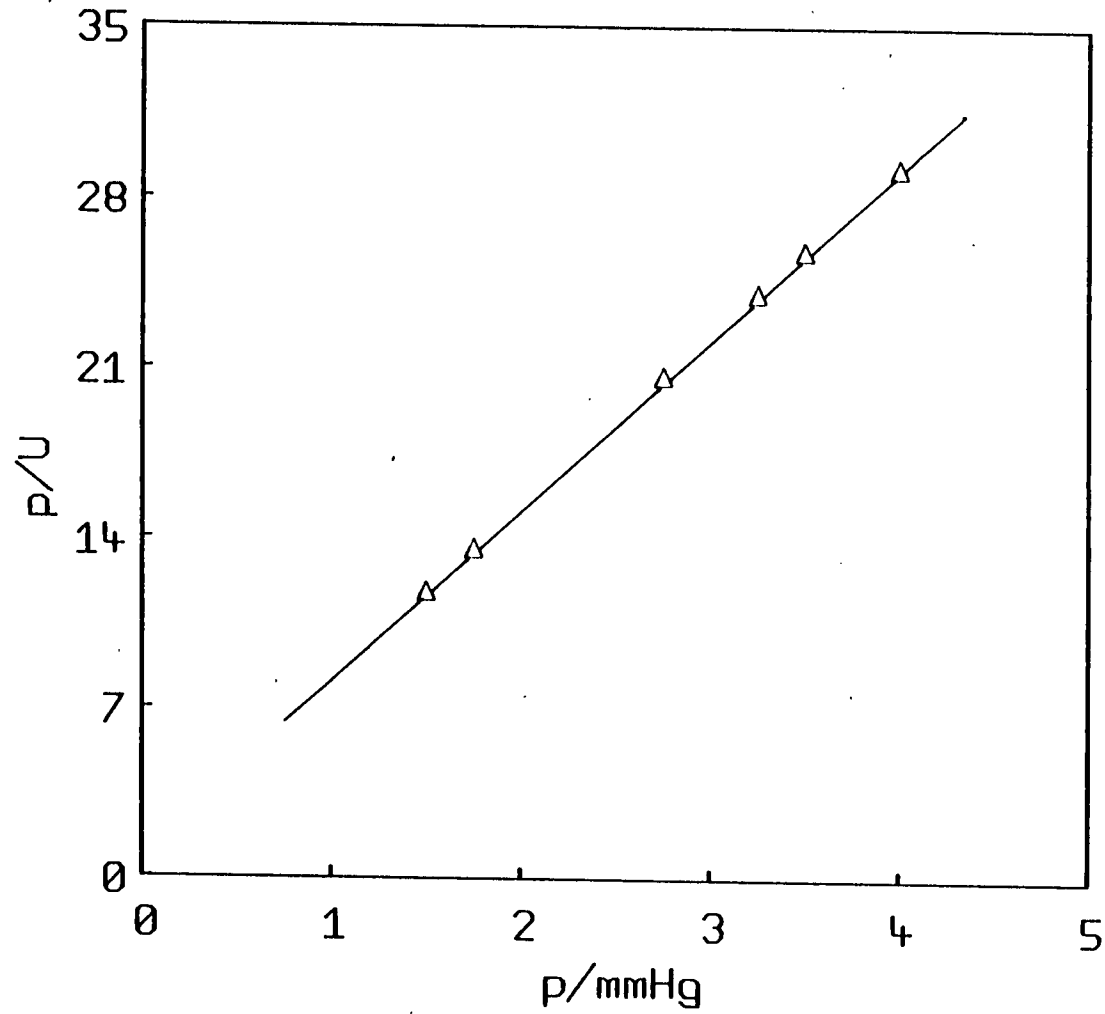


Figure 3.8

The langmuir plot of the p-xylene isotherm shown in Figure 3.7

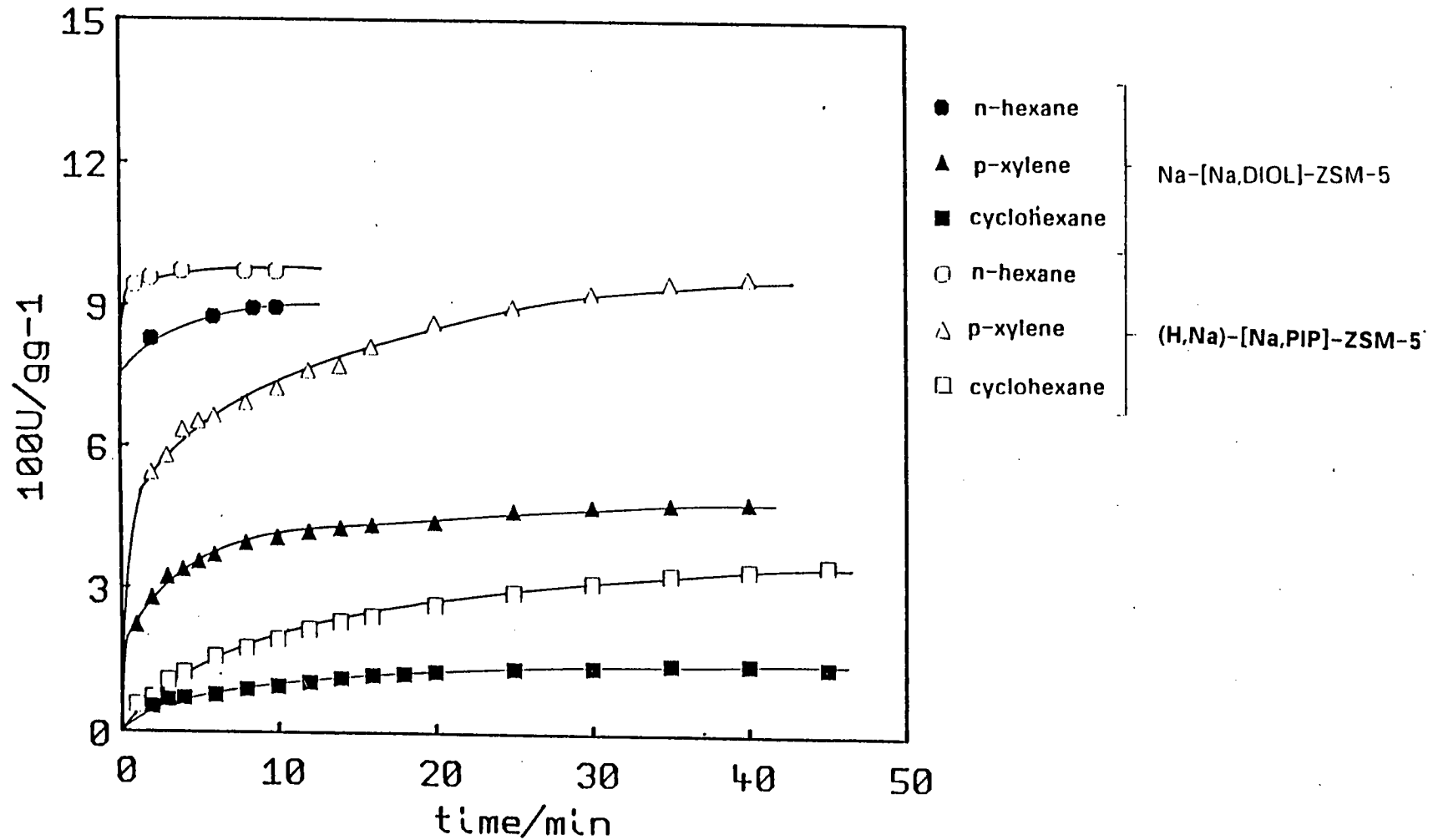


Figure 3.9

The uptakes of n-heptane, p-xylene and cyclohexane by (H,Na)-[Na,PIP]-ZSM-5 and Na-[Na,DIOL]-ZSM-5 with time,  $t$ , at 23°C.

p-xylene is considerably slower than the diffusion of n-heptane into both zeolites. But more revealing is that the (Na,H)-[Na,PIP]-ZSM-5 sample sorbs p-xylene to pore-filling whereas Na-[Na,DIOL]-ZSM-5 only sorbs about 50% of its volume. There is a very small uptake of cyclohexane by Na-[Na,DIOL]-ZSM-5 but a significant amount is taken up by (Na,H)-[Na,PIP]-ZSM-5. Cyclohexane diffused very slowly as equilibrium had not been reached after 45 minutes.

n-Heptane has a kinetic diameter of 4.9Å and can pass easily through the pores of ZSM-5. It has a favourable interaction with the framework because of high dispersion energies of interaction. As a result it is sorbed rapidly by both of the ZSM-5 samples examined. The larger uptake of n-heptane by (Na,H)-[Na,PIP]-ZSM-5 suggests that there is a greater volume available to sorbate molecules in (Na,H)-[Na,PIP]-ZSM-5. The more Na<sup>+</sup> ions in the channels of ZSM-5 the less space there is inside the pores for sorbate molecules. (Na,H)-[Na,PIP]-ZSM-5 sorbs p-xylene to pore-filling but Na-[Na,DIOL]-ZSM-5 sorbs less than 50% of its pore volume. Similar results are obtained for the sorption of cyclohexane. This may be due to the tight fit of p-xylene molecules in the channels of ZSM-5. In (Na,H)-[Na,PIP]-ZSM-5 there is sufficient room for the p-xylene molecules to pack in such a way that all the volume is filled whereas in Na-[Na,DIOL]-ZSM-5 the presence of more Na<sup>+</sup> ions in the channel system prohibits packing of p-xylene molecules so as to fill all the available pore volume.

Plots of  $U_t/U_{max}$  against  $t^{1/2}$  are shown in Figure 3.10. If diffusion is intracrystalline controlled, these plots should yield straight lines at short times, and the lines should pass through the origin. It is observed under the conditions used the only sorbate for which intracrystalline control occurred

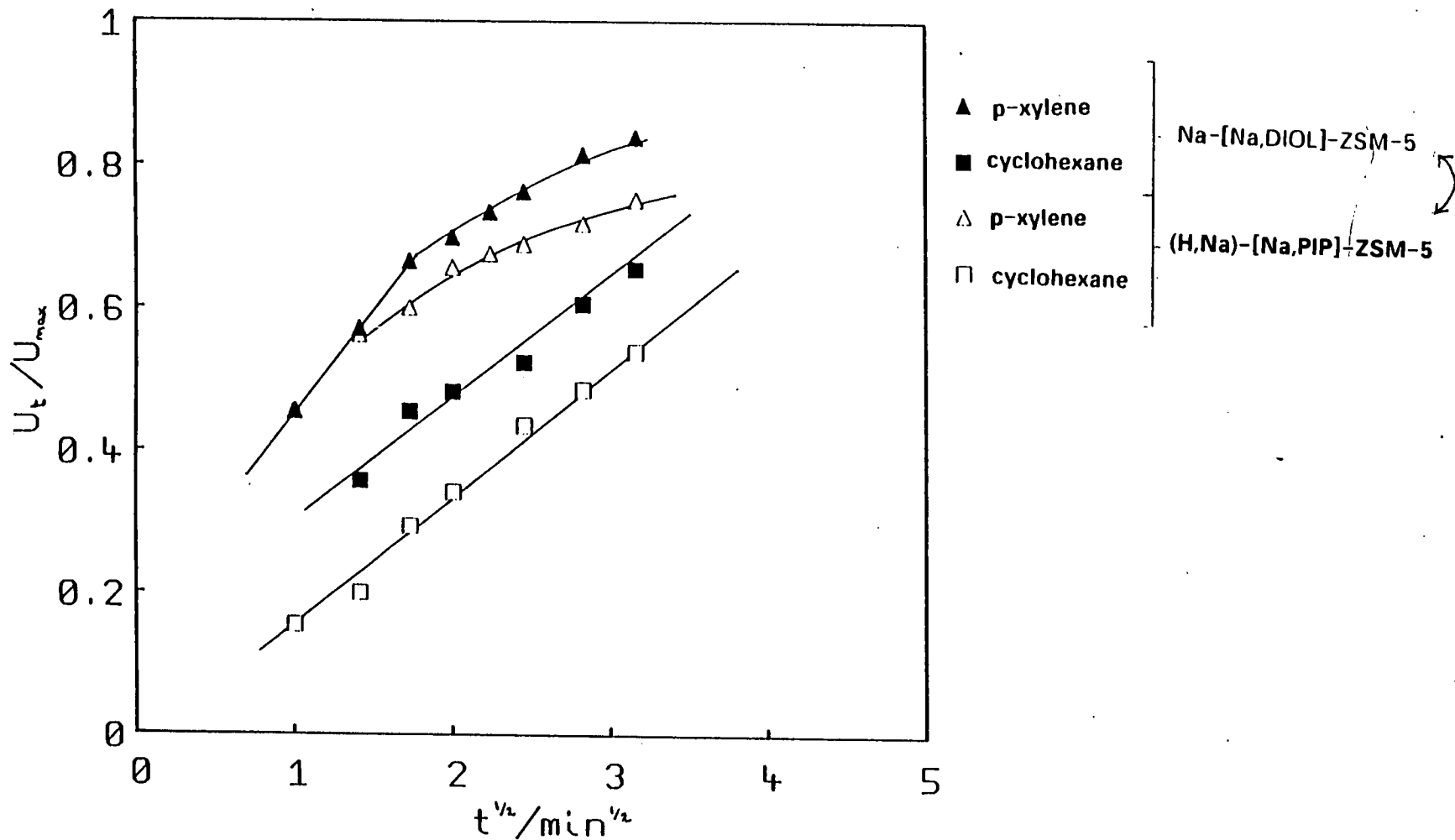


Figure 3.10

Plots of  $U_t/U_{max}$  against  $t^{0.5}/\text{min}^{0.5}$   
for the sorption time curves plotted in Figure 3.9.

over a measurable time range was cyclohexane. It is observed that the diffusion of sorbates into (Na,H)-[Na,PIP]-ZSM-5 is faster than into Na-[Na,DIOL]-ZSM-5. The presence of Na<sup>+</sup> ions in the channel system restricts the diffusion of sorbates into ZSM-5. Intracrystalline diffusion controlled sorption of p-xylene could have been obtained if a smaller sample weight had been used or if a lower pressure of sorbate had been admitted to the sample chamber.

The uptakes of n-heptane were determined by the "multi-equilibration" method. The uptakes by the two different preparations of ZSM-5 are given below. For comparison the results for [TPA,PIP]-SIL-P10 are also given.

<b>Zeolite</b>	<b>U<sub>n-heptane</sub></b>
Na-[Na,DIOL]-ZSM-5	0.107gg <sup>-1</sup>
(Na,H)-[Na,PIP]-ZSM-5	0.131gg <sup>-1</sup>
[TPA,PIP]-SIL-P10	0.132gg <sup>-1</sup>

As expected the uptake of n-heptane by Na-[Na,DIOL]-ZSM-5 is considerably lower than the uptake by the predominantly hydrogen form of ZSM-5. It is interesting to note that the uptake of n-heptane by (Na,H)-[Na,PIP]-ZSM-5 is very similar to that of [TPA,PIP]-SIL.

The uptakes of water by these two ZSM-5 samples were measured using the "multi-equilibration" method and are shown below.

<b>Zeolite</b>	<b>U<sub>water</sub></b>
Na-[Na,DIOL]-ZSM-5	0.126gg <sup>-1</sup>
(Na,H)-[Na,PIP]-ZSM-5	0.050gg <sup>-1</sup>

These results suggest that (Na,H)-[Na,PIP]-ZSM-5 is more hydrophobic than

Na-[Na,DIOL]-ZSM-5, despite similar Si/Al ratios. The higher uptake of water by Na-[Na,DIOL]-ZSM-5 is probably due to the greater solvation of the Na<sup>+</sup> ions in the channels. In (Na,H)-[Na,PIP]-ZSM-5 the protons are present probably as -Si-OH Al-. Although these sites have some hydrophilic nature they are probably not as highly solvated as Na<sup>+</sup> ions.

### 3.12 Sorption Properties of Silicalite

#### 3.12.1 Uptakes of n-alkanes by [TPA,PIP]-SIL

The uptakes of n-alkanes by [TPA,PIP]-SIL were obtained with the previously described "multi-equilibration" method. The alkanes used were C<sub>n</sub>H<sub>2n+2</sub> with n = 6, 7, 8, 9, 10 and 12.

The uptakes are shown in Table 3.6 and expressed in gram of sorbate sorbed per gram of dry silicalite, number of molecules sorbed per unit cell, number of CH<sub>2</sub> groups per unit cell and in cm<sup>3</sup> of sorbate per gram of dry silicalite. The uptakes of n-alkanes obtained experimentally are in good agreement with those reported in the literature[52,53,54,55,56].

Several assumptions were made in the calculation of these results,

1. The unit cell composition was 96SiO<sub>2</sub>.
2. In counting the CH<sub>2</sub> groups in the sorbates, the two terminal CH<sub>3</sub> groups were counted as two CH<sub>2</sub> groups.
3. In the calculation of the uptake as a volume the density of the sorbate in the channels of silicalite was taken to be the same as the density of the sorbate in the liquid phase.

alkane	U/gg-1	molecules/unitcell	CH2/unitcell	V/cm <sup>3</sup> g-1
n-hexane	0.132	8.8	53	0.200
n-heptane	0.134	7.6	53	0.196
n-octane	0.121	6.1	49	0.172
n-nonane	0.118	5.3	48	0.164
n-decane	0.126	5.1	51	0.173
n-dodecane	0.128	4.3	52	0.167

Table 3.6

The uptakes of C<sub>n</sub>H<sub>2n+2</sub>, n = 6,7,8,9,10 and 12 by [TPA,PIP]-SIL at 25°C.

alkane	length of molecules/Å	molecules/unit cell	CH groups/unit cell
n-hexane	10.3	6.4	38
n-heptane	11.56	5.7	40
n-octane	12.82	5.1	41
n-nonane	14.08	4.7	41
n-decane	15.34	4.3	43
n-dodecane	17.86	3.7	44

Table 3.7

The length of n-alkane molecules with the respective number of molecules of this length that should occupy a unit cell of silicalite.

The channel length per unit cell in silicalite has been calculated by other workers and found to be 65.8Å[55]. Since the length of a CH<sub>2</sub> group is 1.26Å[17], it would be expected that 52 CH<sub>2</sub> groups could be accommodated within the channels of one unit cell of silicalite.

If the raw results - uptakes of n-alkanes expressed in gg<sup>-1</sup> - are examined no clear trend is apparent. However, when the uptakes are expressed as molecules per unit cell it is observed that as the length of the molecules increases the number of molecules sorbed per unit cell decreases. The larger the molecule the fewer that can be accommodated in the available space.

When the uptake of n-alkanes is expressed as number of CH<sub>2</sub> groups per unit cell it is found as previously estimated that approximately 52 CH<sub>2</sub> groups are sorbed per unit cell. There are however variations that are outwith experimental error. There are several explanations that could account for these variations.

It is possible that the assumption that a CH<sub>3</sub> group can be counted as a CH<sub>2</sub> group is invalid. In order to examine this further Table 3.7 shows the length of n-alkane molecules as given in the literature along with the number of molecules of this length that could be accommodated within a unit cell of silicalite. Also tabulated is the number of 'CH<sub>2</sub>' groups this would lead to if each CH<sub>3</sub> was counted as a CH<sub>2</sub>.

It is immediately apparent that these figures are not in agreement with the experimental results obtained. If a CH<sub>3</sub> occupies more space than a CH<sub>2</sub> group, then less "CH<sub>2</sub>" groups would be sorbed per unit cell for n-hexane than for n-dodecane. This does not appear to be the case. The molecules sorbed



within the silicalite are packed more densely than expected from their length of chain. They may be in a more coiled configuration. The assumption that a  $\text{CH}_3$  group is equivalent to a  $\text{CH}_2$  group is valid in the light of the experimental results.

The variation in the number of  $\text{CH}_2$  groups sorbed per unit cell could be explained by difficulty in packing molecules of a certain length. It may be that molecules of a given length can not be packed to fill all the space in the silicalite channels.

The volume of the silicalite channels is considered to be constant and to have a value of  $0.19\text{cm}^3\text{g}^{-1}$ . This suggests that the assumption that the density of the sorbate in the silicalite channels is the same as the density of the sorbate in the liquid phase is only a rough approximation.

### 3.12.2 Uptake of n-heptane by silicalite

The uptake of n-heptane by silicalite-1 can be measured with ease by the "multi-equilibration" method. As n-heptane is sorbed to pore filling, any differences in uptake between samples should be due to differences in pore volume. In order to observe any differences in pore volume of silicalites prepared and pretreated using different procedures, the uptakes of n-heptane by these samples was measured. The results obtained are shown in Table 3.8.

The  $\text{Li}^+$ ,  $\text{Na}^+$  and  $\text{K}^+$  cation forms of silicalite-1 all have lower uptakes of n-heptane than [TPA,PIP]-SIL. This is due to the presence of cations in the channels that reduces the space available to sorbate molecules. The uptakes for the  $\text{Na}^+$  and  $\text{K}^+$  forms of silicalite are similar: these two cation forms have approximately the same number of cations in the channels. The  $\text{Li}^+$  cation form

Sample	U/gg-1
Na- [TPA, PIP]-SIL-P18 (550° C)	0.121
Na- [TPA, PIP]-SIL-P18 (800° C)	0.005
soxhletNa- [TPA, PIP]-SIL-P18 (550° C)	0.144
H- [TPA, Na]-SIL-P18 (550° C)	0.148
K- [K, TPA]-SIL-P18 (550° C)	0.120
soxhletK- [K, TPA]-SIL-P18 (550° C)	0.102
H- [TPA, PIP]-SIL-P18 (550° C)	0.140
Li- [TPA, Li]-SIL-P20 (550° C)	0.111
Li- [TPA, Li]-SIL-P20 (800° C)	0.107
soxhletLi- [TPA, Li]-SIL-P20 (550° C)	0.115
H- [TPA, Li]-SIL-P20 (550° C)	0.118
H- (800 C) - [TPA, Li]-SIL-P20 (550° C)	0.115
Cs- [TPA, Cs]-SILP21 (550° C)	0.145
[TPA, PIP]-SIL-P10 (800° C)	0.134
(650 C) - [TPA, PIP]-SIL-P10 (800° C)	0.128

Table 3.8

Uptakes of n-heptane by silicalites prepared and pretreated differently.

has a lower uptake: this can be explained by the larger number of cations in the channels. The uptake of n-heptane by Cs-[Cs,TPA]-SIL-P21 is higher than the uptake of n-heptane by [TPA,PIP]-SIL. This agrees well with the XRF results discussed in chapter two, that showed that no Cs<sup>+</sup> ions were present in this form of silicalite. The crystals of this sample are very small and so the higher uptake may be due to sorption on the external surfaces of the silicalite crystals.

Hydrogen ion-exchange of the cation forms results in higher uptakes of n-heptane. Removal of cations from the channels increases the space available to sorbate molecules. The increase in uptake by H-[Li,TPA]-SIL-P20 is small. This may be because not all the Li<sup>+</sup> ions have been ion-exchanged.

Soxhlet extraction of the Na<sup>+</sup> and Li<sup>+</sup> cation forms result in greater uptakes of n-heptane. This is predictable as the continuous washing process removes some of the cations from the channels. The uptake of n-heptane by soxhlet extracted K-[K,TPA]-SIL-P18 is difficult to explain.

When [Na,TPA]-SIL is calcined at 800°C the resultant structure does not sorb n-heptane. This suggests that the silicalite structure has collapsed to give a more dense, less open structure. In light of later work, this structure is probably α-cristobalite. The collapse of the silicalite structure at below 800°C is considerably lower than the generally quoted temperature for the limit of the thermal stability of silicalite. The presence of sodium ions in the channels must initiate the collapse of the structure at a lower temperature.

When [Li,TPA]-SIL-P20 is calcined at 800°C the framework remains intact as there is only a small reduction in the uptake of n-heptane. The presence of Li<sup>+</sup>

ions in the channels does not initiate collapse of the silicalite structure even at elevated temperatures.

### 3.12.3 Sorption of Methanol

The methanol sorption isotherms of several different silicalites were obtained at a number of different temperatures using a Cahn electrobalance. From such a set of isotherms it is possible with the use of the Clausius-Clapeyron equation to calculate the variation of isosteric heat of sorption with the uptake of sorbate.

#### Uptake of Methanol by [TPA,PIP]-SIL-P10

The methanol sorption isotherms of [TPA,PIP]-SIL-P10 are shown in Figure 3.11. They show as expected that the higher the temperature the lower the uptake at a given pressure and the greater the pressure range over which Henry's law is obeyed. There is an anomaly in these isotherms in the form of a small step at very low pressures. The curves appear to extrapolate to  $0.013\text{gg}^{-1}$  on the y-axis rather than the origin. It is possible that this is due to sorption of methanol onto hydrophilic sites. These sites could be silanol groups. If the hydroxyl group of the methanol molecule interacted with such a site the isotherm would be steeper than if they had been absent. An uptake of methanol of  $0.013\text{gg}^{-1}$  corresponds to 2.3 methanol molecules per unit cell.

The Langmuir plots of these isotherms are shown in Figure 3.12. These isotherms approximate to the Langmuir isotherm over some ranges of pressure. Deviations from the Langmuir isotherm occur because of interaction of the methanol molecules with internal silanol groups.

The heat of sorption for the uptake of methanol by [TPA,PIP]-SIL-P10 can

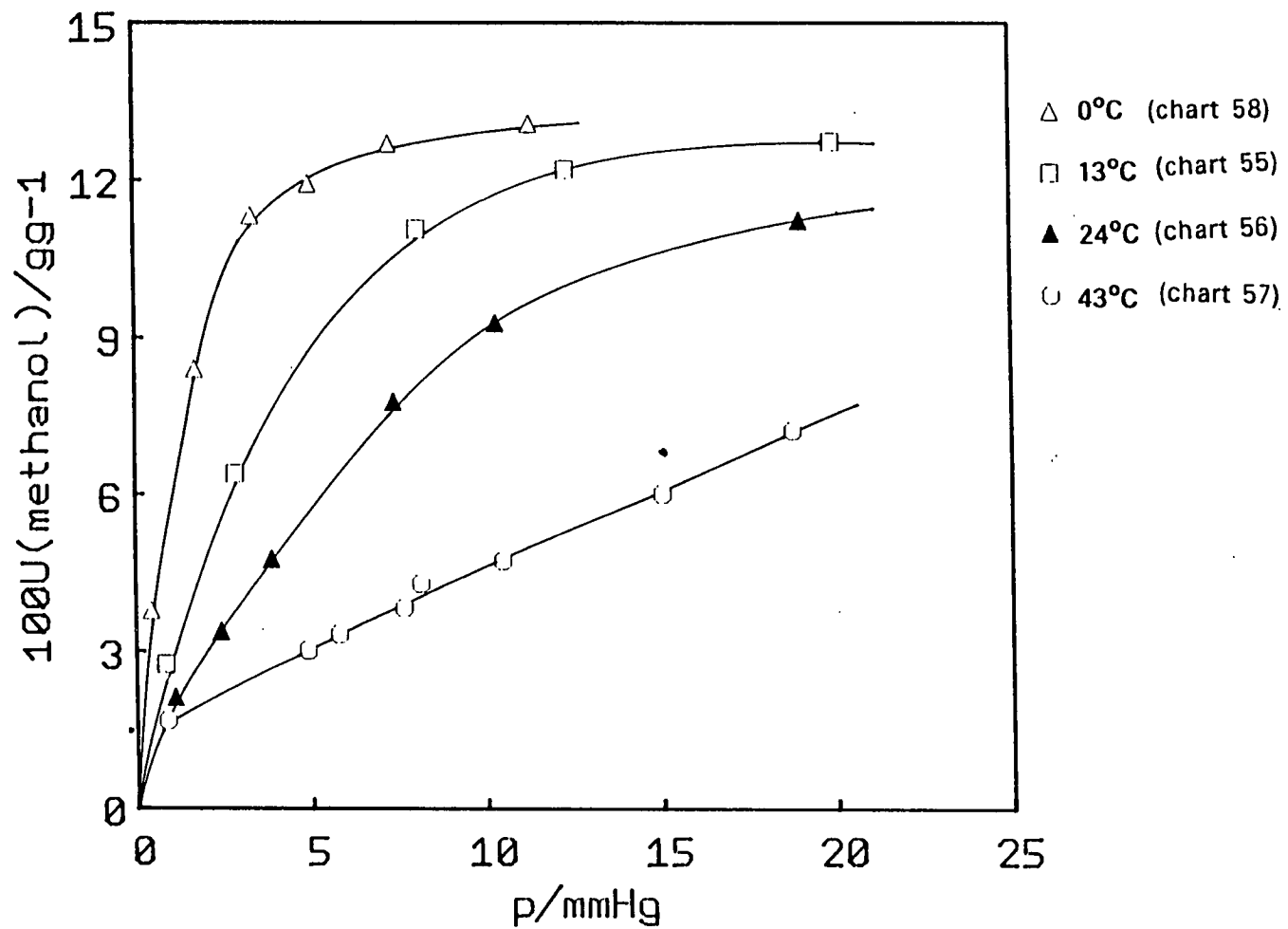


Figure 3.11

Methanol sorption isotherms of [TPA,PIP]-SIL-P10.

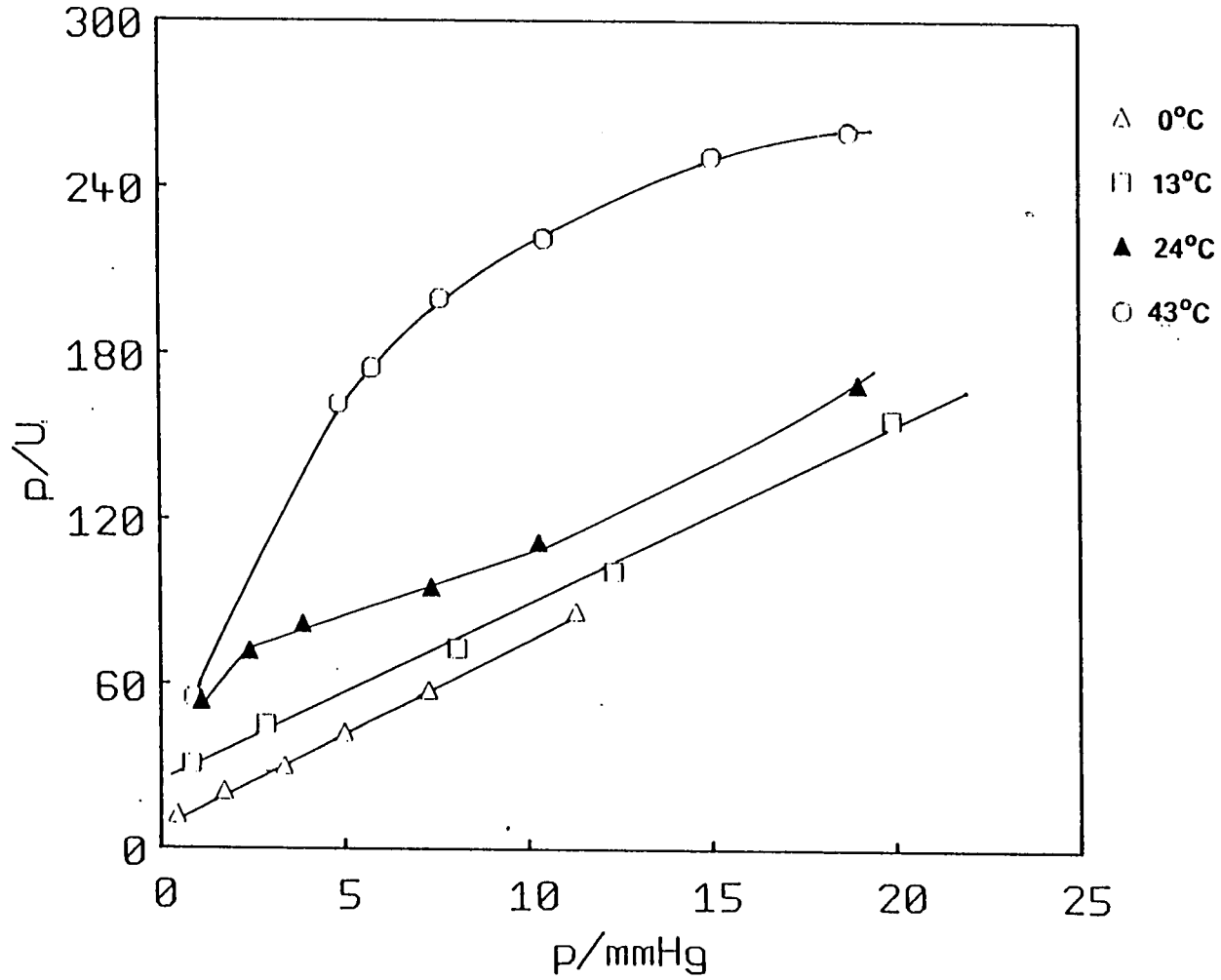


Figure 3.12

Langmuir plots of the methanol sorption isotherms shown in Figure 3.11.

be obtained from the Clausius-Clapeyron equation. The slopes of plots of  $\log p$  against  $1/T$  were determined with a least squares analysis programme on a microcomputer, for different uptakes of methanol. Some examples of these plots are shown in Figure 3.13. The error in these gradients is of the order  $\pm 3\%$ . This is consistent with errors in  $p$ ,  $T$ , and  $U$ .

A plot of isosteric heat of sorption  $q_{st}$ , against the uptake of methanol is shown in Figure 3.14. The heat of liquifaction of methanol is  $39.06 \text{ KJ mol}^{-1}$  and is indicated as a dashed line on the plot. The heat of sorption exceeds this value indicating that there are favourable interactions between methanol molecules and the silicalite framework. The sorption process is not merely one of condensation.

It is of interest that at low uptakes of methanol the variation of  $q_{st}$  with  $U$  is positive. This initially suggests that the silicalite surface is homoenergetic. If the internal surface was heteroenergetic, some sites would be able to interact more strongly with sorbate molecules than others. These sites would be occupied before less polar sites and the isosteric heat of sorption would be higher at low uptakes, decreasing at larger uptakes as the polar sites became occupied. However, the limits of the technique do not allow the variation of  $q_{st}$  with  $U$  to be examined at uptakes less than  $0.02 \text{ gg}^{-1}$ . So there may be a number of hydrophilic sites in [TPA,PIP]-SIL-P10 but an uptake of  $0.02 \text{ gg}^{-1}$  of methanol is sufficient to ensure they are all occupied. There are two possible explanations for the increase in  $q_{st}$  with  $U$ , i.e.

1. Favourable contributions to  $q_{st}$  from methanol-methanol interactions.

2. The possibility that as the uptake of methanol increases the number of hydrophilic sites increases. This could occur if

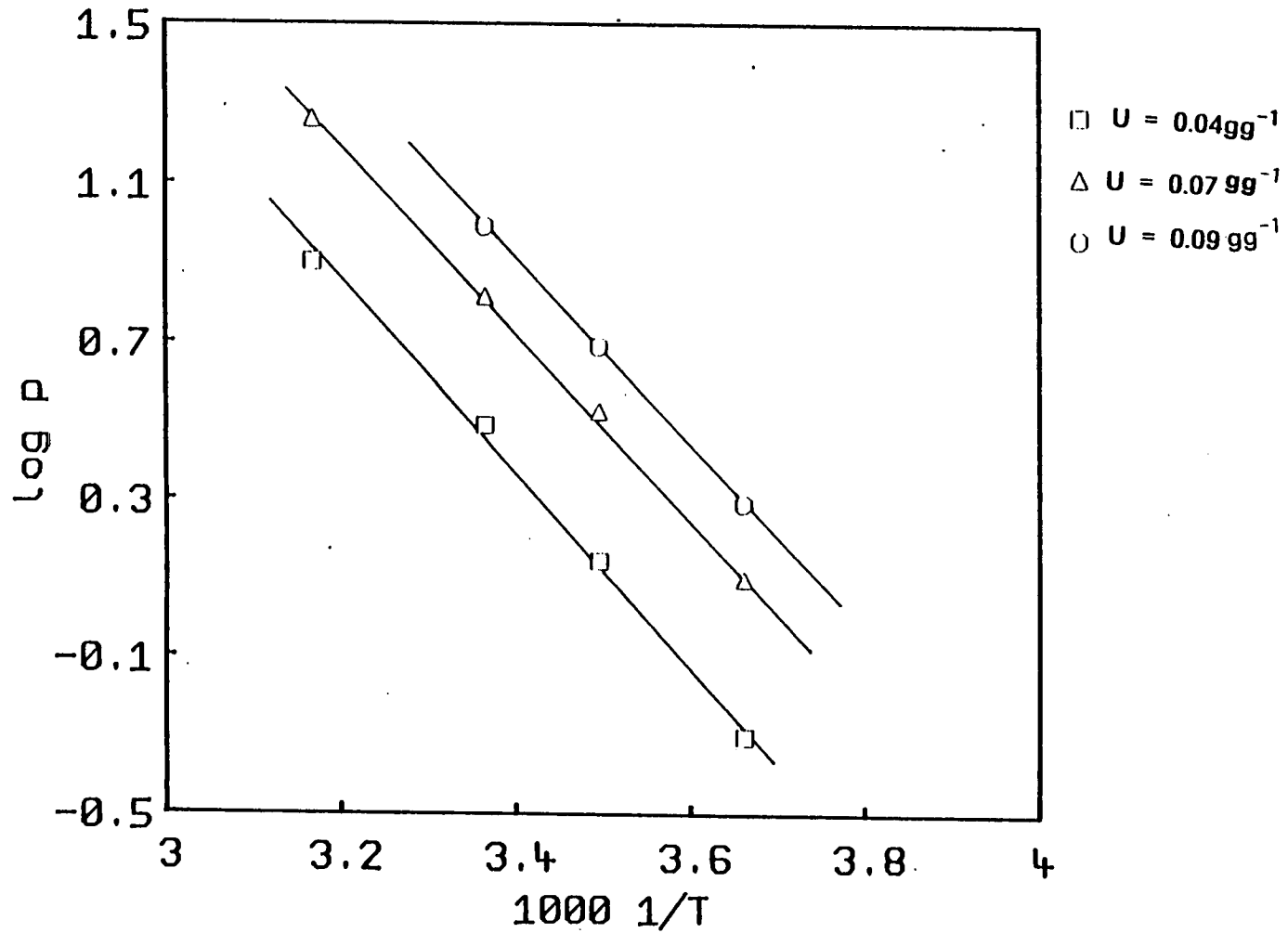


Figure 3.13

Plots of  $\log p$  against  $1/T(^{\circ}\text{K}^{-1})$  at three uptakes of methanol.



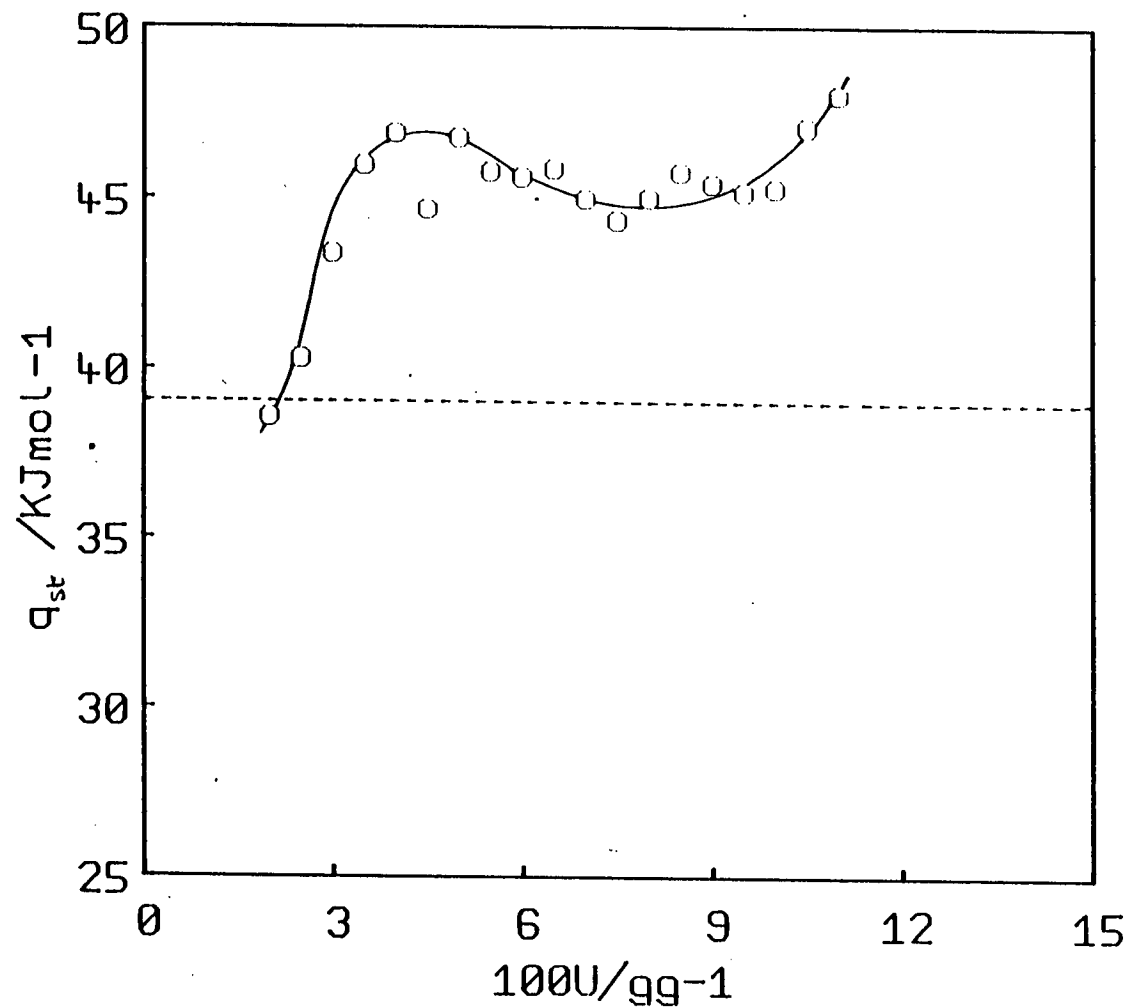


Figure 3.14

Variation of the isosteric heat of sorption,  $q_{st}$ , for the sorption of methanol by [TPA,PIP]-SIL-P10 with the uptake of methanol,  $U$ .

methoxylation/hydroxylation of the surface takes place.

### **Uptake of methanol by Na-[Na,TPA]-SIL-P16**

The sorption isotherms of uptake of methanol by Na-[Na,TPA]-SIL-P16 at 0,15,23,and 42°C are shown in Figure 3.15. The isotherms differ quite markedly when contrasted with the isotherms of [TPA,PIP]-SIL-P10. The uptake of methanol is about  $0.02\text{gg}^{-1}$  less than the corresponding uptake by [TPA,PIP]-SIL. The presence of  $\text{Na}^+$  ions in the channels of silicalite reduces the space available to the methanol molecules. Agreement of these isotherms with the Langmuir isotherm equation is poor except at low temperatures and high pressures. This deviation from the Langmuir model is not surprising when the shape of the isotherms are examined. All the isotherms have a distinct S-shape.

Initially there is a steep increase in the slope  $dU/dp$ . After this initial steep increase,  $dU/dp$  increases more slowly before increasing more sharply again and then levelling out as  $U_{\text{max}}$  is reached. The shape of the these isotherms can be explained in terms of sorbate-sorbate interactions or an increase in hydrophilic sites or both. In the light of later experiments, it is likely that the methoxylation/ hydroxylation of the surface is the most significant factor.

The initial steep increase in uptake with pressure is due to sorption of methanol on sorption sites associated with  $\text{Na}^+$  ions. The interaction of the dipole of a methanol molecule with a  $\text{Na}^+$  ion results in a favourable electrostatic interaction contribution to  $q_{\text{st}}$ , and the slope  $dU/dp$  is steeper than it would have been in the absence of such interactions. At some uptake all the sites associated with the cations are occupied. In subsequent sorption,  $q_{\text{st}}$  will be lower and the slope  $dU/dp$  is less steep. The uptake at which this occurs is

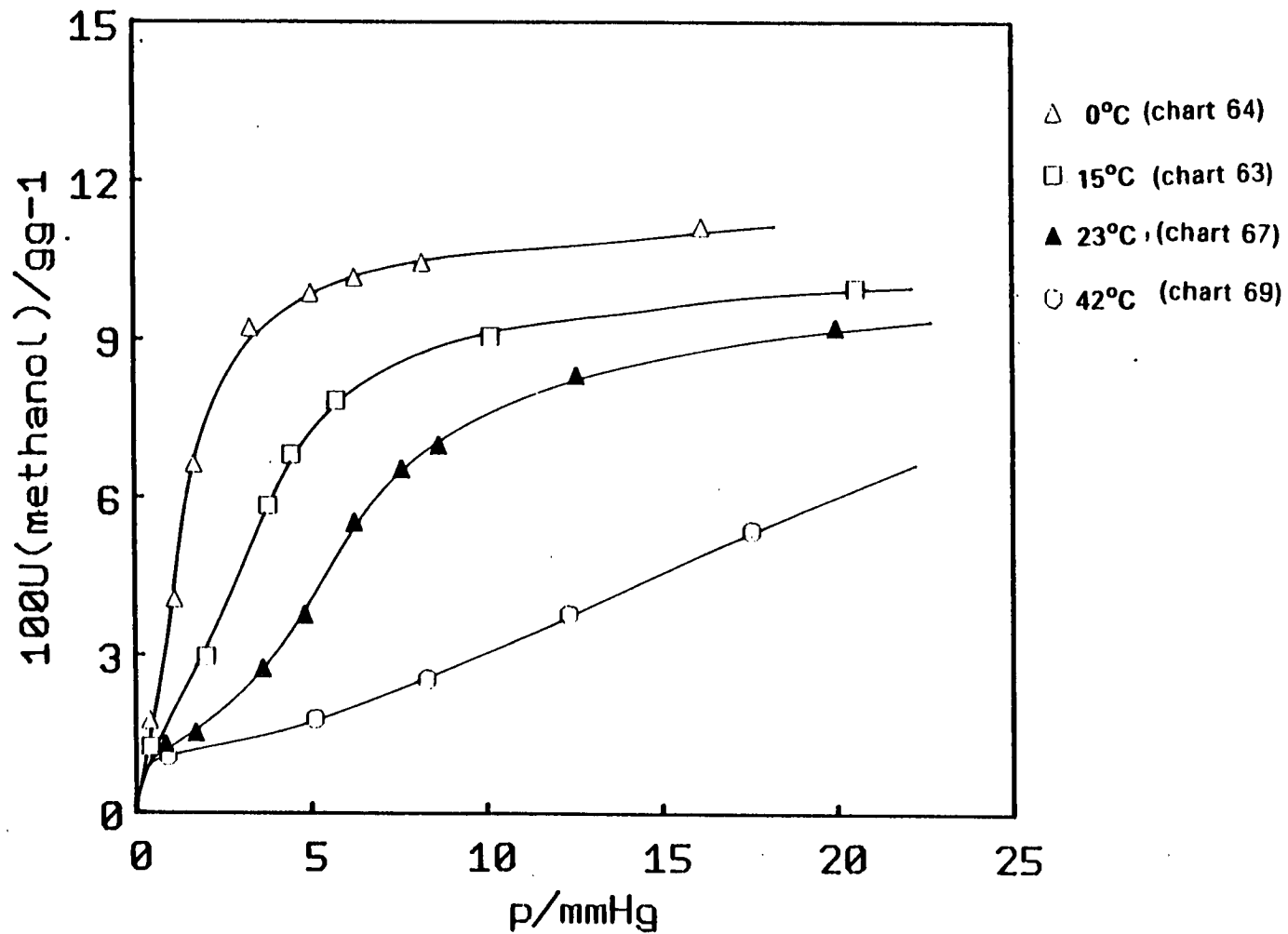


Figure 3.15

Methanol sorption isotherms of Na-(Na,TPA)-SIL-P16  
at  $T = 0, 15, 23$  and  $42^\circ\text{C}$ .

ca.  $0.02\text{gg}^{-1}$  which is equivalent to ca. 3.6 molecules per unit cell. The XRF results indicate that there are  $3.9\text{ Na}^+$ /unit cell. This suggests that there is approximately one methanol molecule strongly sorbed per  $\text{Na}^+$  ion. Once higher uptakes of methanol have been reached, two other factors may become important: methanol-methanol interactions and methoxylation and hydroxylation of the silicalite surfaces. As a result the uptakes of methanol increase with pressure more sharply.

The variation of  $q_{\text{st}}$  with  $U$  is shown in Figure 3.16. The shape of this plot can be explained in the same terms used to account for the shape of isotherms. The initial decrease in  $q_{\text{st}}$  with  $U$  suggests that the internal surface is heterogeneous. There are a number of sorption sites that are more energetically favourable – those associated with  $\text{Na}^+$  ions. At an uptake of  $0.045\text{gg}^{-1}$  which is equivalent to 8 molecules/unit cell, methoxylation and hydroxylation become important. The magnitude of  $q_{\text{st}}$  is similar to the sorption of methanol by [TPA,PIP]-SIL.

The presence of  $\text{Na}^+$  ions in the channels reduces the pore volume available to sorbate molecules and increases the heterogeneity of the internal surfaces.

#### **Uptake of Methanol by H-[Na,TPA]-SIL**

In this silicalite all the  $\text{Na}^+$  ions have been removed from the channels by hydrogen ion exchange. The sorption isotherms of the uptake of methanol by H-[Na,TPA]-SIL are shown in Figure 3.17. The uptakes of methanol by this sample are higher than the uptakes by Na-[Na,TPA]-SIL and at higher pressures are comparable to uptakes by [TPA,PIP]-SIL. The removal of  $\text{Na}^+$  from the channels increases the space available to sorbate molecules. However the strength of the sorbate-molecular sieve interaction is also reduced which

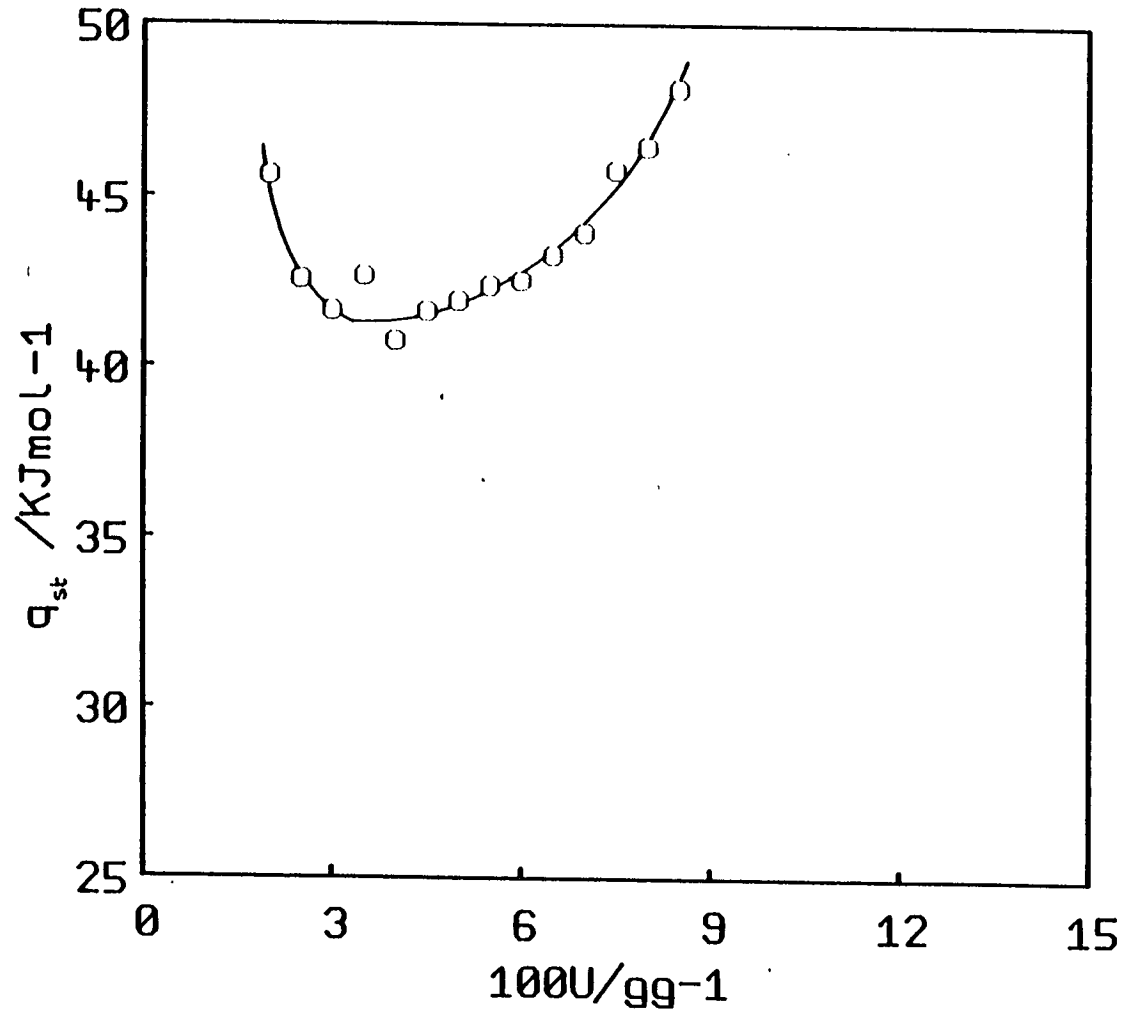


Figure 3.16

Variation of the isosteric heat of sorption,  $q_{st}$ ,  
for Na-[Na,TPA]-SIL-P16, with the uptake of methanol, U.

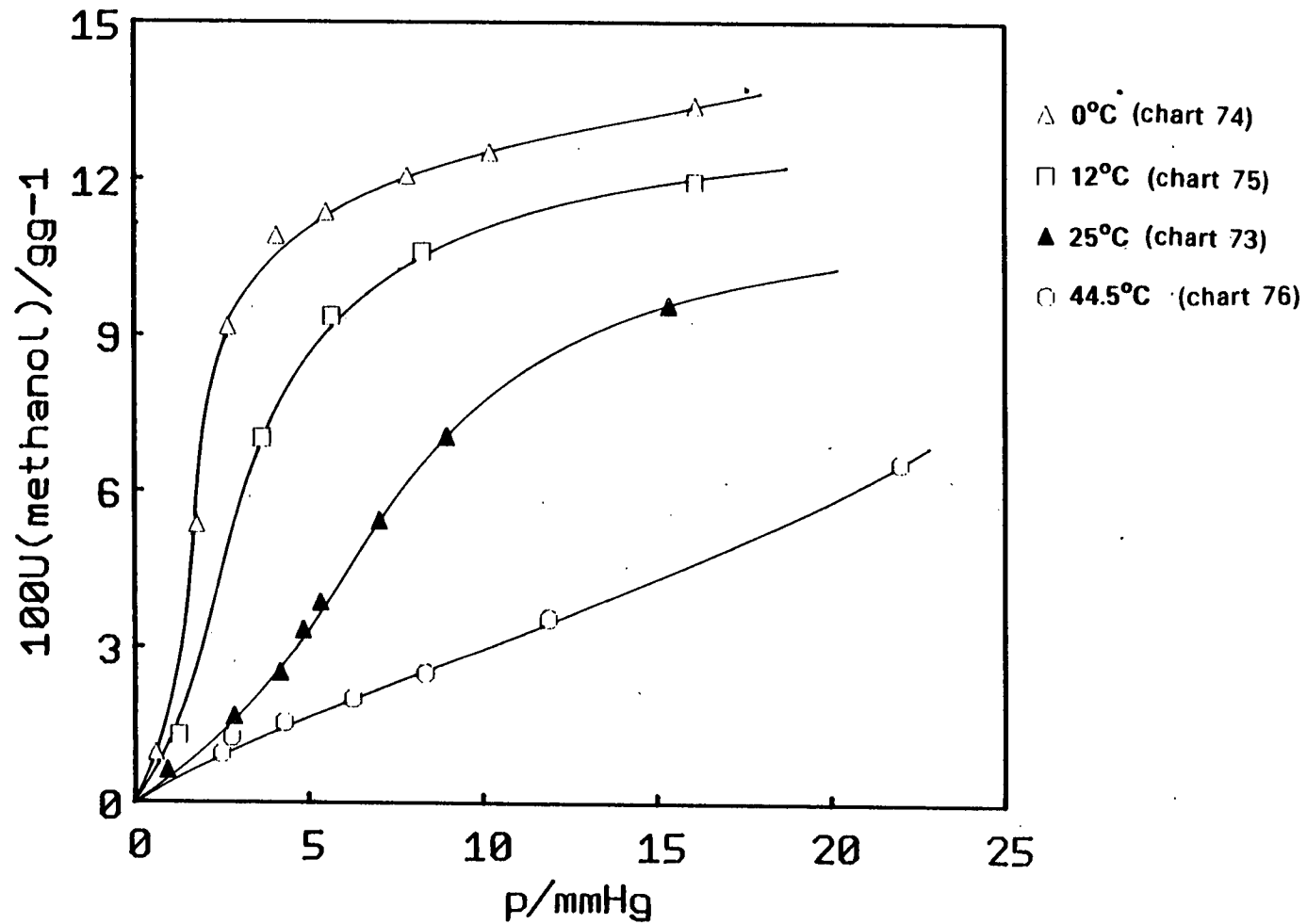


Figure 3.17

Methanol sorption isotherms of H-[Na,TPA]-SIL-P16  
at 0, 12, 25 and 44°C.

results in lower uptakes at lower pressures. No longer are there  $\text{Na}^+$  ions in the channels which interact strongly with methanol molecules.

The variation of  $q_{\text{st}}$  with  $U$  is shown in Figure 3.18. A steady increase is observed in  $q_{\text{st}}$  with  $U$ . This suggests that the internal surface is homoenergetic. However there may be a small number of hydrophilic sites that are occupied by a uptake of methanol less than  $0.02\text{gg}^{-1}$ . This increase in  $q_{\text{st}}$  with  $U$  is probably due to methoxylation/hydroxylation of the silicalite surface and possibly some contribution from sorbate-sorbate interactions.

The magnitude of  $q_{\text{st}}$  is significantly lower than  $q_{\text{st}}$  for  $\text{Na}-[\text{Na,TPA}]-\text{SIL}$  and  $[\text{TPA,PIP}]-\text{SIL}$ . This suggests that  $\text{H}-[\text{Na,TPA}]-\text{SIL}$  is more hydrophobic than the two other silicalites investigated. Prior to ion-exchange treatment  $\text{Na}^+$  ions were present in the channels of this silicalite. Ion-exchange with aqueous  $\text{HCl}$  solution will result in the formation of two hydroxyl groups. Before a sorption run the silicalite is activated at  $550^\circ\text{C}$ . It is possible that at this temperature a number of internal hydroxyl groups are healed. This would render the internal surface of silicalite more hydrophobic. Why does this silicalite appear more hydrophobic than the  $[\text{TPA,PIP}]-\text{SIL}$ ? It is probable that  $[\text{TPA,PIP}]-\text{SIL}$  is less hydrophobic than expected rather than the  $\text{H}-[\text{Na,TPA}]-\text{SIL}$  being more hydrophobic. This may be a consequence of the initial reaction mixture composition. The presence of piperazinehexahydrate in the reaction mixture appears to increase the number of internal hydroxyl groups that are present after synthesis.

#### **Uptake of Methanol by Cation forms of Silicalite**

The sorption isotherms of the uptake of methanol by the  $\text{Li}^+$ ,  $\text{Na}^+$ , and  $\text{K}^+$  cation forms of silicalite and  $[\text{TPA,PIP}]-\text{SIL}$  are shown in Figure 3.19. These

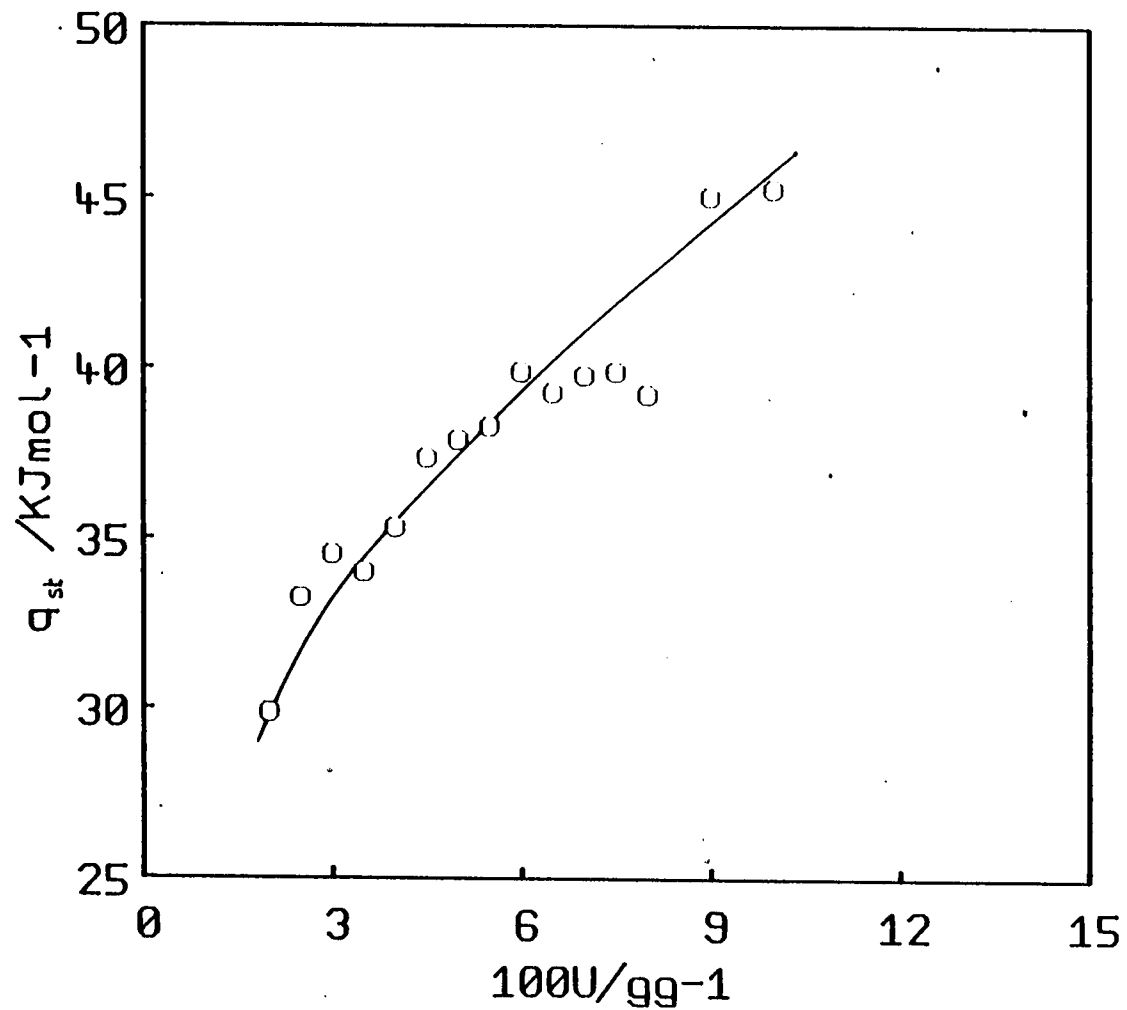


Figure 3.18

Variation of the isosteric heat of sorption of methanol by H-[Na,TPA]-SIL-P16, with the uptake of methanol.



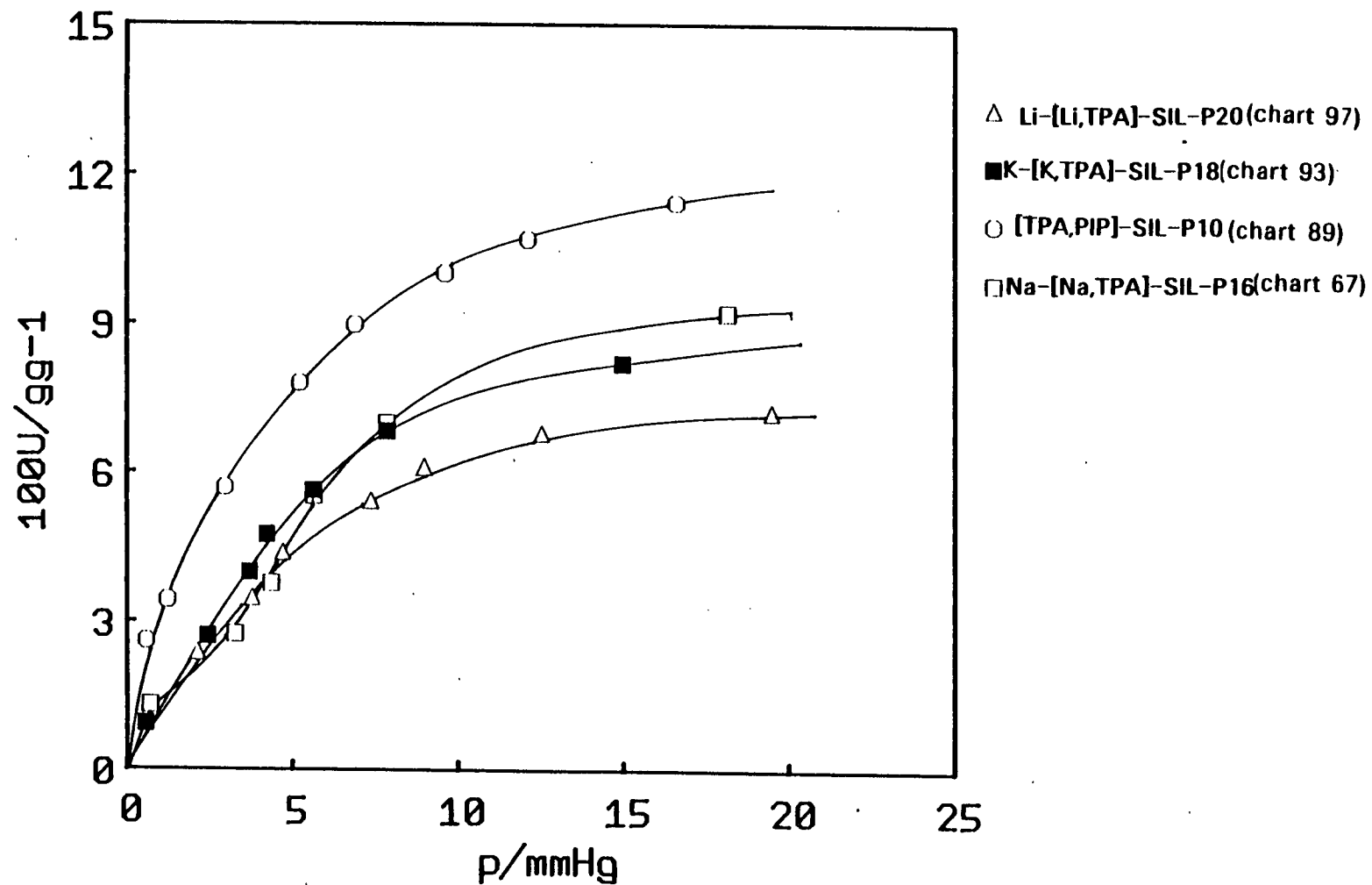


Figure 3.19

Comparison of the uptake of methanol by the different cation forms of silicalite, Li-[Li,TPA]-SIL-P20, Na-[Na,TPA]-SIL-P16, K-[K,TPA]-SIL-P18 and [TPA,PIP]-SIL-P10.

isotherms were determined at 24, 23, 22.5 and 23°C respectively. The most striking feature of this set of isotherms is that the sorption isotherm of [TPA,PIP]-SIL lies well above those of the cation forms of silicalite. Because [TPA,PIP]-SIL contains no cations in its channels the pore space available to sorbate molecules is greater than in the cation forms of silicalite. Comparison of the uptakes of methanol by the different cation forms of silicalite at high pressures show that the uptakes are in the order of Na-[Na,TPA]-SIL-P16 = K-[K,TPA]-SIL-P18 > Li-[Li,TPA]-SIL-P20. The sodium and potassium forms have similar numbers of cations per unit cell, and so similar uptakes. The uptake of methanol by the lithium form is lower than the uptakes by the others. The number of Li<sup>+</sup> ions per unit cell was found to be 11 which exceeds the number of sodium or potassium ions in the equivalent frameworks.

The shape of the isotherms can provide information about the interaction of methanol molecules with the silicalite frameworks. The [TPA,PIP]-SIL and Li-[Li,TPA]-SIL show type 1 isotherms whereas Na-[Na,TPA]-SIL and K-[K,TPA]-SIL give isotherms that have a distinct s-shape.

#### **3.12.4 Uptake of Water by Silicalite**

Water is not sorbed to pore filling by silicalite because it is a more polar molecule than methanol and its uptake is very dependent on the number of hydrophilic sites.

##### **Uptake of water by [TPA,PIP]-SIL-P10**

The sorption isotherms of the uptake of water by [TPA,PIP]-SIL at 24, 36 and 48°C are shown in Figure 3.20.

These isotherms fit the Langmuir isotherm equation. The Langmuir plots

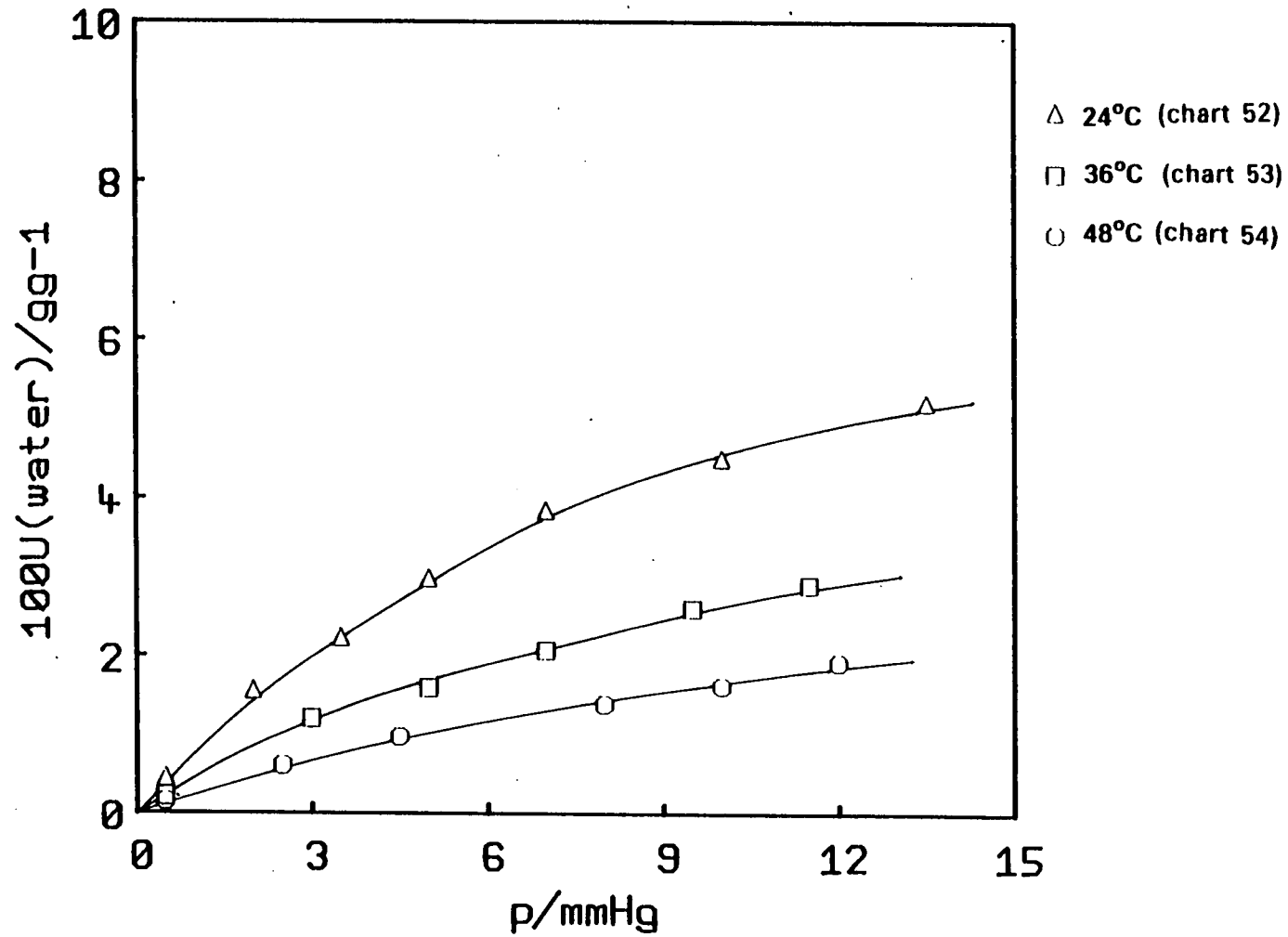


Figure 3.20

Water sorption isotherms of [TPA,PIP]-SIL-P10 at 24, 36 and 48°C.

are shown in Figure 3.21. The maximum uptakes and equilibrium constants are given in the table below.

<u>T/°C</u>	<u>U<sub>max</sub>/gg<sup>-1</sup></u>	<u>K/mmHg<sup>-1</sup></u>
24	0.0899	0.1011
36	0.0661	0.0672
48	0.0398	0.0705

The equilibrium constants are low compared with those of n-heptane(2.7mmHg<sup>-1</sup>) and p-xylene(5.0mmHg<sup>-1</sup>). This is indicative of weak sorbate-sorbent interactions. The maximum uptake varies linearly with temperature as shown in Figure 3.22. The large variation of U<sub>m</sub> is probably a consequence of water not filling the pores to capacity.

The variation of the isosteric heat of sorption, q<sub>st</sub>, with the uptake of water, U, is shown in Figure 3.23. The molar enthalpy condensation for water is 44.35 kJ mol<sup>-1</sup> and is shown as a dashed line on the plot. It is observed that at low uptakes of water, q<sub>st</sub> is less than or close to the value of the heat of condensation. The reason for this is that the heat of condensation involves contributions from four hydrogen bonds that link each molecule to its nearest neighbours. The dimensions of the channels of silicalite prohibit such extensive interactions. The increase of q<sub>st</sub> with U may be due to two factors as discussed with the uptake of methanol by silicalite. At higher uptakes water-water interactions may become significant and the hydroxylation of the internal surface may occur increasing the interaction between internal hydroxyl groups and water molecules.

#### **Uptake of Water by Cation forms of Silicalite**

The isotherms of uptakes of water by various cation forms of silicalite are shown in Figure 3.24. Na-[Na,TPA]-SIL-P-16 and [TPA,PIP]-SIL-P14 have similar

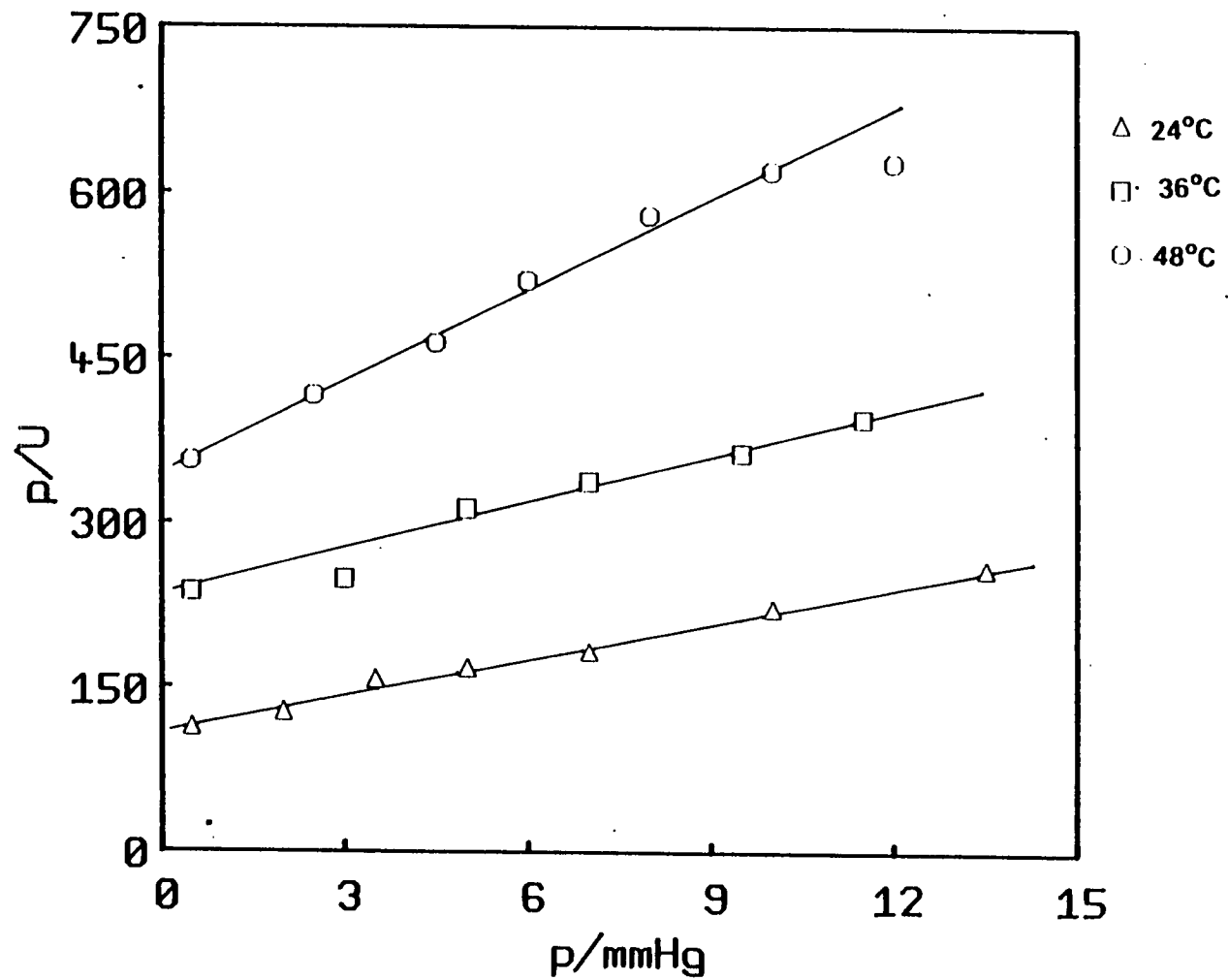


Figure 3.21

Langmuir plots of the water sorption isotherms shown in Figure 3.20.

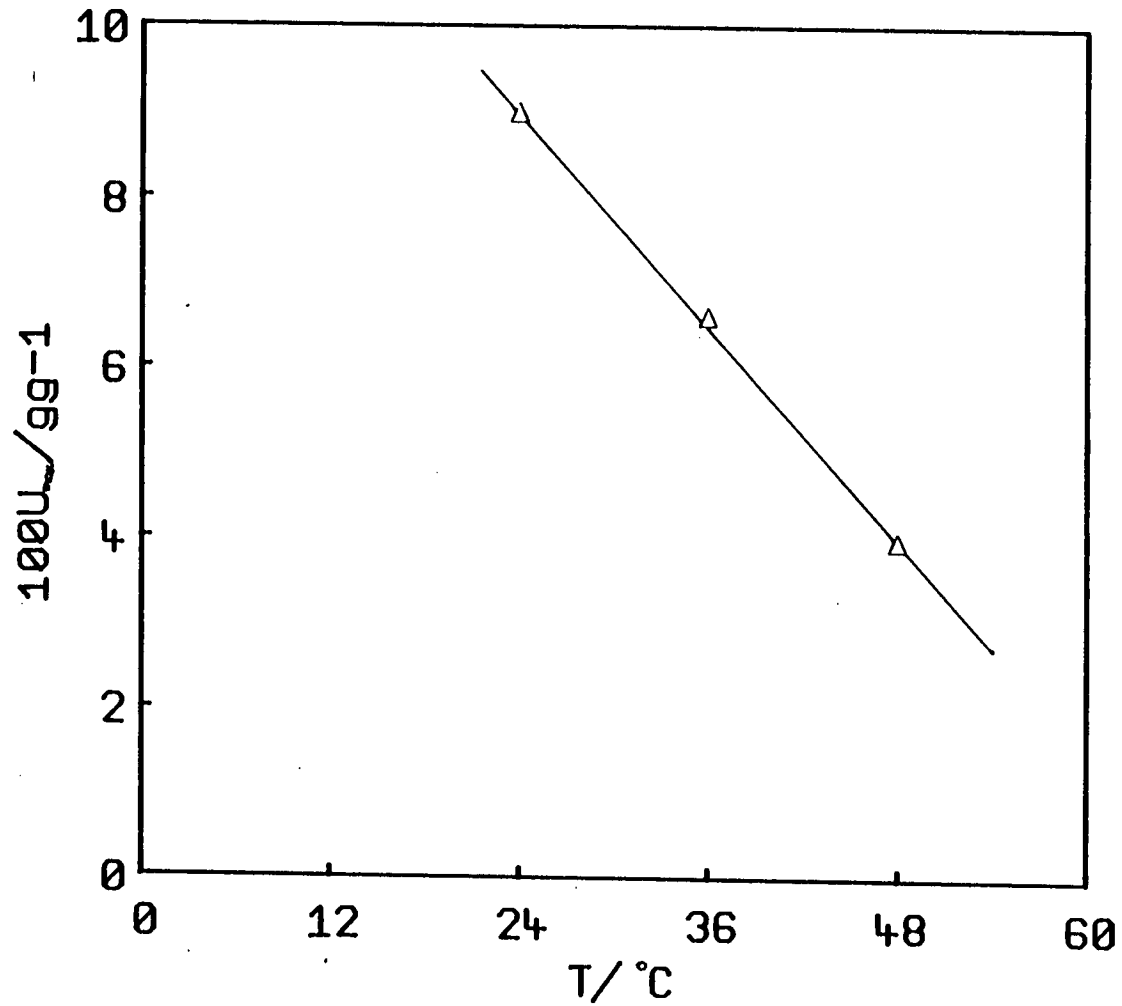


Figure 3.22

The variation of the maximum uptake of water,  $U_{\max}$ , by [TPA,PIP]-SIL with temperature,  $T$ .

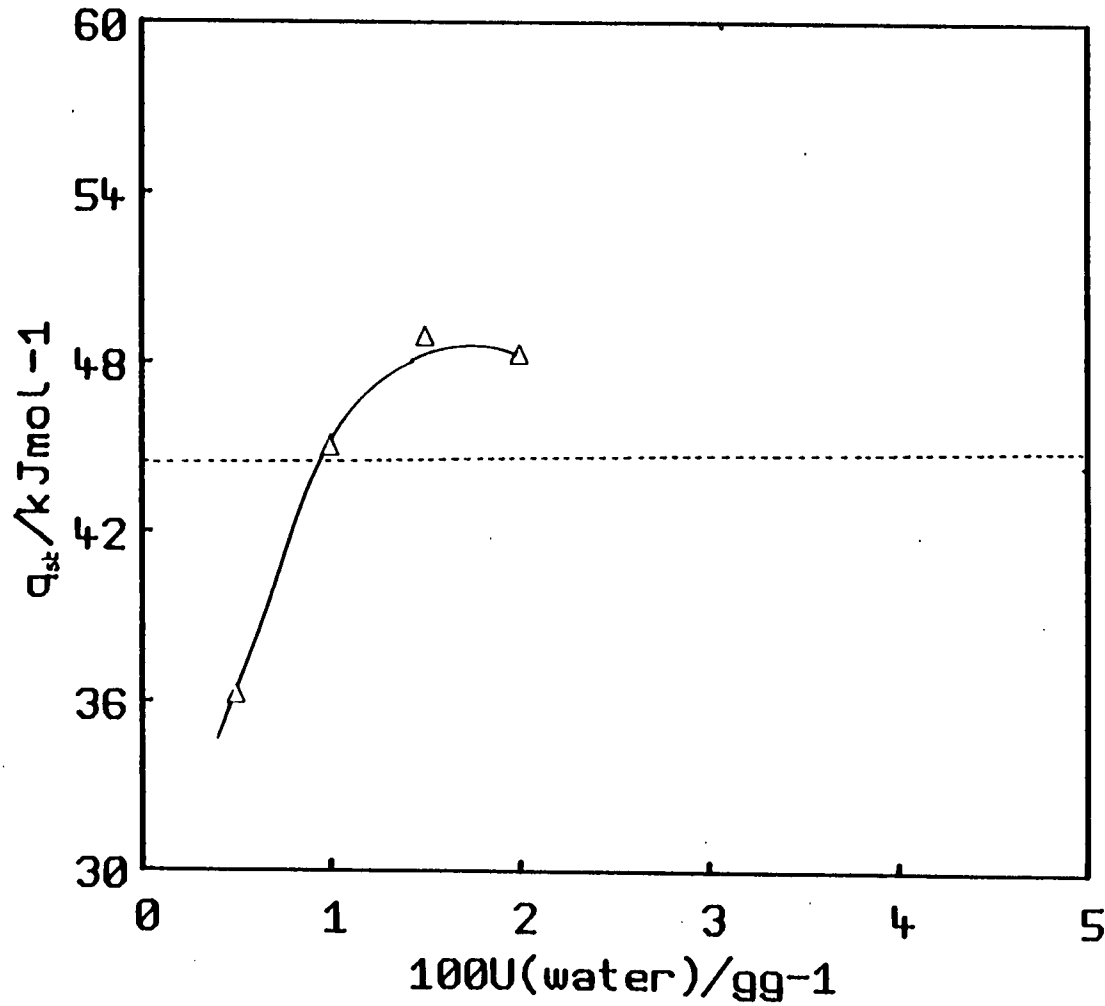


Figure 3.23

Variation of the isosteric heat of sorption,  $q_{st}$ , of water by [TPA,PIP]-SIL-P14 with the uptake of water,  $U$ .

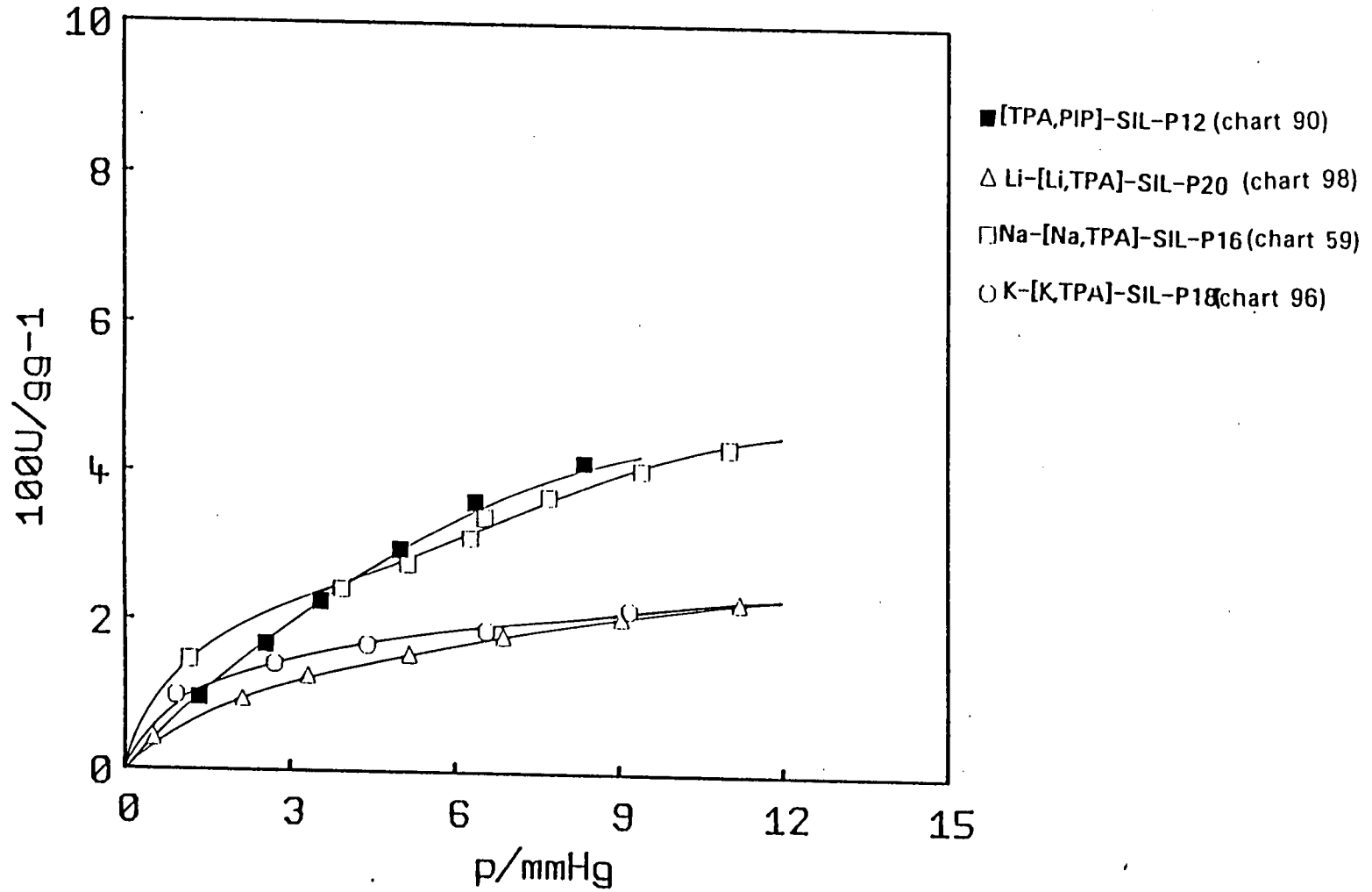


Figure 3.24

Comparison of the uptake of water by the different cation forms of silicalite.



isotherms which lie above the isotherms of Li-[Li,TPA]-SIL-P-20 and K-[K,TPA]-SIL-P-18. It is difficult to explain the uptakes of water by the different cation forms of silicalite. The uptakes are in increasing order of uptake,  $\text{Na} > \text{K} > \text{Li}$  forms of silicalite.

But the enthalpies of hydration, which are a measure of the strength of interaction between the cation and the water molecule, are shown below.

<u>cation</u>	<u><math>\Delta H/\text{kJmol}^{-1}</math></u>
$\text{Li}^+$	-520
$\text{Na}^+$	-400
$\text{K}^+$	-320

It would be expected from these values - particularly at low pressures - that the uptake of water would be greatest for Li-[Li,TPA]-SIL-P20. However, the strength of the molecular-sieve/cation interaction will also be significant. The lithium cation is likely to interact most strongly with the silicalite surface. If it is bound very tightly, it may be less able to interact with the water.

### 3.12.5 Low Pressure Hysteresis of Isotherms

In many of the isotherms discussed previously, the desorption isotherms do not coincide with the sorption isotherms. This is an unusual phenomena in molecular sieves; it is generally accepted that sorption by molecular sieves does not usually exhibit hysteresis. The hysteresis is found to occur in the low pressure region. An explanation for this can found by considering the sorption of polar molecules on silica surfaces. As mentioned in section 3.8, sorption isotherms of water on silica surfaces exhibit low pressure hysteresis. It is in this case attributed to hydroxylation of the surface during isotherm determination. The sorption and desorption curves of the uptake of water and

methanol on silicalites pretreated and synthesised differently are shown in Figures 3.25 - 3.37.

#### **Methanol + [TPA,PIP]-SIL-P14**

The sorption/desorption curve for the equilibration of methanol with [TPA,PIP]-SIL-P14 at 23°C is shown in Figure 3.25. It is observed that the curves are almost coincident except at very low pressures of sorbate. The difference between the sorption and desorption curves is less than  $0.005\text{gg}^{-1}$  which is almost within experimental error. A difference of less than 1°C in sample temperature could produce this magnitude of variation in the isotherm.

#### **Water + [TPA,PIP]-SIL-P14**

Figure 3.26 shows the sorption and desorption of water by [TPA,PIP]-SIL-P14. It is apparent that the two curves do not coincide and that the desorption curve lies well above the sorption curve. This is most pronounced at low pressures.

#### **Methanol + K-[K,TPA]-SIL-P18**

The sorption and desorption curves shown in Figure 3.27 are seen to coincide at higher pressures but at lower pressures they are seen to diverge, the sorption curve being lower than the desorption curve.

#### **Water + K-[K,TPA]-SIL-P18**

The sorption and desorption curves from two separate runs are shown in Figure 3.28. The desorption curve lies above the sorption curve, and it appears that the hysteresis is reproducible.

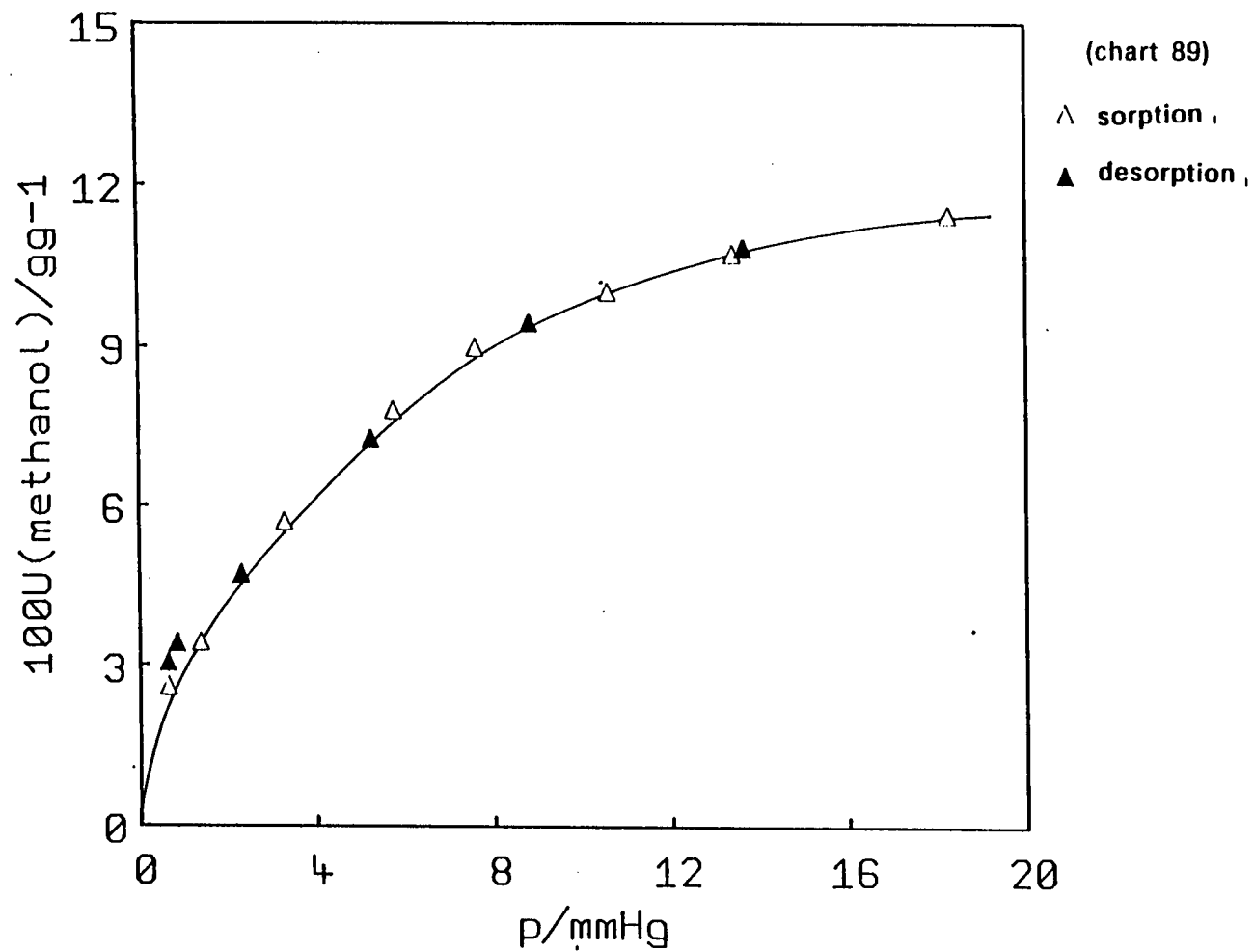


Figure 3.25

Sorption/desorption of methanol by [TPA,PIP]-SIL-P14  
at 23°C.

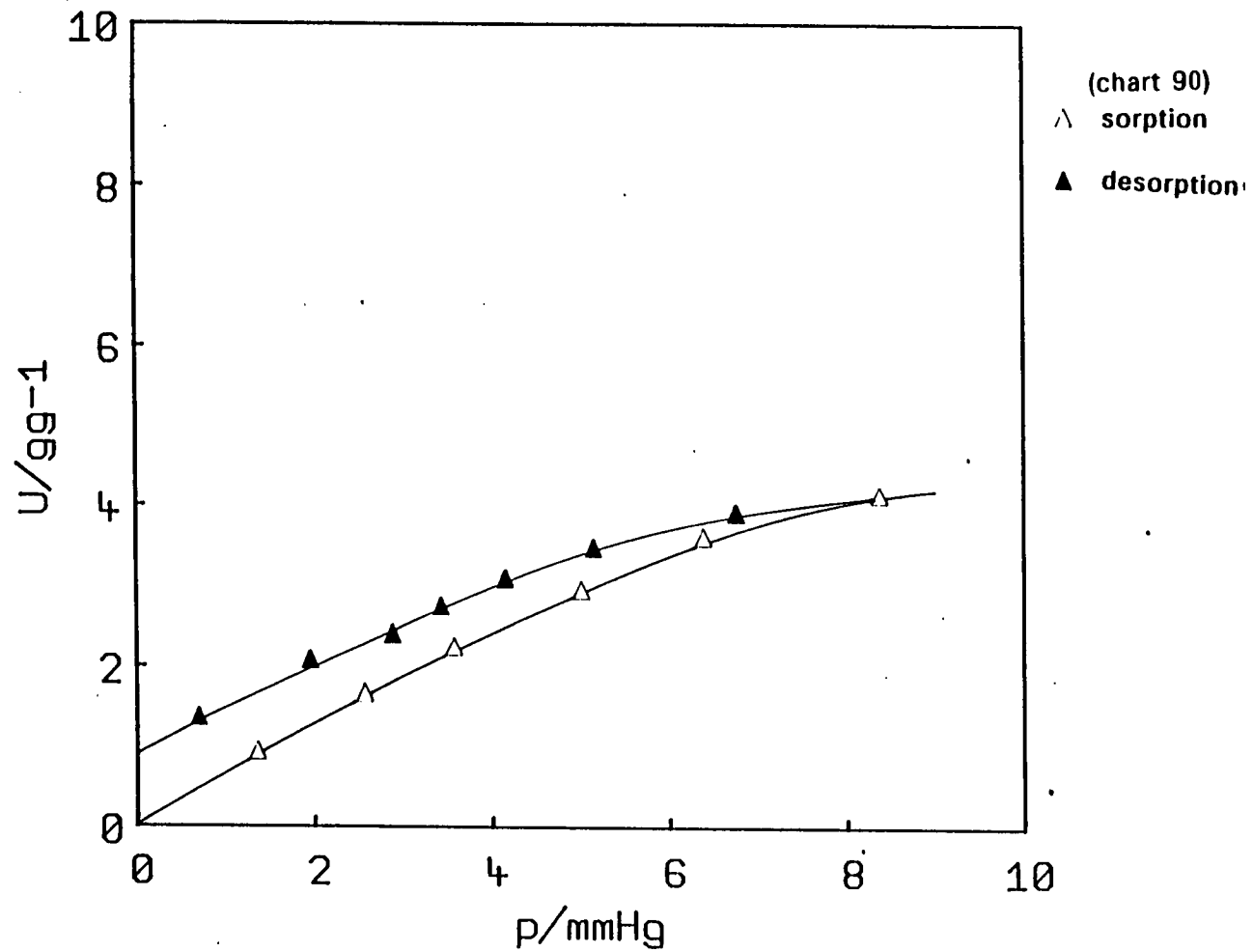


Figure 3.26

Sorption/desorption of water by [TPA,PIP]-SIL-P14  
at 23°C.

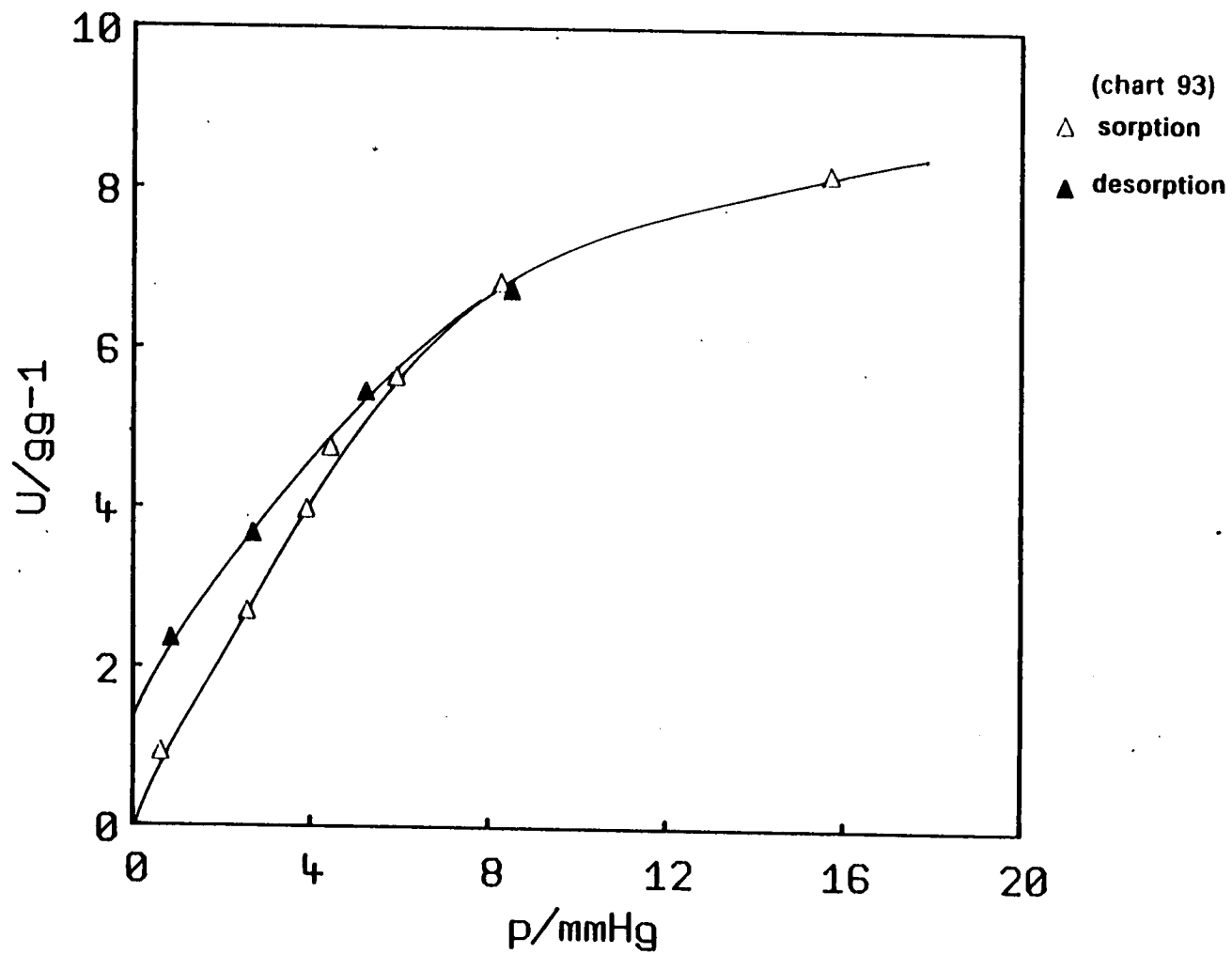


Figure 3.27

Sorption/desorption of methanol by K-[K,TPA]-SIL-P18  
at 23°C.

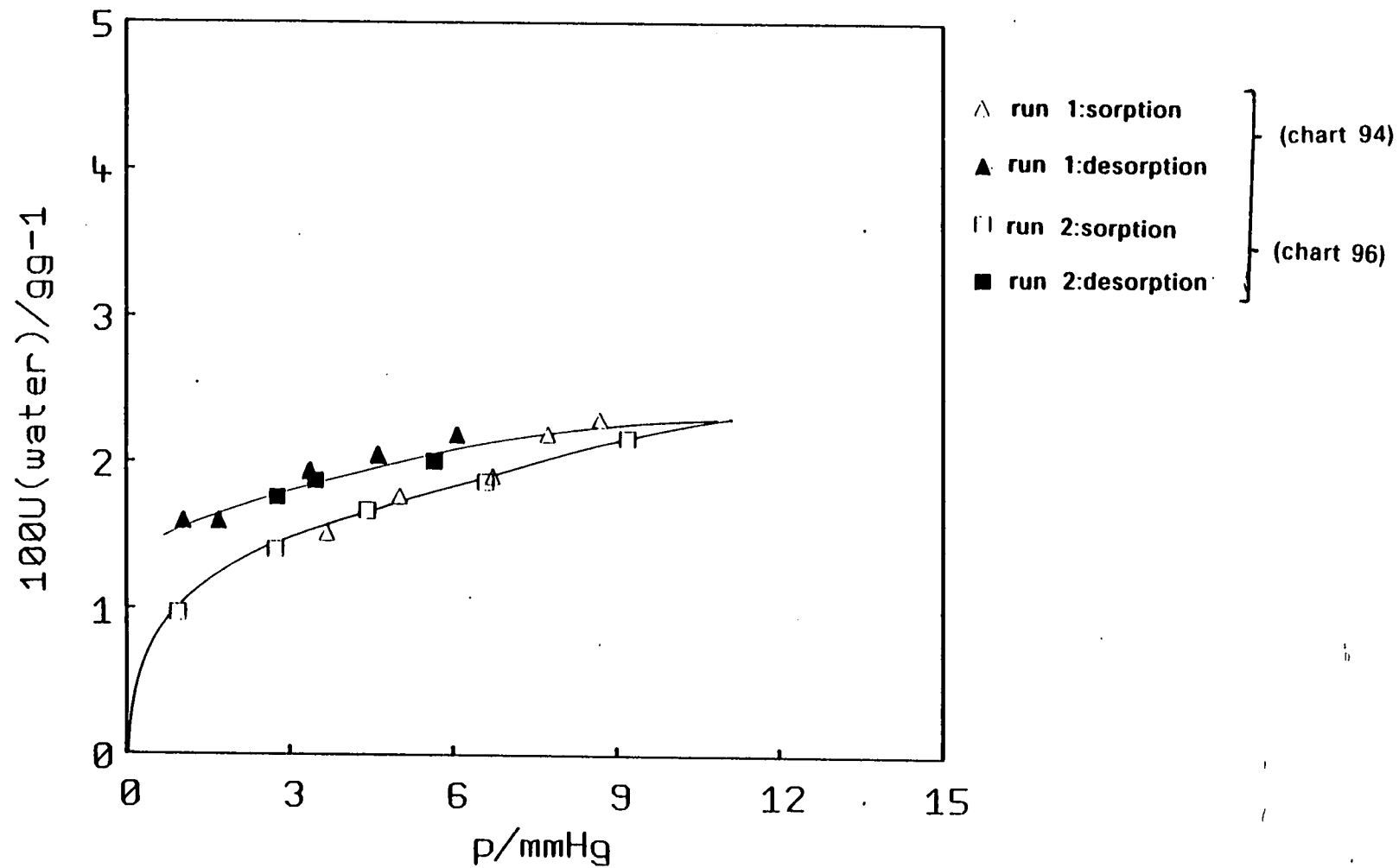


Figure 3.28

Sorption/desorption of water by K-[K,TPA]-SIL-P18.  
The results from two separate runs are plotted.

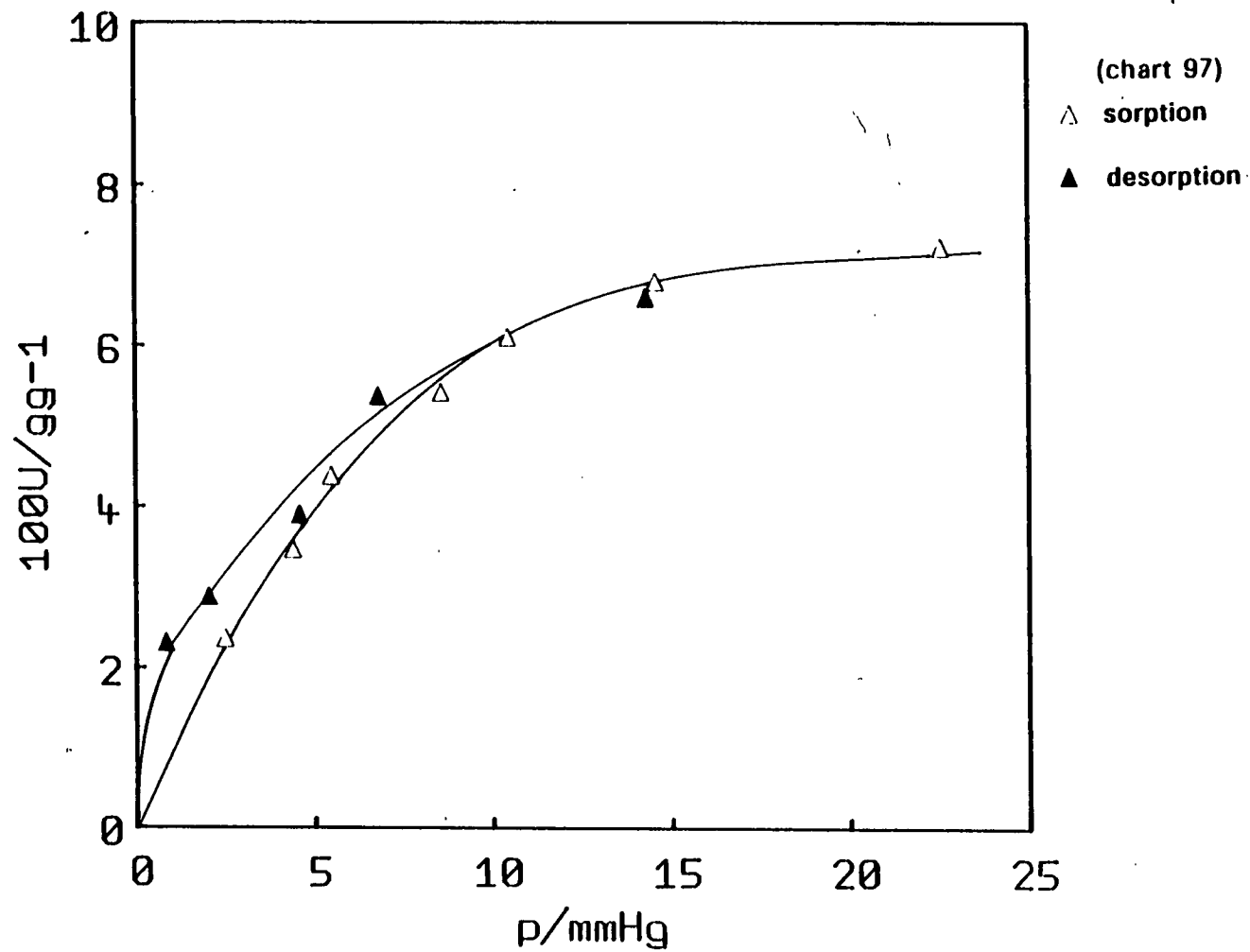


Figure 3.29

Sorption/desorption of methanol by Li-[Li,TPA]-SIL-P20  
at 24°C.

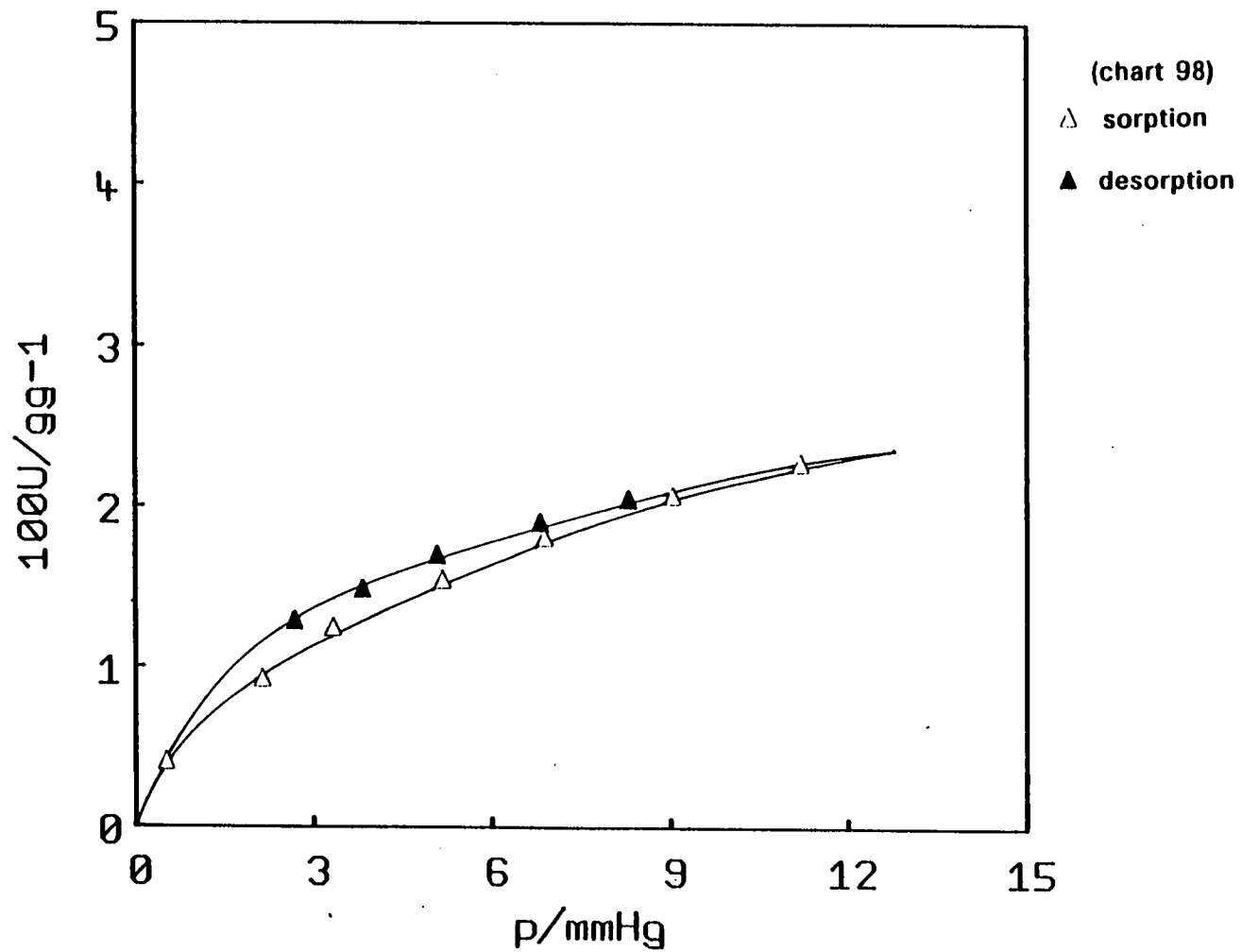


Figure 3.30

Sorption/desorption of water by Li-[Li,TPA]-SIL-P20  
at 24°C.



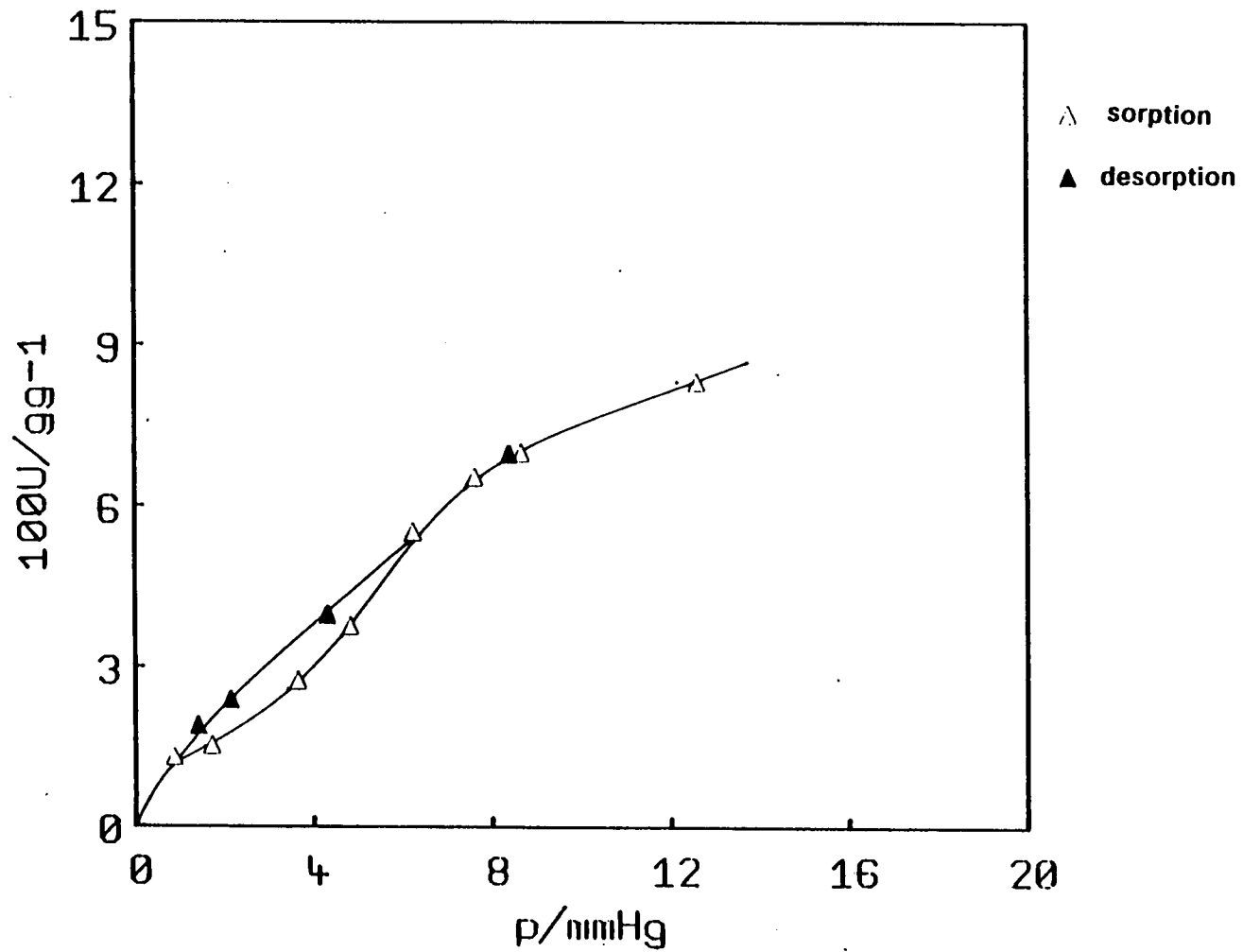


Figure 3.31

Sorption/desorption of methanol by Na-(Na,TPA)-SIL-P16  
23°C.

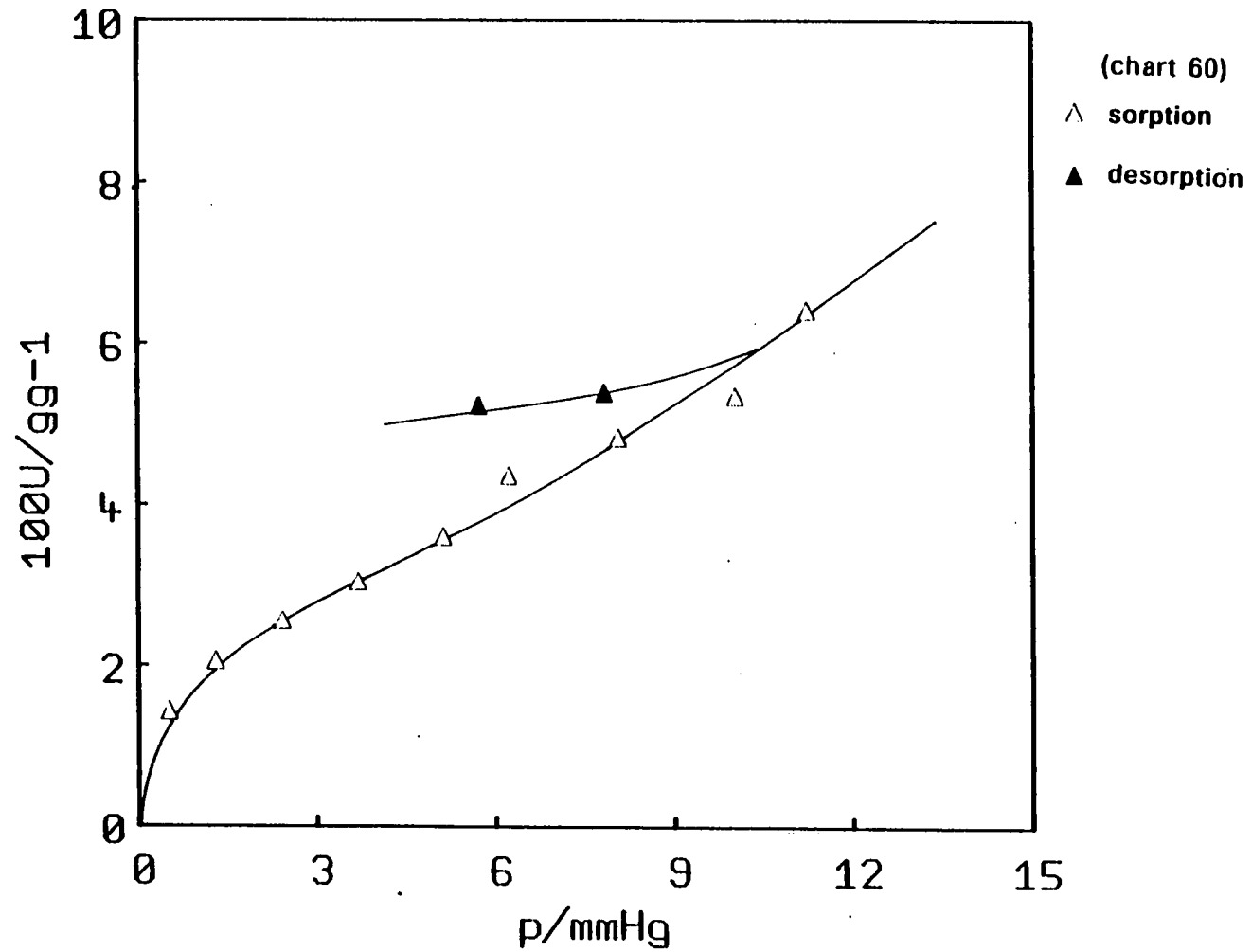


Figure 3.32

Sorption/desorption of water by Na-[Na,TPA]-SIL-P16  
at 23°C.

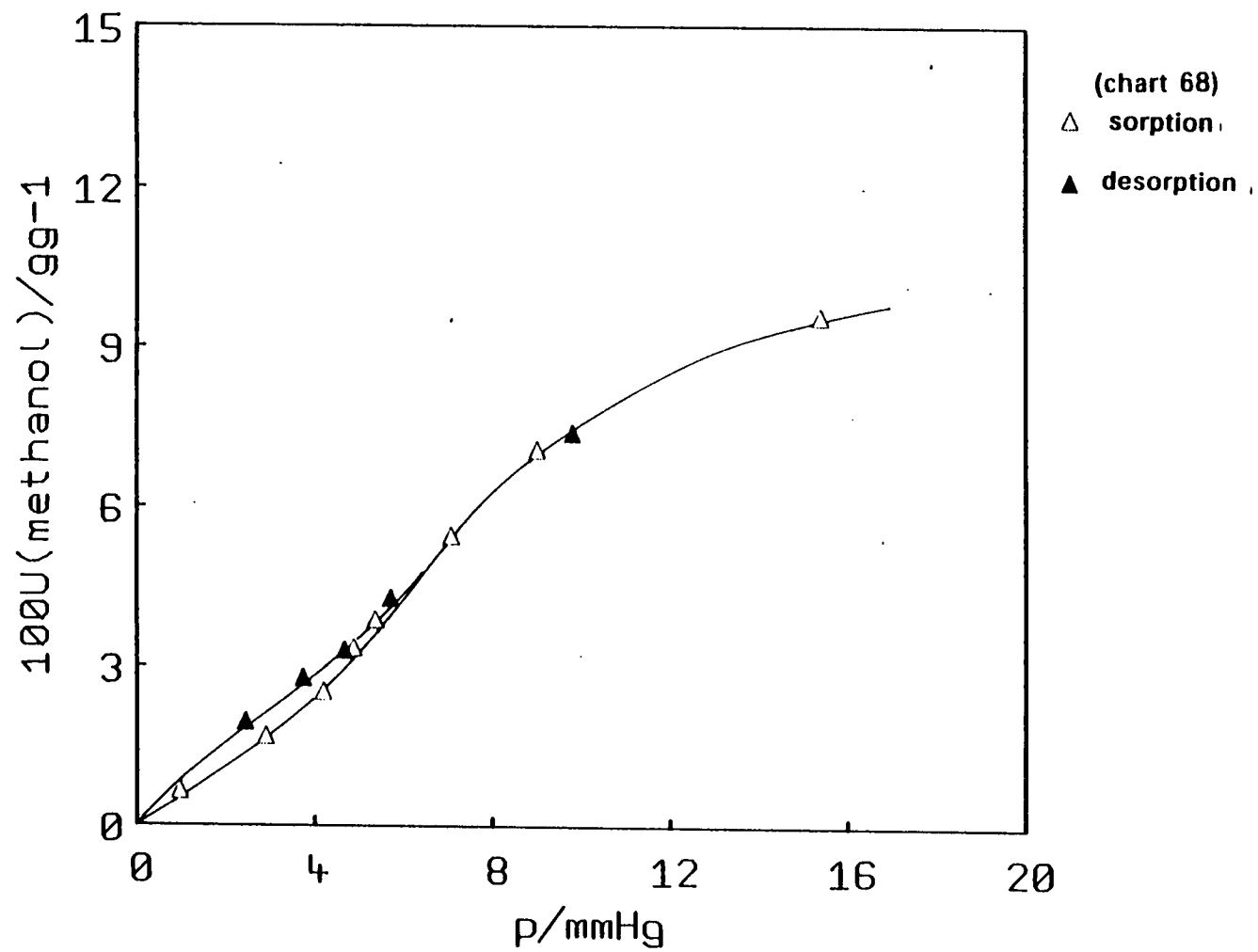


Figure 3.33

Sorption/desorption of methanol by H-[Na,TPA]-SIL-P16  
at 25°C.

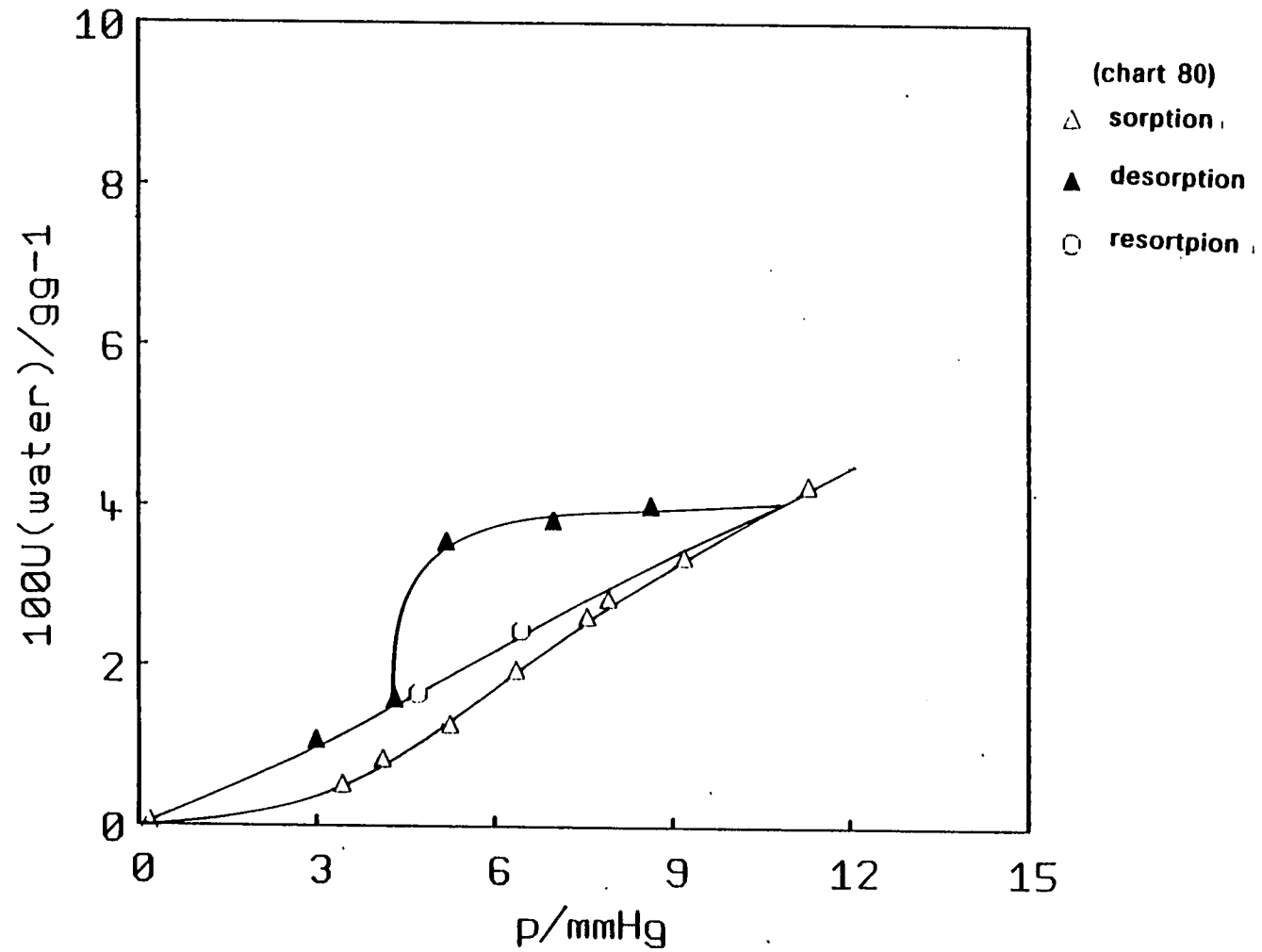


Figure 3.34

Sorption/desorption of water by H-[Na,TPA]-SIL-P16  
at 13°C.

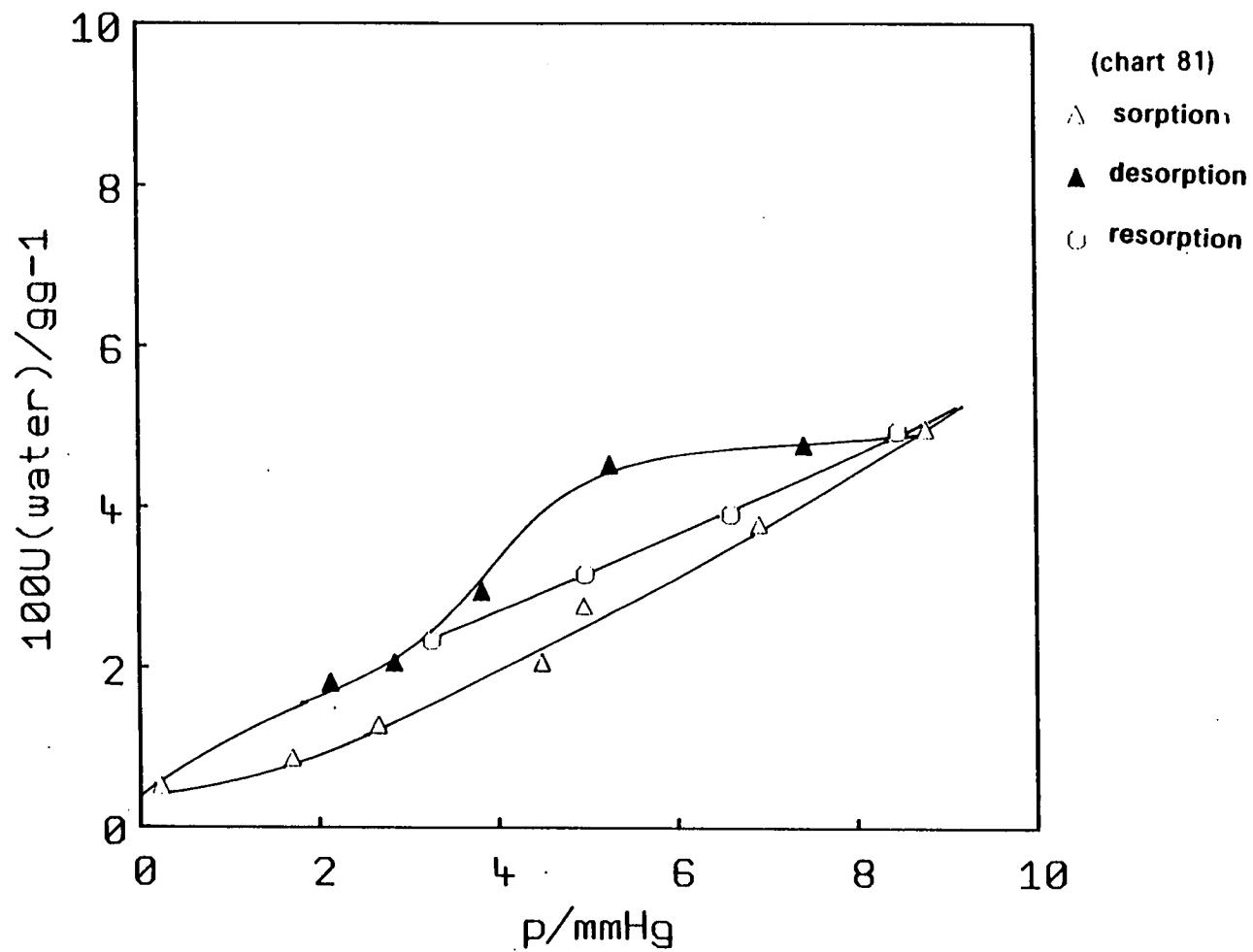


Figure 3.35

Sorption/desorption of water by H-[Na,TPA]-SIL-P16  
at 17°C.

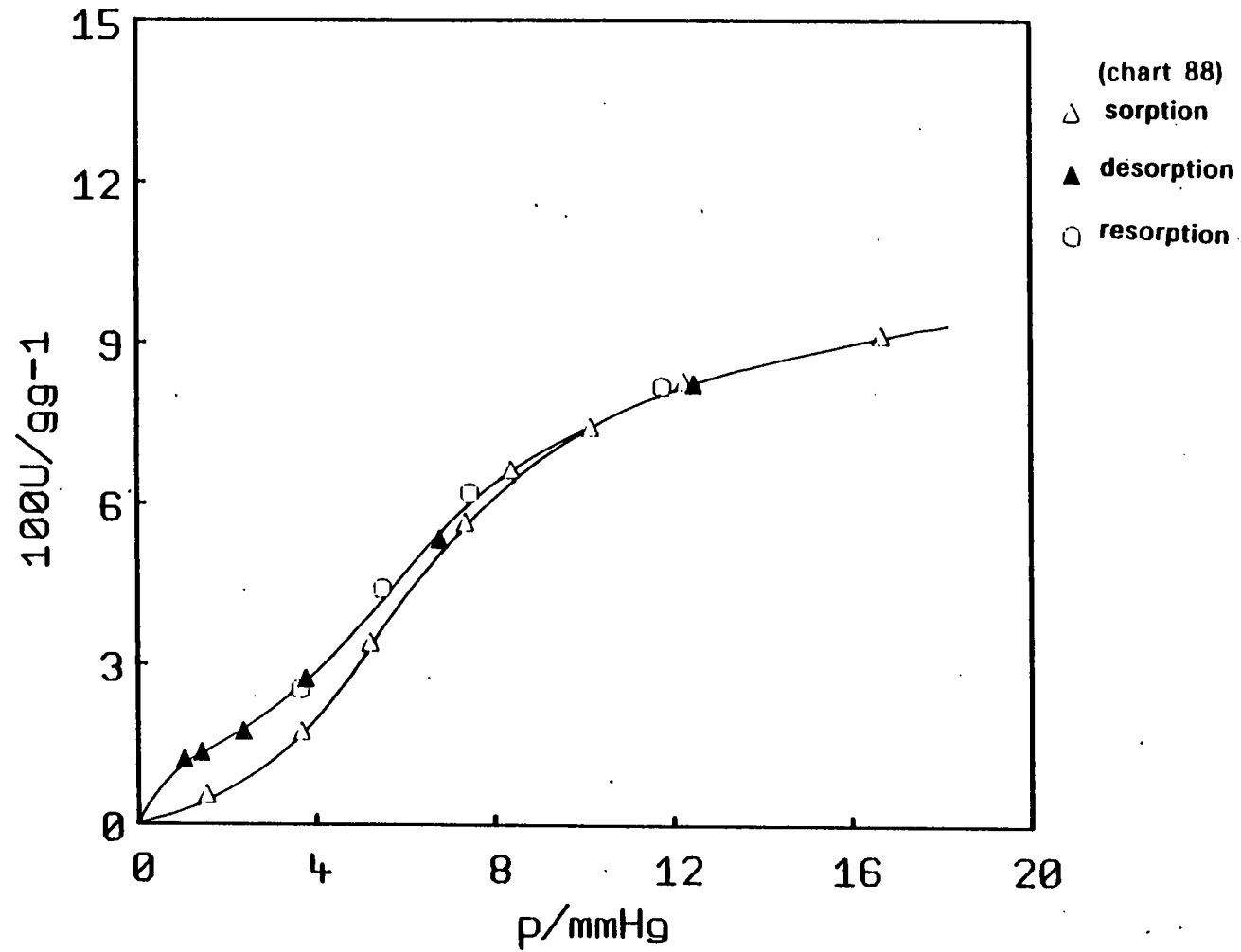


Figure 3.36

Sorption/desorption/resorption of methanol by  
H-(800°C)-[Na,TPA]-SIL-P16.

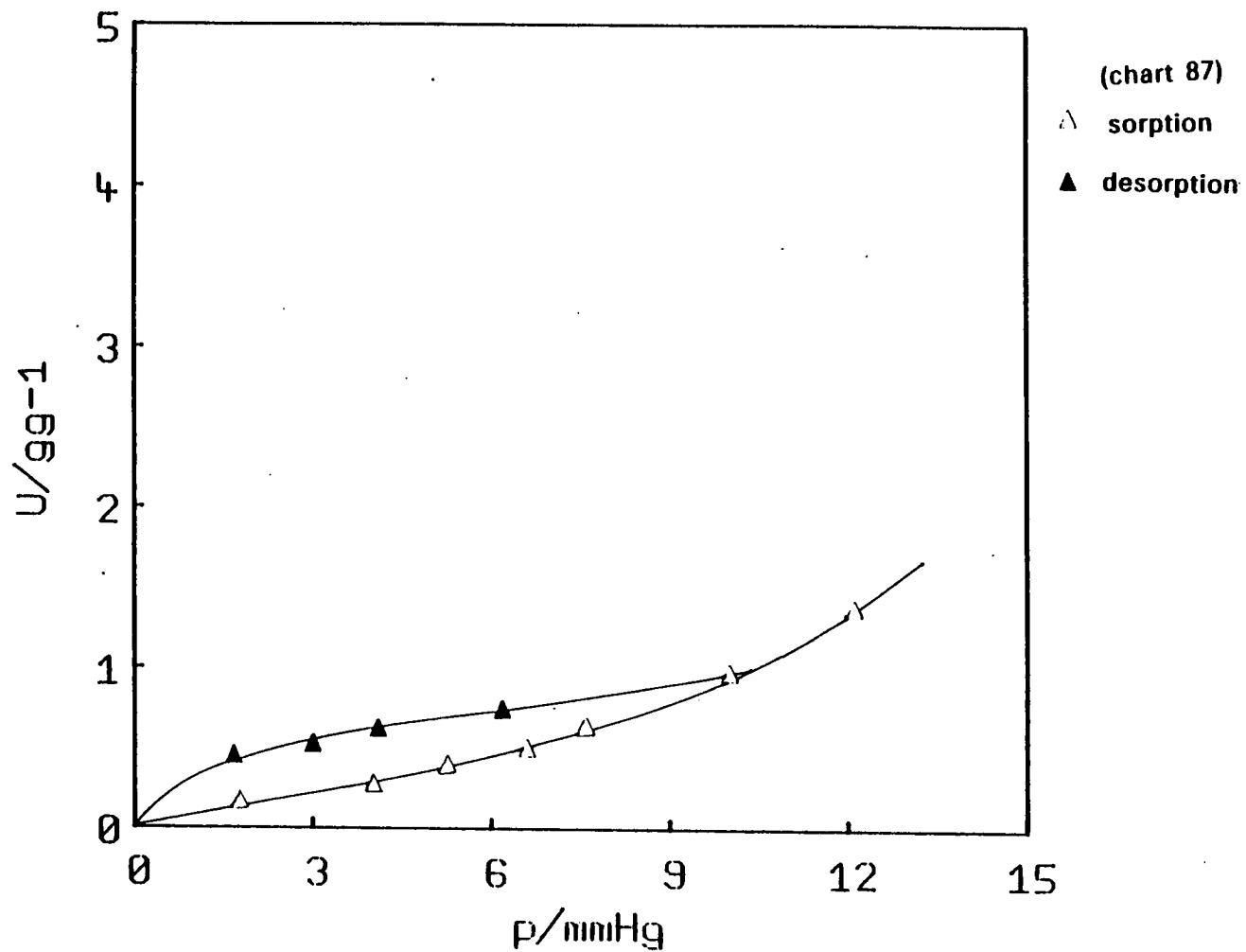


Figure 3.37 Sorption/desorption of water by H-(800°C)-[Na,TPA]-SIL

### **Methanol + Li-[Li,TPA]-SIL-P20**

The sorption and desorption curves seen in Figure 3.29 nearly coincide except at very low pressures where a small amount of hysteresis is observed.

### **Water + Li-[Li,TPA]-SIL-P20**

The sorption of water by this form of silicalite exhibits only a small amount of low pressure hysteresis as shown in Figure 3.30.

### **Methanol + Na-[Na,TPA]-SIL-P16**

In Figure 3.31, the sorption and desorption curves are observed to coincide at higher pressures but at lower pressures hysteresis is observed. It is also noticed that the sorption curve exhibits an S-shape isotherm whereas the desorption curve is much smoother in shape.

### **Water + Na-[TPA,PIP]-SIL-P16**

Considerable hysteresis is observed in this sorption system as shown in Figure 3.32.

### **Methanol + H-[Na,TPA]-SIL-P16**

The sorption and desorption curves lie very close together except at very low pressures as seen in Figure 3.33.

### **Water + H-[Na,TPA]-SIL-P16**

The sorption and desorption curves were obtained in the usual manner for this sorption system. But after the desorption curve was obtained, the silicalite was again exposed to water and the resorption curve found as shown in Figure 3.34. The shape of the isotherm was unexpected and the run was repeated



again to check that it was reproducible. It was, as shown in Figure 3.35. The desorption curve lies well above the first sorption curve at all pressures. However instead of the hysteresis being most extreme at low pressures, greatest hysteresis is observed at intermediate pressures. The shape of the desorption curve is also different from those observed in previous systems. The resorption curve follows the desorption curve at low uptakes but lies below it at higher uptakes. It is as if there are two different effects causing hysteresis in this case.

#### **Methanol + H-{800°C}-[TPA,PIP]-SIL-P16**

Sorption, desorption and resorption curves were obtained for this system. It is observed that as shown in Figure 3.36, at higher pressures all three curves coincide but at lower pressures the desorption curve lies above the first sorption curve. However, it is noted that the desorption and resorption curves coincide. All the isotherms show a distinct S-shape.

#### **Water + H-{800°C}-[TPA,PIP]-SIL-P16**

Considerable hysteresis is observed at all pressures as shown in Figure 3.37.

### **3.12.6 Hydroxylation and Methoxylation of Silicalite**

The extent of hysteresis observed in the isotherms of water or methanol is believed to be a measure of the amount of hydroxylation or methoxylation that occurs during the determination of the isotherm. This indicates the susceptibility of the Si-O-Si bonds to break and form hydroxyl or methoxyl groups on exposure to water or methanol vapour.

Hysteresis does not indicate the number of hydroxyl groups that are

present in the sample before isotherm determination. This quantity is given by the initial uptake of polar molecules at low sorbate pressure.

Both the number of hydroxyl groups present initially and the amount of hydroxylation and methoxylation that occurs on exposure to water or methanol vapour are dependent on the nature and pretreatment of the silicalite.

The [TPA,PIP]-SIL-P14 is observed to uptake a quantity of water comparable to that of Na-[Na,TPA]-SIL-P16. Since there are few cations present in the channels, this suggests that there are a number of hydroxyl groups in the silicalite as a consequence of synthesis and pretreatment. As discussed previously, the presence of piperazine in the reaction mixture may increase the number of internal hydroxyl groups formed. These are not removed even during subsequent heating at elevated temperatures. However, the hysteresis observed in the isotherms of water and methanol for this particular silicalite suggest that subsequent formation of hydroxyl and methoxyl groups does not occur as readily as with other silicalite samples.

All the cation forms of silicalite exhibit hysteresis in their isotherms, although the extent varies with the nature of the cation. Both the sodium and potassium forms are observed to exhibit hysteresis in the low pressure region. Methoxylation and hydroxylation of the silicalite surface occurs during the course of isotherm determination. Surprisingly, the lithium form of silicalite shows very little hysteresis in its isotherms. This suggests that very little methoxylation or hydroxylation of the surface occurs which may be a result of the lithium cation being very tightly bound to the silicalite framework.

Extensive hysteresis is observed in the isotherms of H-[Na,TPA]-SIL. The

removal of the sodium ions from the structure renders the silicalite surface more susceptible to hydroxylation and methoxylation. The unusual shape of the hysteresis curve in the isotherms of water is difficult to explain particularly, as it is not observed for H-{800°C}-[Na,TPA]-SIL-P16.

The isotherms of H-{800°C}-[Na,TPA]-SIL-P16 do not exhibit as extensive hysteresis as H-[Na,TPA]-SIL. Calcination of the sample at 800°C leads to the healing of some of the internal hydroxyl groups and further reduces the susceptibility of the silicalite surface to hydroxylation and methoxylation.

### 3.12.7 Uptake of Water by Various Forms of Silicalite

Silicalite is usually considered to be a hydrophobic molecular sieve and as a consequence it might be expected that the uptake of water would be negligible. However as described above it is found experimentally that the uptake of water is not only significant but dependent on such factors as calcination temperature, and type of cation present. It was therefore decided to use the "multi-equilibration" method to measure the uptake of water by various forms of silicalite subjected to a number of different pretreatments. For these experiments the water vapour pressure was controlled at  $a_w = 0.753$  using saturated NaCl solution.

It was observed that the uptake of water by silicalite also varies with the time allowed for equilibration, and that the variation takes place over several days or even weeks, or months. The variation may result in an increase or decrease in the uptake of water dependent on the type of silicalite under investigation and its pretreatment. If, after the silicalite has been equilibrated for some time, the samples are reactivated at 400°C and then re-equilibrated over the same pressure of water vapour, the uptakes are found to be

significantly lower. The effect of various parameters are now discussed.

### **Effect of Calcination Temperature**

The uptake of water by silicalite samples that were initially calcined at different temperatures are shown in Table 3.9. It is observed that the fact that more broken siloxane bonds are healed at higher calcination temperatures means that there are fewer hydrophilic sites, less water is sorbed, and the molecular sieve becomes more hydrophobic.

### **Effect of Cations**

The uptake of water by different cation forms of silicalite are shown in Table 3.10. The uptakes of water by Li-[Li,TPA]-SIL-P and K-[K,TPA]-SIL-P18 are similar and lower than the uptakes of water by Na-[Na,TPA]-SIL-P16 and [TPA,PIP]-SIL-P14. This agrees well with the results obtained with the Cahn balance.

### **Effect of Soxhlet Extraction**

The effect of soxhlet extraction of cation forms of silicalite on the sorption of water is shown in Table 3.11. The effect of this treatment on Li-[Li,TPA]-SIL-P20 and Na-[Na,TPA]-SIL-P16 is to reduce the initial uptake of water. Soxhlet extraction of the samples removes ions from the channels and so the initial uptake of water tends to be reduced. However with such samples the uptake of water increases with time, whereas for the corresponding untreated forms the uptake of water decreases as the equilibration time increases.

### **Effect of Hydrogen Ion-exchange**

The uptakes of water by hydrogen ion-exchanged silicalite samples are

silicalite	1d	>10d
Na- [Na, TPA] -SIL-P18 (400°C)	0.088	0.108
Na- [Na, TPA] -SIL-P18 (550°C)	0.071	0.055
Na- [Na, TPA] -SIL-P18 (800°C)	0.030	0.043
Li- [Li, TPA] -SIL-P20 (400°C)	0.078	0.088
Li- [Li, TPA] -SIL-P20 (550°C)	0.048	0.037
Li- [Li, TPA] -SIL-P20 (800°C)	0.034	0.033

Table 3.9

The effect of calcination temperature on the uptake of water by silicalite.

silicalite	1d	>10d
Li- [Li, TPA] -SIL-P20 (550°C)	0.048	0.037
Na- [Na, TPA] -SIL-P18 (550°C)	0.071	0.055
K- [K, TPA] -SIL-P18 (550°C)	0.048	0.048
[TPA, PIP] -SIL-P10	0.053	0.053

Table 3.10

The effect of cations on the channels on the uptake of water by silicalite.

silicalite	1d	>10d
Li- [Li, TPA] -SIL-P20	0.048	0.037
soxhletLi [Li, TPA] -SIL-P20	0.025	0.028
Na- [Na, TPA] -SIL-P18	0.071	0.055
soxhletNa- [Na, TPA] -SIL-P18	0.036	0.051
K- [K, TPA] -SIL-P18	0.048	0.048
soxhletK- [K, TPA] -SIL-P18	0.048	0.084

Table 3.11

The effect of soxhlet extraction on the uptake of water by silicalite.

sample	1d	>10d
Li- [Li, TPA] -SIL-P20	0.048	0.037
H- [Li, TPA] -SIL-P20	0.035	0.038
H- (800 C) - [Li, TPA] -SIL-P20	0.018	0.021
Na- [Na, TPA] -SIL-P18	0.071	0.055
H- [Na, TPA] -SIL-P18	0.051	0.038
K- [K, TPA] -SIL-P18	0.048	0.048
H- [K, TPA] -SIL-P18	0.057	0.057
[TPA, PIP] -SIL-P10	0.053	0.053

Table 3.12

The effect of ion-exchange of silicalite on the uptake of water by samples.

given in Table 3.12. Hydrogen ion-exchange of the  $\text{Li}^+$ ,  $\text{Na}^+$  forms of silicalite results in a lower uptake of water initially. However after longer periods of equilibration the uptakes are similar to those of the cation forms. The silicalite, H-[K,TPA]-SIL-P18 seems to sorb slightly more water than the original cation form. The uptakes of water by hydrogen ion-exchange silicalites compare well with the uptake of water by [TPA,PIP]-SIL-P14. Calcination at  $800^\circ\text{C}$  after ion-exchange of the lithium form of silicalite considerably reduces the uptake of water. Heating the samples at elevated temperatures probably heals many of the internal hydroxyl groups.

### **Longer periods of equilibration**

To further examine the uptake of water by silicalite over longer periods of time the following experiment was carried out. Six dishes from a six-seater isopiestic block were weighed and different forms of silicalite were placed in each dish. These dishes were then equilibrated over saturated NaCl solution ( $a_w = 0.753$ ) in contact with excess solid salt.

The dishes were weighed after 1d, 14d and 73d. After this time thermal analysis was carried out on each sample to find the weight of silicalite in each dish from which  $U_{\text{H}_2\text{O}}$  could be calculated. It was also of interest to observe the shape of the desorption curve for the water in the different samples. The uptakes of water by these samples are shown in Table 3.13.

It should be noted that there are differences between this experiment and previous "multi-equilibration" experiments. The silicalite added to the dishes in this experiment had not been activated but had been equilibrated with the atmosphere. This explains why the initial values are higher than obtained by the "multi-equilibration" technique. The uptakes after 73d are in all cases

silicalite	1d	14d	73d
Na- [Na, TPA] -SIL-P18	0.062	0.090	0.121
H- [Na, TPA] -SIL-P18	0.075	0.105	0.177
K- [K, TPA] -SIL-P18	0.068	0.094	0.105
H- [K, TPA] -SIL-P18	0.068	0.098	0.128
soxhletK- [K, TPA] -SIL-P18	0.060	0.076	0.097
[TPA, PIP] -SIL-P10	0.067	0.099	0.117

Table 3.13

Uptakes of water by silicalites after equilibration of 1d, 14d and 73d.



considerable and approach pore filling. The hydrophobicity of the molecular sieve has been reduced.

The TG traces are shown in Figure 3.38. These traces show some unusual features. In some of the traces, the desorption of water is observed to occur in definite stages.

Both Na-[Na,TPA]-SIL-P16 and K-[K,TPA]-SIL-P18 show similar curves, which are initially concave in shape. This suggests that most of the water present is co-ordinated with the cations in the silicalite framework.

The trace for the desorption of water from [TPA,PIP]-SIL-P10 exhibits two distinct steps. The shape of this trace suggests that there are two different types of sorbed water present in the silicalite channels i.e. (a) water that is only loosely sorbed and co-ordinated only to other water molecules and (b) water that is more tightly bound - presumably co-ordinated to hydroxyl groups in the channels. There is a small continuous weight loss that occurs at  $> 400^{\circ}\text{C}$  which is probably due to the healing of hydroxyl groups with the elimination of water.

The H-[Na,TPA]-SIL-P16 and H-[K,TPA]-SIL-P18 samples show similar curves suggesting again two types of sorbed water is present. A slight continuous weight loss at  $> 400^{\circ}\text{C}$  is again observed.

### **3.13 Conclusion**

The results discussed in this Chapter show that the sorption properties of silicalite are dependent on the preparation and pretreatment of samples. When examining the sorption properties of silicalite - particularly the sorption of

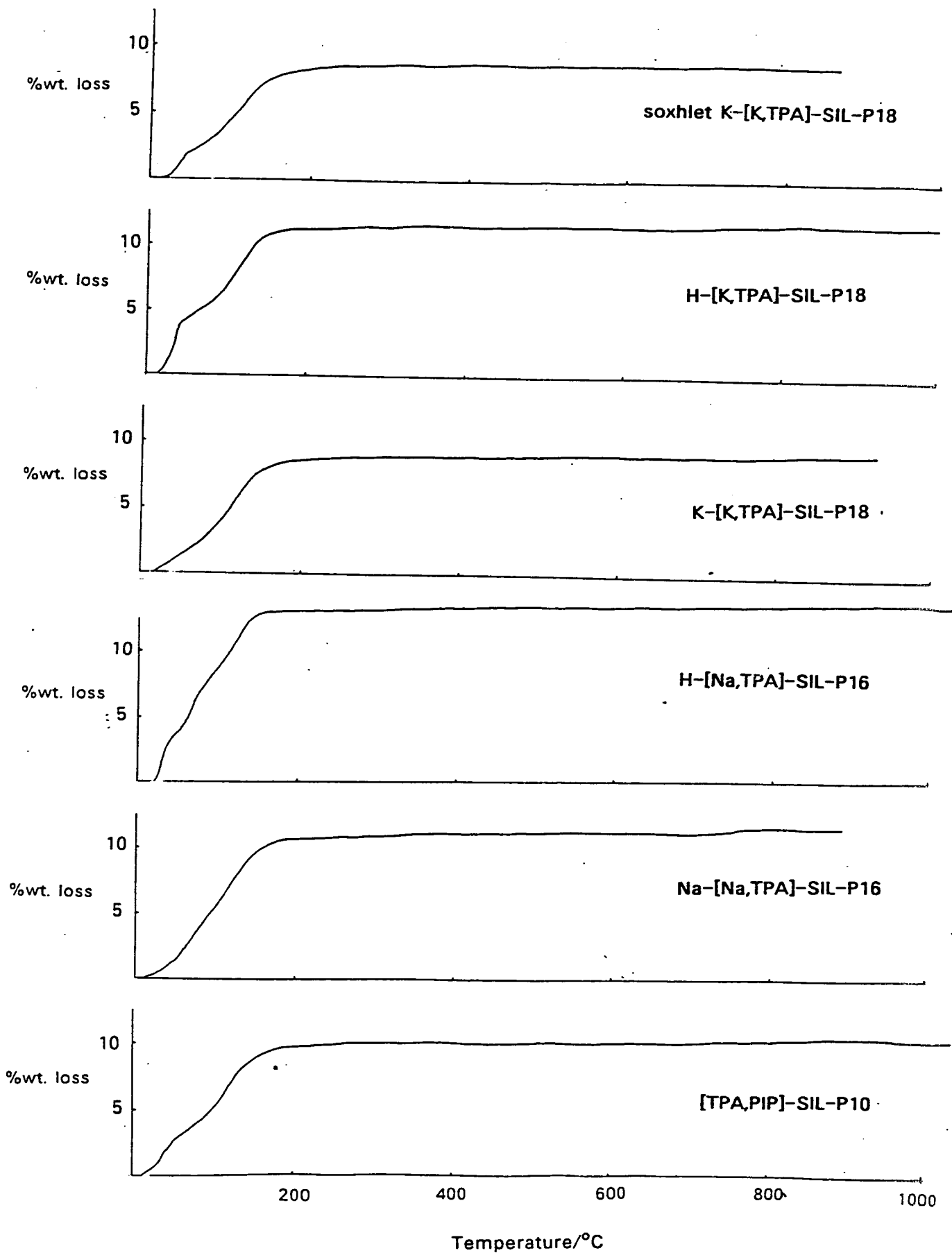


Figure 3.38 TG traces of selected silicalite samples equilibrated with water vapour at  $a_w = 0.753$ .

polar molecules - it cannot be considered as a wholly hydrophobic inert array of siloxane bonds.

The internal surface of silicalite is susceptible to attack by water and methanol molecules. How prone the surface of the silicalite is to attack depends on the synthesis conditions, calcination temperature, cations present and ion-exchange procedures. Methoxylation and/or hydroxylation of the surface of silicalite results in hysteresis in the sorption isotherms for water and methanol and in variation of uptake with equilibration time. It is found to be very difficult to attain a true equilibrium with water vapour. This has far-reaching consequences for the use of silicalite in industrial applications, where the silicalite may be in prolonged contact with water.

The sorption of polar molecules by silicalite is dependent on the method of synthesis, the nature of the cations present, the calcination temperature and the ion-exchange procedures.

### 3.14 References

1. R.M. Barrer, *J. Soc. Chem. Ind.*, 1945, 64, 130.
2. S. Brunauer, "The Adsorption of Gases and Vapours", Princeton University press, Princeton, New Jersey, 1945.
3. M.M. Dubinin, *Adv. Coll. Interface Sci.*, 1965, 2, 214.
4. J.W. M<sup>c</sup>Bain, "The Sorption of Gases and Vapours by Solids", George Routledge and Sons Ltd., London, 1932.
5. G.L. Kington and A.C. Macleod, *Trans. Faraday Soc.*, 1959, 55, 1799.
6. W.K. Lewis, E.R. Gilliland, B. Chertow and W.P. Cadogon, *Ind. Eng. Chem.*, 1950, 42, 1319.
7. I. Langmuir, *J. Amer. Chem. Soc.*, 1916, 38, 2221.
8. S. Brauner, L.S. Denning, W.S. Deming and E. Teller, *J. Amer. Chem. Soc.*, 1940, 62, 1723.
9. R.M. Barrer and J.A. Davies, *Proc. Roy. Soc.*, 1971, A 322, 1.
10. R.M. Barrer, "Zeolites: Science and Technology", NATO ASI series, (ed. F.R. Ribeiro, A.E. Rodrigues, L.D. Rollman, C. Naccache), Martinus Nijhoff, The Hague, 1984, p261.
11. L. Riekert, *Adv. Catal.*, 1970, 21, 218.

12. D.W. Breck, "Zeolite Molecular Sieves", John Wiley and Sons, New York, 1974.
13. R.M. Barrer, *J. Coll. Interface Sci.*, 1966, 21, 415.
14. R.M. Barrer and J.W. Sutherland, *Proc. Roy. Soc.*, 1956, A 237, 439.
15. R.M. Barrer, *Adv. Chem. Ser. No. 102*, 1971, 1.
16. A.P. Vaultitis, D.M. Ruthven and K.F. Loughlin, *J. Col. Interface Sci.*, 1981, 84, 526.
17. R.L. Goring, *J. Catal.*, 1973, 31, 13.
18. D.W. Breck, W.G. Eversole, R.M. Milton, T.B. Reed and T.L. Thomas, *J. Amer. Chem. Soc.*, 1956, 78, 5963.
19. R.M. Barrer and W.I. Stuart, *Proc. Roy. Soc.*, 1959, A249, 464.
20. S. Furuyama and M. Nagato, *J. Phys. Chem.*, 1984, 88, 1735.
21. S. Furuyama, M. Muzayaki and H. Inoue, *J. Phys. Chem.*, 1984, 88, 174.
22. R.M. Barrer, "Zeolites and Clay Minerals as Sorbents and Molecular Sieves", Academic Press, London, 1978.
23. N.Y. Chen, *J. Phys. Chem.*, 1976, 80, 60.

24. H. Nakamoto and H. Takahashi, *Zeolites*, 1982, 2, 67.
25. R.M. Barrer, D.Harding, A. Sikand, *J.C.S. Faraday 1*, 1980,76,180.
26. D.H. Olson, W.O. Haag and R.M. Lago, *J. Catal.*, 1980, 61, 390.
27. E.M. Flanigen, J.M. Bennett, R.W. Grose, J.P. Cohen, R.L. Patton and R.M. Kirchner, *Nature*, 1978, 271, 512.
28. Qin-Hua Xu, Ai-Zhen Yan, Zhong-Yue Meng, Yi-Chan Yan and Ri-Xin Zhou, Proc. 5th Int. Conf. Zeolites, Naples(1980), (ed. R. Sersale, C. Collela and R. Aiello), 1980, p107.
29. S.G. Hill and D. Seddon, *Zeolites*, 1985, 5, 173.
30. H.J. Doelle, J. Herring and L. Riekeit, *J. Catal.*, 1981, 71, 27.
31. H. Lechert and W. Schweitzer, "Proceedings of the 6th Int. Conf. on Zeolites", (eds. D.H. Olson and A. Biso), Butterworths, Guilford, 1984, p210.
32. H. Stach, H. Thamm, J. Janchen, K. Fielder and W. Schirmer, "Proceedings of the 6th International Conference on Zeolites", (eds. D.H. Olson and A. Biso), Butterworths, Guilford, England, 1984, p225.
33. C.G. Pope, *J. Phy. Chem.*, 1986, 90, 835.
34. D.H. Olson, G.T. Kokotailo, S.L. Lawton and W.M. Meier, *J. Phys. Chem.*, 1981, 85, 2238.

35. C.G. Pope, *J. Phys. Chem.*, 1984, 88, 312.
36. R.K. Iler, "The Chemistry of Silica", Wiley-Interscience, New York, 1979.
37. S.J. Gregg and K.S.W. Sing, "Adsorption, Surface Area and Porosity", Academic Press, London, 1982.
38. G. Boxhoorn, A.G.T.G. Kortbeck, G.R. Hays and N.C.M. Alma, *Zeolites*, 1984, 4, 15.
39. G.L. Woolery, L.B. Alemany, R.M. Dessau and A.W. Chester, *Zeolites*, 1986, 6, 15.
40. K.F.M.G.J. Scholle, W.S. Veeman, J.G. Post and J.H.C. van Hooff, *Zeolites*, 1983, 3, 214.
41. A.W. Chester, Y.F. Chu, R.M. Dessau, G.T. Kerr and C.T. Kresge, *J. Chem. Soc. Chem. Comm.*, 1985, 5, 289.
42. S.G. Fegan and B.M. Lowe, *J. Chem. Soc. Comm.*, 1984, 437.
43. R. von Ballmoos and W.M. Meier, *J. Phys. Chem.*, 1982, 86, 2698.
44. A. Ison and R.G. Gorte, *J. Catal.*, 1984, 89, 150.
45. "Ultraweight Determination in Controlled Enviroments", ed. Wolsky and Zdanuk, Wiley-Interscience, 1969.

46. G.R. Landolt, *Anal. Chem.* 1971, 43, 613.
47. R. Le Van Moa, *React. Kinet. Catal. Lett.*, 1979, 12, 69.
48. P.E. Eberly, Jr., *Ind. Eng. Chem. Prod. Res. Develop.*, 1969, 4, 140.
49. R.M. Barrer and S. Wasilewski, *Trans. Faraday Soc.*, 1961, 57, 1140.
50. C.G.V. Burgess, R.H.E. Duffett, G.J. Mintoff and R.G. Taylor, *J. Appl. Chem.*, 1964, 14, 350.
51. I.H. Doetsch, D.M. Ruthven and K.F. Loughlin, *Can. J. Chem.*, 1974, 52, 2717.
52. R.E. Richards and L.V.C. Rees, *Zeolites*, 1986, 6, 17.
53. J. Janchen and H. Stach, *Z. Chem.*, 1984, 24, 158.
54. P.A. Jacobs, H.K. Beyer and J. Valyon, *Zeolites*, 1983, 1, 161.
55. P. Wu, A. Debebe and Yi Hua Ma, *Zeolites*, 1983, 3, 119.
56. R.L. Pallon, R.M. Kirchner and J.V. Smith, *Nature*, 1978, 271, 521.



## CHAPTER 4

# OCCLUSION OF SALTS BY SILICALITE

### 4.1 Introduction

The occlusion of salts by molecular sieves is a property that can be used to 'tailor' their catalytic and sorptive character. Salts may be occluded during the course of synthesis or post-synthesis from melts or aqueous solutions. The amount of salt taken up from a melt cannot be readily controlled, whereas the amount occluded from aqueous solution depends on the concentration. In order for occlusion of a salt to take place the diameter of the ions must be smaller than the pore diameter. If this condition is not satisfied, then the salt will be excluded from the framework. As in ion exchange processes it is the diameter of the unhydrated ions that governs whether or not occlusion may occur. However, the size and strength of the solvation shell will be significant as in many cases this shell is momentarily shed as the ion passes through the pore openings. If the energy of solvation is high, diffusion of the salt into the molecular sieve will be slow.

The occlusion of salts into molecular sieves will depend on the relative strengths of the following interactions:

1. zeolite-water
2. zeolite-salt
3. water-salt

These interactions will depend on the nature of both the salt and the molecular sieve. If no water was sorbed by a molecular sieve, occlusion would depend only on whether the salt interacted more strongly with the water molecules or the zeolite framework. However, many molecular sieves sorb water to pore

capacity and so occlusion of salt usually necessitates displacement of water molecules from the framework. Occlusion is favoured by strong interaction of the salt and the molecular sieve, weak interaction between the salt and water molecules and weak interactions of water molecules and the zeolite framework.

The strength of the water-zeolite interaction will depend on the nature of the framework: is the internal surface hydrophobic or hydrophilic? It will also be related to the nature and number of cations present in the framework.

A measure of the strength of the water-salt interaction is the solubility of the salt. Small ions with large charge will have the strongest water-salt interaction, whereas larger ions with small charge interact less strongly with the water molecules.

The salt-molecular sieve interaction depends on the strength of attraction of the cation for the anionic framework and vice versa and also the repulsion between the anion and the anionic framework. Not only will the interaction depend on the charge on the framework but also on the dimensions of the channels and cages.

It can be seen that the occlusion properties of aluminous zeolites and high silica molecular sieves will differ considerably. In the following sections the occlusion properties of aluminous zeolites and high silica molecular sieves are examined in more detail.

#### **4.1.1 Aluminous Zeolites**

The occlusion of an anion from dilute aqueous solution into an anionic framework even with an accompanying cation, is unfavourable. However, as the

concentration of the solution increases, ion-ion interactions in the solution become significant and the occlusion of the cation-anion pair becomes more favourable. The cation occupies one of the usual cation sites and becomes indistinguishable from the ion-exchange cations present. The anion occupies a position that allows it to minimise the repulsion from the anionic framework and other anions already occluded and to maximise the attraction with the cations. Salts are not usually occluded to such an extent that they fill all the available pore space. This is a result of like ion-like ion repulsion of anions occluded in the channels. Barrer explained this behaviour in terms of a Donnan membrane effect[1]. This effect occurs when a solution contains diffusible and non-diffusible ions, the non-diffusible ions being located on one side of a semi-permeable membrane[2]. The distribution of the diffusible ions is unequal when equilibrium is reached, being greater on the side of the membrane which contains the non-diffusible ions.

At equilibrium the concentrations of species can be described as follows:

	Solution	Zeolite
Species	$M^+, X^-$	$M^+, X^-, R^-$
Concentration	$c, c$	$c_m, c_i, c_r$
Activity	$a, a$	$a_m, a_i$

where  $c$  is the concentration of the solution,  $c_r$  the "concentration" of the anionic framework,  $c_m$  the concentration of cations and  $c_i$  the concentration of anions in the zeolite, and  $a, a_m$  and  $a_i$  are the corresponding activities.

If it is considered that  $n$  moles of  $H_2O$  are displaced from the zeolite to the solution phase, then the Donnan membrane treatment[1,2,3] gives the equilibrium constant for the occlusion process as:

$$K = (a_i a_m / a^2) \{ (a_{H_2O})_{aq}^n / (a_{H_2O})_z^n \} \quad (4.1)$$

This may be rewritten as

$$c_i c_m / c^2 = R \quad (4.2)$$

where  $R = K(a_{H_2O})_z^n y^2 / (a_{H_2O})_{aq}^n y_z^2$ .  $y$  and  $y_z$  are the activity coefficients of the solution and zeolite respectively. For electrical neutrality

$$c_m = c_i + c_r \quad (4.3)$$

As  $c_i$  is small compared to  $c_r$  this equation may be simplified to

$$c_i = Rc^2 / c_r \quad (4.4)$$

As  $c_r$  is a constant,  $c_i$  will vary with  $c^2$ , provided  $R$  does not vary with  $c$  or  $c_i$ , that is the ratio  $c_i(c_i + c_r) / c^2 = R$  is constant. Barrer has shown that this is the case for the occlusion of some salts such as NaCl in Na-X and KCl in K-X but for some other salts such as CaCl<sub>2</sub> in Ca-X or Ca-A,  $R$  is not a constant. Equation (4.4) shows  $c_i$  is very low at low solution concentrations but increases rapidly as the concentration increases. This gives rise to the concave curves in a plot of  $c_i$  against  $c$ , that are associated with occlusion of salts into aluminous zeolites.

Barrer and Walker[3] found that for the occlusion of group 1 halides in zeolite-X the order of preference was KCl > NaCl > LiCl and suggested that occlusion becomes more favourable as the cation radius increases. When the occlusion of different halides of a given cation were examined, the occlusion process showed little dependence on the anion. This is probably due to its relatively larger size and it is only the charge on the anion that is of significance. This order of preference is the same as the affinity series for ion-exchange in zeolite-X. This is easily understood when it is remembered that the occluded cations occupy similar positions to exchange cations.

### 4.1.2 High Silica Molecular Sieves

High silica molecular sieves, particularly silicalite, are expected to show marked differences in occlusion behaviour from more aluminous zeolites, as there is a negligible charge on their framework. The non-polar environment within silicalite, makes the occlusion of ionic salts such as NaCl unfavourable. The occlusion of more covalent salts, especially if they contain an organic part, will be more favourable, because of their higher dispersion energy of interaction with the molecular sieve framework. As water does not fill the pores of silicalite it is not a prerequisite for the occluded salt to displace water molecules.

Consider the concentration of species present in the silicalite channels and solution.

	Solution	Silicalite
Species	$M^+, X^-$	$M^+, X^-$
Concentration	$c, c$	$c_m, c_i$
Activities	$a, a$	$a_m, a_i$

The equilibrium constant may be written as

$$K = a_m a_i / a^2 = (c_m c_i / c^2) (y_z^2 / y^2) \quad (4.5)$$

where  $y_z$  and  $y$  are the mean activities of the ions in the silicalite and solution phases. In the ideal case silicalite contains no exchangeable cations,  $c_m = c_i$ , and we can write,

$$\log K^{1/2} = \log c_i / c + \log y_z / y \quad (4.6)$$

A problem now arises because of a lack of knowledge of how  $y_z$  and  $y$  vary with concentration. As the solutions are not dilute, the Debye-Huckel theory can not be used to calculate  $y$ , and neither theoretical nor experimental values of  $y_z$  are available. However, it can be seen that the occlusion properties of high silica molecular sieves are likely to differ considerably from the those of

more aluminous zeolites. If  $y_2/y$  was constant then  $c_i$  would vary linearly with  $c$ .

## 4.2 Introduction to Experimental Techniques

The techniques used to measure the uptake of salt by zeolites involved separation of the zeolite from the solution phase. This procedure involves many experimental problems. Not least, there is the difficulty of assessing the amount of water present in the zeolite. Previous workers have found it necessary to make assumptions about the amount of water in the channels of the molecular sieve. These difficulties can be overcome by use of a technique developed by Fegan and Lowe [4]. This technique makes use of isopiestic vapour pressure equilibration to obtain the weights of water and salt both in the zeolite and the solution phase, thereby eliminating the need for assumptions about the distribution of water.

The technique relies on the principle that if two or more solutions of non-volatile solutes are allowed to equilibrate in a closed system, then solvent will distil from one to another until the vapour pressure of all the solutions are the same.

To illustrate this, consider two dishes which each contain a known weight of salt. If an arbitrary amount of water is added to these dishes they will initially have different water activities. But when they are placed in a closed system, water will distil from one dish to another until finally both solutions will have the same water activity,  $a_w$ . If the same salt was present in both dishes then at equilibrium the solutions would be of equal concentration. Such solutions are said to be isomolar. If a dish that contains saturated solid salt solution in contact with excess salt solution is introduced into the system, the

water activity of the system will be controlled by this solution. At equilibrium all the solutions will have the same  $a_w$  as the saturated salt solution. The concentration of solution in the dishes is obtained simply by reweighing.

Considerable care has to be taken in the experimental procedure to obtain meaningful and accurate isopiestic results. Equilibration of concentrated solutions is obtained within days but equilibration of dilute ones may take considerably longer. The time required for equilibrium to be reached can be reduced if the system is evacuated. As solvent distils from one dish to another temperature and concentration gradients may result. This is overcome by placing the dishes on a metal block and by gently 'rocking' the system as it is equilibrated. Further details are given in reference [5].

The experimental procedure by which data regarding salt occlusion is obtained from isopiestic measurements is outlined below. Known weights of molecular sieve, different known amounts of salt and some water are added to a series of dishes. The dishes are placed in an evacuated chamber. This chamber also contains a dish of saturated salt solution in contact with excess solid salt which controls the vapour pressure within the chamber. The solutions will all have different water activities, so water will distil from one dish to another until all have the same water activity as that of the saturated solution

At the same time occlusion of salt into the molecular sieve will occur and this will alter the amount of salt in solution. At equilibrium however all the dishes will have the same water activity. By reweighing the dishes the weight of water in each dish can be found. So the weights of molecular sieve, salt and water in each dish are known. From the information so far the distribution of the salt between the molecular sieve and solution phase remains unknown,

so too is the weight of water in the molecular sieve. However, these problems can be overcome as follows. If only a small quantity of salt is present in one of the dishes, all this salt will be occluded into the molecular sieve and no solution phase will be present in the dish. All water and salt in this dish are intracrystalline. Imagine a set of dishes with known weights of molecular sieve and increasing quantities of salt, to which water has been added and the whole system equilibrated. As the amount of salt increases an increase in the amount of salt occluded is observed. Concomitantly, the water sorbed decreases as the occlusion of salt displaces sorbed water molecules. A point will be reached when no more salt can be occluded in the molecular sieve under the given conditions. Any salt in excess of this will be present on the exterior of the zeolite crystals and will form a solution of appropriate concentration. As a result the weight of water in the dishes will increase in a linear fashion. If these results are plotted as  $WW/WZ$  against  $WS/WZ$  a v-shaped graph is obtained as shown in Figure 4.1. The equation for the line known as the "intercrystalline phase" line, is given by

$$\frac{WW}{WZ} = \frac{WS}{WZ} \left( \frac{ww_s}{ws_s} \right) + \frac{ws_z}{WZ} \left( \frac{ww_z}{ws_z} - \frac{ww_s}{ws_s} \right) \quad (4.7)$$

where  $WW$ ,  $WS$  and  $WZ$  are the total weights of water, salt and zeolite in the dishes respectively.  $ww_s$  and  $ws_s$  are the weights of intercrystalline water and salt and  $ww_z$  and  $ws_z$  are the weights of intracrystalline water and salt. From this equation it is seen that the gradient of this line is  $ww_s/ws_s$  which is the reciprocal of the solution concentration. As the gradient of the line is the inverse of the solution concentration, a dilute solution has a steep gradient. If the water activity of the system is below that of the water activity of a saturated solution of the occluded salt, then any salt present on the exterior of the crystals will be present as crystalline anhydrous or hydrated salt. In this case the "intercrystalline phase" line will be horizontal, or alternatively it will



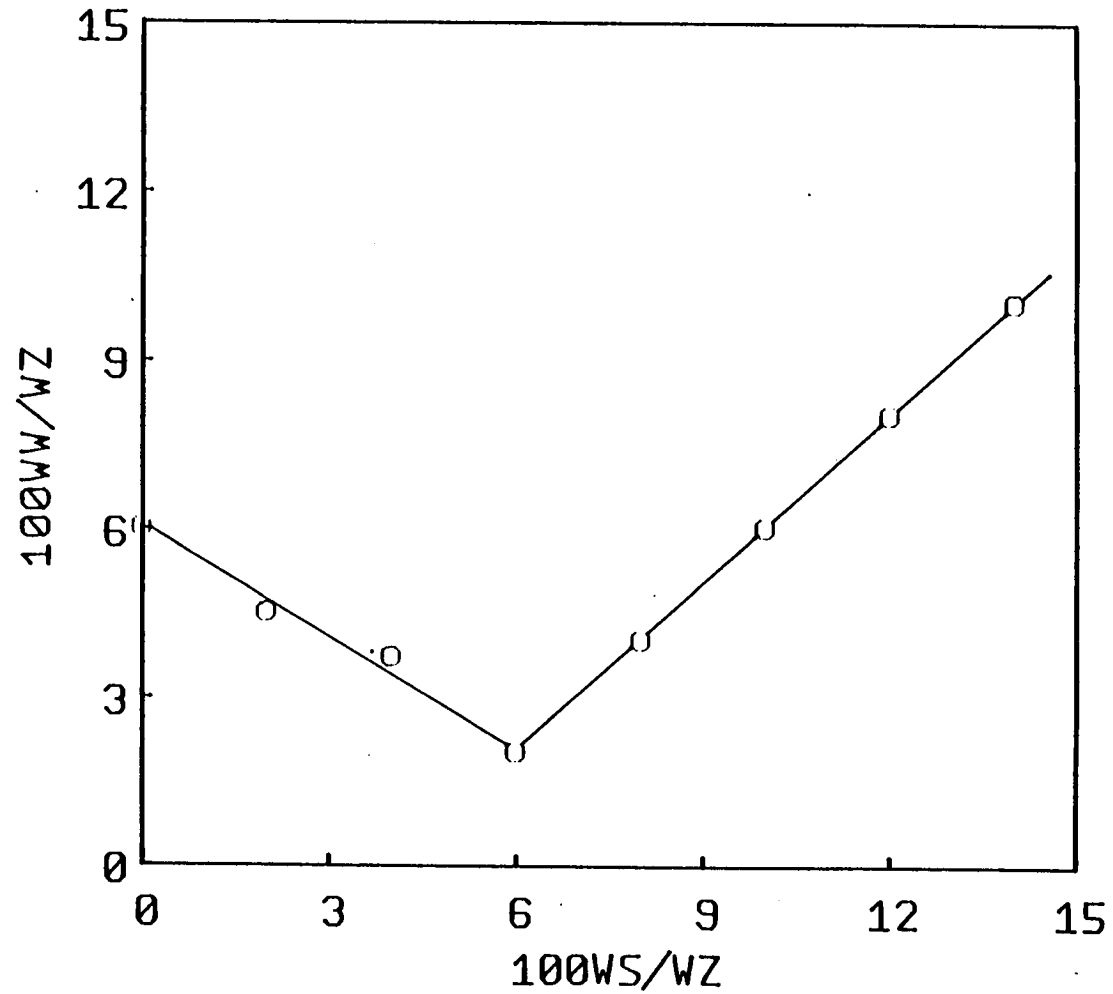


Figure 4.1

Set of occlusion results for an imaginary typical salt system, shown as a plot of  $WW/WZ(gg^{-1})$  against  $WS/WZ(gg^{-1})$ .

have a positive slope independent of the water activity. If the intercrystalline line is extrapolated back to the y-axis, the intercept,  $(ww_z/WZ) - (ws_z \cdot ww_s / ws_s \cdot WZ)$ , corresponds to the weight of water in the zeolite minus the weight of water that would have been associated with the salt if it had been in solution rather than in the zeolite. This depends on two factors - how much salt has been occluded and how much water is displaced by the salt.

The intracrystalline line, that is for the dishes which contain only solid phase, may be represented by the equation (4.8).

$$WW/WZ = U_w + kWS/WZ \quad (4.8)$$

where  $k$  is a measure of how much water is displaced by occlusion of salt. If the presence of salt in the channels of the molecular sieve leads to an increase in the uptake of water then  $k$  will be positive. Unlike the "intercrystalline phase" line there is no thermodynamic requirement for this line to be linear.

The intersection of the two lines is indicative of the maximum amount of salt that may be occluded under the given set of conditions. It is essential that this intersection point can be determined accurately. In order to do this, it is necessary to have dishes with the appropriate mixtures to appear on either side of the intersection, so care must be taken when initially choosing the quantities of salt to be added.

The experiment may be repeated over a range of different water activities and so the variation of the maximum amount of salt occluded with water activity and/or solution concentration can be obtained.

## **4.3 Experimental**

### **4.3.1 Apparatus**

Jencons Type 4 6 inch dry-seal desiccators were used as the closed system. A metal block made of gold plated copper or stainless steel was used to hold the dishes and to ensure that they were isothermal. The dishes were of gold plated silver or stainless steel. Lids of these dishes could be lowered and raised without releasing the vacuum in the desiccator. A schematic diagram of the desiccator "set-up" which was used is shown in Figure 4.2.

### **4.3.2 Procedure**

The procedure used in the measurement of occlusion of salt into molecular sieves is given below.

1. Approximately 0.5g molecular sieve was added to the weighed dish.
2. These samples were equilibrated over saturated NaCl solution, weighed, and the weight of dry silicalite found by thermal analysis.
3. Different quantities of salt were accurately weighed into the dishes.
4. Sufficient boiled distilled water was added to cover the molecular sieve in the dishes.
5. A petri-dish of saturated salt solution in contact with excess solid salt was placed in the bottom of the desiccator to control the water vapour pressure of the system.
6. The desiccator was evacuated slowly by use of a water pump taking care to avoid 'spluttering' of the contents.

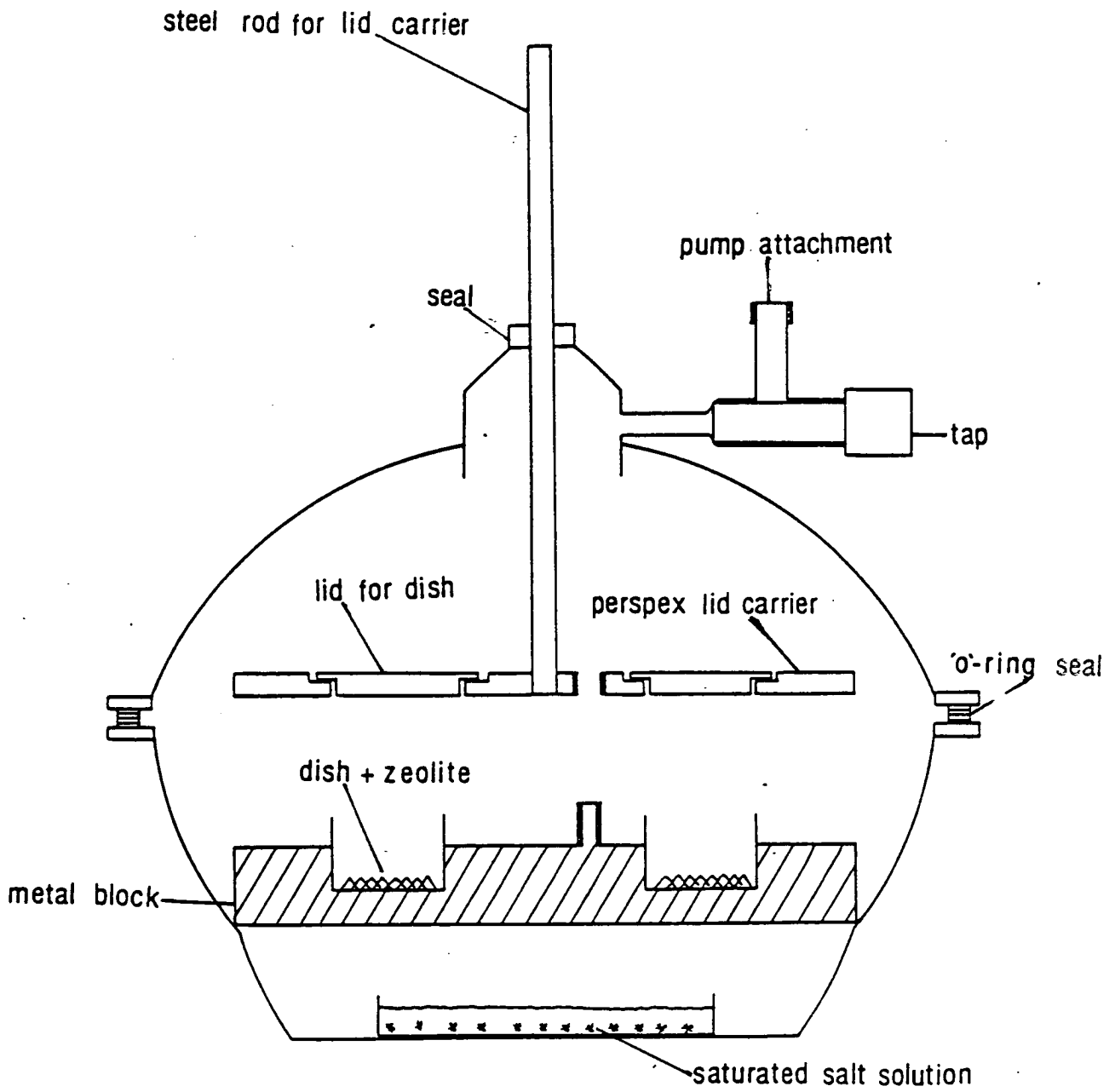


Figure 4.2 The desiccator "set-up" used in isopiestic measurements.

7. The desiccator was then equilibrated in a 'rocking' water bath at 25°C.
8. After equilibration the dishes were reweighed to find the weight of water.
9. The results were calculated using a computer programme written by S.Fegan.
10. The dishes were then re-equilibrated at a different water activity and the procedure from 6. onwards repeated.

### 4.3.3 Materials

The silicalite used for all the work described in this chapter was [TPA,PIP]-SIL. Several different preparations were used and these are denoted in the usual way. The method of preparation was discussed in chapter two.

The source and purity of the salts used in the occlusion experiments are shown below.

<u>salt</u>	<u>purity</u>	<u>source</u>
Sodium propanesulphonate monohydrate	>97%	Fluka A.G.
Sodium pentanesulphonate monohydrate	98%	Aldrich Chemical Co.
Sodium octanesulphonate monohydrate	>99%	Fluka A.G.
Sodium benzenesulphonate	>99%	Fluka A.G.
Tetramethylammonium bromide	>99%	Fluka A.G.
Hexamethonium bromide	>98%	Fluka A.G.
Decamethonium bromide	>98%	Fluka A.G.
Caesium nitrate	99%	BDH Chemicals
Caesium chloride	99%	Sigma Chemical Co.
Sodium chloride	99.5%	Fisons Scientific

### Saturated salt solutions

The water activity of saturated salt solutions used in this work are shown

below[6].

<u>Solid Phase</u>	<u>water activity</u>
KNO <sub>3</sub>	0.925
ZnSO <sub>4</sub>	0.871
KBr	0.807
NH <sub>4</sub> Cl	0.771
NaCl	0.753
NaNO <sub>3</sub>	0.738
NH <sub>4</sub> NO <sub>3</sub>	0.618
MgNO <sub>3</sub>	0.529
K <sub>2</sub> CO <sub>3</sub>	0.428
MgCl <sub>2</sub>	0.330
LiCl	0.111

#### 4.4 Isopiestic results

The isopiestic technique was used to investigate several different salt systems.

##### 4.4.1 Hexamethonium bromide + Silicalite

This system was equilibrated at two different water activities,  $a_w=0.753$  and  $a_w=0.330$ . The isopiestic results obtained for this system are plotted in Figure 4.3 as WW/WZ against WS/WZ. No occlusion of hexamethonium bromide into silicalite was observed, and the line which represents the solution phase may be extrapolated back to  $U_w^0$ . The slopes of these two lines are equal to the reciprocal of the solution concentration. It appears that hexamethonium bromide is completely excluded from the silicalite channels. This is probably because the diameter of the ends of the hexamethonium ion,  $(Me_3N(CH_2)_6NMe_3)^{2+}$ , exceed that of the silicalite pores at 25°C.

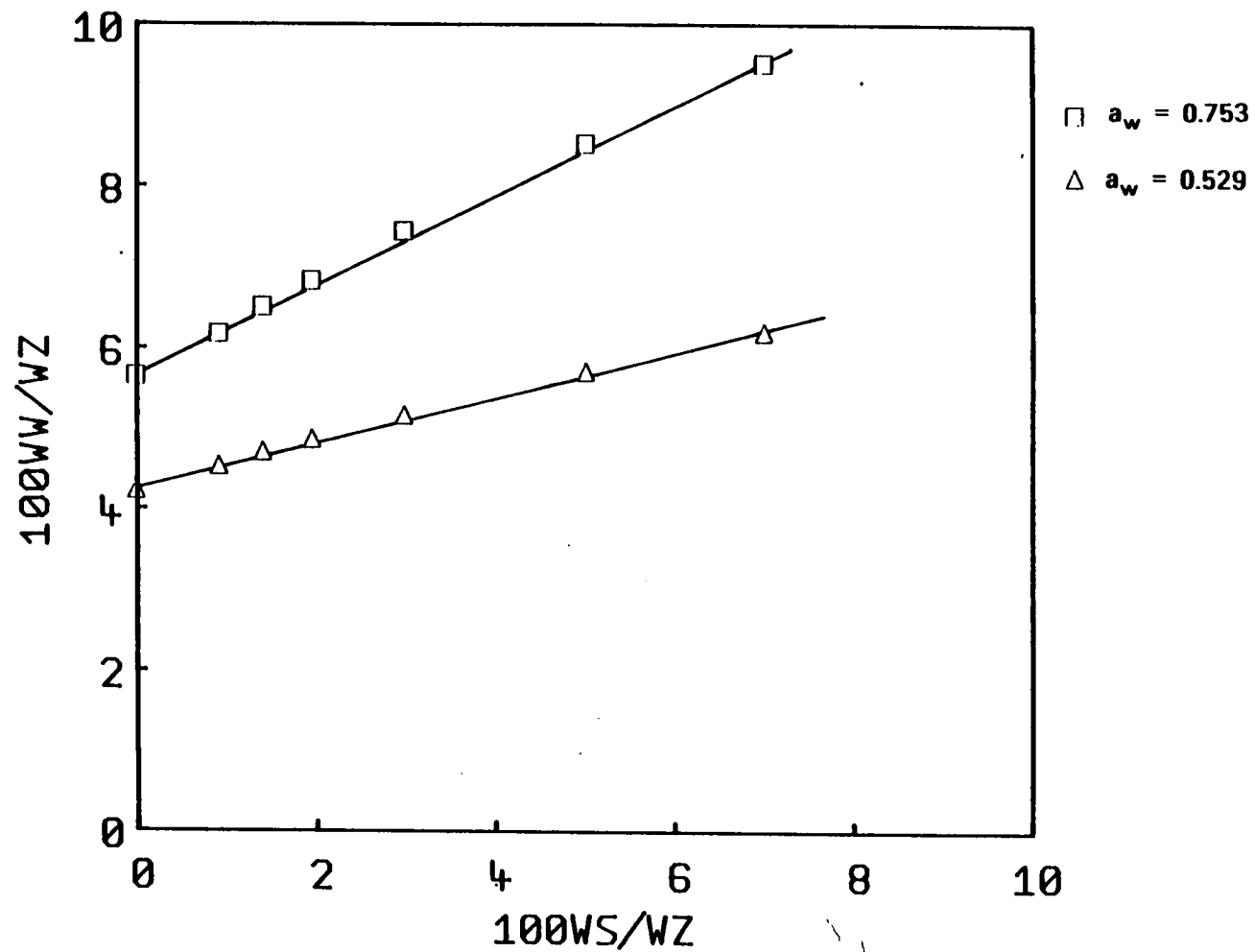


Figure 4.3

The occlusion results obtained from isopiestic measurements for the system, hexamethoniumbromide + [TPA,PIP]-SIL-P-16.

#### 4.4.2 CsNO<sub>3</sub> + Silicalite

The occlusion results for the CsNO<sub>3</sub> + Silicalite system at three different water activities are shown in Figure 4.4. The slope of the "intracrystalline" line described by equation (4.8) and representative of dishes in which no solution phase is present, is negative. This indicates that water molecules are displaced from the silicalite channels by the occlusion of CsNO<sub>3</sub> molecules. This is an initially surprising observation. Water fills only approximately 25% of the silicalite channels. There is more than sufficient space in the channels for both the water and the salt molecules. Indeed, it might have been anticipated that the presence of such ionic species as Cs<sup>+</sup> and NO<sub>3</sub><sup>-</sup> might have led to an increase in the uptake of water by silicalite-1. This occurrence suggests there are a small number of specific sites present in the framework. These sites could be unhealed -O-Si-OH HO-Si-O- groups. The salt molecules are occluded on these sites and the water molecules associated with them are displaced. This idea is further strengthened by the observation that the maximum uptake of salt is invariant with the water activity of the system. As there are a limited number of these hydrophilic sites only a small amount of salt is taken up by the silicalite. The maximum uptake of CsNO<sub>3</sub> is 0.02gg<sup>-1</sup> which is equivalent to 0.6 CsNO<sub>3</sub> per unit cell. Such an uptake is reasonable when the ionic nature of the CsNO<sub>3</sub> and the hydrophobic nature of the silicalite are considered.

#### 4.4.3 Tetramethylammoniumbromide + Silicalite

Figure 4.5 shows the occlusion results obtained for this system at four different water activities. At the three lower water activities the intercrystalline lines are horizontal. This is a consequence of the system being equilibrated at water activities below that of saturated TMABr solution. In such a situation, any excess salt is present as an anhydrous solid in contact with the silicalite



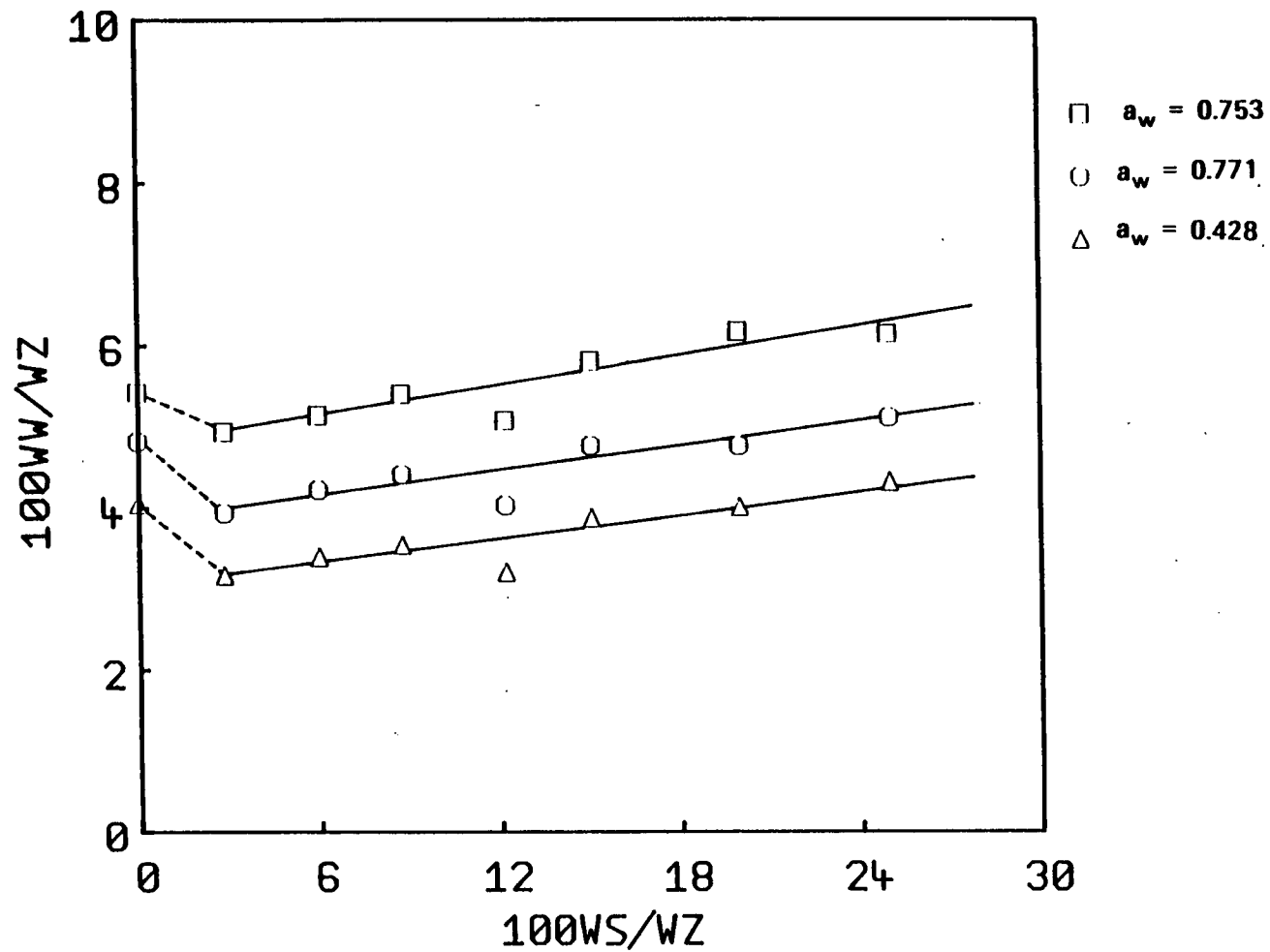


Figure 4.4

Occlusion results for  $\text{CsNO}_3$  + [TPA,PIP]-SIL-P-12.

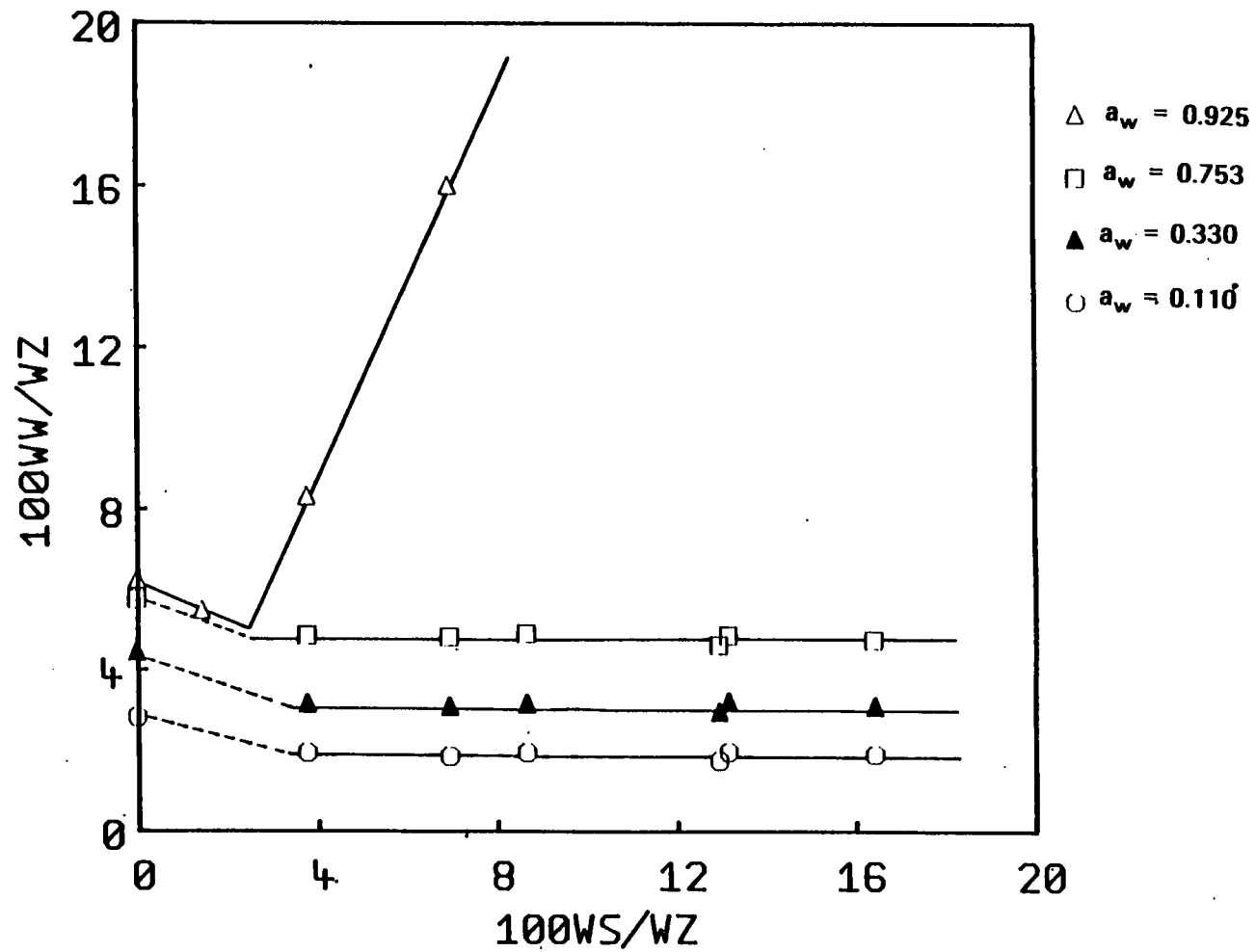


Figure 4.5

Occlusion results for TMABr + [TPA,PIP]-SIL-P-7.

crystals. At  $a_w = 0.925$ , excess salt is present as a solution on the exterior of the crystals. It is again observed that the occlusion of TMABr results in displacement of water from the framework. The maximum amount of salt occluded can only be determined precisely for the highest water activity. At  $a_w = 0.925$ ,  $0.024 \text{ g g}^{-1}$  of TMABr is occluded. This is equivalent to 0.9 TMABr per unit cell. This limited uptake of TMABr by silicalite may be due to its size; TMA has an equilibrium diameter of  $6.2 \text{ \AA}$ [7]. This is larger than the pore diameter of silicalite. As a consequence there is a large energy barrier associated with the occlusion of this salt.

#### 4.4.4 Sodium benzenesulphonate + Silicalite

The isopiestic measurements obtained for this system are shown in Figure 4.6. Sodium benzenesulphonate is present as a monohydrate on the exterior of the silicalite crystals. A small amount of the salt is occluded, as shown by the fact that the plots do not extrapolate back to  $U_w^0$ . The exact uptake of salt cannot be quantified due to a lack of points at  $WS/WZ < 0.02 \text{ g g}^{-1}$ . It is significant that sodium benzenesulphonate is not occluded to any great extent into silicalite as benzene is readily sorbed by silicalite and other sulphonates are occluded. It may be that the shape of the molecule and its inability to adopt the correct configuration for occlusion into the silicalite pores is responsible for its low uptake.

#### 4.4.5 Occlusion of Sodium alkylsulphonates

The occlusion of sodium alkylsulphonates with alkyl = propyl, pentyl and octyl into silicalite was investigated. The plots of  $WW/WZ$  against  $WS/WZ$  at different water activities are shown in figures 4.7, 4.8 and 4.9. It is apparent from these plots that these salts are readily occluded into the channels of silicalite. These salts possess considerable organic character. The dispersion energy of interaction between the alkyl chains and the silicalite framework will

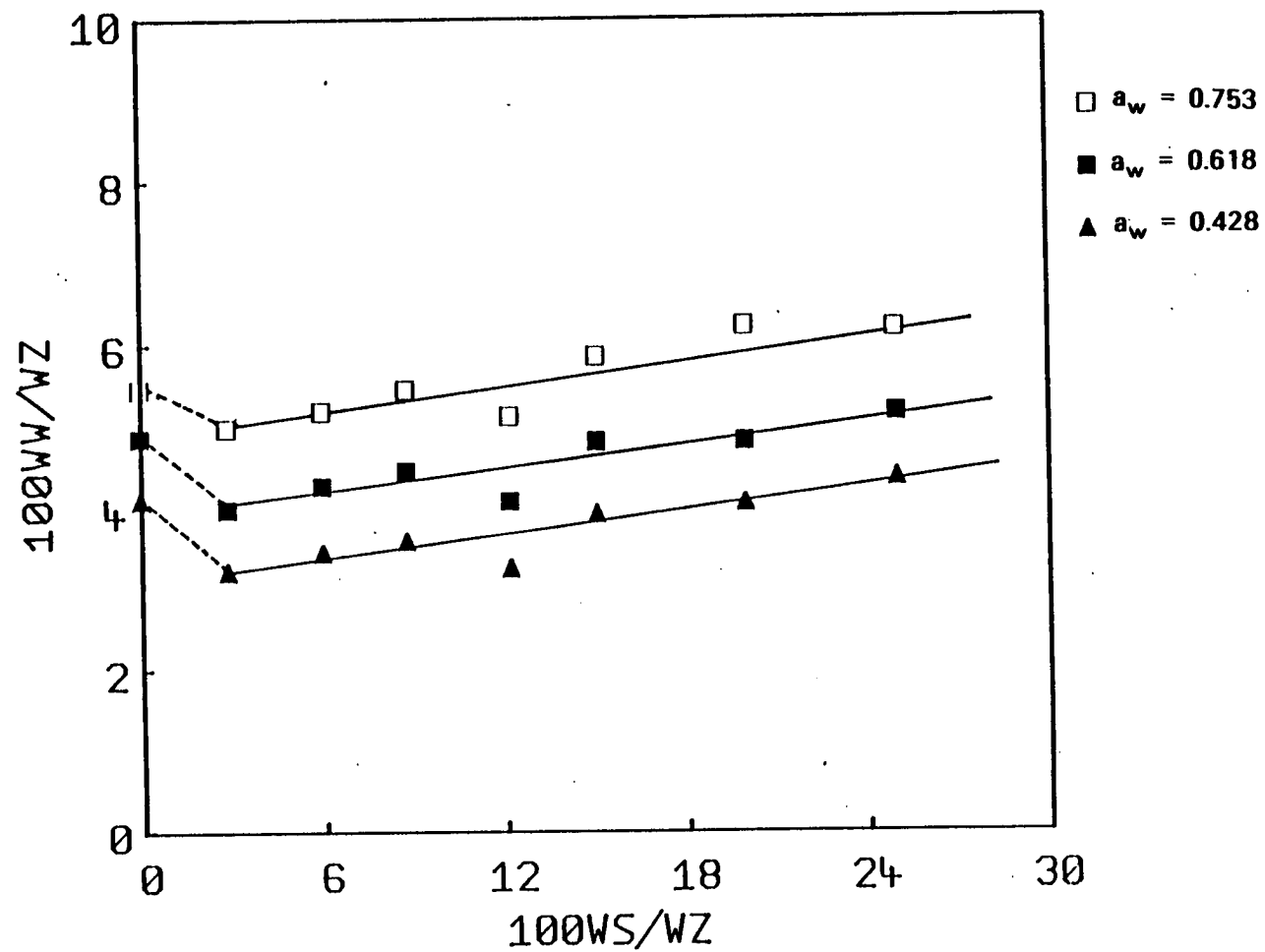


Figure 4.6

Occlusion results for sodium benzenesulphonate + [TPA,PIP]-SIL-P14.

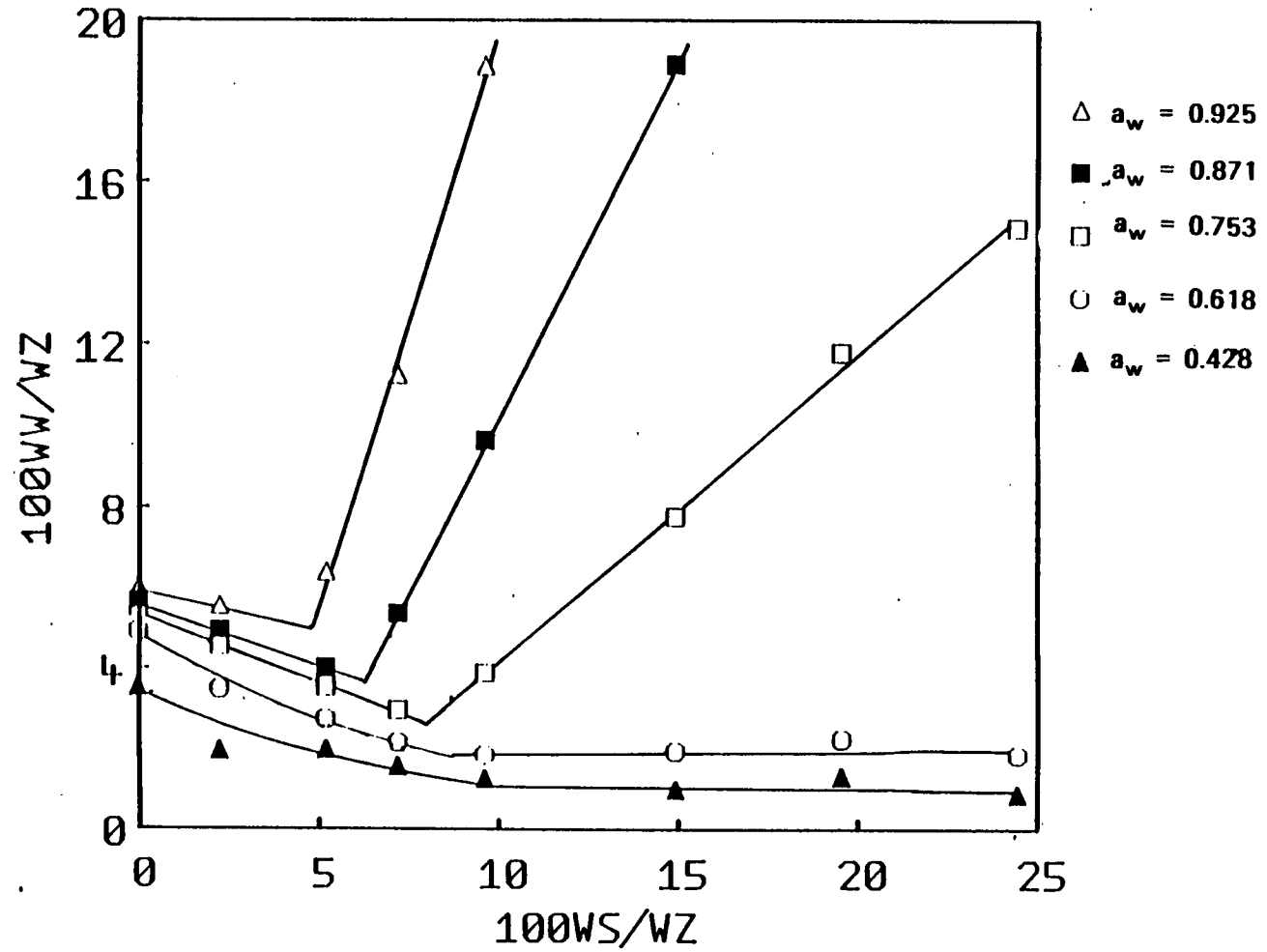


Figure 4.7 Occlusion results for sodium propanesulphonate + [TPA,PIP]-SIL-P15.

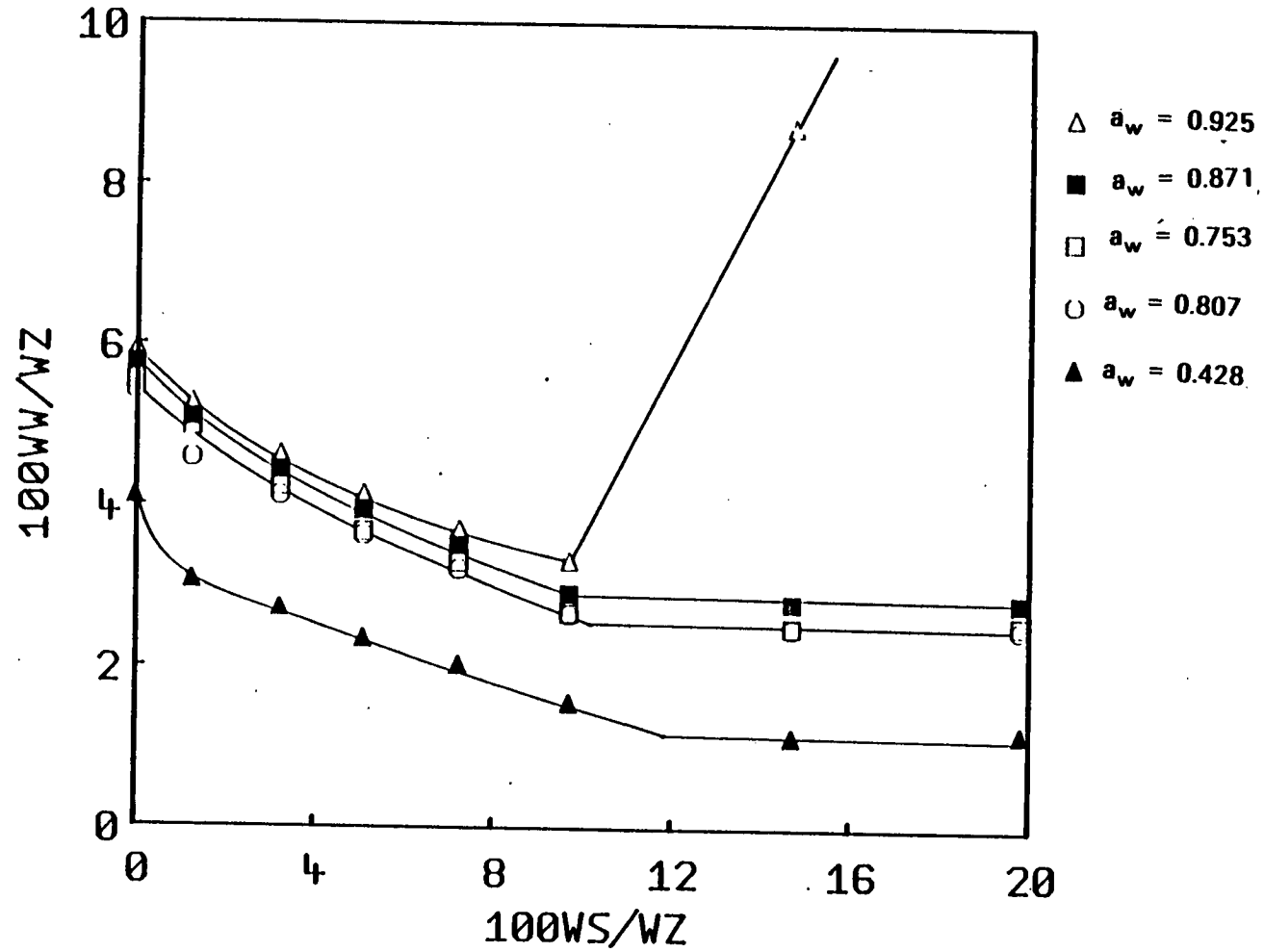


Figure 4.8

Occlusion results for sodium pentanesulphonate + [TPA,PIP]-SIL-P15.

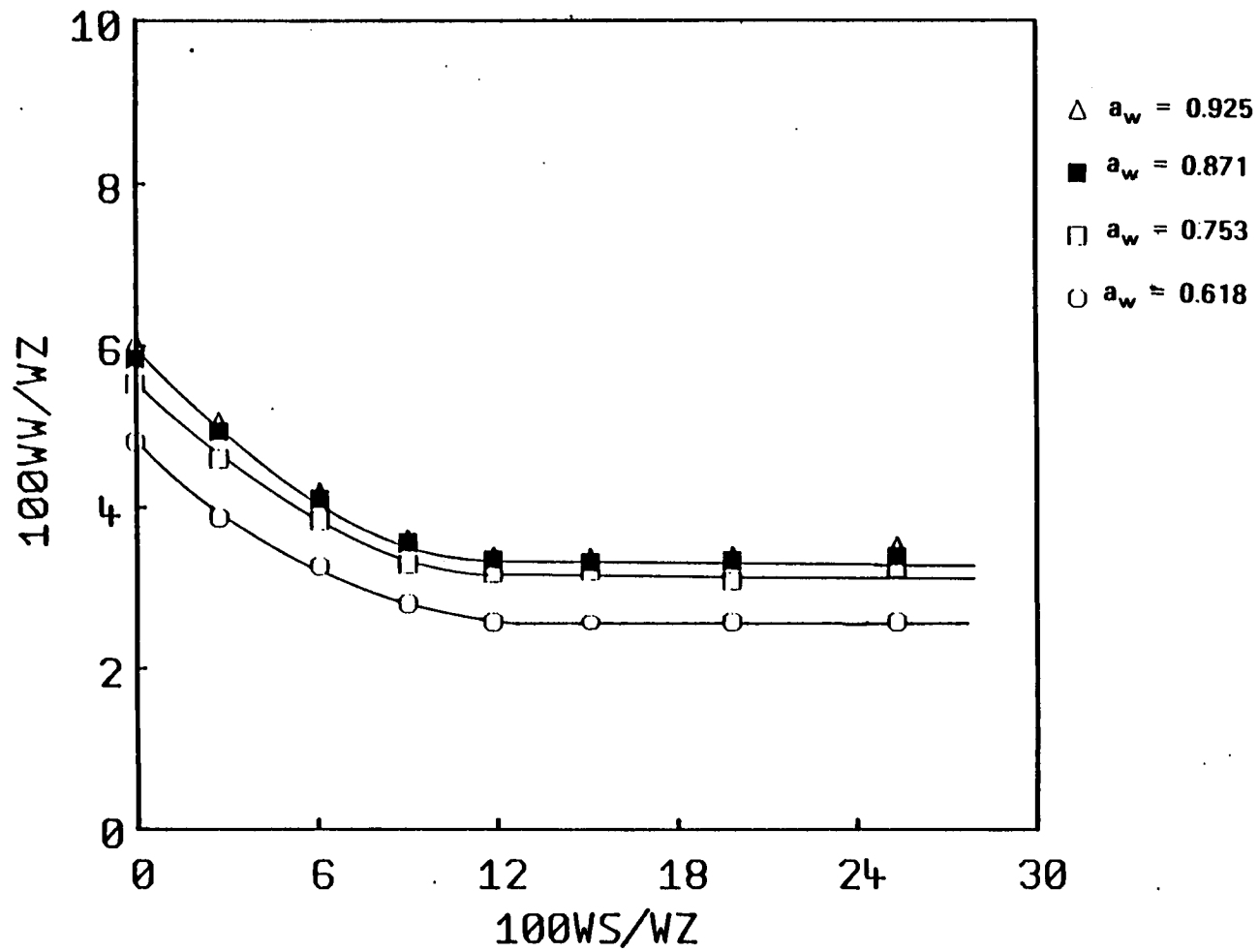


Figure 4.9 Occlusion results for sodium octanesulphonate + [TPA,PIP]-SIL-P14.

be high and so can overcome the less favourable interaction of the sulphonate and sodium ions with the framework. The occlusion of these salts is also aided by the unfavourable interaction of the alkyl group with water molecules in solution. The shape of the salt molecules is such that they can pack easily into the channel network of silicalite. It is noted that as in previous systems occlusion of salt results in a lower uptake of water by the silicalite.

#### **Sodium propanesulphonate + Silicalite**

At all water activities examined except  $a_w=0.428$  any salt not occluded is present as a solution on the exterior of the crystals. As the water activity of the system decreases the concentration of the solution increases and the maximum amount of salt occluded,  $U_s^T$ , increases. The magnitude of  $U_s^T$  is very dependent on  $a_w$  or the concentration of the solution unlike some of the other systems investigated. This is depicted in Figure 4.10 as a plot of internal molality of salt  $m_i$ , against external molality  $m$ . The uptake of salt by silicalite even at low solution molality is significant. This is unlike the occlusion of more ionic salts into aluminous zeolites where the uptake of salt is very low at dilute concentrations.

#### **Sodium pentanesulphonate + Silicalite**

In this experiment any excess salt that is not occluded into the framework of silicalite is present in an anhydrous form on the surface of the crystals. In this system the value of  $U_s^T$  shows little dependence on the water activity of the system in contrast to the previous system. The lines which correspond to the weight of salt and water in the "dry" dishes are concave in shape. Initially occluded salt displaces more water molecules than subsequent occlusion of salt.



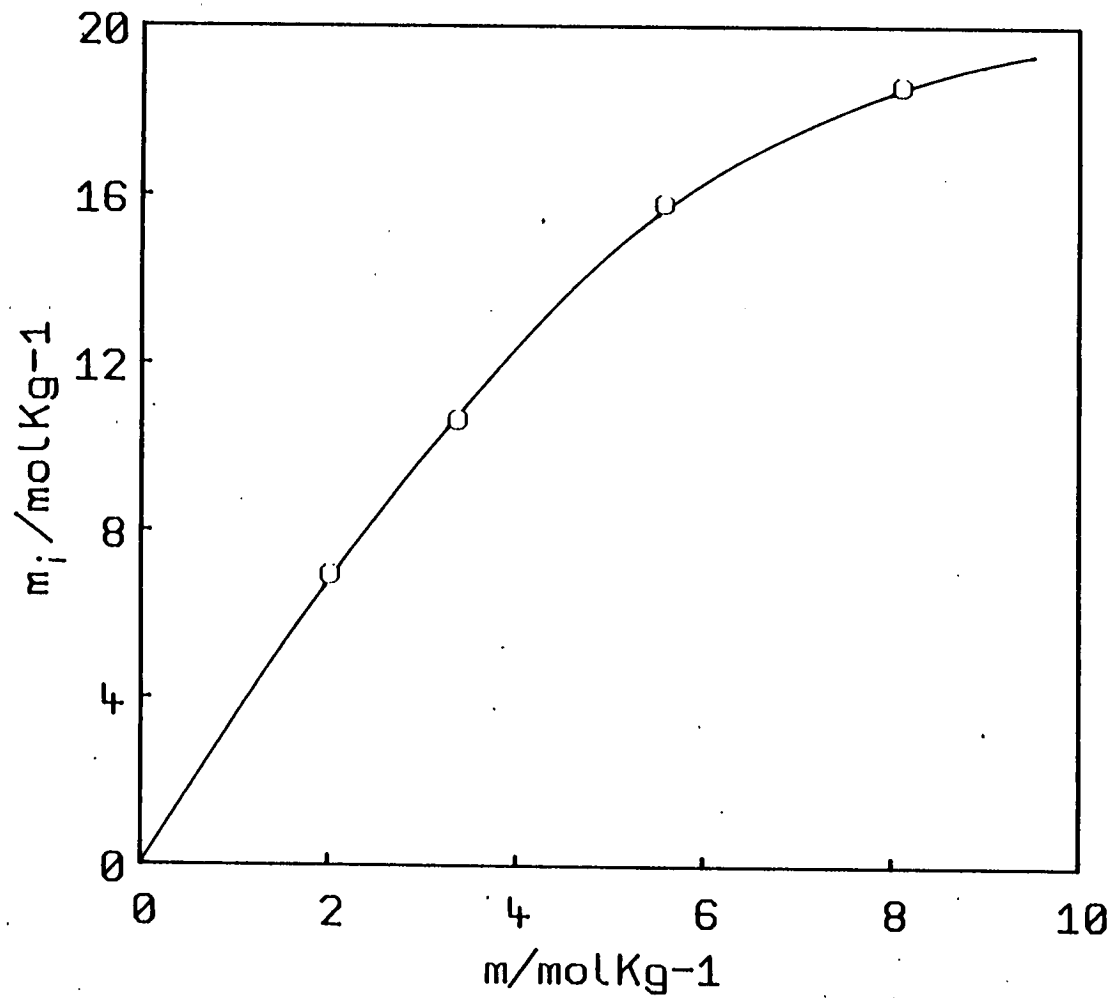


Figure 4.10

A plot of internal molality,  $m_i$ , against external molality,  $m$  of sodium propanesulphonate solution.

## Sodium octanesulphonate + Silicalite

Sodium octanesulphonate that is not occluded is present as anhydrous salt on the surface of the crystals. The maximum amount of salt occluded appears to be almost independent of the water activity of the system. The intracrystalline line that represent the dry dishes are again curved in shape.

### Comparison of the sodium alkylsulphonate systems

The maximum amount of salt that is occluded  $U_s^T$ , at water activities  $a_w = 0.925, 0.871, 0.753$  and  $0.618$  for the three different alkylsulphonates is shown in Tables 4.1-4.4.  $U_s^T$  is expressed in  $gg^{-1}$ , molecules per unit cell and the number of  $CH_2$  groups per unit cell. No systematic trend is observed in the number of molecules occluded with an increase in alkyl chain length. This is because of two opposing factors. The longer the alkyl chain the more favourable the occlusion of salt, but the longer the chain the fewer salt molecules that can be accommodated in the channel network. A systematic trend is observed when the uptake of salt is expressed in number of  $CH_2$  groups per unit cell. The longer the alkyl chain the more  $CH_2$  groups that are occluded.

A plot of  $U_s^T/mol\ g^{-1}$  against  $a_w$  is shown in Figure 4.11. A considerable uptake of salt is observed even at high water activities. At high water activities the curve of sodium propanesulphonate lies well below those of sodium pentanesulphonate and sodium octanesulphonate. This can be rationalised as sodium propanesulphonate has the shortest hydrophobic chain and so its occlusion is presumably not as favourable as the occlusion of sulphonates with longer alkyl chains. The situation becomes more complicated when the curves of sodium pentanesulphonate and sodium octanesulphonate

Table 4.1 The maximum amount of salt,  $U_s^T$  occluded at  $a_w = 0.925$  for three sodiumalkylsulphonates.

sodium alkylsulphonate	$U_s^T/gg$	$U_s^T$ (molecules/unitcell)	$U_s^T$ ( $CH_2$ /unitcell)
propyl	0.047	1.65	4.96
pentyl	0.105	3.15	15.76
octyl	0.112	2.76	22.06

Table 4.2 The maximum amount of salt,  $U_s^T$  occluded at  $a_w = 0.871$  for three sodiumalkylsulphonates.

sodium alkylsulphonate	$U_s^T/gg$	$U_s^T$ (molecules/unitcell)	$U_s^T$ ( $CH_2$ /unitcell)
propyl	0.062	2.18	6.54
pentyl	0.104	3.12	15.61
octyl	0.113	2.78	22.26

Table 4.3 The maximum amount of salt,  $U_s^T$  occluded at  $a_w = 0.753$  for three sodiumalkylsulphonates.

sodium alkylsulphonate	$U/gg$	$U_s^T$ (molecules/unitcell)	$U_s^T$ ( $CH_2$ /unitcell)
propyl	0.079	2.78	8.34
pentyl	0.102	3.08	15.31
octyl	0.109	2.68	21.47

Table 4.4 The maximum amount of salt,  $U_s^T$  occluded at  $a_w = 0.618$  for three sodiumalkylsulphonates.

sodium alkylsulphonate	$U_s^T/gg$	$U_s^T$ (molecules/unitcell)	$U_s^T$ ( $CH_2$ /unitcell)
propyl	0.100	3.00	9.00
pentyl	0.105	3.15	15.76
octyl	0.118	2.86	22.85

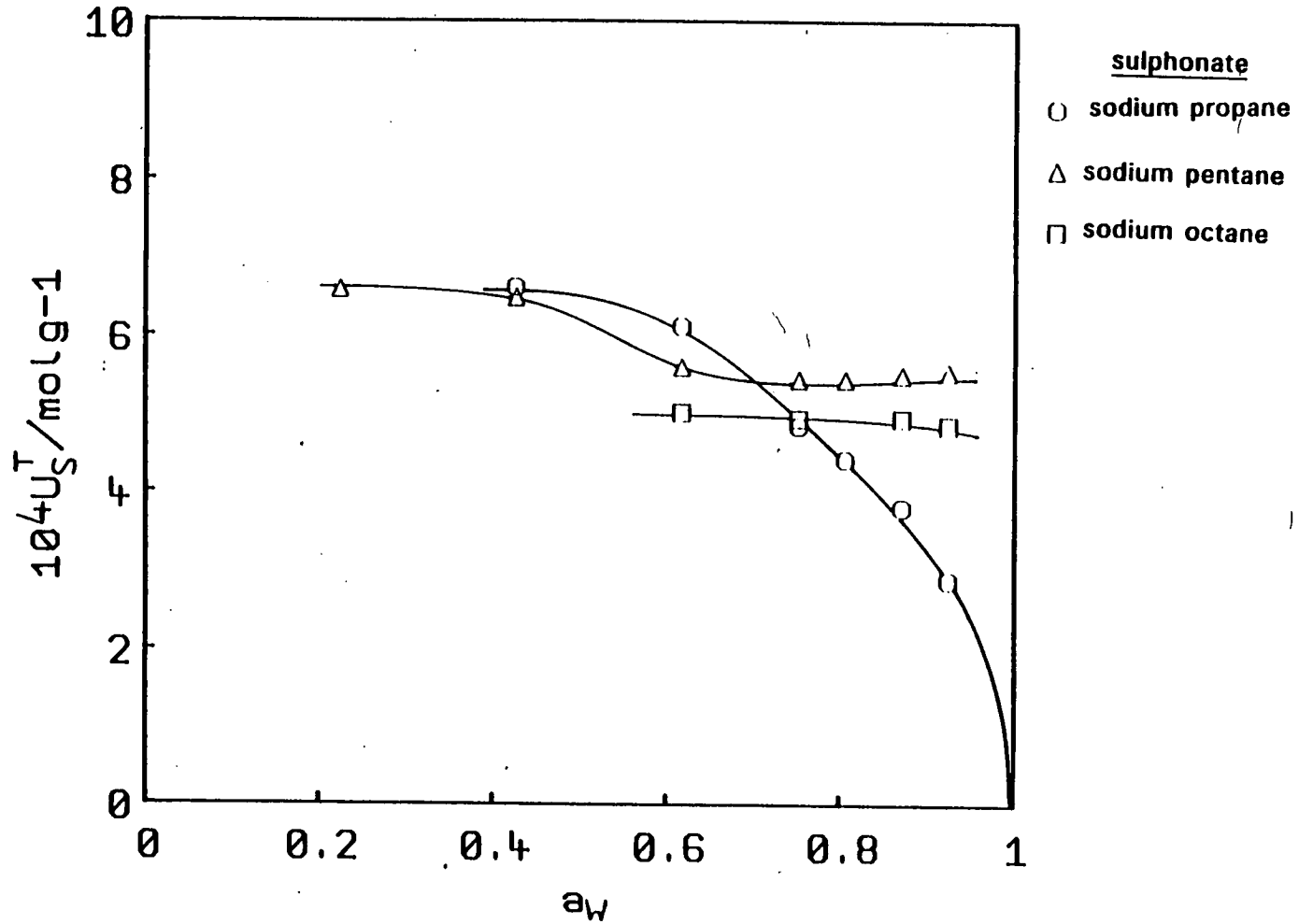


Figure 4.11

A plot of the maximum uptake of salt,  $U_s^T$  in units of mol per gram against water activity,  $a_w$  for three sodium alkylsulphonates.

are examined. The curve for sodium pentanesulphonate lies above the curve for sodium octanesulphonate at all water activities and at some lower water activities the curve for sodium propanesulphonate is the highest. This is a consequence of trends already mentioned. The uptakes of sodium pentanesulphonate and sodium octanesulphonate depend little on the water activity of the system. This can be compared to the sorption of organic molecules by silicalite where maximum sorption is achieved at very low pressures of sorbate. The maximum amount of salt that may be occluded does not correspond to pore filling of the silicalite pores. This is because of ion-ion repulsion of like ions in the channel system.

An abrupt increase in  $U_s^T$  is observed in the occlusion of sodium pentanesulphonate at  $a_w = 0.5$ . This may be due to rearrangement of salt in the silicalite channels. It is possible that this also occurs for sodium octanesulphonate but occlusion at lower activities was not investigated. If this was so, then at low water activity the three curves may converge at  $U_s^T = 6.6 \times 10^{-4} \text{ mol g}^{-1}$  which is equivalent to 3.8 salt molecules per unit cell. This is close to four salt molecules per unit cell which corresponds to the number of intersections in a unit cell of silicalite.

When  $U_s^T$  in units of  $\text{CH}_2$  groups per gram is plotted against  $a_w$  the trends observed are more systematic (Figure 4.12). It is observed that at any given water activity the number of  $\text{CH}_2$  groups occluded per unit cell increase as the length of the alkyl chain in the salt increases.

The molality of the intracrystalline salt,  $m_i$ , in units of moles salt per kg of  $\text{H}_2\text{O}$  plotted against uptake of salt in units of  $\text{mol g}^{-1}$  for two different water activities,  $a_w = 0.618$  and  $0.925$  are shown in Figures 4.13 and 4.14. No obvious

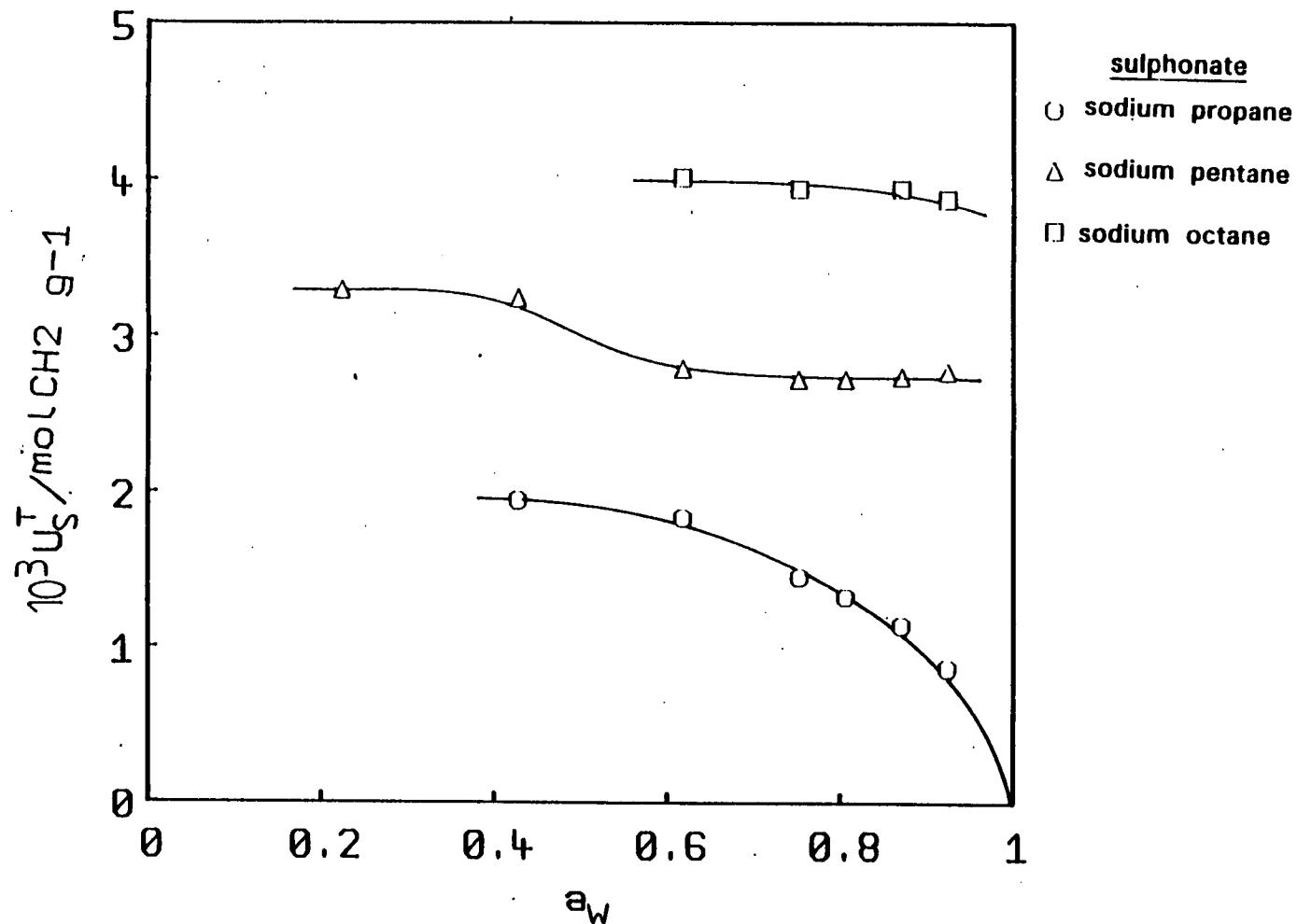


Figure 4.12

Plot of the maximum uptake of salt,  $U_s^T$ , in units of  $\text{molCH}_2\text{g}^{-1}$ , as a function of water activity for three sodiumalkylsulphonates.

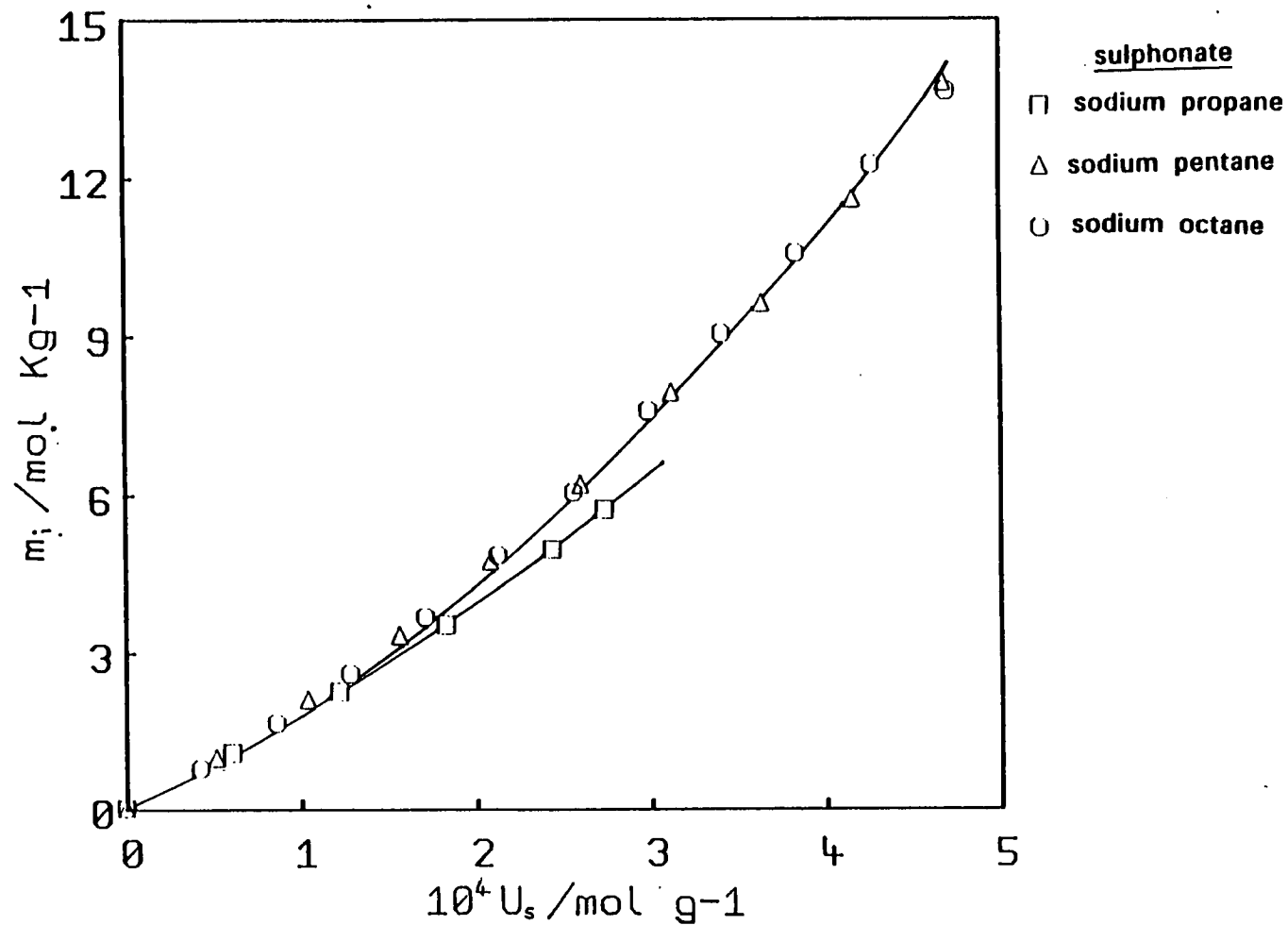


Figure 4.13

Variation of internal molality,  $m_i$ , in  $\text{mol Kg}^{-1}$  with the uptake of salt in  $\text{mol g}^{-1}$  for the three sodium alkyl sulphonates at a water activity of 0.925.

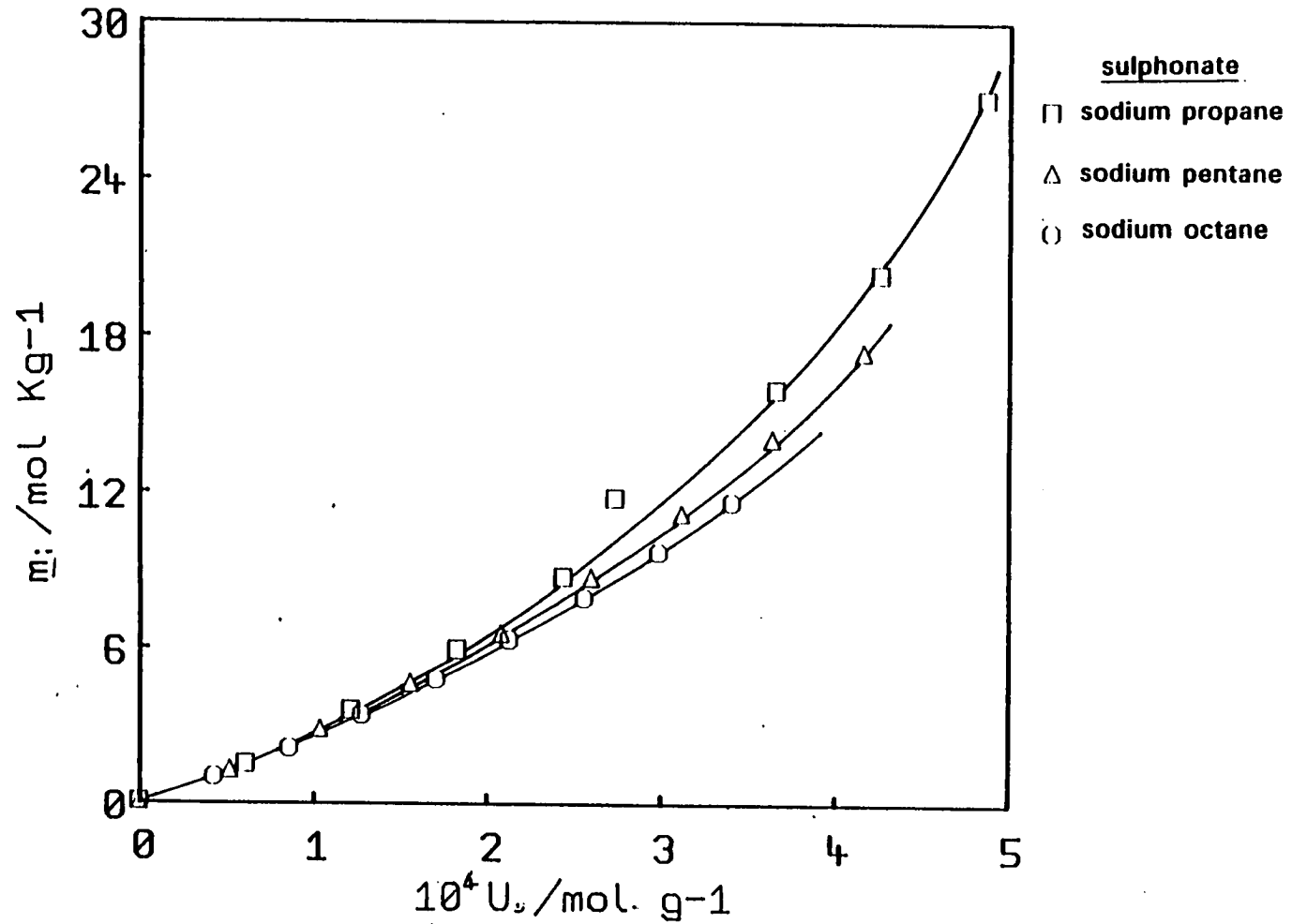


Figure 4.14

Variation of internal molality,  $m_i$ , in mol Kg<sup>-1</sup> with the uptake of salt in mol g<sup>-1</sup> for three sodium alkylsulphonates at a water activity of 0.618.



trends are observed with increasing length of alkyl chain. For all three salts at both water activities an increase in internal molality is observed as  $U_s$  is increased. The increase in internal molality is greatest at large uptakes of salt. This is a consequence of water molecules being displaced from the channels of silicalite by the uptake of salt molecules. At low uptakes of salt the internal molality is the same irrespective of the length of alkyl chain. This suggests that occlusion of a small number of molecules will displace a certain number of water molecules whatever the dimensions of the salt occluded. Perhaps, the first salt molecules occluded are associated with sites that are occupied by water molecules. As aforementioned, such sites could be internal silanol groups. The different trends observed at higher uptakes of salt at different water activity is a consequence of the the differences already discussed. The variation of the internal molality in units of moles of salt per Kg of  $H_2O$  with uptake of salt in units of  $CH_2$  groups per unit cell at two different water activities is shown in Figures 4.15 and 4.16. The trends at both water activities are now similar. At all uptakes of salt, the concentration of  $CH_2$  groups is greatest for sodium octanesulphonate and least for sodium propane sulphonate. There are fewer water molecules per  $CH_2$  group in sodium octanesulphonate than per  $CH_2$  group in sodium propanesulphonate.

#### **Variation in Isopiestic Plots with Time**

In order to ascertain whether or not the results were dependent on the equilibration time, the system was periodically re-equilibrated at  $a_w = 0.783$ . The plots of  $WW/WZ$  against  $WS/WZ$  at  $a_w = 0.783$  for three different equilibration times are shown in Figure 4.17. It is notable that the value of  $U_s^T$  and the concentration of the solution phase is constant with time, so the results discussed in the previous section hold true whatever the equilibration time. However, the uptake of water varies with time. This effect is most

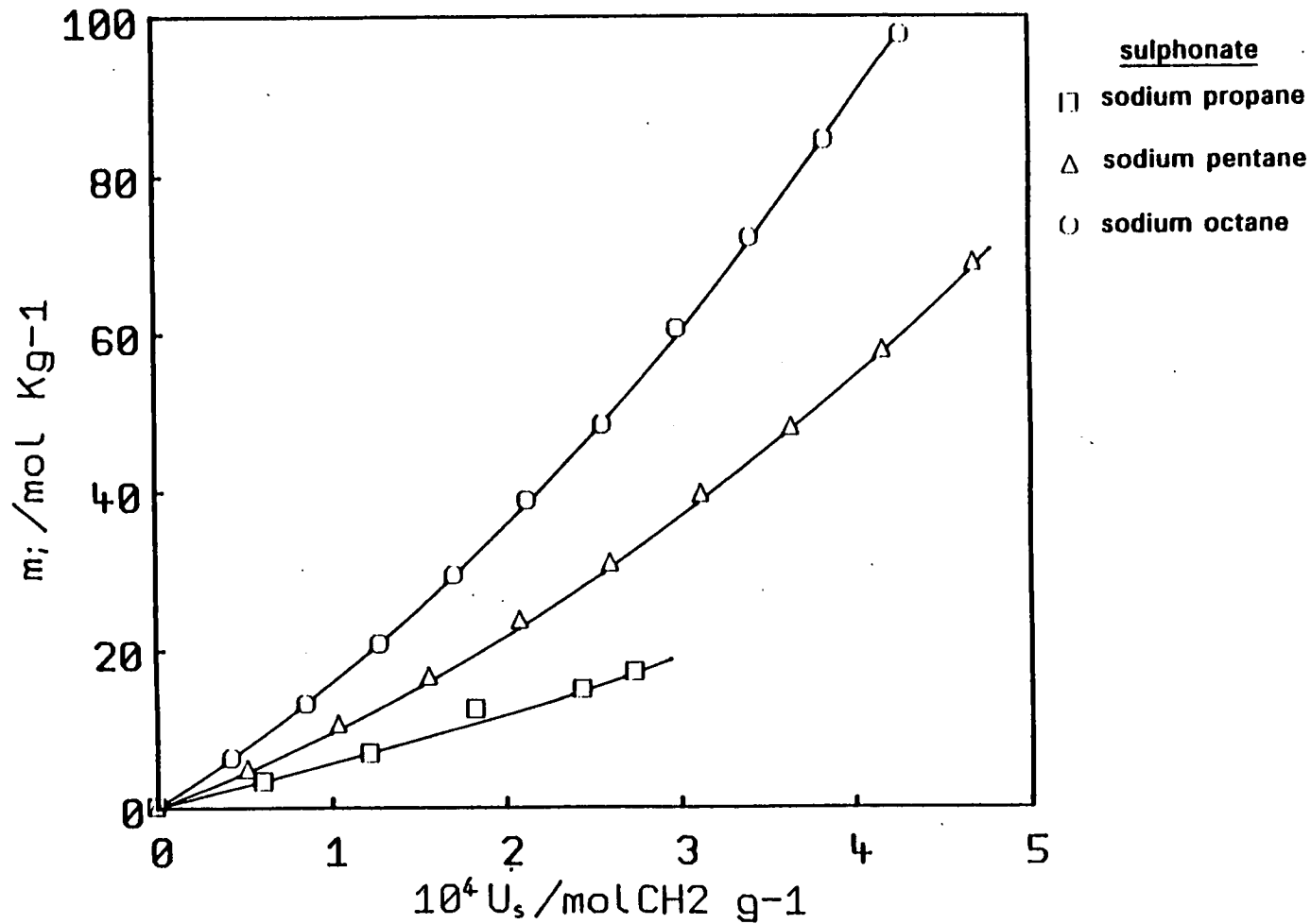


Figure 4.15

A plot of internal molality,  $m_i$ , against the uptake of salt in units of  $\text{mol CH}_2 \text{ g}^{-1}$ , at  $a_w = 0.925$ .

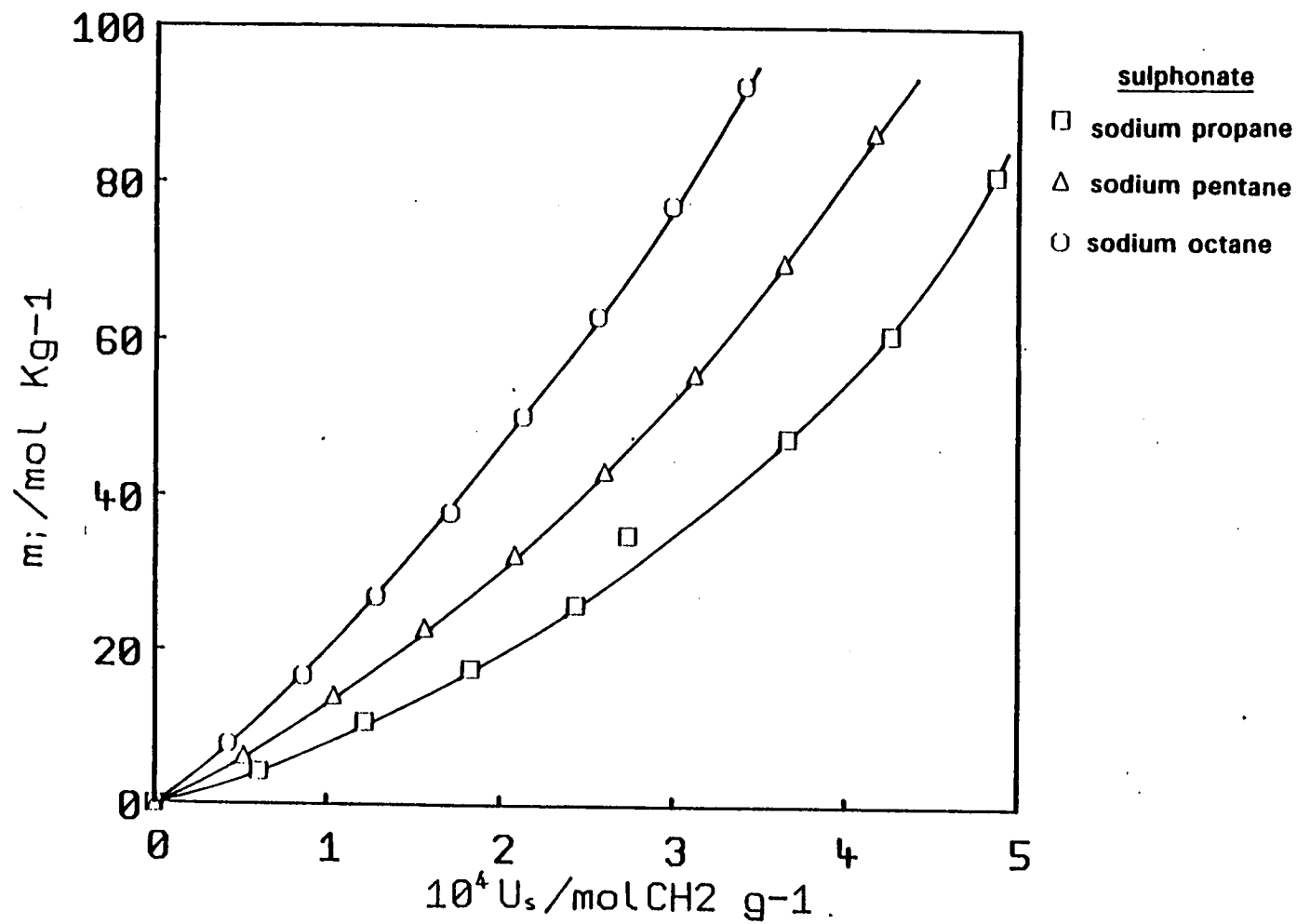


Figure 4.16

A plot of internal molality,  $m_i$  against the uptake of salt in units of  $\text{mol CH}_2 \text{ g}^{-1}$ , at  $a_w = 0.618$ .

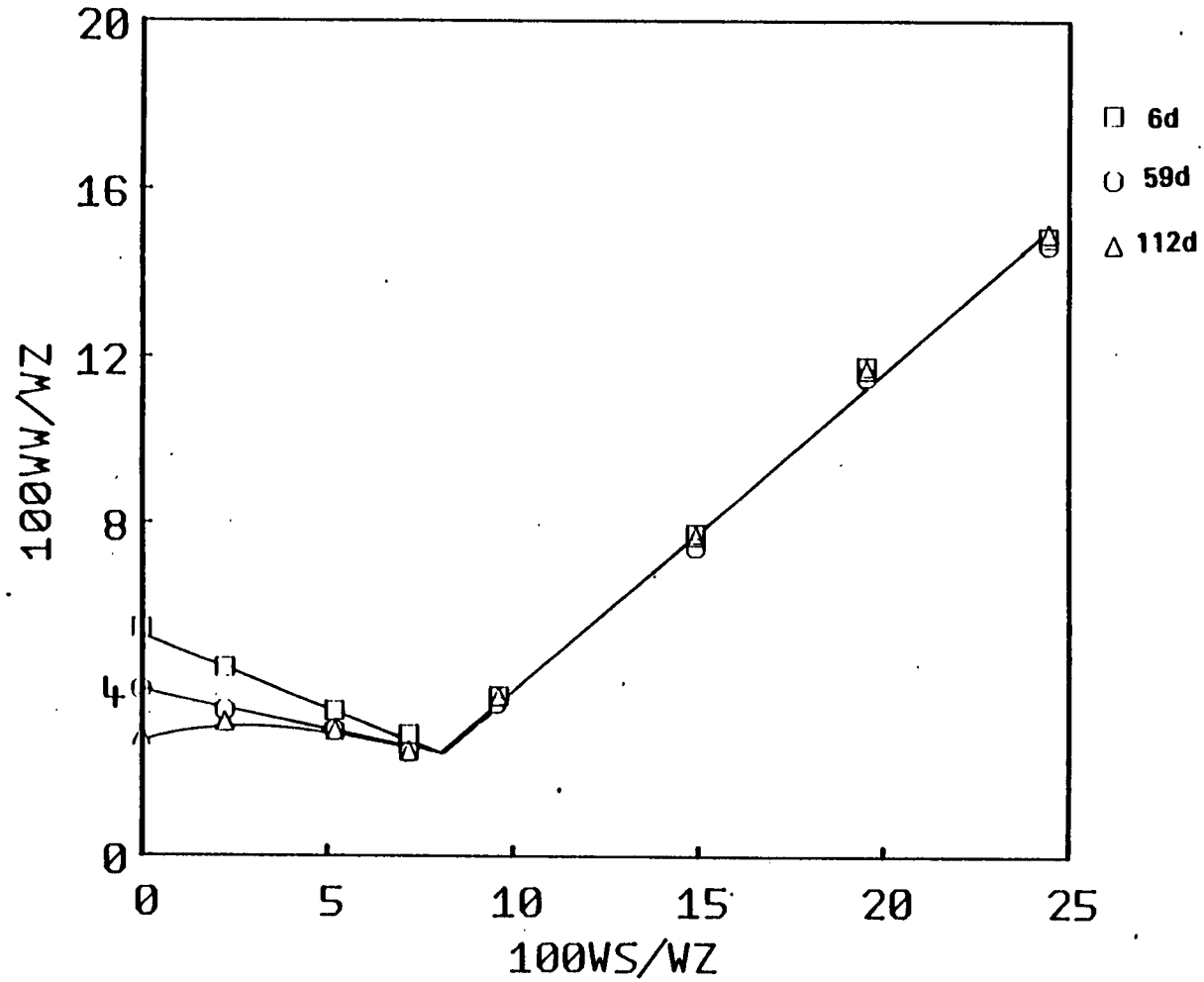


Figure 4.17

The effect of equilibration time on plots of  $WW/WZ$  against  $WS/WZ$  for the system sodiumpentanesulphonate + silicalite,  $a_w = 0.783$ .

pronounced in the dish that contains silicalite alone. The number of water molecules displaced by the occlusion of salt decreases in later equilibrations. Indeed, plot three exhibits a different shape at low uptakes of salt than that of the two earlier equilibrations. The uptake of water initially increases with occlusion of salt, prior to decreasing as in previous equilibrations. These observations suggest that the silicalite becomes more hydrophobic as the equilibration time increases.

It is difficult to account for these observations. Healing of lattice faults - internal hydroxyl groups - would account for such observations, as a decrease in such faults would render the framework more hydrophobic.

X-ray diffraction patterns were obtained of all the salt/silicalite samples after a final equilibration at  $a_w = 0.723$ . These patterns are shown in Figures 4.18, 4.19 and 4.20. The XRD patterns of sodium propanesulphonate show changes in relative peak heights at high WS/WZ. This applies to samples in dishes 6, 7, and 8. In these samples there is an excess salt which forms a solution on the exterior of the silicalite crystals. At  $a_w=0.723$ , any excess sodium pentanesulphonate or sodium octanesulphonate is present on the exterior of the crystals in an anhydrous form. Samples of silicalite with sodium pentanesulphonate or sodium octanesulphonate occluded in the pores but no salt present on the surface of the crystals exhibit XRD patterns similar to that of the parent silicalite. However, the XRD patterns of samples with salt present on the surface of the crystals show peaks due to the salt. The height of these "salt" peaks increases as the amount of salt on the surface of the silicalite increases. These results confirm that at low WS/WZ, all the salt is intracrystalline with no salt present on the exterior of the crystals.

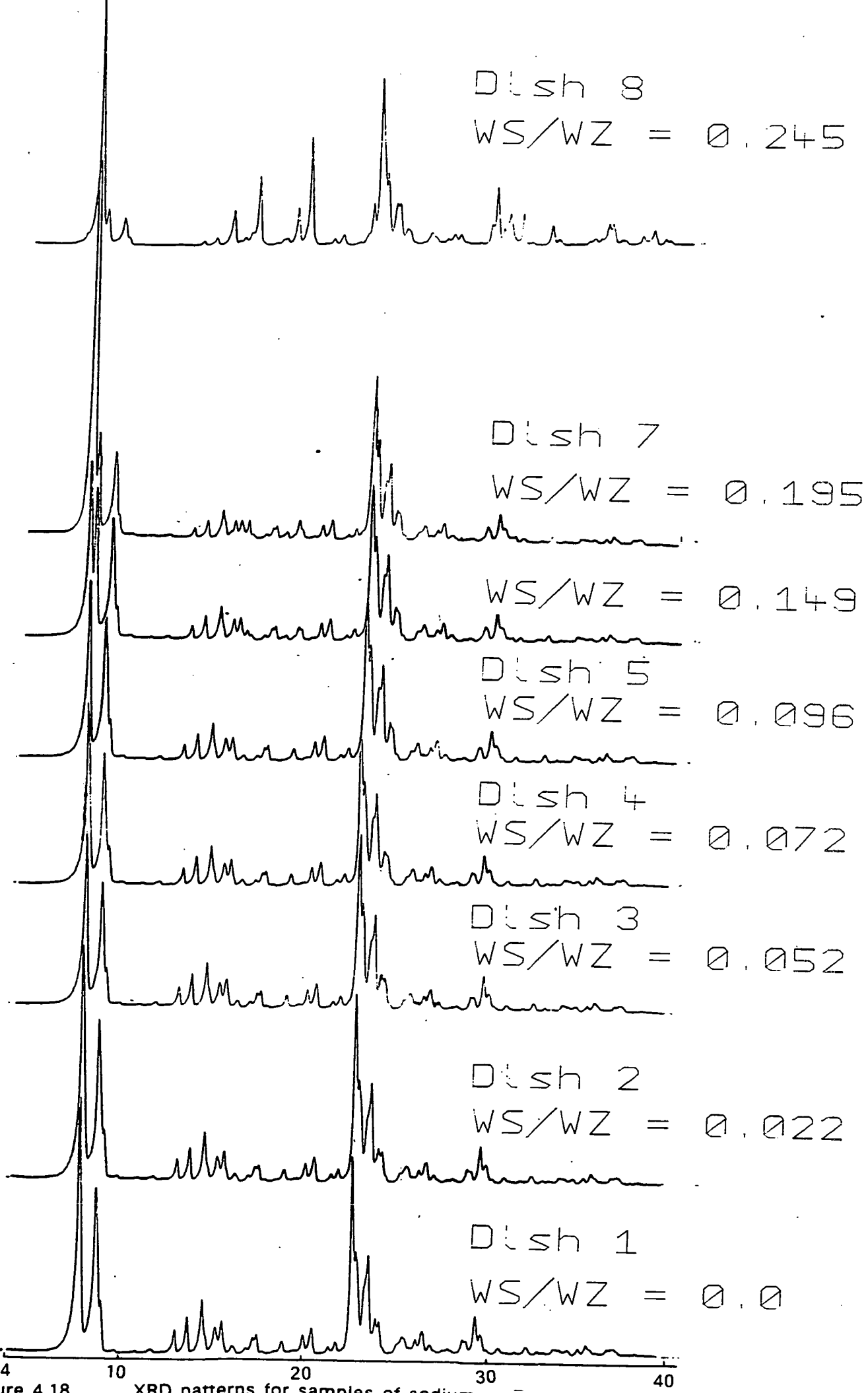


Figure 4.18 XRD patterns for samples of sodium propenesulphonate/silicalite.

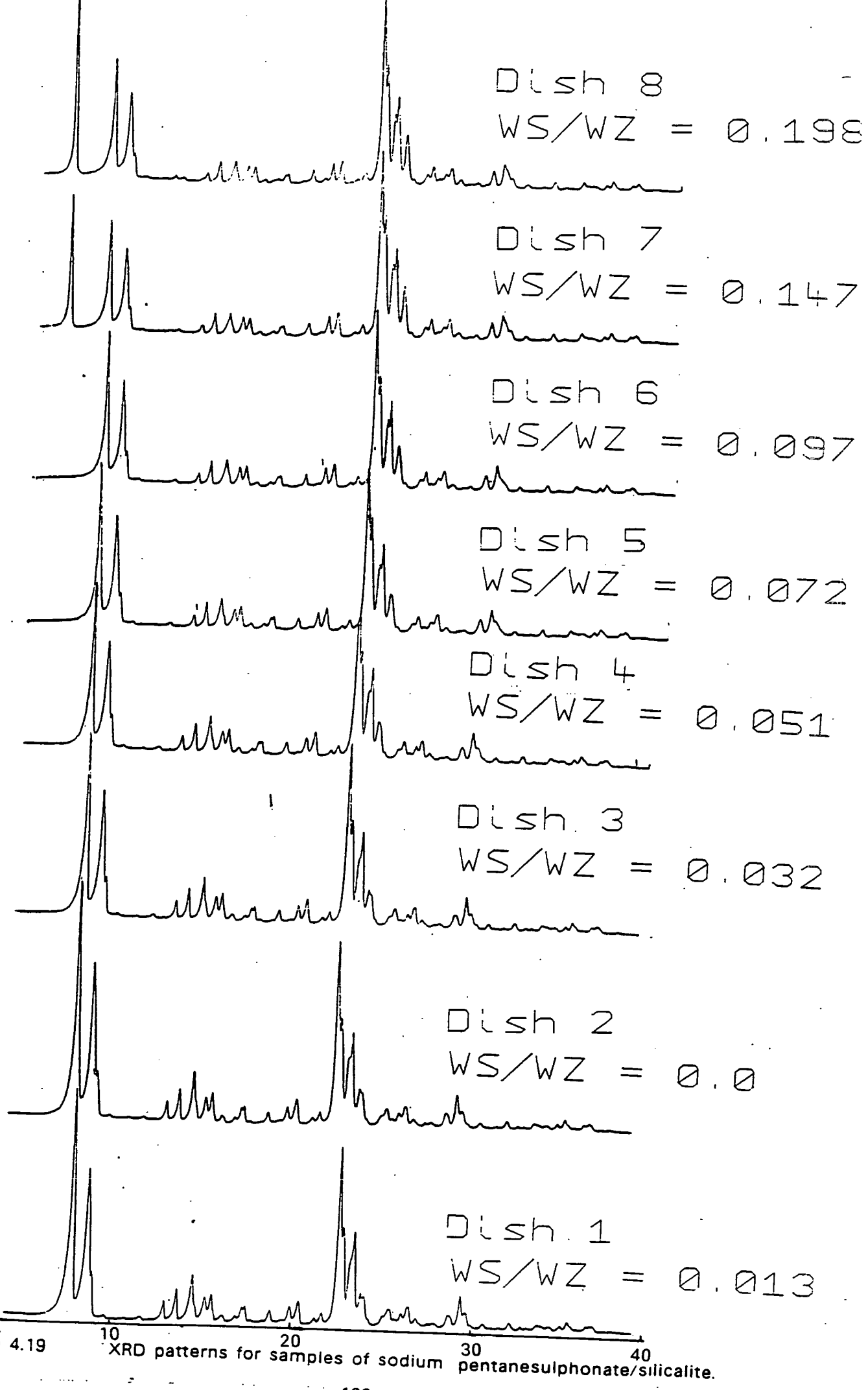


Figure 4.19 XRD patterns for samples of sodium pentanesulphonate/silicalite.

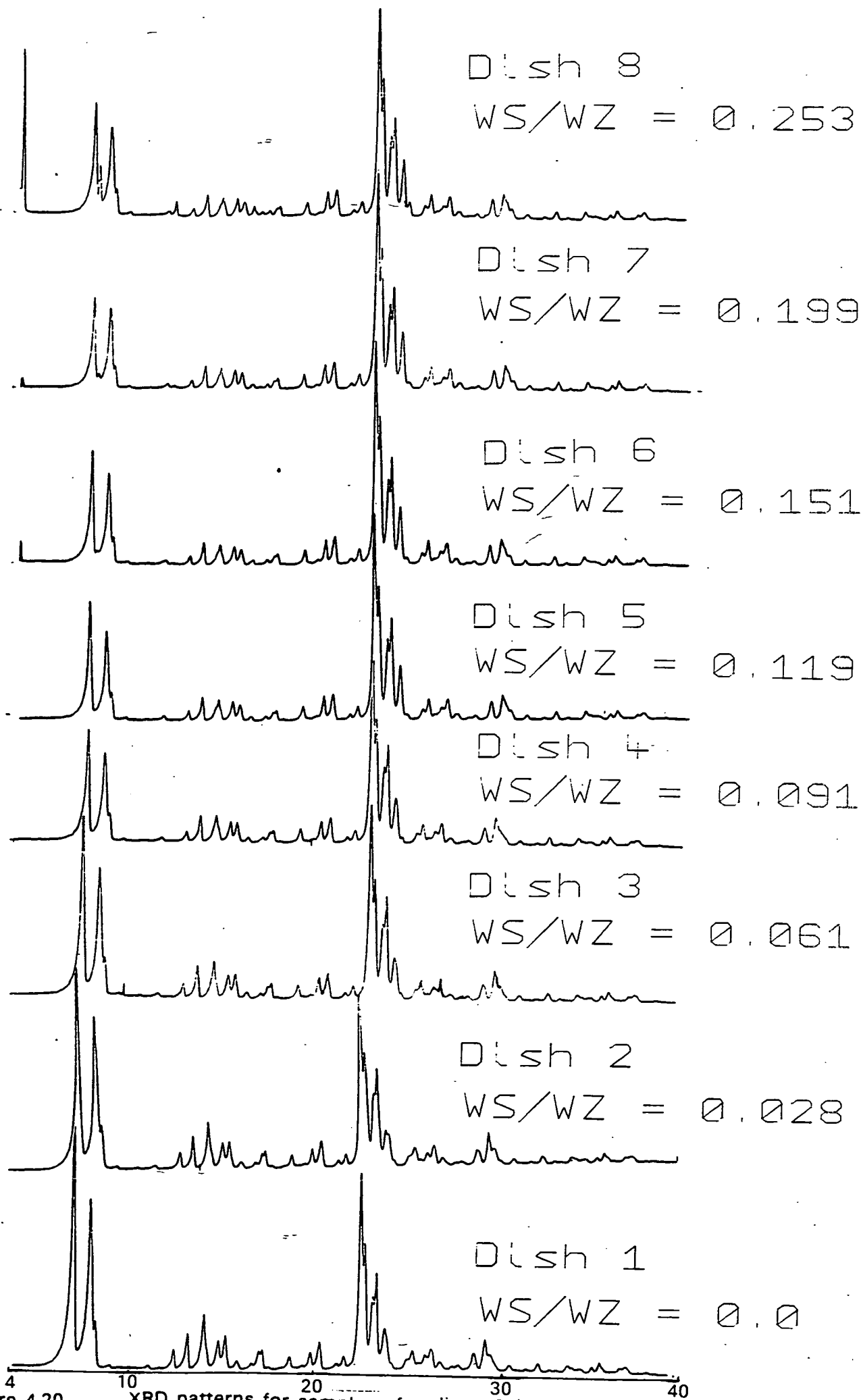


Figure 4.20 XRD patterns for samples of sodium octanesulphonate/silicalite.



## 4.5 Sorption Properties of Salt Occluded Silicalite

The sorption behaviour of silicalite with varying amounts of salt occluded was investigated using the "multi-equilibration" method. The procedure followed was:

1. The weight of anhydrous molecular sieve was found as on page 80.
2. Small amounts of salt were weighed into the sample tubes that contained silicalite.
3. Water was added to the sample tubes.
4. Samples were dried in an oven at 70°C.
5. Samples were heated at 200°C to remove any remaining water and sorbed gases.
6. Samples cooled to room temperature in vacuo over P<sub>2</sub>O<sub>5</sub>.
7. Samples reweighed prior to equilibration with 2cm<sup>3</sup>/2cm<sup>3</sup> DBP/sorbate at 25°C.
8. After equilibration the samples were reweighed to obtain uptake of sorbate per gram of anhydrous silicalite.

In this technique all the water is slowly removed from the samples. This will result in larger amounts of salt being occluded than if water had been

present as in the isopiestic technique.

The results are plotted as uptake of sorbate against weight of salt added per gram of anhydrous silicalite, WS/WZ. An example of a typical plot is shown in Figure 4.21. If salt is occluded a decrease in  $U_{\text{sorbate}}$  with WS/WZ is observed. The gradient of this line is a measure of the volume that the salt prohibits the sorbate from occupying. A value of WS/WZ is reached when no more salt can be occluded, any salt in excess is present on the surface of the crystals. At this point there will be no further decrease in uptake of sorbate and the experimental points lie on a line horizontal with the WS/WZ axis.

Because of its simplicity and quickness this technique can also be used to discover whether or not a salt is occluded by a molecular sieve before carrying out more lengthy explorations with the isopiestic technique. It is also useful to know approximately how much salt may be occluded so appropriate amounts of salt may be added to dishes in the isopiestic technique.

#### 4.5.1 Sorption Properties of CsCl/Silicalite and NaCl/Silicalite

The uptakes of *n*-heptane by silicalite to which quantities of CsCl or NaCl have been added are shown in Figure 4.22. WS/WZ is expressed in units of  $\text{mol g}^{-1}$  so the two plots may be compared. Very little decrease in  $U_{\text{n-heptane}}$  is observed when NaCl is in contact with the silicalite. But when CsCl is added to the silicalite a decrease in  $U$  is observed at low WS/WZ. The maximum amount of CsCl that could be occluded under these conditions is  $0.4 \times 10^{-3} \text{ mol g}^{-1}$ . CsCl is occluded to a small extent whereas NaCl is excluded by silicalite because  $\text{Cs}^+$  is a much larger ion than  $\text{Na}^+$  and so the  $\text{Cs}^+$  ion has a

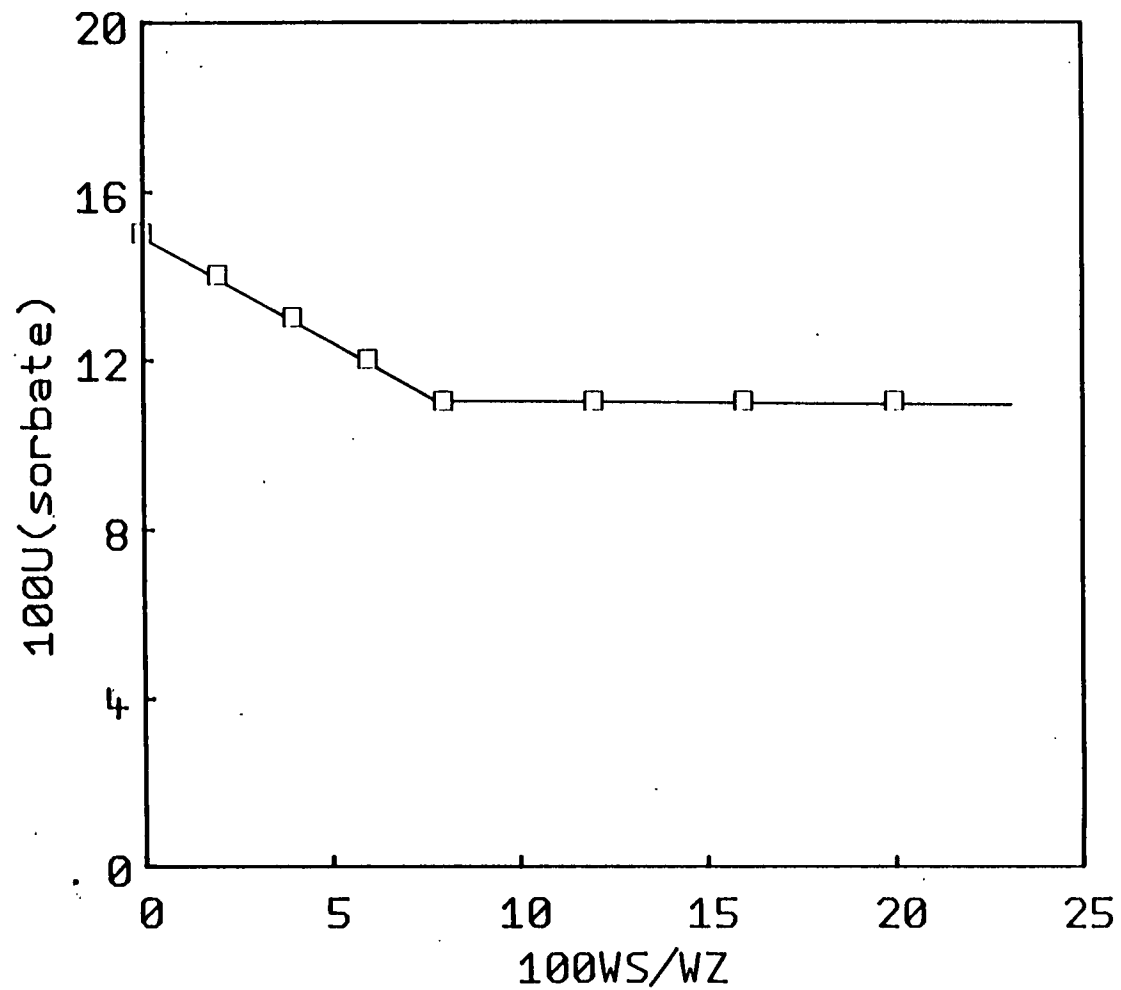


Figure 4.21

Set of sorption results for an imaginary typical salt system, shown as a plot of uptake of sorbate,  $U$  against weight of salt per gram of molecular sieve,  $WS/WZ$ .

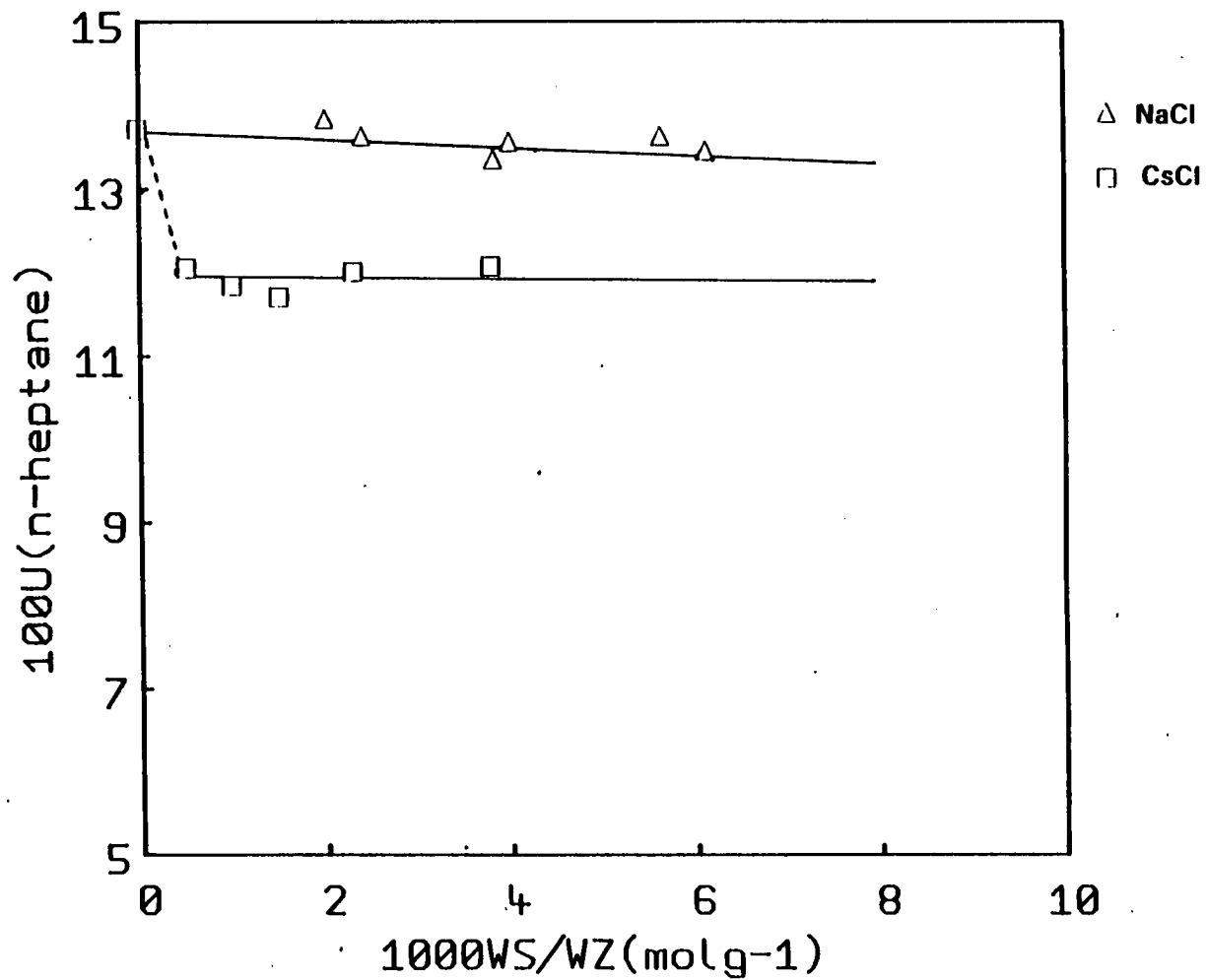


Figure 4.22

The variation in the uptake of n-heptane with the weight of salt for the CsCl/silicalite and NaCl/silicalite systems.

higher dispersion energy of interaction with the silicalite framework than the  $\text{Na}^+$  ion.

#### 4.5.2 Uptake of n-heptane by Hexamethonium bromide/Silicalite and Decamethonium bromide/Silicalite

The uptakes of n-heptane by silicalite contacted with different quantities of hexamethonium bromide or decamethonium bromide, are shown in Figure 4.23 as a plot of  $U_{\text{n-heptane}}$  against WS/WZ. The plot for hexamethonium bromide suggests that  $0.05\text{gg}^{-1}$  of salt is occluded. This is equivalent to 0.8 salt molecules per unit cell. The occlusion results obtained from isopiestic measurements showed that hexamethonium bromide was excluded from the silicalite framework. However, occlusion in the isopiestic technique occurs at  $25^\circ\text{C}$ . In the "multi-equilibration" technique samples are heated to  $200^\circ\text{C}$ . The higher the temperature, the larger the vibrational amplitudes of the oxygen atoms in the framework and so as the temperature increases the pore size increases. At  $25^\circ\text{C}$ , hexamethonium bromide is excluded from the silicalite framework. But at  $200^\circ\text{C}$  the pore diameter has increased sufficiently to permit hexamethonium molecules to pass through the pores into the channel system beyond.

The decamethonium bromide plot shows that very little salt is occluded, somewhat less than  $0.01\text{gg}^{-1}$ . The diameter of decamethonium bromide is similar to that of hexamethonium bromide so presumably it is the longer length of decamethonium bromide that prevents its occlusion into the silicalite framework.

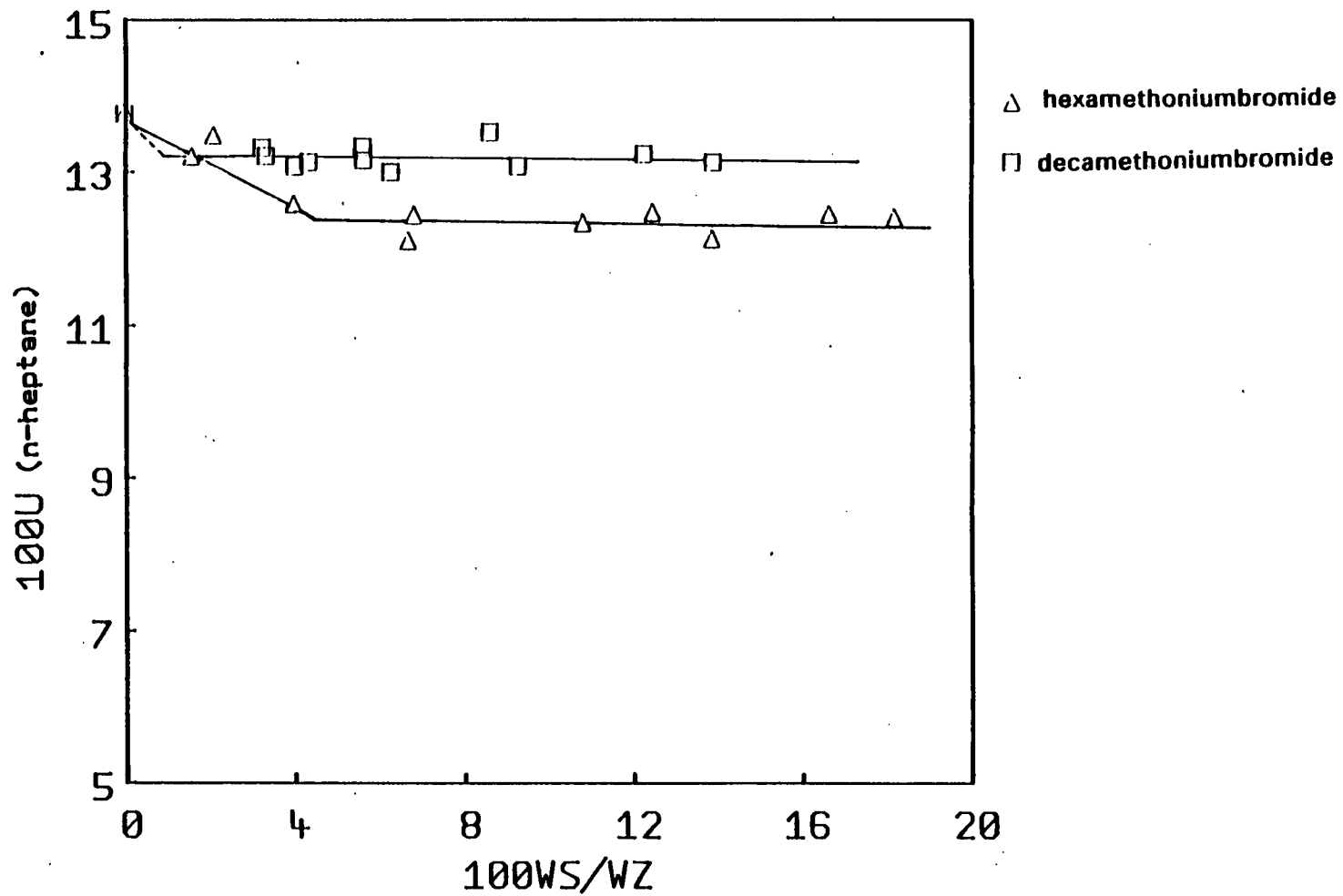


Figure 4.23

A plot of uptake of n-heptane against WS/WZ for hexamethonium bromide/silicalite and decamethonium bromide/silicalite.

#### 4.5.3 Uptake of N-heptane by Sodium benzenesulphonate/Silicalite

The uptake of n-heptane by silicalite with different amount of salt occluded in the channels was measured using the "multi-equilibration" method and the results are shown as a plot of  $U_{\text{heptane}}$  against WS/WZ in Figure 4.24. At low weights of added salt a reduction in  $U_{\text{heptane}}$  occurs but at  $\text{WS/WZ} > 0.035\text{gg}^{-1}$  no further reduction in  $U_{\text{heptane}}$  occurs. These results agree well with the results obtained from the isopiestic technique. Less than  $0.035\text{gg}^{-1}$  of sodium benzenesulphonate is occluded and reduces the  $U_{\text{heptane}}$  from  $0.135\text{gg}^{-1}$  to  $0.115\text{gg}^{-1}$ . Any further salt added in excess of this quantity remains on the surface of the silicalite and does not affect the uptake of n-heptane.

#### 4.5.4 Uptakes of sorbates by Sodium alkylsulphonates

The variation of uptakes of n-heptane, n-dodecane and p-xylene by silicalite with different amount of salt occluded in the channels, is shown for sodium propanesulphonate, sodium pentanesulphonate and sodium octanesulphonate in Figures 4.25, 4.26 and 4.27 as a plot of  $U_{\text{sorbate}}$  against WS/WZ. The quantities  $U_{\text{sorbate}}$  and WS/WZ are expressed in  $\text{gg}^{-1}$ . The plots show that the occlusion of alkylsulphonate results in a decrease in the uptake of sorbate. Obviously, this is due to the salt occupying space in the channels that the sorbate would have occupied. The weight of salt after which no further reduction in uptake of sorbate occurs, corresponds to the maximum amount of occlusion of that the salt under the given conditions. This value  $U_s^T$  should be the same for a given salt irrespective of the sorbate. This is observed within experimental error. Although occlusion of sodium alkylsulphonates reduces the uptake of sorbates by silicalite, it does not appear to alter the molecular sieving properties.

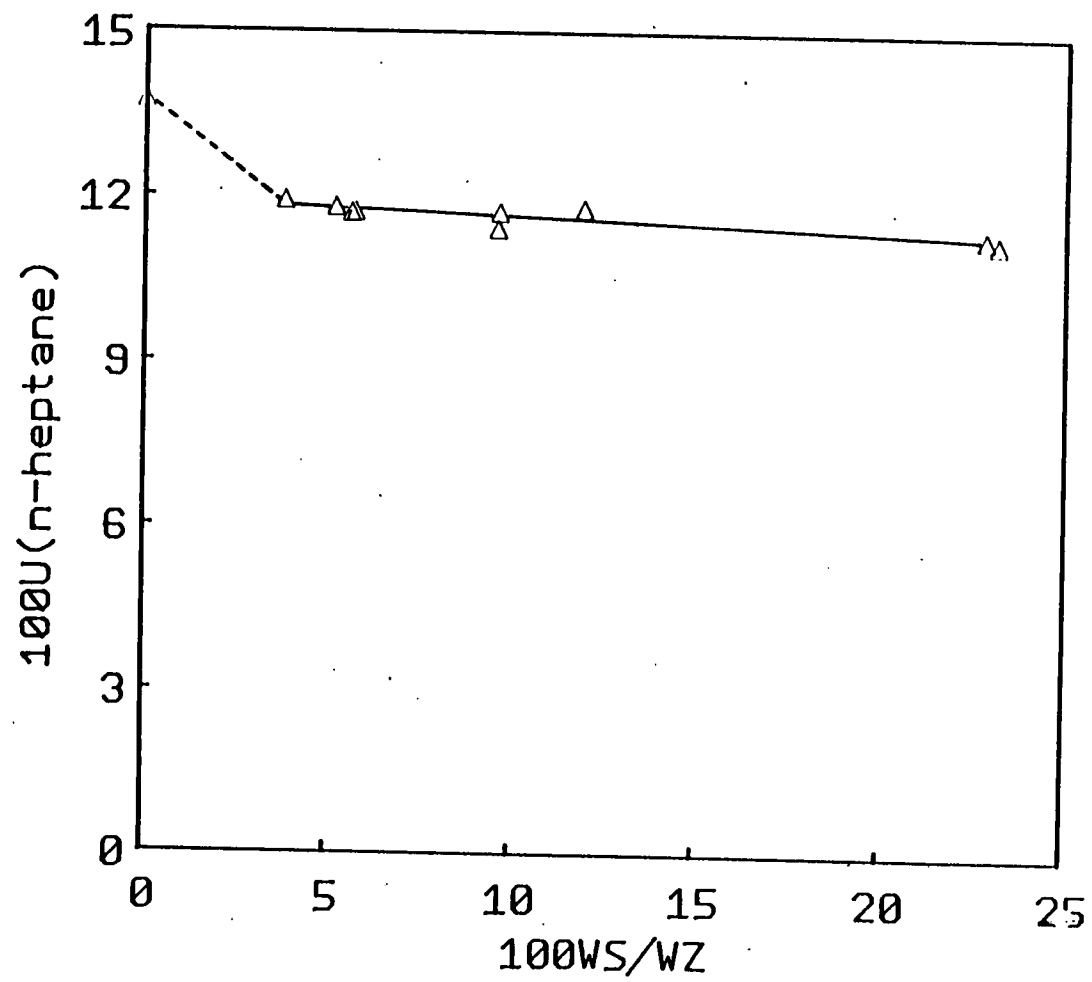


Figure 4.24 The variation in uptake of n-heptane with weight of salt for the system sodium benzenesulphonate/silicalite.



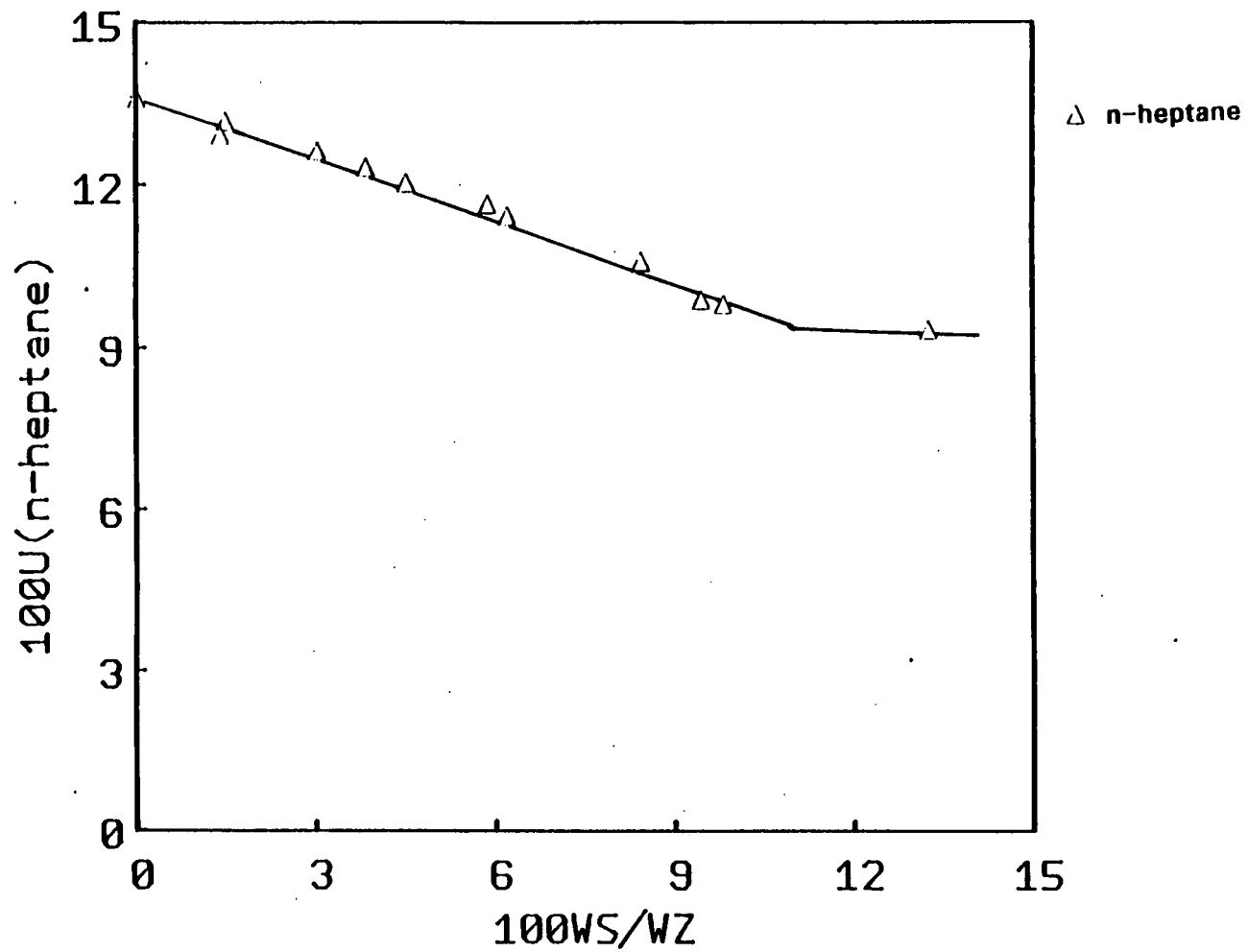


Figure 4.25

Uptake of n-heptane plotted against  
WS/WZ for sodium propanesulphonate.

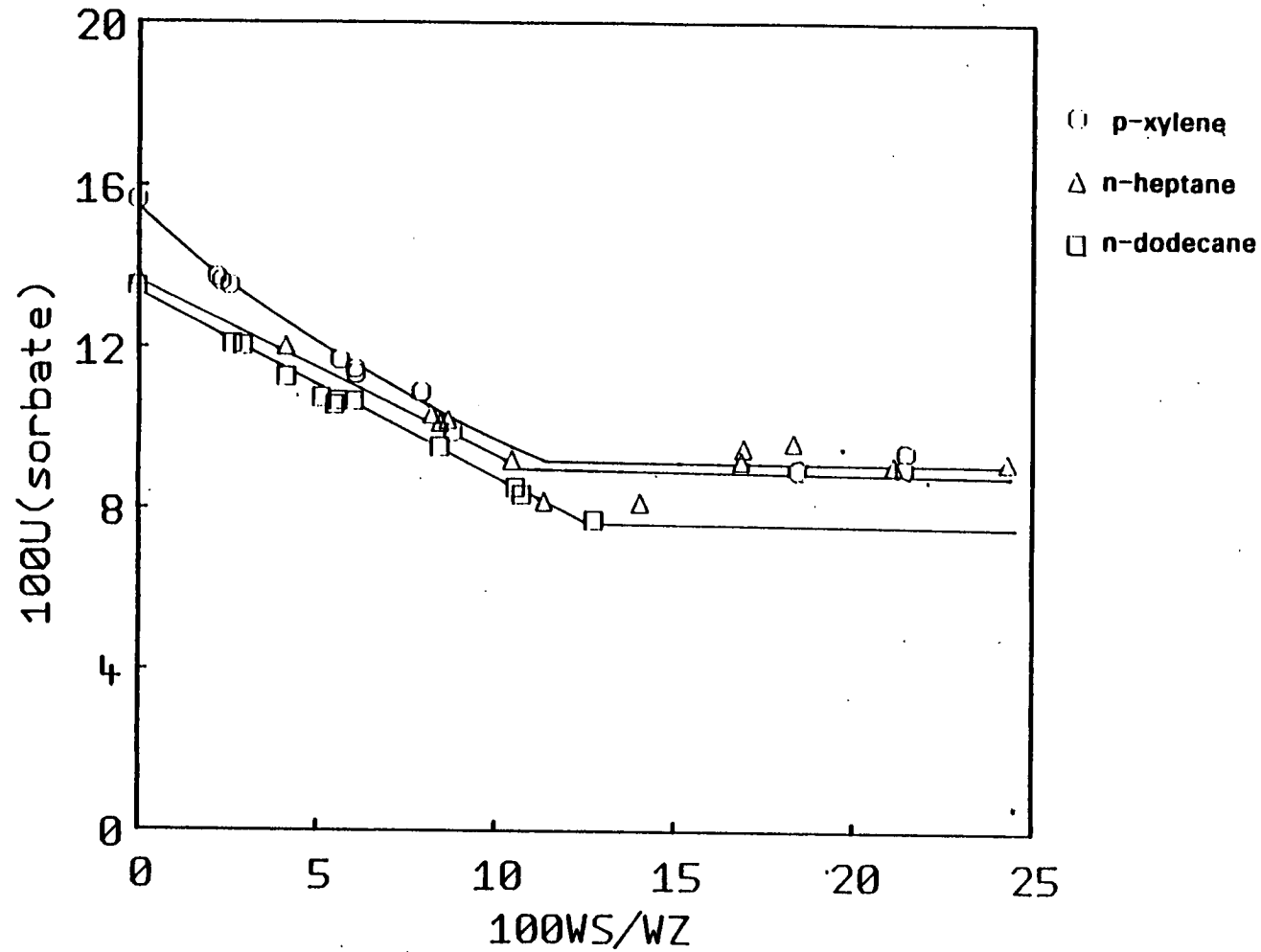


Figure 4.26 Uptakes of n-heptane, n-dodecane and p-xylene plotted against WS/WZ for sodium pentanesulphonate.

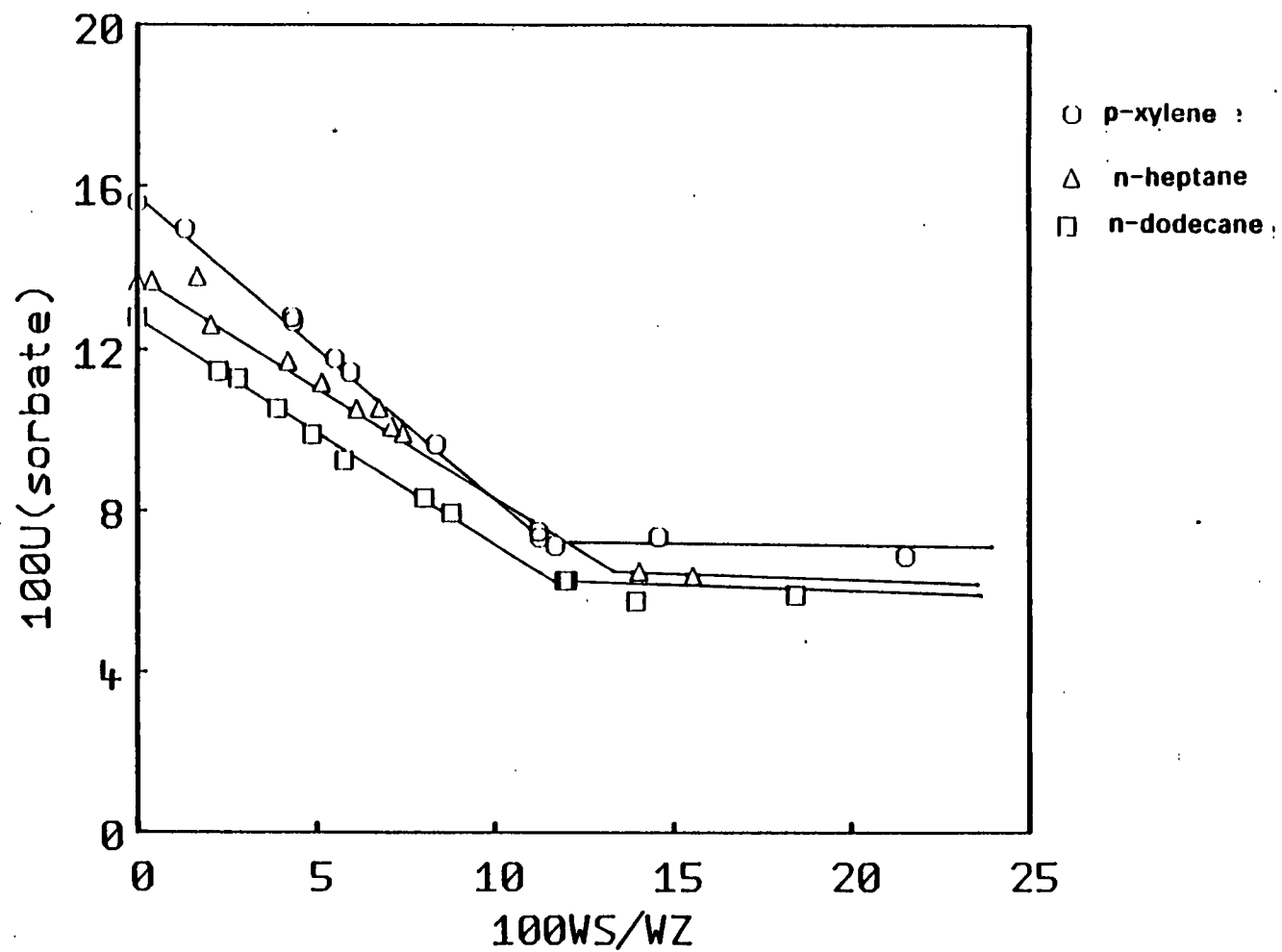


Figure 4.27

Uptakes of n-heptane, n-dodecane and p-xylene plotted against WS/WZ for sodium octanesulphonate.

The variation of  $U_{n\text{-heptane}}/\text{gg}^{-1}$  with  $W_S/W_Z$  when  $W_S/W_Z$  is expressed in units of  $\text{mol g}^{-1}$  is shown in Figure 4.28. The reduction in the uptake of n-heptane is greatest the longer the length of alkyl chain. This is simply a consequence of a sodium propanesulphonate molecule occupying less volume than a sodium octanesulphonate molecule. The maximum amount of salt that may be occluded under these conditions shows no systematic trend as was also observed in the isopiestic technique.

However, as previously, if  $W_S/W_Z$  is expressed in mol  $\text{CH}_2$  groups per g silicalite a trend becomes apparent, as seen in Figure 4.29. The longer the alkyl chain the greater the number of  $\text{CH}_2$  groups occluded in the silicalite framework. This agrees well with the isopiestic measurements. The slope  $dU/d(W_S/W_Z)$  is greatest for sodium propanesulphonate and least for sodium octanesulphonate. This is a result of the volume occupied by the sodium ions and the sulphonate ions. For a sodium propanesulphonate, there is a sodium ion and a sulphonate ion associated with every three  $\text{CH}_2$  groups whereas for sodium octanesulphonate there is only a sodium and a sulphonate ion associated with every eight  $\text{CH}_2$  groups.

## 4.6 Conclusion

Silicalite occludes salts readily if they have considerable organic character and are of the correct size and shape to pass through the pores. Sodium alkylsulphonates are occluded in considerable quantities by silicalite even at high water activities or low solution concentrations. It is observed that the dependence of salt occlusion on water activity is far less for high silica molecular sieves than for more aluminous zeolites. The higher the temperature at which the occlusion process is undertaken at, the greater is amount of salt occluded. Indeed, salts that are too large to be occluded at  $25^\circ\text{C}$  may be

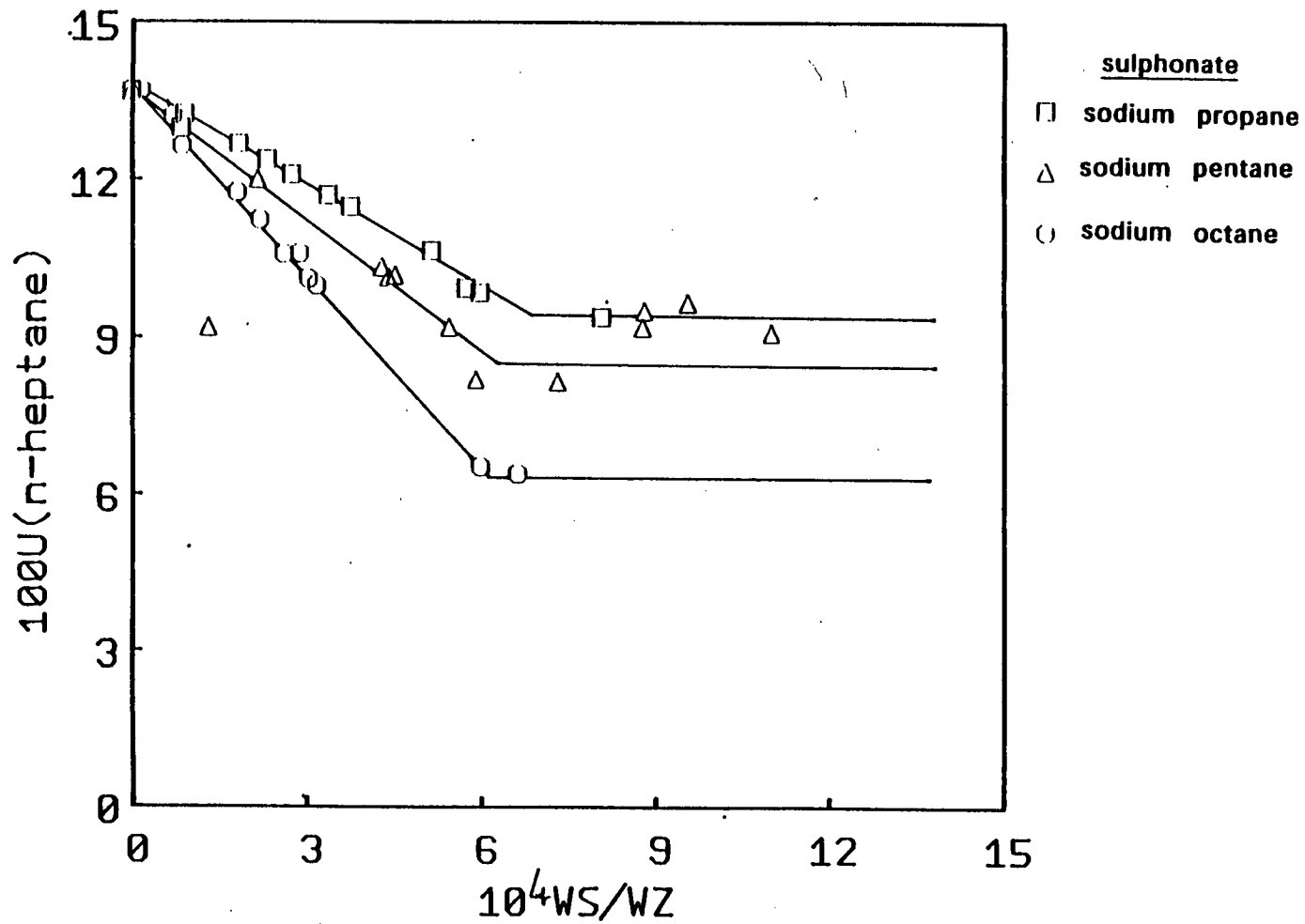


Figure 4.28 A plot of uptake of n-heptane by silicalites with sodium propane sodium pentane, and sodium octanesulphonate occluded. The amount of salt being expressed in units of  $\text{mol g}^{-1}$ .

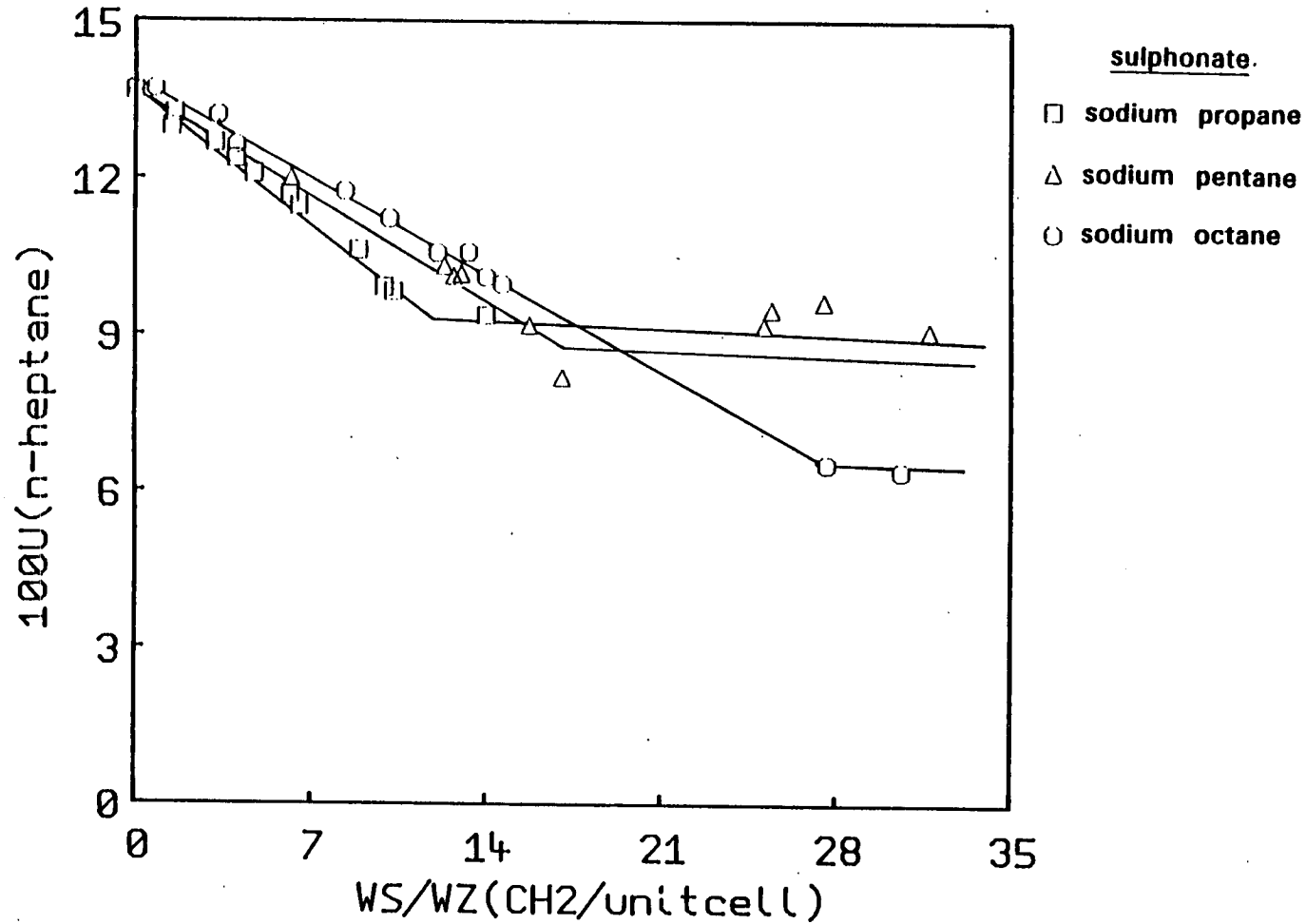


Figure 4.29

A plot of uptake of n-heptane by silicalites with sodium propane, sodium pentane and sodium octanesulphonate occluded. The amount of salt being expressed in units of CH<sub>2</sub> groups per unit cell.

occluded at 200°C. Some salts that are ionic in nature are occluded in small quantities, e.g. CsNO<sub>3</sub> and CsCl but other ionic salts, particularly those with small ionic radii such as NaCl are excluded from the silicalite framework as a consequence of their very weak interaction with the framework. Ionic salts that are occluded are probably associated with hydrophilic sites within the framework.

The occlusion of salt alters the sorption properties of molecular sieves. However the salts occluded in this work did not alter the molecular sieving properties of the silicalite.

## 4.7 References

1. R.M. Barrer and W.M. Meier, *J. Chem. Soc.*, 1958,299
2. D.J. Shaw, "Introduction to colloid and surface chemistry", Butterworths, 1970
3. R.M. Barrer and A.J. Walker, *Trans. Faraday Soc.*, 1964,60,171
4. S.G. Fegan and B.M. Lowe, Proceedings of the 6th International Conference on Zeolites(Reno,1983)
5. S.G. Fegan, Ph.D. Thesis, University of Edinburgh, 1984
6. R.A. Robinson and R.H. Stokes, "Electrolyte Solutions", Butterworths, London, 1955.
7. R.M. Barrer, "Hydrothermal Chemistry of Zeolites", Academic Press, London, 1982, p37.



## CHAPTER 5

### OCCLUSION AND DECOMPOSITION OF

#### ACETATES IN SILICALITE

Group 1 and Group 2 acetates possess some organic character and are sufficiently small to pass through the pores of silicalite. The decomposition of these acetates occurs at relatively low temperatures - around 450°C[1]. Consequently, the occlusion of these salts into silicalite and subsequent decomposition may be carried out conveniently in pyrex glass sample tubes. The products of decomposition of group 1 and 2 acetates are the respective carbonates[2,3].

The work in this chapter was initiated by several ideas and aims.

1. Occlusion of salts followed by decomposition may be a feasible technique with which to introduce ions or salts into the channel system. This could not be accomplished by direct occlusion.
2. It would be of interest to investigate the occlusion of a series of group 1 acetates into silicalite and examine the variations due to the effect of different cations.
3. Repeated occlusion, decomposition and ion-exchange cycles may alter the sorption properties of silicalite. If the framework was attacked at specific points, an increase in pore volume could result.

Unfortunately, during the pursuit of this work, it became apparent that these aims could not be realised. This was due to the occurrence of other phenomena that were not foreseen. However, these are of interest in

themselves and are described and discussed in this chapter.

## 5.1 Isopiestic Measurements

The isopiestic technique was used to study the occlusion of lithium, sodium, potassium, caesium and barium acetates by silicalite.

### 5.1.1 Experimental

#### Materials

The purity and sources of salts used during the work discussed in this chapter are given below.

<u>Chemical</u>	<u>Purity</u>	<u>Source</u>
CH <sub>3</sub> CO <sub>2</sub> Li	99%	BDH Chemicals
CH <sub>3</sub> CO <sub>2</sub> Na	99%	BDH Chemicals
CH <sub>3</sub> CO <sub>2</sub> Na.3H <sub>2</sub> O	99.5%	BDH Chemicals
CH <sub>3</sub> CO <sub>2</sub> K	98%	Fisons Scientific
CH <sub>3</sub> CO <sub>2</sub> Cs	98%	Fluka AG
Na <sub>2</sub> CO <sub>3</sub>	99%	BDH Chemicals
K <sub>2</sub> CO <sub>3</sub>	99%	BDH Chemicals
(CH <sub>3</sub> CO <sub>2</sub> ) <sub>2</sub> Ba	98%	BDH Chemicals

The type of silicalite used was [TPA,PIP]-SIL. The synthesis of this material was described in section 2.2.3.

#### Procedure

The procedure followed was the same as described in section 4.3.2.

### 5.1.2 Results

The occlusion results obtained from isopiestic measurements are shown in Figures 5.1 to 5.4, as plots of WW/WZ against WS/WZ. The uptake of water by the parent silicalite, the maximum uptake of salt and the concentration of the solution phase for the different salt systems after various equilibration times

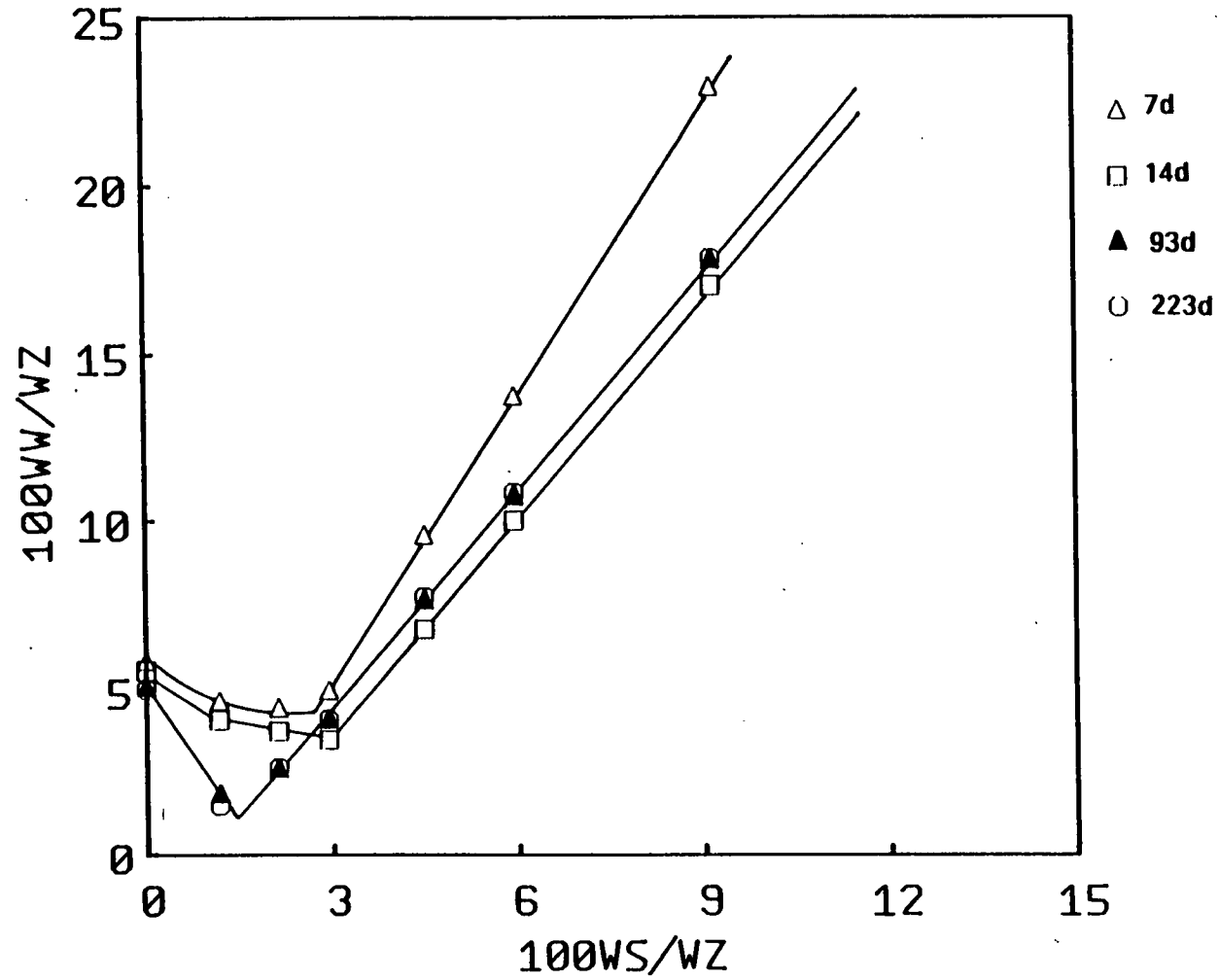


Figure 5.1

Occlusion results for [TPA,PIP]-SIL-P10 +  
lithium acetate after different equilibration times,  
at  $a_w = 0.753$ .

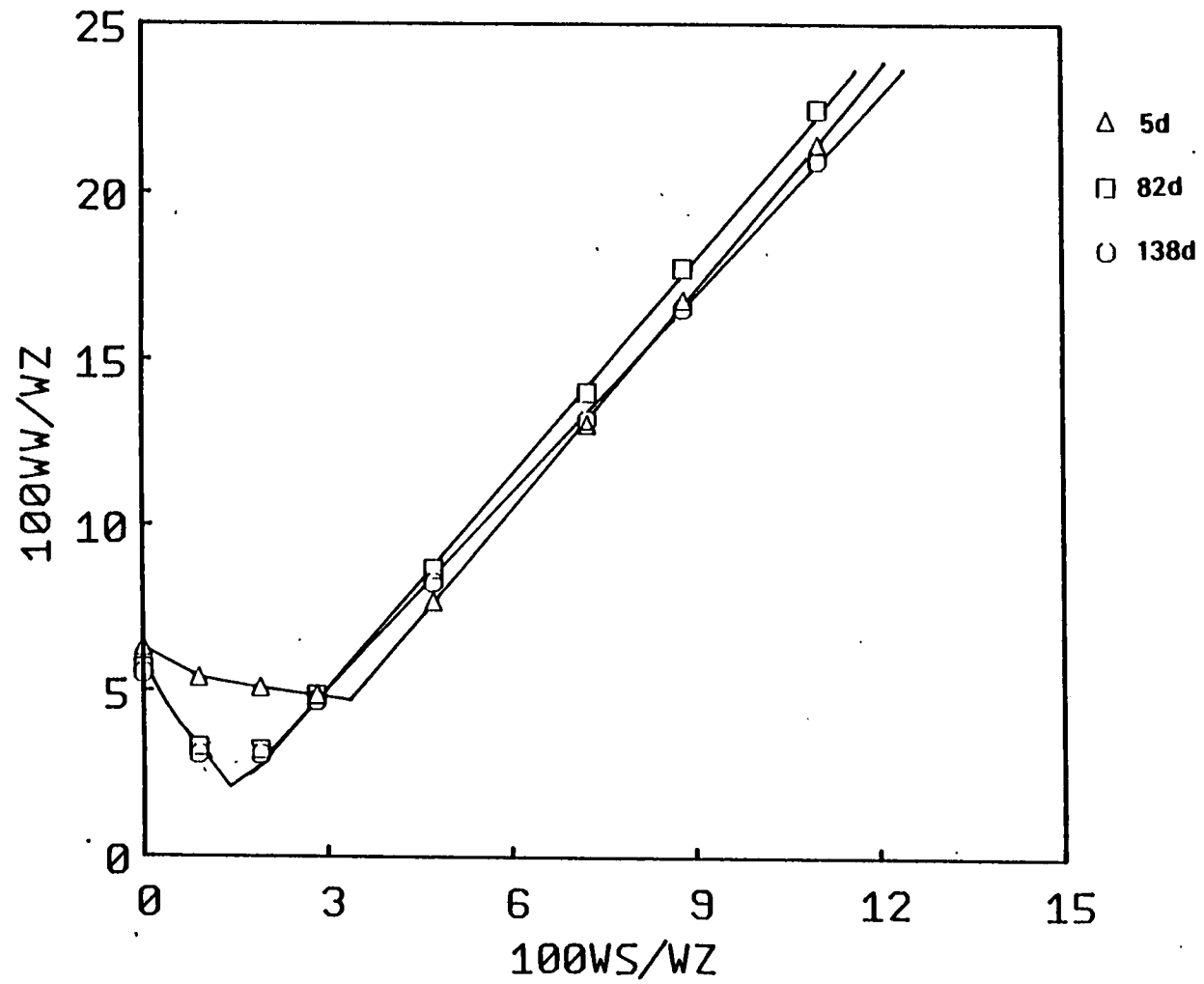


Figure 5.2

Occlusion results for [TPA,PIP]-SIL-P8 +  
sodium acetate at  $a_w = 0.753$ .

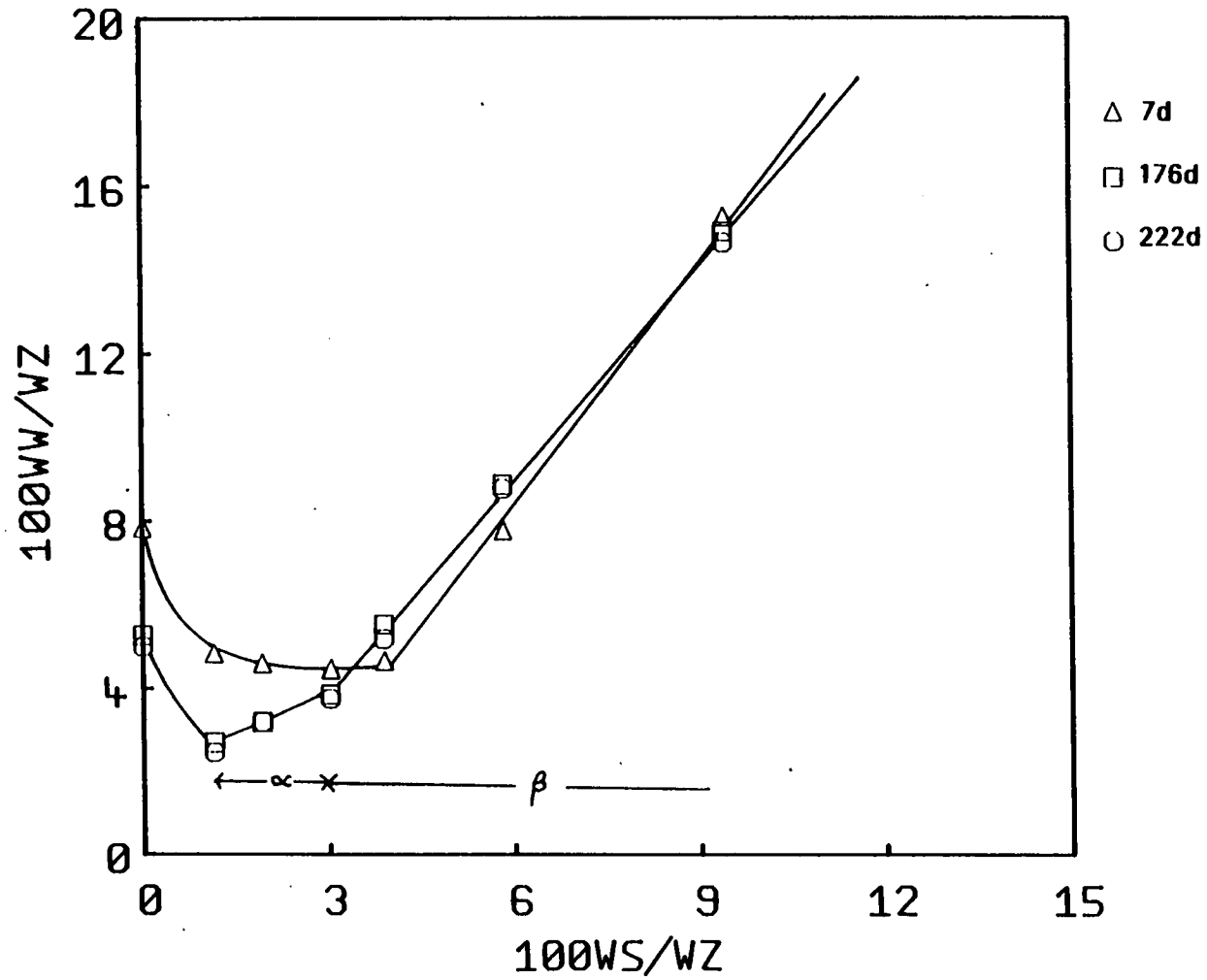


Figure 5.3

Occlusion results for [TPA,PIP]-SIL-P8 + potassium acetate at  $a_w = 0.753$ .

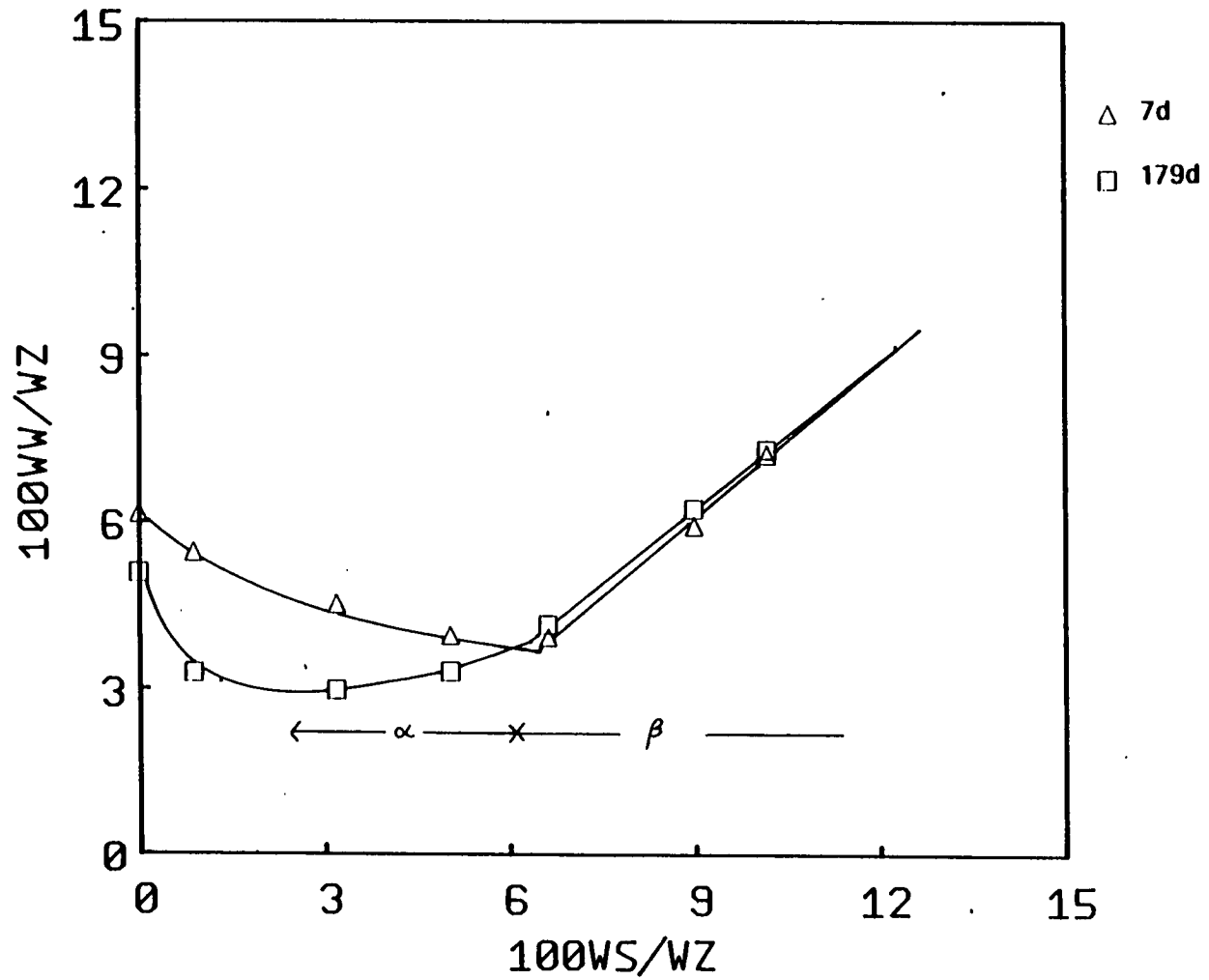


Figure 5.4

Occlusion results for [TPA,PIP]-SIL-P12 +  
caesium acetate at  $a_w = 0.753$ .

are given in Table 5.1. The plots show results obtained at the same water activity ( $a_w = 0.753$ ) after different equilibration times. It is observed that the uptake of salt and water by the silicalite varies quite dramatically with the length of equilibration. Examination of the plots reveals the following observations.

1. The uptake of water by the parent silicalite,  $U_w^0$ , decreases with time. It is noted that there are variations in the uptake of water between the different experiments after short equilibration times. However, after longer periods of time – approaching 200d – the uptake of water is close to  $0.050\text{gg}^{-1}$  in all the experiments.
2. The maximum amount of salt occluded,  $U_s^T$ , is observed to decrease with equilibration time.
3. The slope of the intracrystalline line becomes more negative with time. The amount of water displaced by the occlusion of a salt molecule increases.
4. The slope of the solution phase line alters with time. In general, the concentration of the solution apparently increases.
5. After longer equilibration times in the potassium and caesium acetate systems, there appears to be some variation in the solution phase concentration with the amount of salt present, WS/WZ. Two different regions can be identified. These are denoted as  $\alpha$  and  $\beta$  on the appropriate figures.
6. After long periods of times, an equilibration of the system appears to be

Salt	Equilibration Time	$U_w^o/gg^{-1}$	$U_s^T/gg^{-1}$	$10^4 U_s^T/mol\ g^{-1}$	solution conc /mol $Kg^{-1}$
Lithium acetate	7d	0.0583	0.027	1.53	3.4
Lithium acetate	14d	0.0558	0.028	1.58	4.5
Lithium acetate	83d	0.0509	0.014	0.78	4.6
Lithium acetate	223d	0.0489	0.013	0.73	4.6
Sodium acetate	8d	0.0830	0.034	2.39	5.5
Sodium acetate	82d	0.0570	0.015	1.06	5.7
Sodium acetate	138d	0.0554	0.014	0.89	6.3
Potassium acetate	7d	0.0784	0.038	2.23	5.5
Potassium acetate	178d	0.0529	0.017	1.00	5.8
Potassium acetate	222d	0.0489	0.017	1.00	5.8
Cesium acetate	7d	0.0611	0.068	2.00	5.4
Cesium acetate	179d	0.0507	0.025	0.78	5.4

Table 5.1

Results obtained from the isopiestic experiments for the group 1 acetate + silicalite systems.



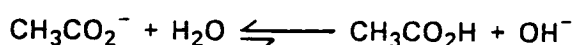
reached. This is shown by the reproducibility of results after 93d and 223d in the lithium acetate system and after 176d and 222d in the potassium acetate system.

The long equilibration times suggest that an activated process is involved. For example, the rearrangement or cleavage of framework bonds or atoms.

The decrease in the uptake of water by the parent silicalite has been explained in terms of increasing hydrophobicity as a result of slow healing of siloxane bonds (Chapter 4).

It seems unlikely that this process takes place when there are species such as  $M^+$  or  $OH^-$  present. So some other explanation must be sought to account for observations 2-6.

It is well known that the acetate ion undergoes hydrolysis.



This equilibrium lies to the far left and only a small number of species will be present as  $CH_3CO_2H$  and  $OH^-$ . When only small quantities of salt are present, all species must be occluded as there is no external solution phase present. These will be predominantly acetate ions and metal cations.

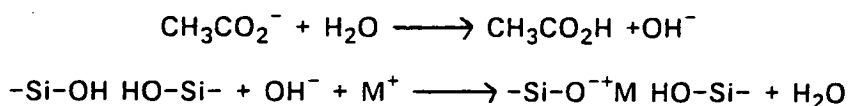
Therefore, it is reasonable to start with the occlusion of  $CH_3CO_2^-M^+$  and to speculate whether this could account for the observations 2-5.

There are a number of reactions that could occur involving the occluded salt and the framework.

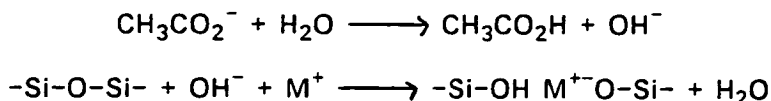
1. Abstraction of a proton from a  $-Si-OH$  group by  $CH_3CO_2^-$ .



2. Abstraction of a proton from a Si-OH group by a hydroxide ion. The hydroxide ion being formed from the hydrolysis of the acetate ion.



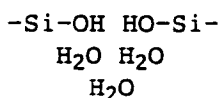
3. Attack of a siloxane bond by a hydroxide ion formed from the hydrolysis of the acetate ion.



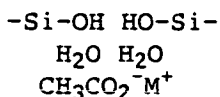
Reaction one would appear to be the least likely of the three. Reaction two requires the least rearrangement and so is the most likely although reaction 3 might also occur.

Can the occurrence of these reactions account for the observed changes with equilibration time? At short equilibration times, few water molecules are displaced by the occlusion of salt molecules. After longer equilibration times, a much greater number are displaced.

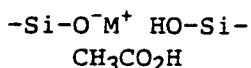
Initially, there are a certain number of hydrophilic sites with associated sorbed water molecules.



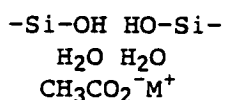
A number of  $\text{CH}_3\text{CO}_2^- \text{M}^+$  ions are occluded. It is possible that initially they are only physisorbed; loosely associated with the hydrophilic sites through the sorbed water molecules.



As a result few water molecules are displaced by the occlusion of salt molecules. After this initial occlusion, some of the salt molecules become chemisorbed; they react with the framework. This is an activated process so the equilibration times are long.



The acetic acid becomes sorbed onto the  $\text{-Si-O}^{-}\text{M}^{+} \text{HO-Si-}$  sites and so water molecules are displaced. Now, it is also observed that the minimum uptake of salt decreases with longer equilibration times. At short equilibration times, the situation could be imagined as follows. When small weights of salt are present, all the salt species are occluded. There is no external solution phase.

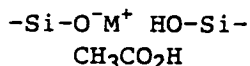


As the weight of salt is increased, a point is reached where no more of the salt is occluded. Any salt in excess of  $U_s^T$ , remains on the exterior of the silicalite crystals and forms a solution of the appropriate concentration. This external solution will be in equilibrium with the internal solution.



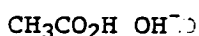
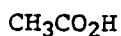
After longer equilibration times, hydroxide ions inside the framework, resulting from the hydrolysis of the acetate ion attack the framework.

If only small amounts of salt present, we have as postulated before.



At higher weights of salt, for example  $WS/WZ > U_s^T$ , acetate solution is present on the exterior of the crystals.





The concentration of acetic acid in the external solution will be very low. It is possible that some of the acetic acid comes out of the pores into the solution and water is sorbed on the hydrophilic sites. This would result in a decrease in the weight of salt present in the silicalite - although not in the number of moles present. Thus if such a process does occur, the maximum weight of salt,  $U_s^T/\text{gg}^{-1}$ , would decrease with equilibration time. The occurrence of such a process could also account for the change in the slope of the solution phase line with equilibration time. If the distribution of acetic acid between the silicalite and the solution phase alters, the composition and so the concentration will both change.

There is still the problem of why after longer equilibration times the slope of the solution phase line alters with WS/WZ in the experiments carried out with potassium and caesium acetate. At short equilibration times the situation is as previously described. Now after longer equilibration times at low weights of added salt, again all species have been occluded so it is as before. However, after longer equilibration times in dishes with greater amounts of added salt, we have:-



Now as caesium and potassium ions are larger than the sodium and lithium ions their occlusion into the silicalite framework is more favourable. It is possible that the acetic acid molecules egress into the solution phase and are replaced by a cation and hydroxide ion. If hydroxide ions are removed from the solution, this will have the effect of shifting the equilibrium to the right. The solution will become less like that of the acetate solution. This will alter the composition of the solution and so the concentration will change. If there

is only a small amount of solution phase present, then the removal of a small number of hydroxide ions will cause a considerable change in composition. However, if there is a large amount of external solution present, then the removal of a small number of hydroxide ions will not alter the composition significantly. As a consequence, the composition of the solution varies with the weight of salt present, and so the concentration of the solution is observed to vary with WW/WZ.

Interpretation of the barium acetate isopiestic data proved difficult, as it was impossible to obtain reproducible results. The problem here may well be caused by dissolution of atmospheric CO<sub>2</sub> in the salt solution to form insoluble BaCO<sub>3</sub>.

## **5.2 Sorption Properties**

### **5.2.1 Experimental**

The method used to measure the uptake of n-heptane by a number of different acetate + silicalite samples was based on the "multi-equilibration" technique.

#### **Procedure**

1. Sample tubes and tops were weighed. Silicalite was added.
2. Samples were heated at 400°C for 2h to remove any sorbed water or gases.
3. The samples were allowed to cool and then reweighed to obtain the weight of dry silicalite in each sample tube.

4. Small different quantities of the appropriate acetate were added to each sample.
5. Water was added to each sample tube to dissolve the acetate.
6. The water was slowly removed from the samples over  $\sim 18\text{h}$  at  $70^\circ\text{C}$ . As the water is removed the concentration of the solution increases and occlusion of the salt should occur.
7. The samples were then reheated at various temperatures from  $200^\circ\text{C}$  to  $500^\circ\text{C}$  for 4h. If a temperature above  $400^\circ\text{C}$  is used, it was expected that the acetate would be decomposed to give the corresponding carbonate.
8. The samples are allowed to cool and reweighed.
9. The sorption mixture of  $2\text{cm}^3$  DBP +  $2\text{cm}^3$  n-heptane was added to the desiccator.
10. Samples are equilibrated for 18h at  $25^\circ\text{C}$  before being reweighed to obtain the weight of n-heptane sorbed.

### 5.2.2 Results

The results are shown in Figures 5.5 to 5.8 as plots of uptake of n-heptane  $U_{\text{n-heptane}}$  against weight of salt added WS/WZ. The temperature used to heat the salt + silicalite mixture is shown in the key of the diagrams. In the lithium acetate system (Figure 5.5) the uptake of n-heptane decreases linearly with the weight of salt per g silicalite, WS/WZ, until it approaches  $0.100\text{gg}^{-1}$  at  $\text{WS/WZ} \sim 0.192\text{gg}^{-1}$ .

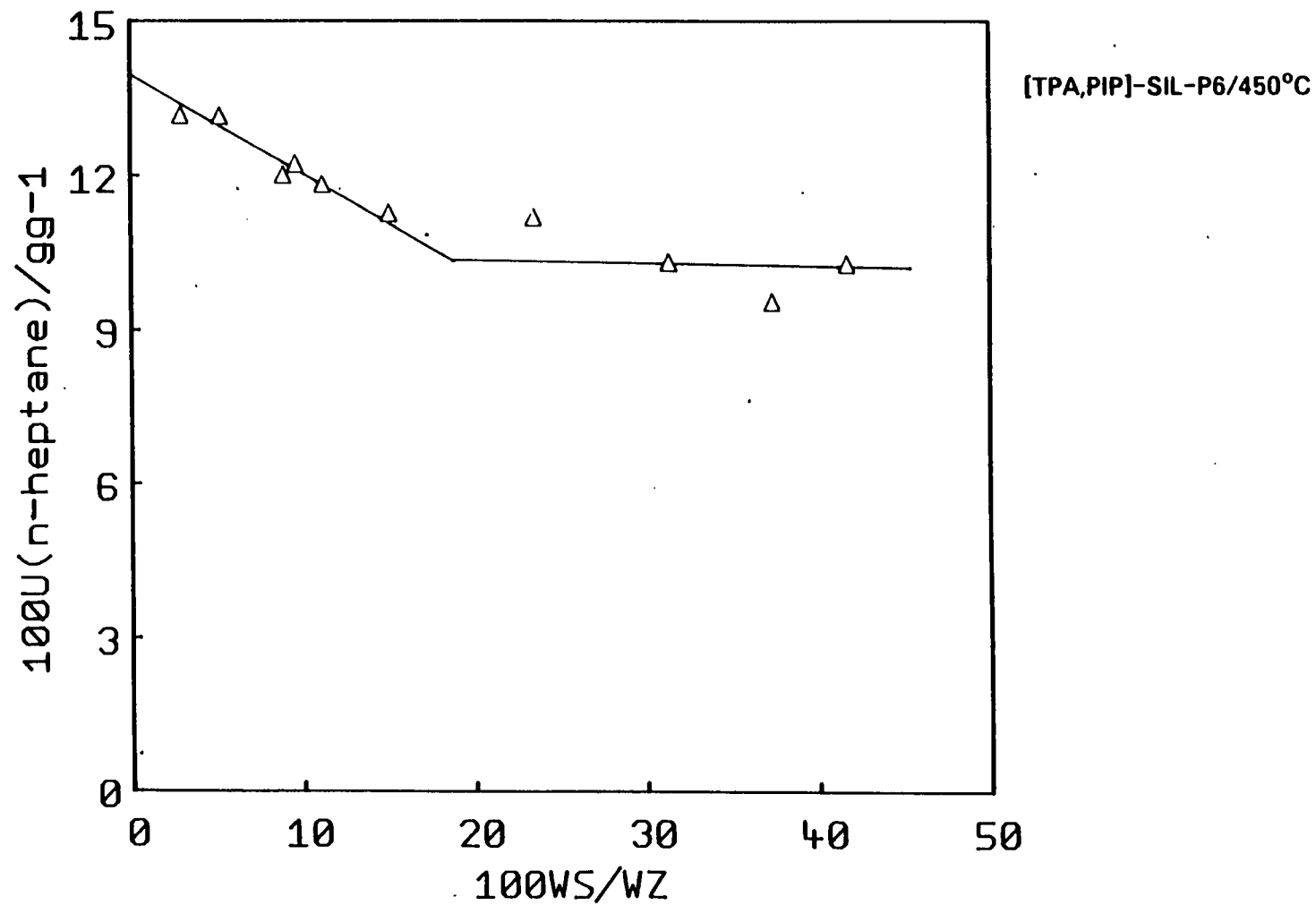


Figure 5.5

The variation of the uptake of n-heptane  $U(n\text{-heptane})$ , with the weight of salt,  $WS/WZ$ , for [TPA,PIP]-SIL + lithium acetate.

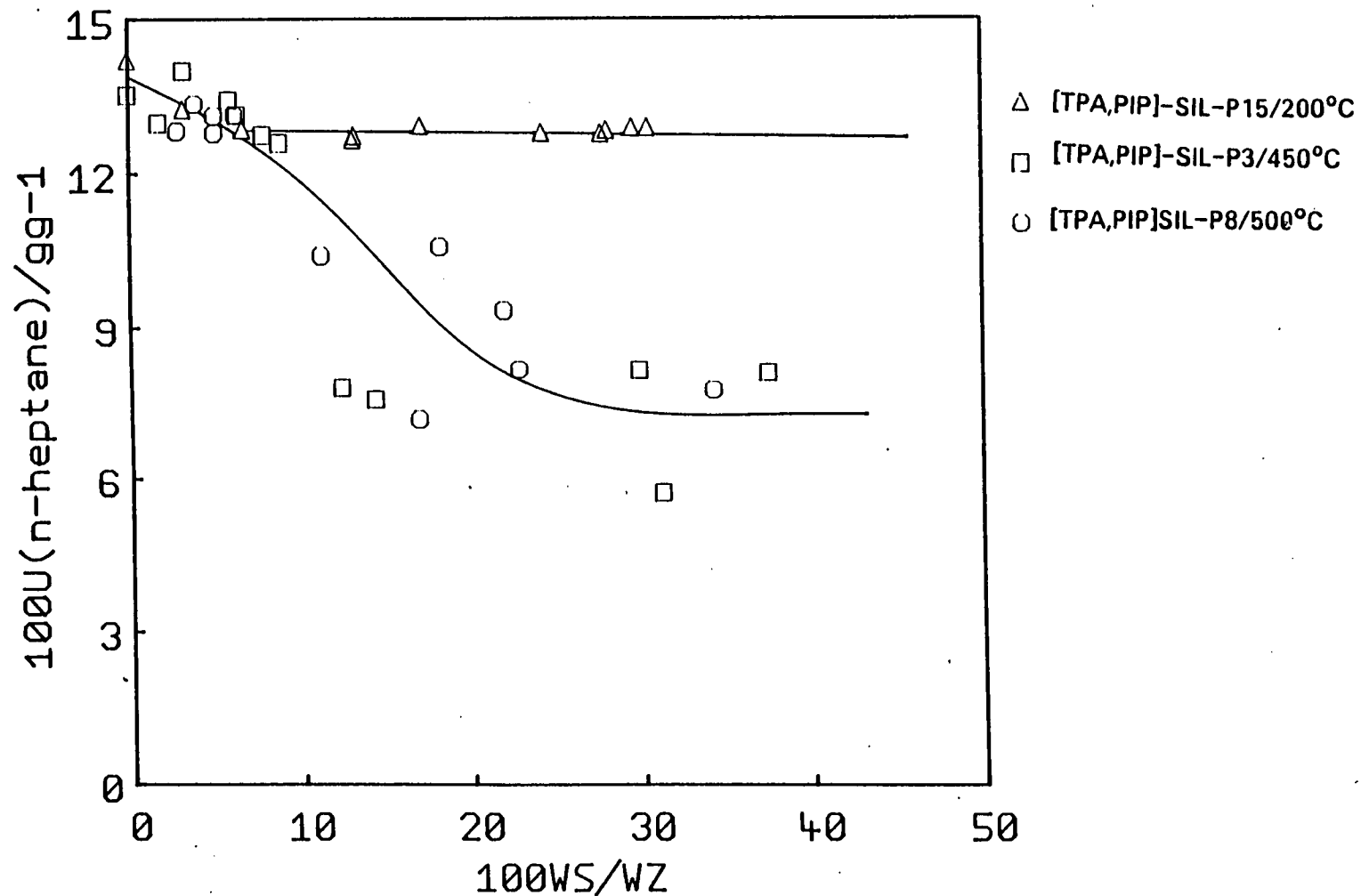


Figure 5.6

The variation of the uptake of n-heptane,  $U(n\text{-heptane})$ , with the weight of salt added,  $WS/WZ$ , for [TPA,PIP]-SIL + sodium acetate. Results from three separate experiments are shown.



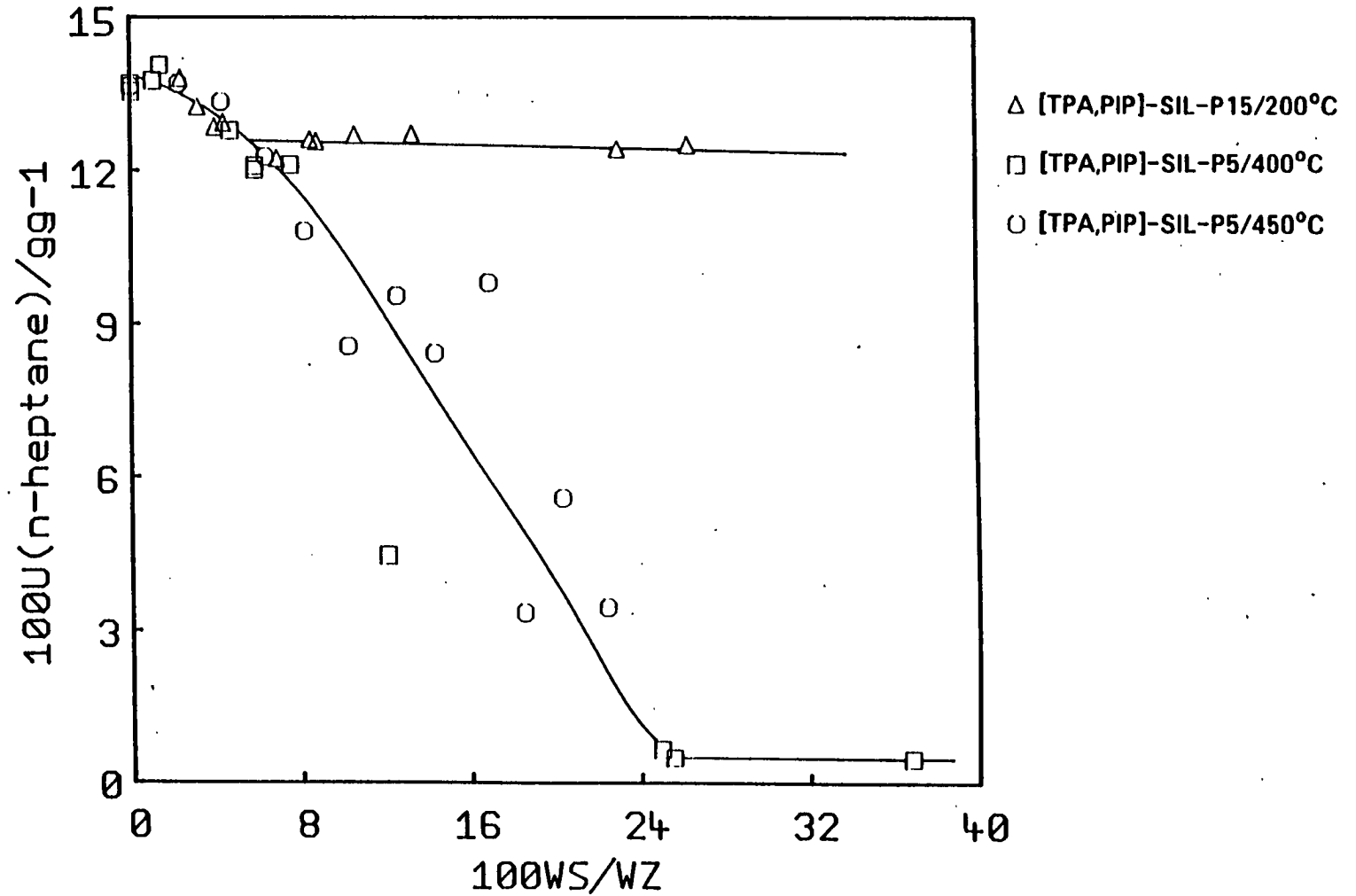


Figure 5.7

The variation of uptake of n-heptane,  $U(n\text{-heptane})$ , with the weight of salt,  $WS/WZ$ , for [TPA,PIP]-SIL + potassium acetate. Results from three separate experiments are plotted.

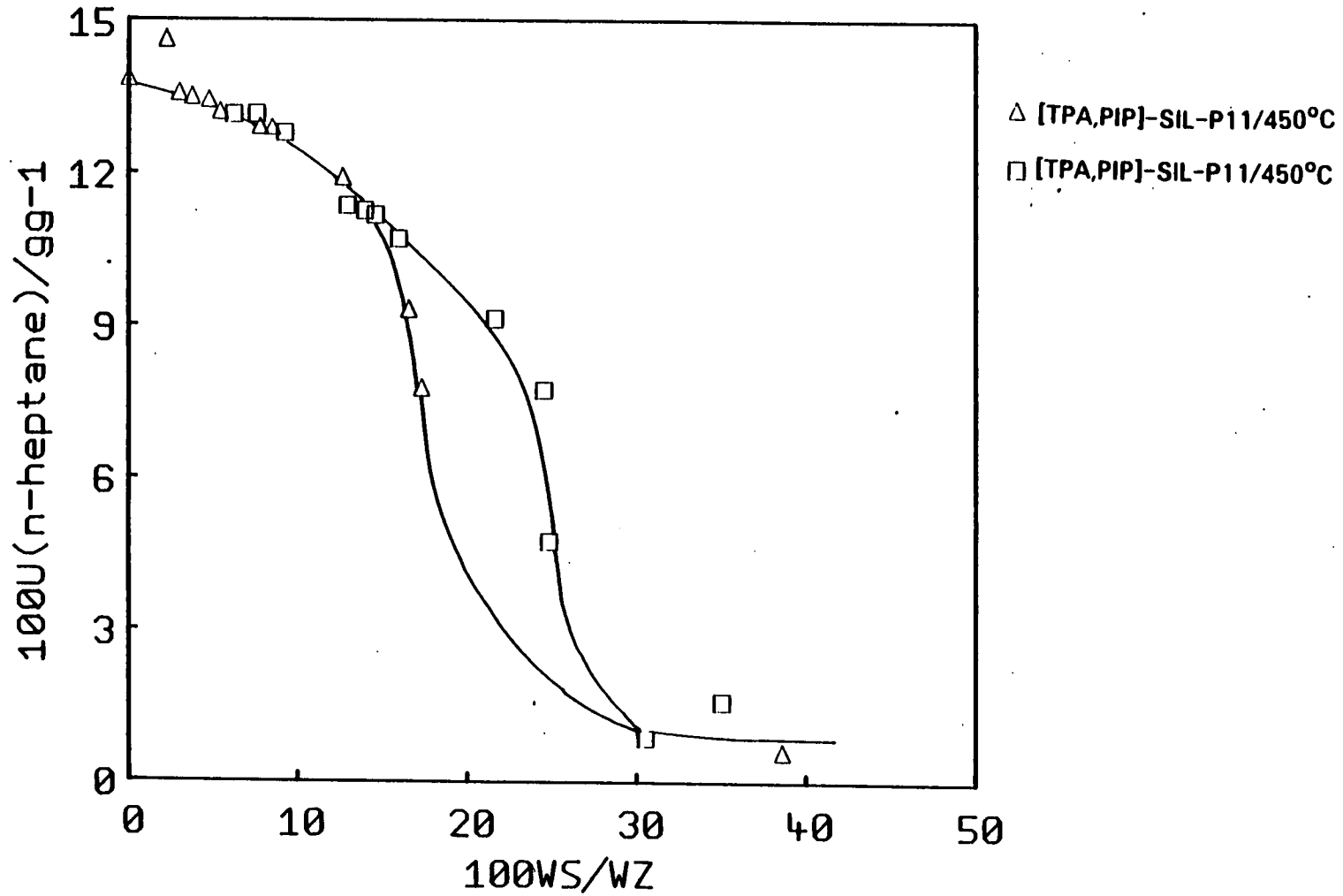


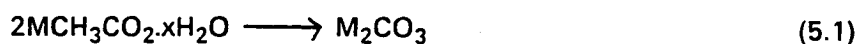
Figure 5.8

The variation of the uptake of n-heptane,  $U(n\text{-heptane})$ , with the weight of salt,  $WS/WZ$ , for [TPA,PIP]-SIL + caesium acetate. Results from two experiments are plotted.

In the other three acetate systems, the reproducibility of results is reasonable at low values of WS/WZ. But at higher values of WS/WZ, large discrepancies between runs are observed. When a temperature of 200°C is used to heat the salt + silicalite samples a small decrease in the uptake of n-heptane is observed at low WS/WZ and then the uptake of n-heptane remains constant at  $\sim 0.11 \text{gg}^{-1}$ . However, when the salt + silicalite samples are heated at temperatures above 400°C, there is a similar decrease in the uptake of n-heptane at small values of WS/WZ, but at higher weights there is an abrupt decrease in the uptake of n-heptane. In some runs the uptake of n-heptane is reduced to almost zero.

These results cannot be accounted for purely in terms of salt molecules blocking the channels. In order to interpret these results, it is necessary to examine the results from further experiments.

It was noted that the heating of the salt + silicalite samples gave inconsistent % weight losses. This is illustrated in Tables 5.2-5.4 which give the % weight losses for samples in an experiment in which acetate + silicalite samples were heated. Theoretically the % weight loss for the decomposition,



is 63.8%, 60.5%, and 29.6% for lithium acetate, sodium acetate and potassium acetates respectively. Experimentally the % weight losses observed during the determination of the uptake of n-heptane are considerably higher than these values. This was observed even when samples were heated at 200°C.

A TGA trace of sodium acetate trihydrate which displays the % weight loss with temperature is shown in Figure 5.9. The % weight losses observed in this trace agree well with those calculated as shown below.

WS/WZ	wt. salt/g	wt. salt after 2h at 450°C	%wt. loss
0.0289	0.0084	0.0004	93.8
0.0521	0.0097	0.0008	93.8
0.1114	0.0280	0.0025	90.4
0.1503	0.0382	0.0032	81.8
0.2341	0.0509	0.0088	88.8
0.3129	0.0734	0.0104	85.8

Table 5.2 Weights of [TPA,PIP]-SIL + lithium acetate samples, sample weights after 2h at 450°C and the corresponding %weight losses.

WS/WZ	wt. salt/g	wt. salt after 2h at 450°C	%wt. loss
0.0498	0.0110	0.0012	89.1
0.0748	0.0220	0.0059	73.2
0.0845	0.0204	0.0057	72.1
0.1040	0.0312	0.0124	80.3
0.1815	0.0414	0.0189	55.8
0.2074	0.0580	0.0273	54.1

Table 5.3 Weights of [TPA,PIP]-SIL + sodium acetate samples, sample weights after 2h at 450°C and the corresponding %weight losses.

WS/WZ	wt. salt/g	wt. salt after 2h 450°C	%wt. loss
0.0558	0.0132	0.0038	72.7
0.0855	0.0153	0.0058	83.4
0.1238	0.0304	0.0114	82.5
0.1358	0.0335	0.0128	81.8
0.2415	0.0588	0.0254	57.8
0.3284	0.0732	0.0305	58.3

Table 5.4 Weights of [TPA,PIP]-SIL + potassium acetate samples, sample weights after 2h at 450°C and the corresponding %weight losses.

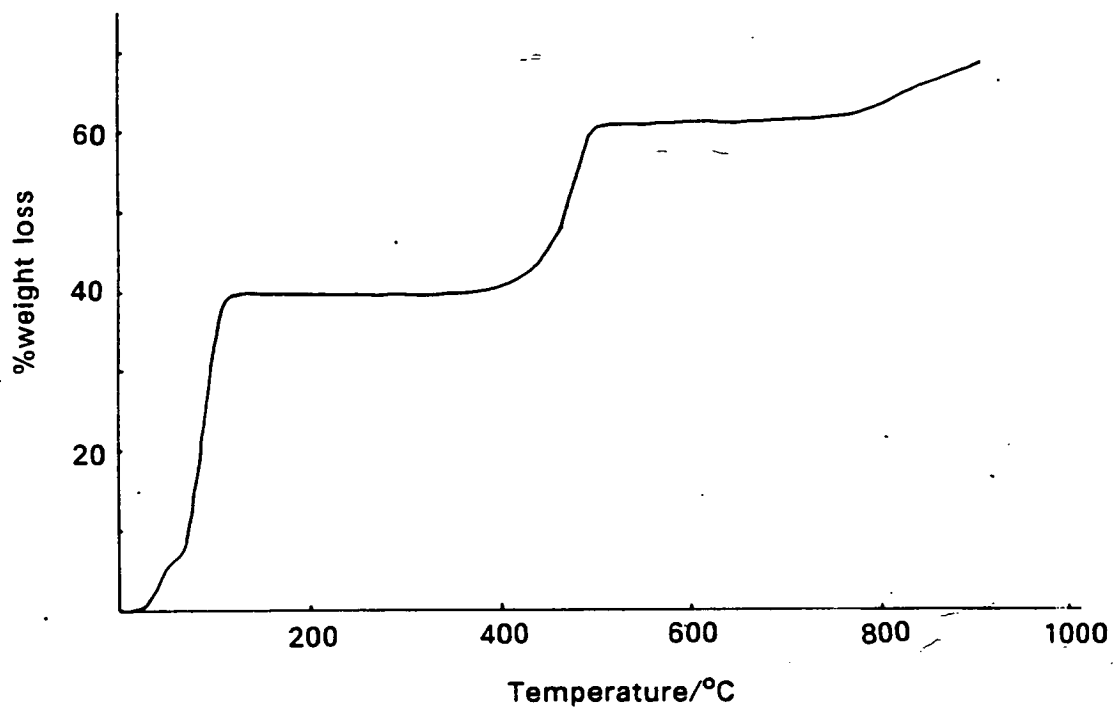


Figure 5.9 TGA curve of sodium acetate trihydrate.

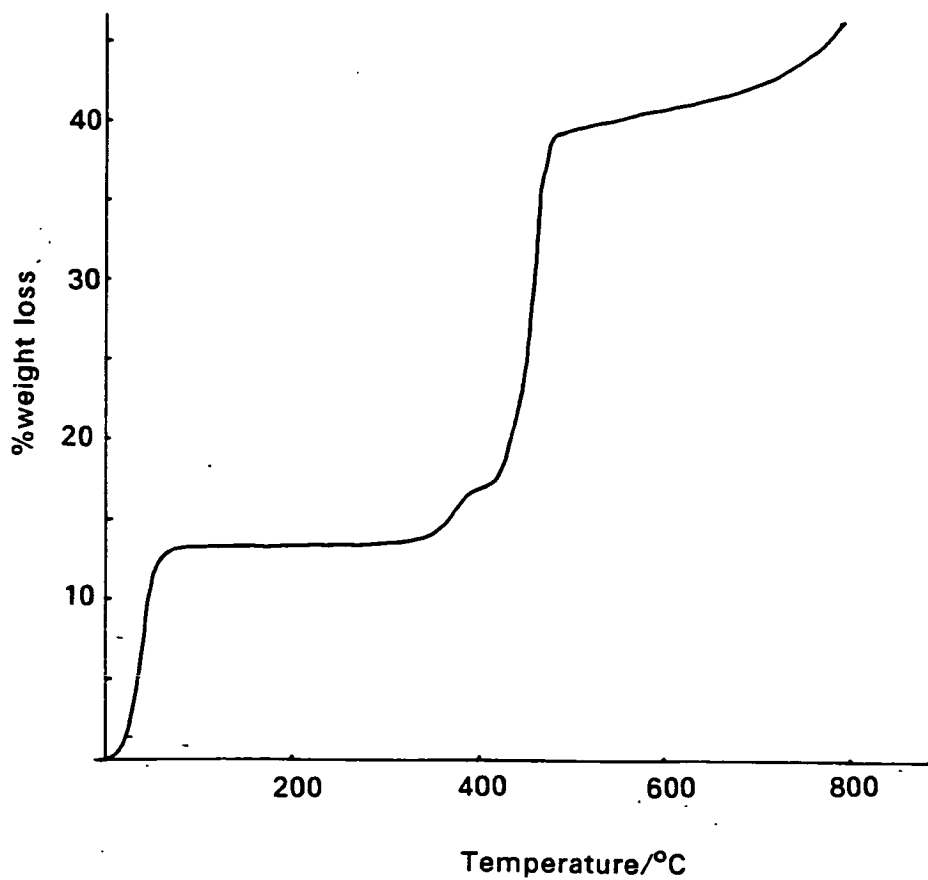


Figure 5.10 TGA curve of potassium acetate.

	<u>Calculated</u>	<u>Experimental</u>
%wt. loss of H <sub>2</sub> O	39.7	39.5
total %wt. loss	60.5	60.5

A TGA trace of potassium acetate is shown in Figure 5.10. The %weight losses observed are shown below along with the calculated values. The potassium acetate was supposedly supplied as anhydrous salt. However, the TGA trace shows that 13.5 wt.% water is present. The calculated %weight loss on decomposition takes into account the experimentally determined %weight of water.

	<u>Calculated</u>	<u>Experimental</u>
%wt. loss of H <sub>2</sub> O	-	13.5
%wt. loss of decomposition	29.6	30.5

Another experiment was carried out in an attempt to determine the source of these high %weight losses observed on heating acetates with silicalite. Samples of lithium, sodium and potassium acetate were added to sample tubes and the weight noted. They were heated at 450°C for 2h and then cooled in vacuo over P<sub>2</sub>O<sub>5</sub>. Once cool the sample tubes were reweighed to find the %weight losses on heating. The results are given in Table 5.5.

In each case the experimental % weight loss is less than the theoretical weight loss. This is probably a result of deposition of carbon due to a lack of oxygen. It is also noted that the variation in the % weight losses is only of the order of 1 or 2 % or so, unlike the large variations observed in the % weight losses in the salt + silicalite experiments. The high % weight losses observed in the salt + silicalite experiments must be due to the reaction of either the acetate or the carbonate with the silicalite framework. There are several

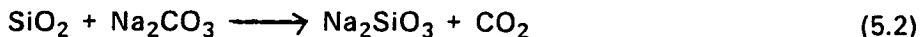
Lithium acetate dihydrate			
wt. salt/g	wt. salt after 2h at 450 C	Experimental %wt. loss	Calculated %wt. loss
0.0907	0.0245	20.2	89.8
0.0982	0.0282	28.2	89.8
0.0894	0.0828	24.8	89.8
0.1177	0.0828	21.2	89.8
Sodium acetate trihydrate			
wt. salt/g	wt. salt after 2h at 450 C	Experimental %wt. loss	Calculated %wt. loss
0.1378	0.0738	48.4	80.5
0.1549	0.0844	48.5	80.5
0.1734	0.0738	47.3	80.5
0.2283	0.1259	45.1	80.5
Potassium acetate			
wt. salt/g	wt. salt after 2h at 450 C	Experimental %wt. loss	Calculated %wt. loss
0.0848	0.0478	28.7	29.8
0.1085	0.0818	25.3	29.8
0.1827	0.1453	24.8	29.8
0.2134	0.1607	24.7	29.8

Table 5.5

The initial weights of lithium, sodium and potassium acetates, the weights after 2h at 450°C and the experimental %weight losses. Also included are the calculated %weight losses.

possible reactions.

It is known that sodium carbonate reacts with silica, as follows,



So once the acetate had decomposed to carbonate, reaction could occur between the carbonate and the silicalite framework.



As aforementioned, it is also possible that the acetate could attack the framework. The resultant acetic acid when heated may be removed as a number of possible species depending on the availability of oxygen and nitrogen. Both reaction of carbonate and acetate with the silicalite framework would result in higher % weight losses of salt than predicted.

High %weight losses and large variations between samples were observed even when the silicalite + acetate samples were heated at 200°C. In this case, the acetate must be reacting with the silicalite framework.

When temperatures sufficient to decompose the acetate to carbonate are used, the framework is probably attacked by both the acetate and carbonate.

When the uptake of n-heptane by silicalite samples with magnesium, calcium, strontium or barium acetate added, was measured, no significant decrease in the uptake of n-heptane with the weight of salt added was observed. This suggests that group two acetates are excluded from the silicalite framework. Such salts are highly charged and highly hydrated and consequently prefer to remain in the solution phase rather than enter the silicalite pores.



### 5.3 Further Experiments

In an attempt to clarify the anomalies discovered in the experiments in the previous section, the decomposition of sodium acetate and potassium acetate in contact with silicalite was explored further.

#### Experiment 1

In order to ascertain the effect of varying the temperature used to decompose the acetate salts occluded in silicalite the following experiment was carried out with both sodium and potassium acetate.

Samples of [TPA,PIP]-SIL with similar quantities of either sodium or potassium acetate in contact with silicalite were heated at 400, 600 and 900°C. After this heat treatment, XRD patterns were obtained and the uptake of n-heptane was measured.

The following procedure was followed.

1. A known weight of salt was dissolved in a known quantity of water.
2. Silicalite was weighed in to the solution. The weight of salt per gram of silicalite, WS/WZ, was  $0.111\text{gg}^{-1}$  for the sodium acetate experiment and  $0.117\text{gg}^{-1}$  for the potassium acetate experiment. This silicalite + salt + water mixture was stirred for 18h.
3. The water was removed over 2d at 70°C.
4. The remaining salt + silicalite mixture was split into three smaller samples. These samples were labelled A, B, and C in the sodium acetate experiment and D, E, and F in the potassium acetate experiment.

5. The samples A and D, B and E, and C and F, were heated at 400, 600 and 900°C respectively for 4h.

6. After heating, the samples were equilibrated with the atmosphere and XRD patterns then obtained. The XRD patterns for samples A, B, and C from the sodium acetate experiment are shown in Figure 5.11, and those from the potassium acetate experiment are shown in Figure 5.12.

7. The uptakes of n-heptane were measured using the "multi-equilibration" technique. The results are given in Table 5.6.

After calcination at 400°C, the XRD patterns differ little from those of the untreated silicalite.

When calcination of the salt + silicalite samples is carried out at 900°C, the XRD patterns are considerably altered. The peaks due to silicalite have disappeared and peaks characteristic of  $\alpha$ -cristobalite are observed. The literature values of  $2\theta$  for  $\alpha$ -cristobalite are given in Table 5.7. When potassium acetate is present and the samples heated at 600°C, a loss of crystallinity is observed but no peaks indicating the  $\alpha$ -cristobalite phase are present. In the case of the silicalite + sodium acetate mixture, calcination at 600°C results in some appearance of the  $\alpha$ -cristobalite although there is still some silicalite present.

The uptakes of n-heptane follow the same trends that were seen in the XRD patterns. After heating at 400°C the samples still sorb considerable amounts of n-heptane. But after 900°C, the uptake of n-heptane is negligible.

Silicalite is usually considered to be stable to temperatures above 1000°C.

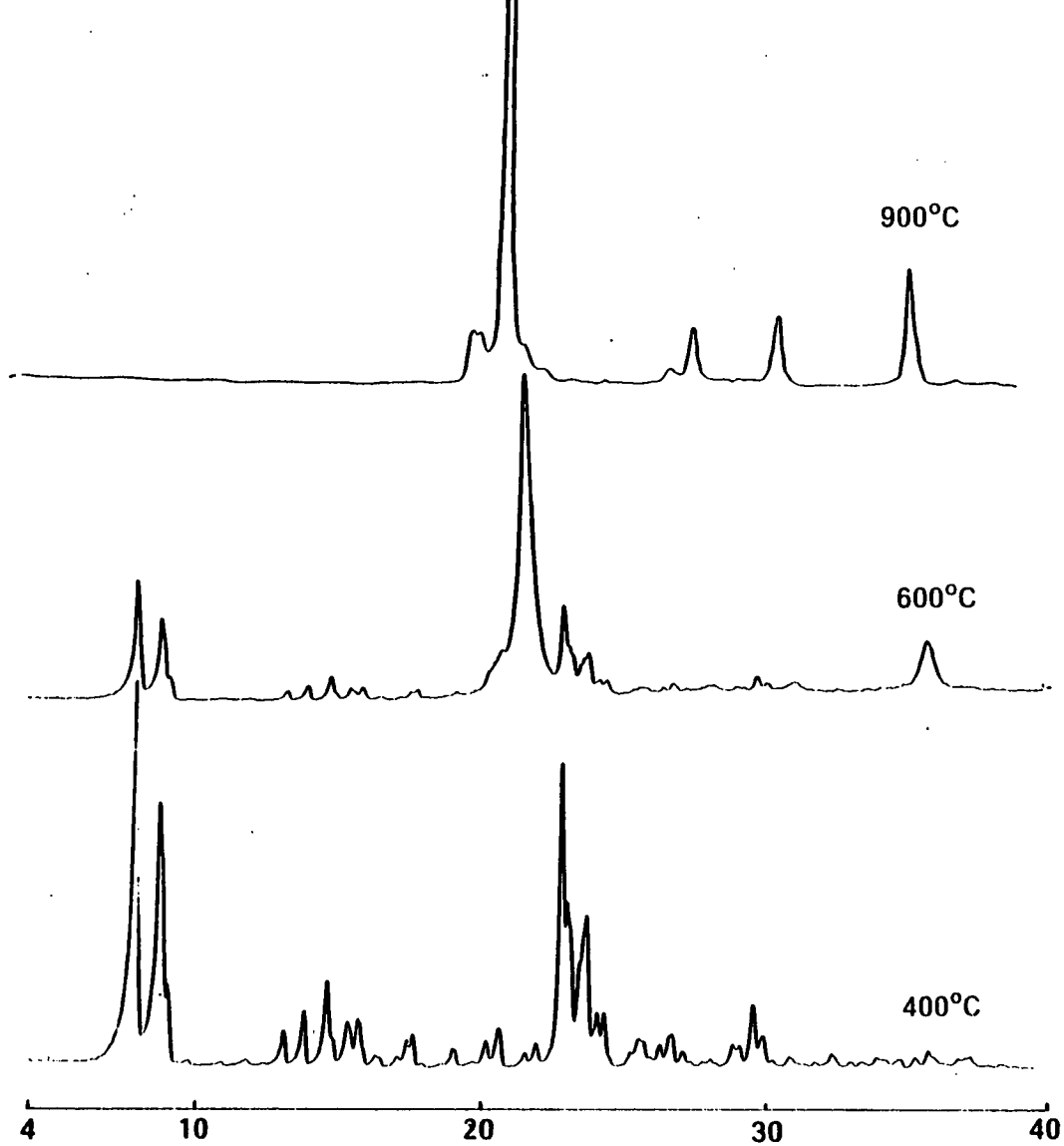


Figure 5.11

XRD patterns of [TPA,PIP]-SIL-P9 + sodium acetate heated at 400, 600 and 900°C.

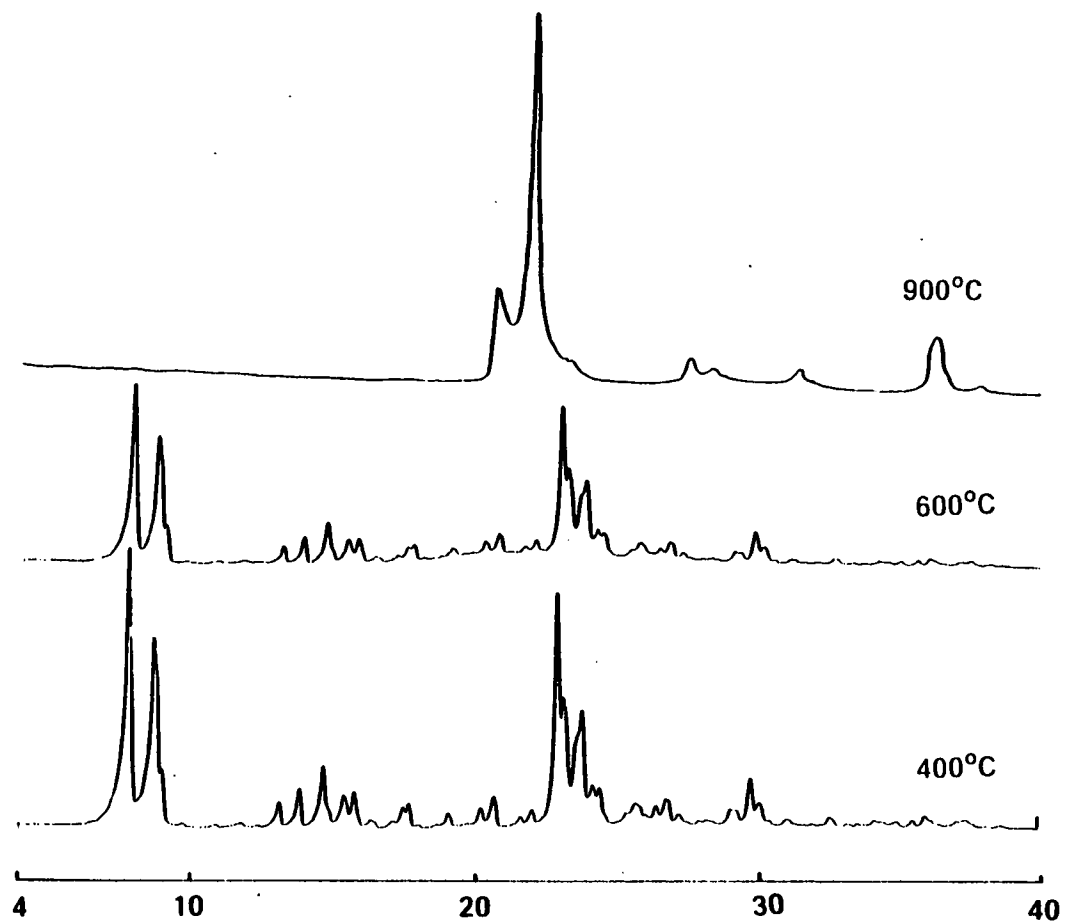


Figure 5.12

XRD patterns of [TPA,PIP]-SIL-P9 + potassium acetate heated at 400, 600 and 900°C.

Sodium acetate + Silicalite			Potassium acetate + Silicalite		
Sample	T/°C	U/gg-1	Sample	T/°C	U/gg-1
A	400	0.127	D	400	0.108
B	800	0.037	E	800	0.031
C	800	0.008	F	800	0.003

Table 5.6

Uptakes of n-heptane by samples A, B, C, D, E, and F.

$2\theta$	$I/I_0$
21.92	100
25.21	3
28.45	11
31.48	13
38.11	20
38.42	5

Table 5.7

The  $2\theta$  values and relative intensities of the XRD patterns lines for  $\alpha$ -cristobalite.

Although it was noted in section 3.12.2, that Na-[TPA,PIP]-SIL-P16 sorbed little n-heptane if heated at 800°C for any length of time. However, here it is observed that a solid phase transformation to a denser phase ( $\alpha$ -cristobalite) is occurring below 600°C. This conversion to a much denser phase is apparently initiated by the presence of sodium or potassium ions in contact with the silicalite. This occurs because group 1 acetates and the carbonates to which they decompose are alkaline in nature and so react with the silicalite framework. Neutral sodium salts such as Na<sub>2</sub>SO<sub>4</sub> do not attack the framework of silicalite in the same way. This is shown by the result of Experiment 2.

The samples of salt + silicalite after the heat treatment were examined by S.E.M. The morphology of the crystals after the heat treatment appeared to be the same as the original samples - spherical in shape and 1µm in diameter. However, the higher the temperature used to decompose the salt, the more "pitted" became the surface of the crystals.

This experiment has shown that the uptake of n-heptane by acetate + silicalite mixtures is dependent on the temperature at which the samples are treated.

## **Experiment 2**

Silicalite was added to a sodium sulphate solution and stirred. The water was removed over several days at 70°C. This sample was then heated at 600°C for 6h and an XRD pattern was obtained as shown in Figure 5.13. It is observed that the silicalite structure has not been adversely affected by heating with sodium sulphate.

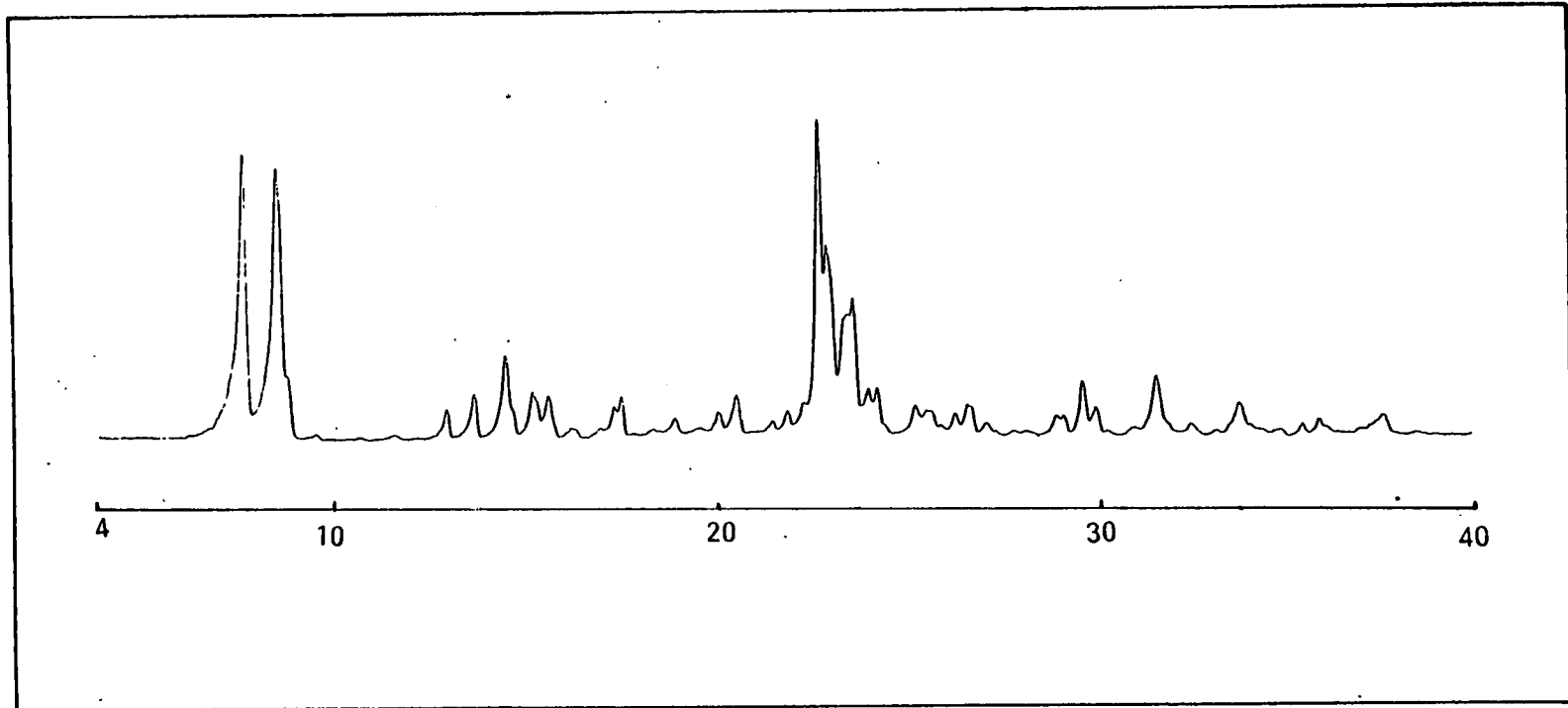


Figure 5.13

XRD pattern of sodium sulphate + silicalite  
heated at 600°C.



### Experiment 3

In order to discover how the collapse of the silicalite framework depends on the quantity of salt, the following experiment was carried out.

Different amounts of sodium acetate or potassium acetate were added to a known quantity of water. Silicalite was added to these solutions and stirred for 18h. The water was removed over 2d at 70°C. The weights of salt in contact with silicalite are given in Table 5.8.

The samples were then heated at 600°C. Approximately 1g of sample was removed after 35min, 1.5h, 3h, 21h or 24h and 48h. The XRD patterns of samples are shown in Figures 5.14–5.16 and Figures 5.17–5.19. The uptake of n-heptane or p-xylene and water by the samples were measured and these are given in Tables 5.9 and 5.10.

In the sodium acetate experiment, sample G exhibits little decrease in crystallinity and there is no appearance of the  $\alpha$ -cristobalite phase until after heating for 21h. Similar results were observed for sample H. The XRD patterns of sample I show peaks due to  $\alpha$ -cristobalite after all heating stages. The uptakes of p-xylene by these samples follows the trend observed in the XRD patterns. The uptake of water in all samples was reduced by the heat treatment.

In the experiment with potassium acetate, no appearance of  $\alpha$ -cristobalite is observed in any of the samples. However, some of the samples show a considerable reduction in crystallinity, after heating at 600°C. The greater the weight of salt in contact with the silicalite and the longer the heating time, the

Sodium acetate + Silicalite			Potassium acetate + Silicalite		
Sample	(MS/WZ) /gg-1	(MS/WZ) /molg-1	Sample	(MS/WZ) /gg-1	(MS/WZ) /molg-1
G	0.069	$5.04 \times 10^{-4}$	J	0.048	$4.84 \times 10^{-4}$
H	0.119	$12.65 \times 10^{-4}$	K	0.072	$7.32 \times 10^{-4}$
I	0.172	$12.65 \times 10^{-4}$	L	0.126	$12.87 \times 10^{-4}$

Table 5.8

Weights of salt in  $\text{gg}^{-1}$  and  $\text{molg}^{-1}$  used in Experiment 3.



Figure 5.14

XRD patterns of sample G.

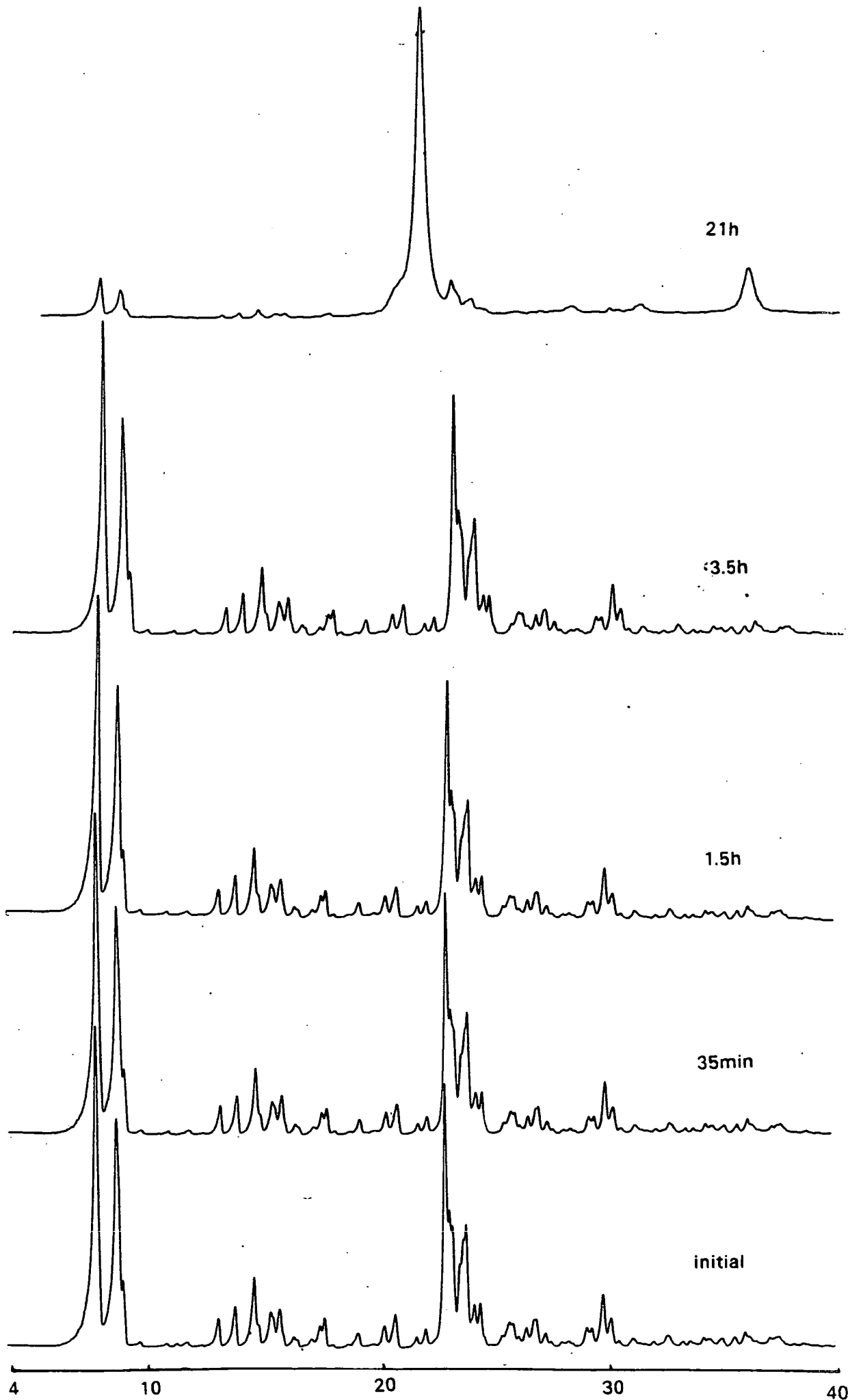


Figure 5.15

XRD patterns of sample H.

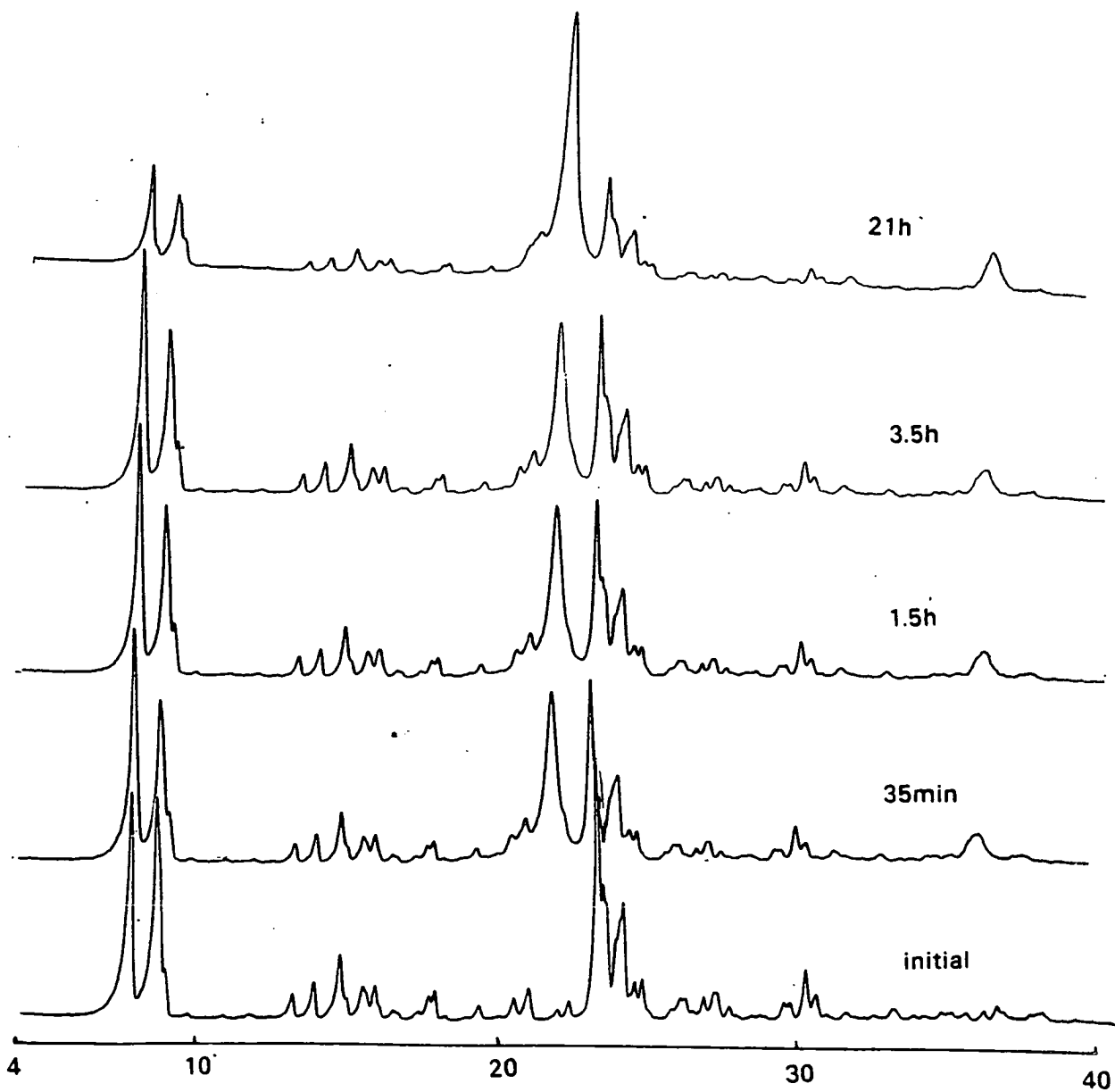


Figure 5.16

XRD patterns of sample I.

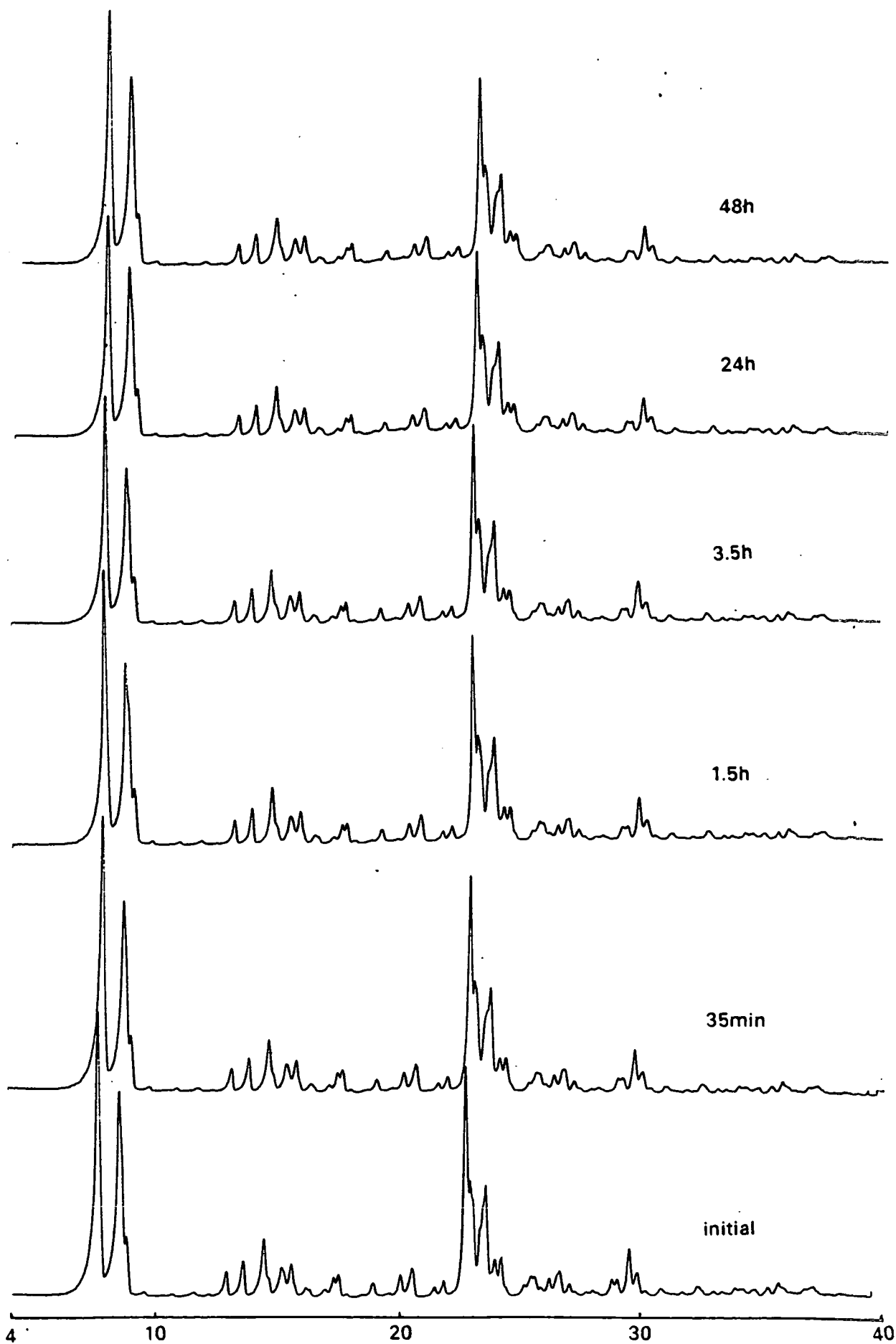


Figure 5.17

XRD patterns of sample J.

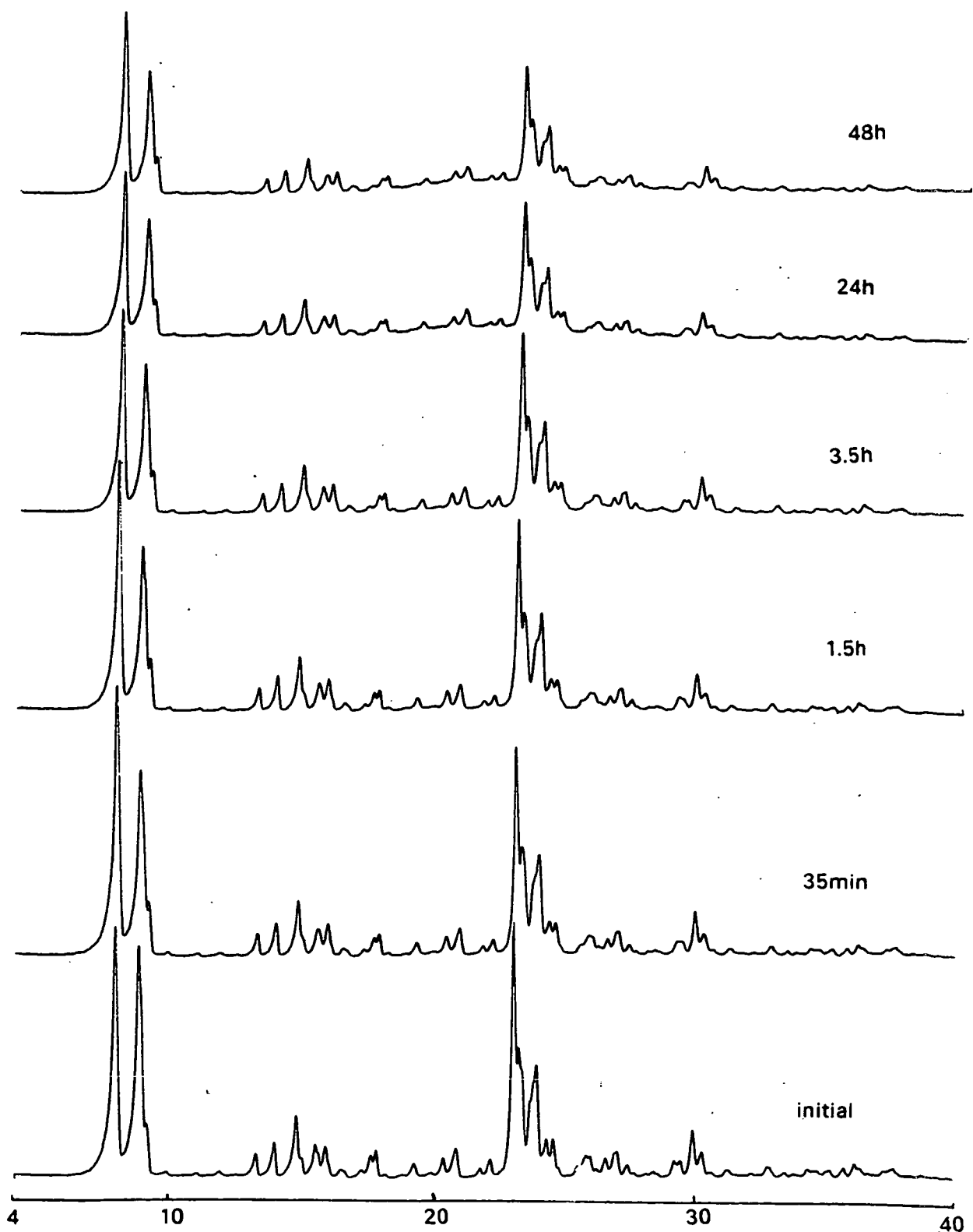


Figure 5.18

XRD patterns of sample K.

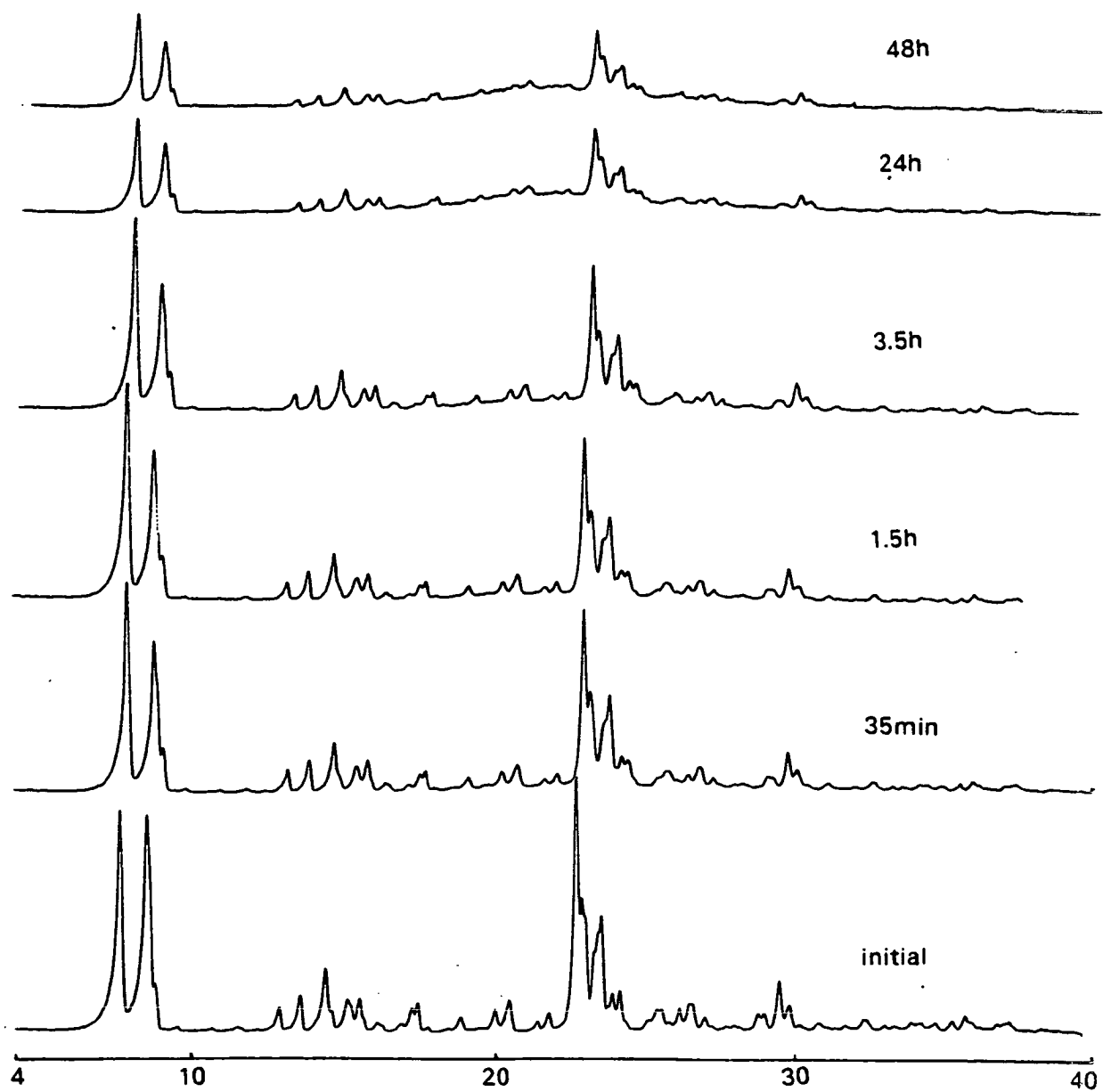


Figure 5.19

XRD patterns of sample L.



Sample	G		H		I	
WS/NZ (molg <sup>-1</sup> )	5.04 x 10		8.75 x 10		12.65 x 10	
Heating Time	U(p-xylene) /gg <sup>-1</sup>	U(water) /gg <sup>-1</sup>	U(p-xylene) /gg <sup>-1</sup>	U(water) /gg <sup>-1</sup>	U(p-xylene) /gg <sup>-1</sup>	U(water) /gg <sup>-1</sup>
initial	0.143	0.049	0.136	0.084	0.081	0.029
35min	0.140	0.047	0.126	0.046	0.080	0.026
1.5h	0.137	0.047	0.124	0.059	0.080	0.028
3.5h	0.138	0.047	0.120	0.056	0.080	0.027
21h	0.024	0.033	0.047	0.047	0.049	0.028

Table 5.9

Uptakes of p-xylene and water by samples of G, H, and I after 0, 35min, 1.5h, 3.5h and 21h at 600°C.

Sample	J		K		L	
MS/NZ (molg <sup>-1</sup> )	4.85 x 10		7.33 x 10		12.89 x 10	
Heating time	U (n-heptane) /gg <sup>-1</sup>	U (water) /gg <sup>-1</sup>	U (n-heptane) /gg <sup>-1</sup>	U (water) /gg <sup>-1</sup>	U (n-heptane) /gg <sup>-1</sup>	U (water) /gg <sup>-1</sup>
initial	0.120	0.042	0.118	0.074	0.100	0.084
35min	0.112	0.028			0.054	0.041
1.5h	0.112	0.028	0.090	0.033	0.013	0.027
3.5h	0.108	0.027	0.066	0.027	0.010	0.015
24h	0.098	0.025	0.019	0.013	0.005	0.007
48h	0.098	0.023	0.021	0.012	0.004	0.005

Table 5.10

Uptakes of n-heptane and water by samples of J, K, and L after 0, 35min, 1.5h, 3.5h, 24h and 48h at 600°C.

greater the reduction in crystallinity. The uptakes of n-heptane follow the same trends as those observed in the XRD patterns. Again, it is observed that the uptake of water is reduced and does not fill the pore volume that is available.

From the results of this experiment, it is seen that the uptake of n-heptane (or other sorbates) by the acetate + silicalite samples depends on the quantity of salt in contact with the silicalite and also on how long the samples are heated at elevated temperatures.

In light of these experiments, it is now possible to interpret the plots of uptake of n-heptane,  $U$ , against  $WS/WZ$ .

Once the acetate and water has been added to the silicalite in the sample tubes and the water has been slowly removed, a small amount of acetate is occluded and the rest remains on the surface of the crystals. Some reaction of the acetate and the silicalite occurs.

Subsequent heating of the salt + silicalite samples removes any acetic acid that has been formed. The remaining acetate is decomposed to the respective carbonate. This carbonate then reacts with the silicalite framework as given in equation (5.3).

At low weights of salt, this does not have a detrimental effect on the framework of silicalite. Any reduction in the uptake of n-heptane must be the result of the presence of cations in the channels of silicalite.

As the weight of salt is increased, a weight is reached that is sufficient to

begin to destroy the silicalite structure. Consequently the uptake of n-heptane is severely reduced. As this process is dependent on several factors - temperature, heating time and weight of salt - the reproducibility of results is very poor in this region. It is also noted that the nature of the cation influences the extent to which the framework is attacked (Figures 5.5-5.8). Samples of lithium acetate + silicalite and sodium acetate + silicalite heated at  $> 400^{\circ}\text{C}$  still sorb n-heptane to a significant extent. In contrast, in the same experiment repeated with potassium acetate and caesium acetate, the sorption capacity for n-heptane was negligible.

If the salt + silicalite mixture is heated only at  $200^{\circ}\text{C}$ , no collapse of the structure occurs. Some of the acetate present reacts with the silicalite framework. The small decrease in the uptake of n-heptane is due to the presence of one or more of several possible species - cations, acetate ions, and acetic acid.

#### **Experiment 4**

In order to discover whether sodium or potassium carbonate in contact with silicalite would lead to conversion to  $\alpha$ -cristobalite or a loss in crystallinity, the experiment discussed below was carried out.

Quantities of  $\text{Na}_2\text{CO}_3$  and  $\text{K}_2\text{CO}_3$  were separately ground with silicalite in a mortar for ten minutes. The quantity of salt added in units of  $\text{g g}^{-1}$  and  $\text{mol g}^{-1}$  are given in Table 5.11. The samples were then heated at  $600^{\circ}\text{C}$  for 3.5h. XRD patterns were obtained and the uptakes of n-heptane measured. The uptakes of n-heptane are also given in Table 5.11. The XRD patterns are shown in Figure 5.20.

	WS/WZ (gg-1)	WS/WZ (molg-1)	U (n-heptane) /gg-1
Na <sub>2</sub> CO <sub>3</sub> + Silicalite	0.137	1.29 x 10	0.056
K <sub>2</sub> CO <sub>3</sub> + Silicalite	0.191	1.38 x 10	0.039

Table 5.11 Uptakes of n-heptane by samples of [TPA,PIP]-SIL + Na<sub>2</sub>CO<sub>3</sub> and [TPA,PIP]-SIL + K<sub>2</sub>CO<sub>3</sub>, after 3.5h at 600°C.

	cycle 1	cycle 2	cycle 3	cycle 4
stage 1	sample 2	sample 6	sample 10 0.110	sample 14 -
stage 2	sample 3 -	sample 7 0.117	sample 11 0.108	sample 15 0.110
stage 3	sample 4 0.115	sample 8 -	sample 12 -	sample 16 -
stage 4	sample 5 0.129	sample 9 0.118	sample 13 0.113	-

Table 5.12 Uptakes of n-heptane and water by samples in Experiment 5.

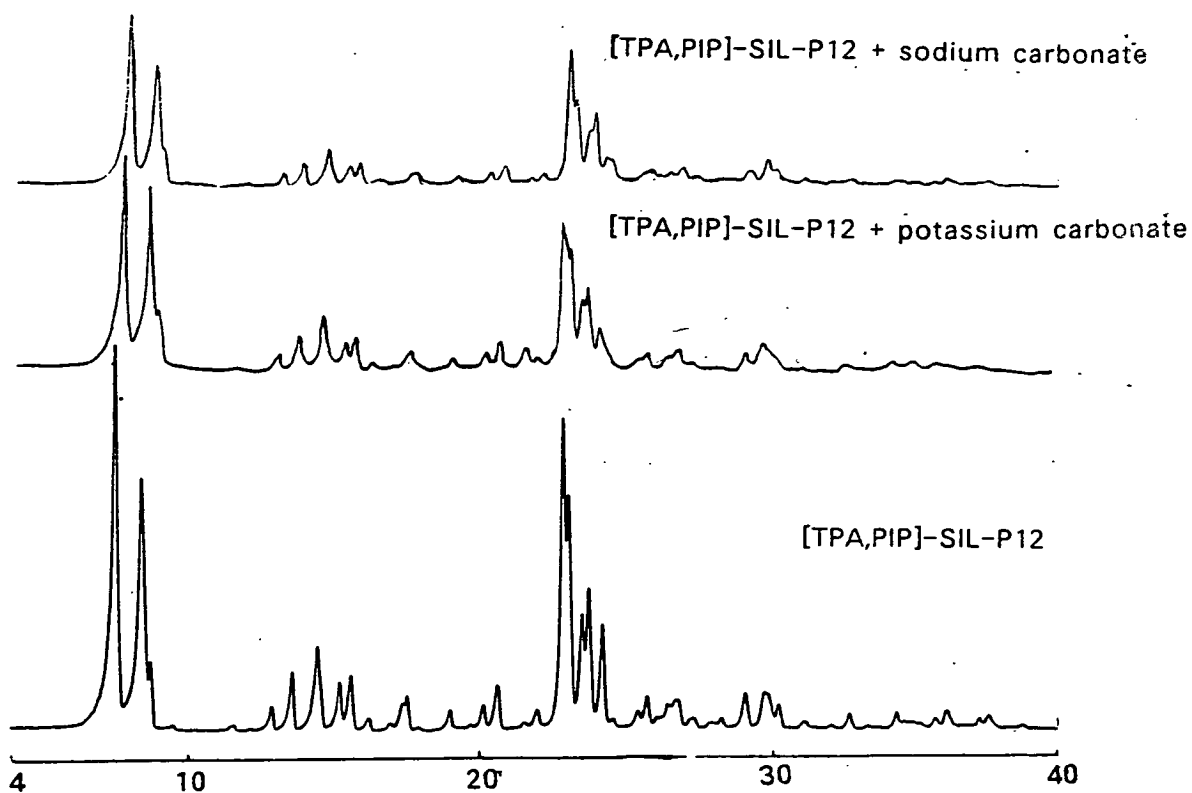


Figure 5.20

XRD patterns of [TPA,PIP]-SIL-P12 + sodium carbonate and [TPA,PIP]-SIL-P12 + potassium carbonate, both heated at 600°C for 3.5h. For comparison the XRD pattern of the untreated form of silicalite is included.

The silicalite sample ground with  $K_2CO_3$  and heated at  $600^\circ C$  exhibits some reduction in crystallinity, and a considerable reduction in the uptake of n-heptane is observed. The corresponding sample that was ground with  $Na_2CO_3$  shows a smaller reduction in crystallinity, no appearance of  $\alpha$ -cristobalite but a substantial reduction in the uptake of n-heptane. In previous experiments the presence of an equivalent number of sodium ions had initiated the conversion of silicalite to  $\alpha$ -cristobalite, and reduced the uptake of n-heptane to an insignificant amount.

Both  $Na_2CO_3$  and  $K_2CO_3$ , in contact with silicalite at elevated temperatures can cause a reduction in crystallinity. However, it appears that the decomposition of sodium or potassium acetate at elevated temperatures in contact with silicalite is more destructive to the silicalite structure. Possibly this is because the acetate starts the attack on the lattice and this is continued by the carbonate. However, the enhanced effect of the acetates, probably reflects the fact that they are more readily occluded than carbonates.

#### **5.4 Repeated Occlusion/Decomposition/Ion-exchange Cycles**

To observe the effects of repeated occlusion of sodium acetate into silicalite, followed by decomposition of the salt and finally hydrogen ion-exchange, several occlusion/decomposition/ion-exchange cycles were carried out.

##### **Experiment 5**

Silicalite was stirred in a sodium acetate solution. The proportion of silicalite to sodium acetate solution was 1:0.12. The water was slowly removed over 2d at  $70^\circ C$ . The salt + silicalite mixture was heated at  $475^\circ C$  and then ion-exchanged with  $NH_4Cl$ . This procedure was repeated four times(Figure

[TPA,PIP]-SIL-P4 calcined at 550°C for 18h and 800°C for 1h.

sample 1

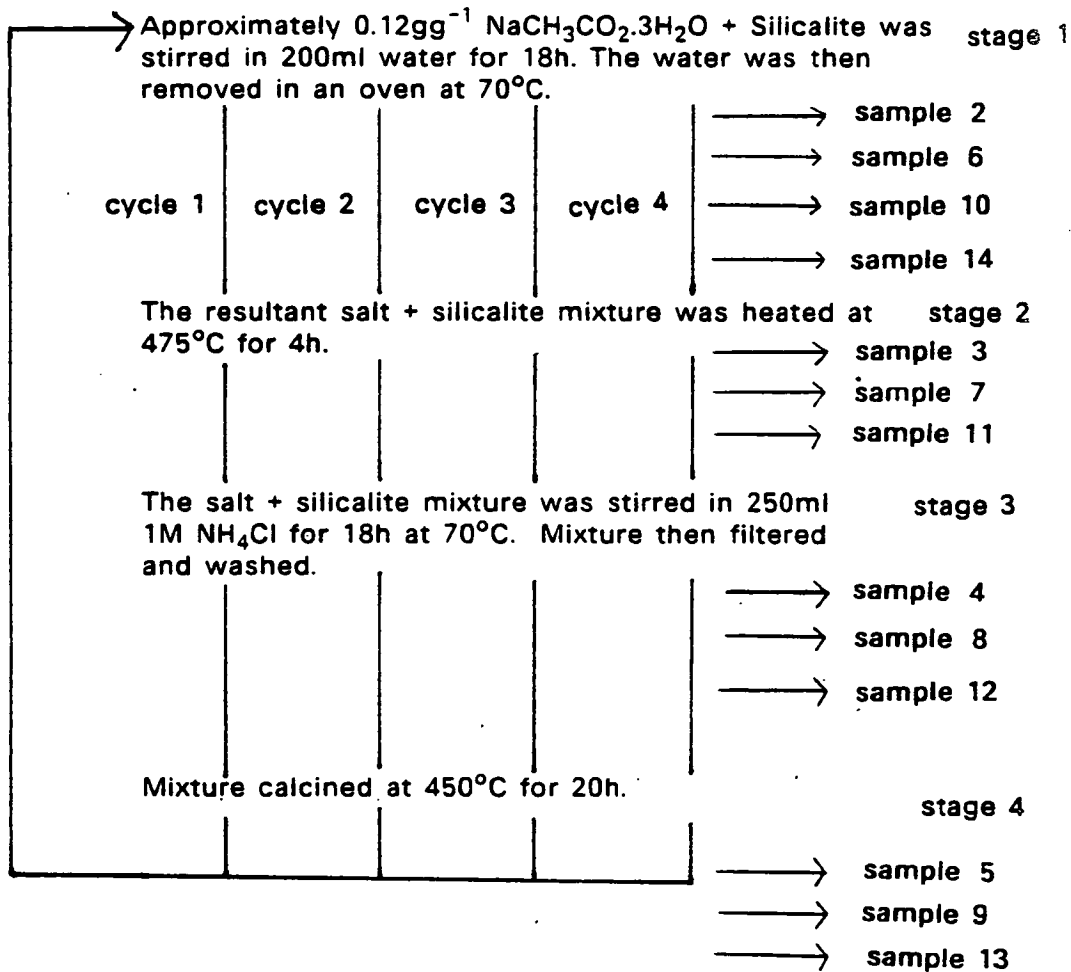


Figure 5.21

Procedure followed in Experiment 5.



5.21). Samples were taken after each stage. The uptakes of n-heptane by the samples were measured with the "multi-equilibration" technique. The results are given in Table 5.12. Differential thermal analysis was carried out on the samples. Some DTA traces are shown in Figure 5.22. For comparison, a DTA trace of sodium acetate/alumina is shown in Figure 5.23. XRD patterns of the samples were also obtained. These showed very little variation from the parent silicalite and that the silicalite structure is little affected by this treatment. This suggests that the small reductions observed in the uptake of n-heptane are due to the presence of cations, acetate ions, and/or acetic acid in the channels.

After the first occlusion/decomposition of salt, the uptake of n-heptane was reduced from  $0.135\text{gg}^{-1}$  to  $0.115\text{gg}^{-1}$ . Ion-exchange of the silicalite only causes a small increase to  $0.122\text{gg}^{-1}$ . Further treatment causes even smaller variations in the uptake of n-heptane. This is compatible with a situation in which no further occlusion of salt occurs after the first occlusion stage.  $\text{NH}_4\text{Cl}$  seems to be very poor at exchanging the sodium ions in the silicalite framework.

When the DTA curve of alumina + sodium acetate trihydrate is examined several peaks are observed. There is a sharp endothermic peak at  $\sim 325^\circ\text{C}$  attributed to the sodium acetate melting. The exothermic peak at  $\sim 450^\circ\text{C}$  results from the decomposition of the acetate to carbonate. The exothermic peak observed in the DTA curve of sample 3 prior to melting is a consequence of changes occurring in the species in the channels of silicalite-1. It may be the result of decomposition of sodium acetate in the channels or it may be the oxidation of acetic acid in the channels. The DTA trace of sample 3 shows an exothermic peak prior to melting of the salt but the DTA traces of 6, 10 and 12 do not. This agrees well with the suggestion that no further occlusion of salt

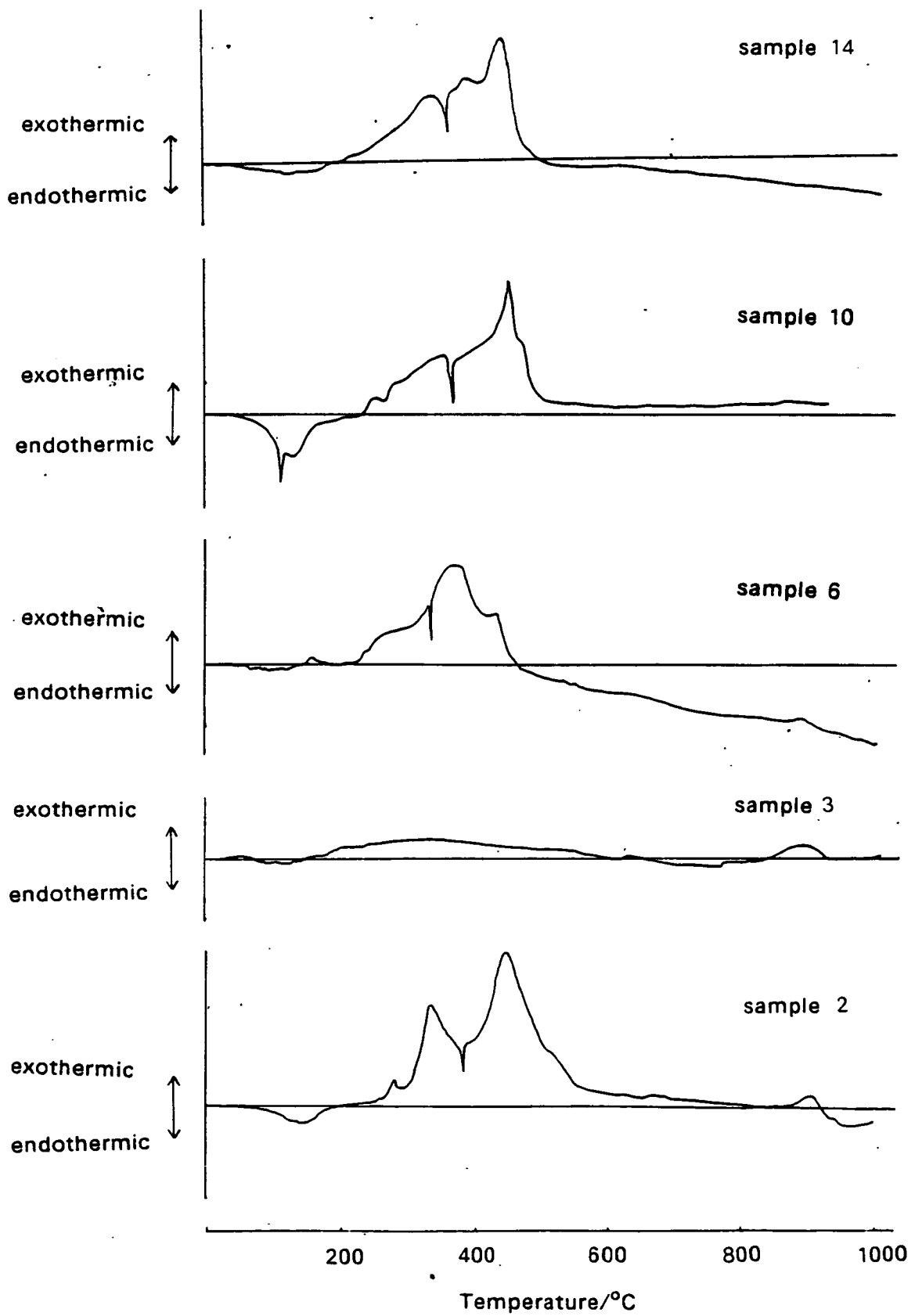


Figure 5.22 DTA curves of samples in Experiment 5.

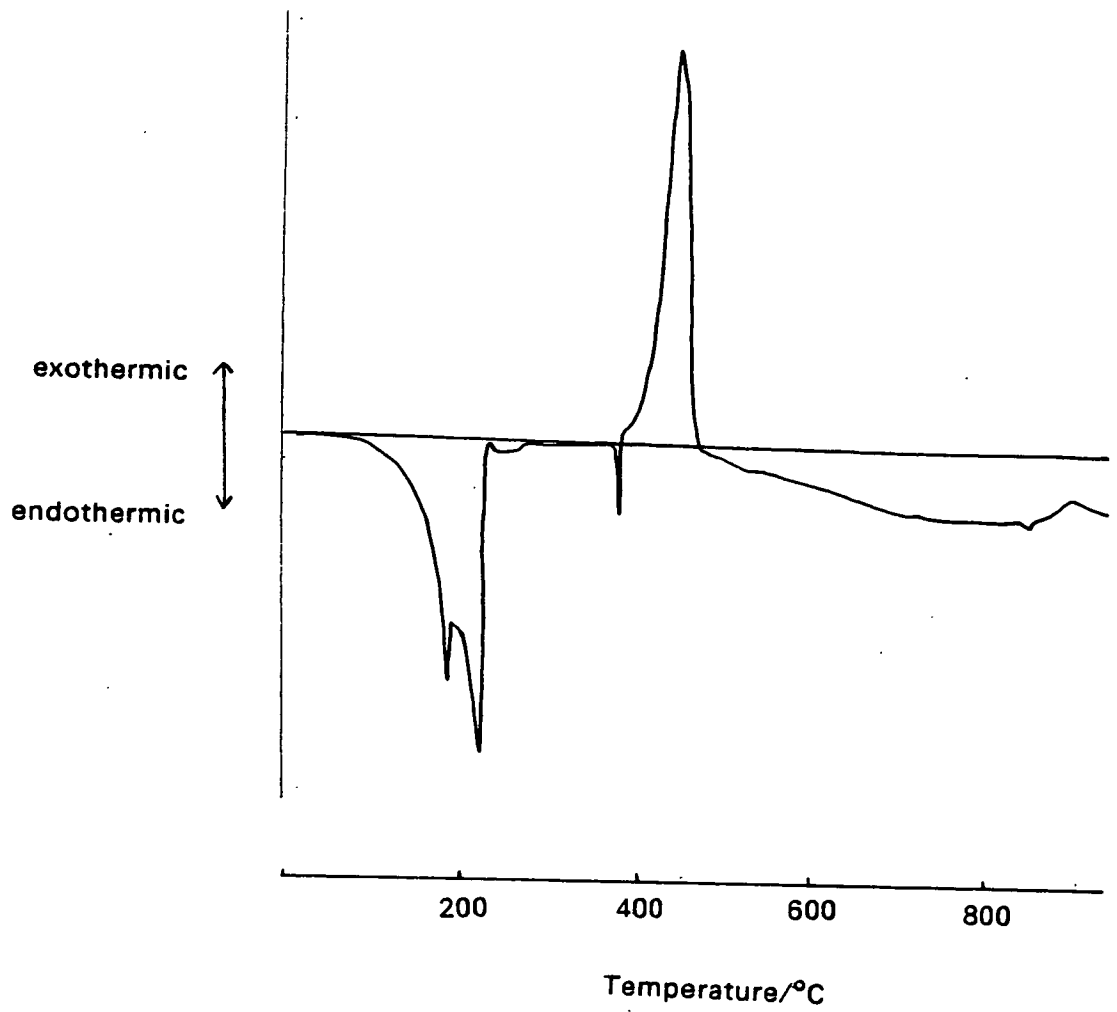


Figure 5.23

DTA curve of alumina/sodium acetate trihydrate.

occurs after the first occlusion stage. The DTA trace of sample 4 shows that all the acetate has been decomposed by this treatment.

Although the uptake of n-heptane has been reduced slightly by this treatment, even after four cycles there is still a considerable uptake and the structure remains crystalline.

### **Experiment 6**

Experiment 6 was similar to Experiment 5 except the silicalite + salt samples were heated at 600°C and samples were ion-exchanged with HCl solutions. The exact procedure is shown in Figure 5.24. The XRD patterns are shown in Figure 5.25 and the uptakes of n-heptane in Table 5.13.

Occlusion of sodium acetate followed by decomposition at 400°C results in a considerable decrease in the uptake of n-heptane. Whether collapse of the structure has occurred or not is unknown since the XRD pattern of sample 3 was obtained prior to heating at 400°C to activate the silicalite for sorption. Decomposition of sample 3 at 600° followed by ion-exchange with HCl leads to the appearance of some  $\alpha$ -cristobalite phase. The uptake of n-heptane has increased suggesting that ion-exchange of sodium ions has occurred. Further occlusion and decomposition results in further conversion to  $\alpha$ -cristobalite and corresponding further decreases in n-heptane. Ion-exchange increases the capacity for n-heptane to a small extent. Stirring with water and soxhlet extraction do little to increase the sorption capacity. Soxhlet extraction appears to increase the crystallinity of the sample which could be due to the loss of amorphous material during the continuous washing process.

Calcination at 850°C reduces the sorption capacity to a negligible amount.

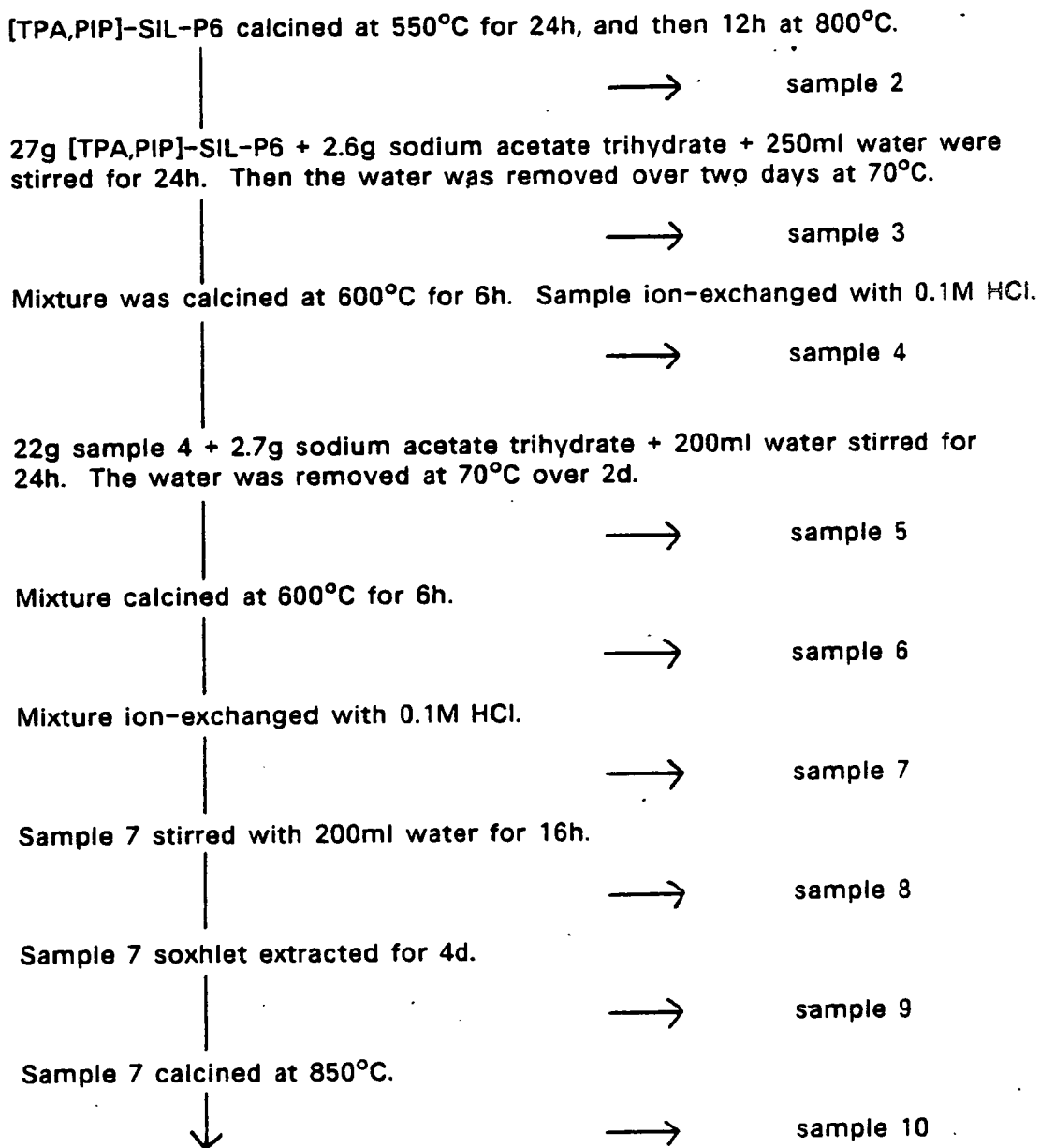


Figure 5.24

Procedure followed in Experiment 6.

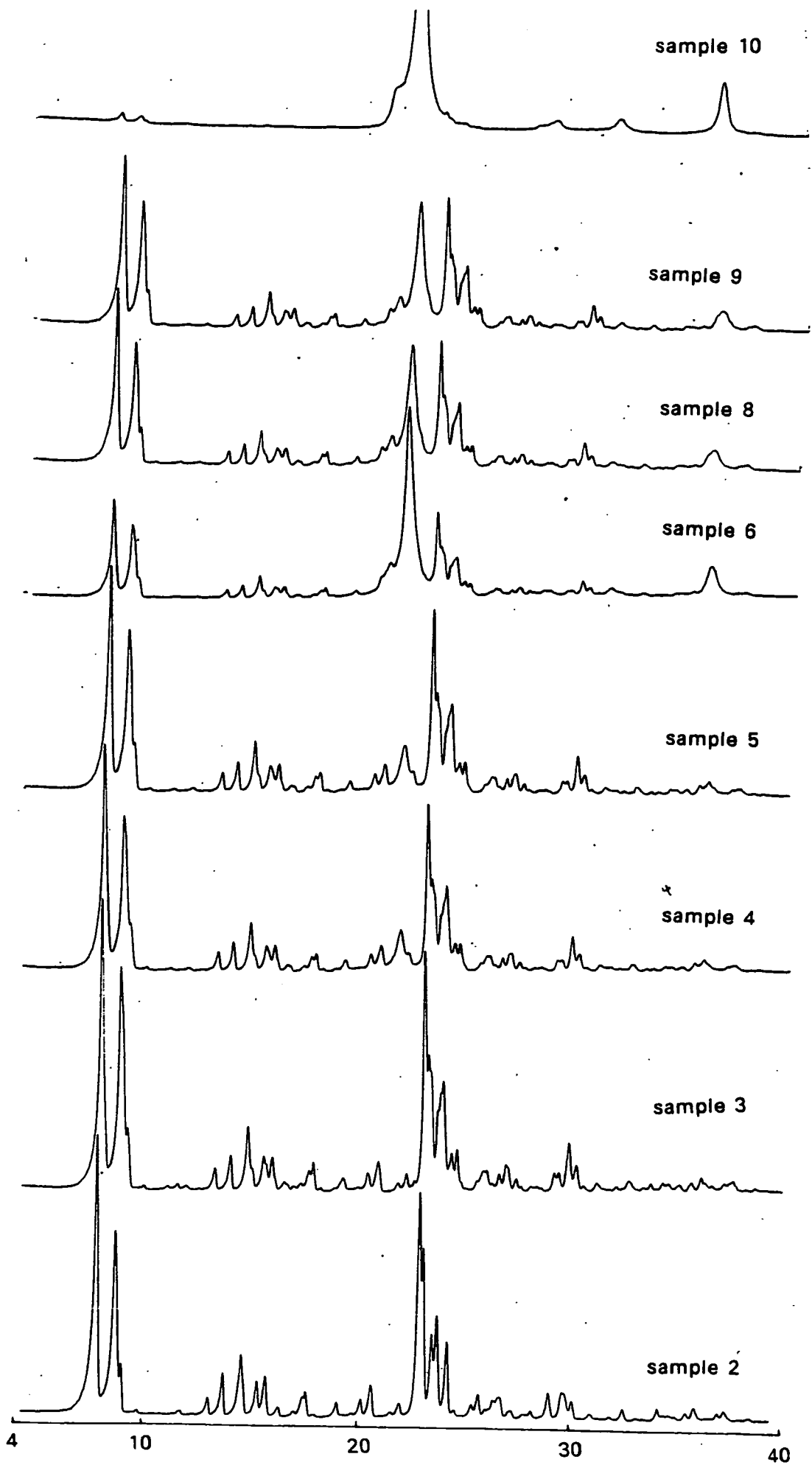


Figure 5.25

XRD patterns of samples in Experiment 6.

sample	U (n-heptane) /gg-1	U (water) /gg-1
2	0.134	0.087
3	0.099	0.072
4	0.107	0.028
5	0.103	0.025
6	0.052	0.022
7	0.075	0.018
8	0.076	0.017
9	0.076	0.013
10	0.010	-

Table 5.13 Uptakes of n-heptane and water by samples in Experiment 6.

The uptakes of water suggest that although the silicalite structure is partially destroyed by this treatment the resultant structure appears to be more hydrophobic than the original structure.

## 5.5 Conclusion

The work in this chapter has shown that group 1 acetates attack the framework of silicalite-1 at temperatures as low as 200°C. It is possible that this phenomena occurs even at ambient temperatures. If sufficient salt is present, decomposition of acetate in contact with the silicalite-1 results in considerable loss of crystallinity or even conversion to  $\alpha$ -cristobalite. The extent of the attack depends on the quantity of salt, temperature, and length of heating. It is also probably dependent on the pretreatment and synthesis of samples although this was not investigated.



## 5.6 References

1. "Handbook of Chemistry and Physics", Chemical rubber publishing Co., Cleveland, Ohio.
2. N.R. Chaudliuri, S.M. Ka and G.K. Pathak, *J. Thermal Chem.*, 13, 16, 1979.
3. M.D. Judd, B.A. Plunkett and M.I. Pope, *J. Thermal Anal.*, 83, 9, 1976.

## CHAPTER 6 CONCLUSION

Throughout this work, silicalite-1 was found to be a more complex material and its framework more "reactive" than is often appreciated.

Samples of silicalite-1 used in this research were synthesised from reaction mixtures that contained TPABr and piperazine or lithium, sodium, potassium, rubidium or caesium hydroxide. Relative to the TPABr + piperazine mixture, all the metal ions affected the rate of reaction and were incorporated into the channels of silicalite-1, except for caesium and possibly rubidium.

The measurement of the sorption properties of silicalite-1 was carried out using two techniques - the Cahn electrobalance and the "multi-equilibration" method. The latter technique was developed particularly for this work. Results were presented that show that this technique is an ideal way in which to obtain sorption uptakes of many samples at one time, quickly, simply and in a reproducible manner.

An investigation of the sorption of straight chain alkanes by silicalite-1 revealed that this process was relatively straightforward. Filling of the channels was achieved at low values of  $p/p_0$ , due to the high dispersion energies of interaction. Any variation observed between samples was due to the presence or absence of different cations in the channels.

The sorption of polar molecules by silicalite-1 was found to be more complicated than the sorption of non-polar molecules. The sorption of these molecules was very sensitive to the nature of the internal surface of silicalite-1. In turn, the nature of the internal surface was found to be very

dependent on the synthesis and pretreatment conditions used for the preparations of samples.

The uptake of methanol and water varied as the synthesis mixture, calcination temperature, ion-exchange and washing procedures were altered. The uptake of water and methanol at a given pressure was found to vary with the equilibration time. The timescale of the variations was much longer than could be explained by the simple diffusion of molecules into the channel system.

This was due to the chemisorption of the polar molecules. For every molecule sorbed in this way, two silanol groups or a silanol and a Si-O-CH<sub>3</sub> group may be formed. This process is an activated process and so it occurs over considerable lengths of time.

As this process occurs during the determination of an isotherm, hysteresis was observed in the sorption/desorption curves of methanol and water. The extent of hysteresis was found to vary between samples prepared or pretreated in different ways. But it was observed to be reproducible between runs of a given sample and sorbate.

Evidence of hydroxylation and methoxylation was also observed in the plots of heats of sorption against uptake of sorbate. As the number of hydroxyl or methoxyl groups increases the heat of sorption increases due to increased contributions to the heat of sorption from interaction of water or methanol with hydroxyl or methoxyl groups.

The initial uptake of a polar molecule depends on the number of hydroxyl

groups present initially. The "final" uptake of water or methanol depends on the degree of hydroxylation and/or methoxylation that has occurred. This in turn depends on the susceptibility of the silicalite-1 framework to attack by the polar molecules.

Both these factors were found to be affected by the synthesis conditions, calcination temperature, ion-exchange and washing processes used in the preparation of samples.

In a few instances, the molecular sieve appeared to become more hydrophobic with time. This was an unexpected observation. However, it is possible that some internal silanol groups that remained after calcination of the silicalite slowly heal with time.

Silicalite was found to readily occlude salts that possess considerable organic character provided they are of the correct size and shape to pass through the pores into the channel system. Occlusion of such salts was found not to occur to a pore-filling extent. The reason for this is the repulsion of like-ion/like-ion interactions. The maximum uptake of salt was achieved at relatively low concentrations. The longer the alkyl chain the less sensitive the occlusion to water activity. This compares well with results obtained from gas phase sorption. The occlusion of salts, for example, sulphonates was found to reduce the sorption uptakes but did not alter the molecular sieving properties of silicalite-1.

Small quantities of inorganic salts such as sodium chloride were occluded. In such cases, the salt was considered to be associated with a number of 'hydrophilic' sites within the channel system, such as hydroxyl groups.

The framework of silicalite was found to be very prone to attack from alkaline salts. Both acetates and carbonates were found to attack the lattice at relatively low temperatures. In particular, the decomposition of acetate in contact with silicalite caused loss of crystallinity and/or conversion to  $\alpha$ -cristobalite. This was effected by the weight of salt and the decomposition temperature.

Many potential uses have been proposed for silicalite-1. This work has shown that great care must be taken when investigating or applying the properties of silicalite. Its simple structure -  $96\text{SiO}_2$  - belies the complex nature of its properties.

## APPENDIX A LECTURE COURSES

The following lecture courses were attended during the period October 1982 and September 1985.

Least Squares Analysis - Prof. J. Tellinghausen (Vanderbilt University, Tennessee).

Molecular Electronics - Prof. R.W. Munn and J.O. Williams (UMIST).

Microcomputers and Instrumentation - Dr. A. Rowley and Mr. A. King (University of Edinburgh).

Chemical Technology and Industrial Chemistry - Dr. A.J.S. Nicoll, Dr. L.H. Mustoe and R.S. Sinclair (Paisley College of Technology).

X-Ray Diffraction Techniques - Dr. R.O. Gould, Dr. B.M. Lowe and Dr. A. Blake (University of Edinburgh).

Characterisation of Surfaces - Dr. H.F. Leach (University of Edinburgh).

Fortran 77 Computing Course - Edinburgh Regional Computing Centre

Also group and departmental seminars were attended.